SYNTHESIS AND CHARACTERIZATION OF METALLOCALIXARENES AS PRECURSORS FOR THE SOHIO MODEL CATALYST

by

Daniel Mendoza-Espinosa

Bachelor of Science, 2004
Universidad Autónoma del Estado de Hidalgo
Pachuca de Soto, Hidalgo, México

Submitted to the Graduate Faculty of the
College of Science and Engineering
Texas Christian University
in partial fulfillment of the requirements
for the degree of

Doctor of Philosophy

August 2009

SYNTHESIS AND CHARACTERIZATION OF METALLOCALIXARENES AS PRECURSORS FOR THE SOHIO MODEL CATALYST

by

Daniel Mendoza-Espinosa

Dissertation approved:

Major Professor

For the College of Science and Engineering

AKNOWLEDGEMENTS

I thank God for all the blessings in my life.

I would like to express my deepest gratitude to my advisor Professor Tracy A. Hanna. Thank you for all the encouragement, guidance and invaluable advices during this doctorate period. Thank you for gave me the opportunity to come to TCU as an undergrad student, for allowed me to belong to your research group, and for all the knowledge that I received from you. Without your kind guidance this journey could have been very difficult.

I am very grateful to professor Anne F. Richards for all her support and interest in my scientific career. Thanks a lot for all your advices and guidance in the X-ray diffraction field.

I also thank the members of my committee, Professor Jeffery Coffer and Professor Sergei Dzyuba for their time, advices and continuous support.

I would like to thank my parents and brothers to whom I dedicate this thesis. Thank you for all the support, love, and patience, and for all the shared efforts in order to achieve all of my goals. Thanks for all your motivation that kept me going and reaching for more. Thanks especially to my mom for being my angel and my main inspiration.

I would like to thank specially Yamina Belabassi for sharing with me these last five years of good and hard times. You were an essential part of my life during this period. Thanks for cheering me up and for your kindness, I could not have gone this far without you.

Thanks to my older brother Bernat Martinez for his friendship and for giving me priceless assistance during all this doctorate period. I wish you the best always.

Thanks to the Hanna group members for their help and the good moments that we shared.

I acknowledge the National Science Foundation (CHE-133866), the Welch (P-1459) and Texas Christian University Research Fund for financial support.

TABLE OF CONTENTS

LIST OF EQUATIONS

LIST OF SCHEMES

LIST OF TABLES

LIST OF FIGURES

CHAPTER 1

BACKGROUND AND PURPOSE

1.1 The SOHIO process

1.1 1 Introduction

The Standard Oil of Ohio Company (SOHIO) process refers to the selective oxidation and ammoxidation of propene to produce acrolein (equation 1.1) and acrylonitrile (equation 1.2), used on large scales in industry.[1] Acrolein is an important precursor for the preparation of polyester resin, polyurethane, propylene glycol, acrylic acid, and glycerol, while acrylonitrile is utilized primarily as a co-monomer in the production of acrylic fibers.

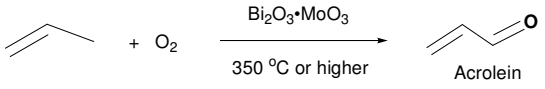

(1.1)

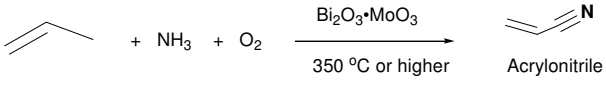

(1.2)

The predominant commercial processes for acrylonitrile and acrolein production use multicomponent catalysts based on the $Bi_2O_3 \cdot MoO_3$ oxide phase developed by SOHIO workers in 1959-1962.[2,3] The pure bimetallic oxide phase was used for the industrial production of acrylonitrile until it was discovered that metal oxide additives increased the selectivity and yields. Nowadays, the simple heterobimetallic formulation has been replaced by multicomponent catalysts that significantly improve the process performance. The SOHIO process currently represents approximately 90% of the acrylonitrile worldwide production with plants installed in sixteen countries. In 2005 the annual global production of acrylonitrile was calculated to be 5 million tons.[4]

The ammoxidation of propene in the SOHIO process is highly selective but the maximum acrolein yield at high propene conversion (90-95%) using the multicomponent catalyst is approximately 80%.[4] Commercial interest in improving the acrolein selectivity and decreasing the temperature of the process has encouraged the fundamental investigation of the mechanistic pathway of the catalyst.[5-7] It is believed that a more detailed knowledge of the mechanism of the substrate activation could enable different approaches such as the use of the cheaper propane substrate.[8-12]

1.1.2 Mechanism of Reaction

The outstanding performance of the SOHIO process has stimulated much fundamental research on its mechanistic details, but four decades after its discovery, the mode of action of the "simple" bimetallic oxide remains controversial.[6,13] Analyses of heterogeneous SOHIO systems using techniques such as Raman spectroscopy, neutron diffraction, X-ray diffraction, pulse kinetic, and isotopic studies have led to mechanistic proposals of acrolein and acrylonitrile formation (Scheme 1.1).[5] The mechanism for acrolein oxidation has been proposed as follows:

1 coordination of propene to a molybdenum site of the catalyst (B);

2 H abstraction at a bismuth site resulting in an allyl intermediate (C, slow step);

3 C-O bond formation at a molybdenum site (D);

4 a second hydrogen abstraction;

5 reoxidation of the active site by oxygen migration from the bulk catalyst accompanied by water elimination (E).

The ammoxidation of acrylonitrile is similar but includes an initial NH_3 substitution for a terminal Mo=O moiety, and subsequent C-N bond formation rather than C-O bond formation.[6] Graselli's proposed reaction mechanism[5] is depicted in Scheme 1.1.

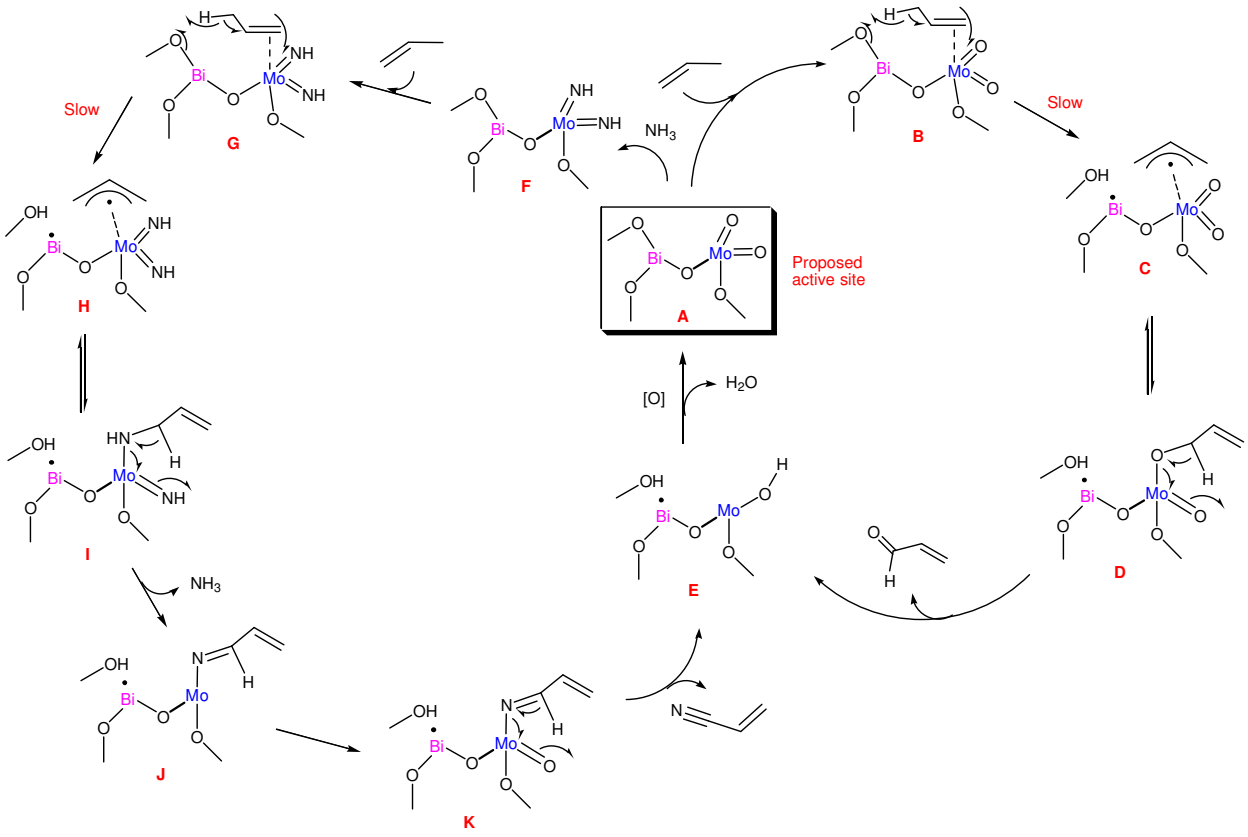

Scheme 1.1 Graselli's proposed mechanism for the selective oxidation (right) and ammoxidation (left) of propene over bismuth molybdate catalysts.[5] Proposed active site (A).

Although very extensive studies on the heterogeneous systems have provided a realistic reaction mechanism, there are important drawbacks that hinder the full elucidation of the heterogeneous chemistry in the system:

i) the multiple sites found on the surface of heterogeneous catalysts makes the identification of active sites very difficult;

ii) different catalyst synthetic methods and reaction conditions could lead to different reaction mechanisms;

iii) conclusions made on the basis of activity or selectivity when a variable is changed, cannot safely define the role of that variable in an otherwise unchanged mechanism;

iv) the current multicomponent catalyst can contain Bi, Mo, Fe, Ce, etc, that of course, may make a big difference in the reaction mechanism compared to simple Bi/Mo catalysts.

All of the above drawbacks are reflected in the significant decrease in the number of mechanistic studies performed using heterogeneous systems during the last two decades. Currently, SOHIO research based on homogeneous models has become more popular, including several molybdenum-containing models and a few bismuth-containing models in the last decade.[6]

1.2 Homogeneous model studies

The complications arising from the chemical and physical interactions of heterogeneous catalyst surfaces with the substrates and products make it difficult to perform mechanistic studies of heterogeneous catalytic reactions. One of the main problems in heterogeneous systems is the fact that the catalyst/substrate interactions are not particularly amenable to spectroscopic or kinetic analysis.

In contrast, homogeneous catalysis reactions can be studied via a variety of spectroscopic techniques, allowing in some cases the isolation of important reaction intermediates. Mechanistic studies of homogeneous catalytic reactions of mononuclear or polynuclear organometallic complexes have allowed mechanistic analogies to similar reactions occurring on heterogeneous catalyst. These mechanistic analogies can be of considerable value if they result in the development of new, more efficient catalysts or the improvement of existing catalysts.

During the last two decades research on the mechanism of the SOHIO process has focused on the synthesis and reactivity of Bi/Mo homogeneous models. This information can be retrieved from two recent reviews.[6,13] In the next subsections (1.2.1 and 1.2.2), some of the most relevant results will be highlighted to provide a better understanding of where our research is located and our goals.

1.2.1 Mo and Bi monometallic models

Graselli's proposed first step in the mechanism of reaction SOHIO process involves the coordination of propene to a molybdenum site of the catalyst (structure **B**, Scheme 1). This intermediate is characteristic of a high oxidation state Mo center buried in an oxo environment. The coordination of olefins to the molybdenum center has been observed[14] and modeled using allylic ligands.[15-17]

Models of the radical-like intermediates **C** and **D** are unknown, presumably due to the instability of such type of intermediates. However, some complexes containing a π-allylmolybdenum unit covalently bound to an oxo or an imido ligand have been prepared[13,15-19] and some examples are shown in Figure 1.1.

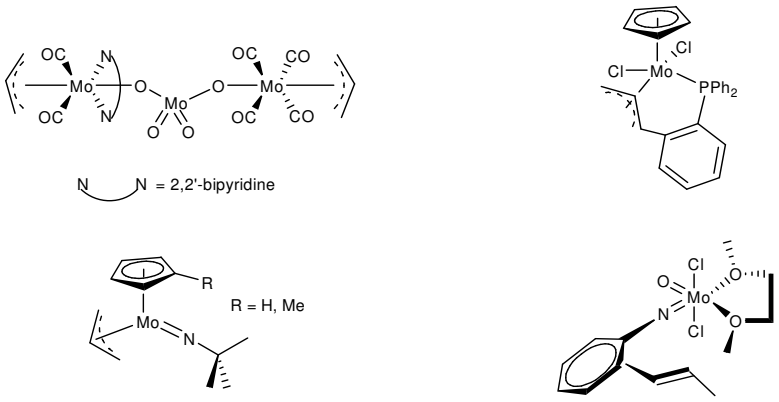

Figure 1.1 Model molecules[13,15-19] for the intermediates **C** and **D** in the Graselli's proposed SOHIO reaction mechanism (Scheme 1.1).

Several other studies using modybdenum(VI)/tungsten(VI)-based models have been performed and have provided information about C-O and C-N forming steps in the SOHIO process (structures **D** and **I**, Scheme 1).[6] These modeling results suggested that the C-O or C-N bond forming routes can be a consequence of three different reaction mechanisms; i) ligand radical trapping followed by oxidation,[20,21] ii) allylic migration,[22,23] or iii) deprotonation of allylimido moieties.[24-30]

The amount of work that has been done to model the role of bismuth in the Bi/Mo catalyst is relatively small in comparison to that of molybdenum. Rademann and coworkers have found that bridging atoms in clusters of the type $Bi_3O_4^+$ (Figure 1.2a) and $Bi_5O_7^+$ (Figure 1.2b) can participate in propene oxidation rate-determining steps.[31]

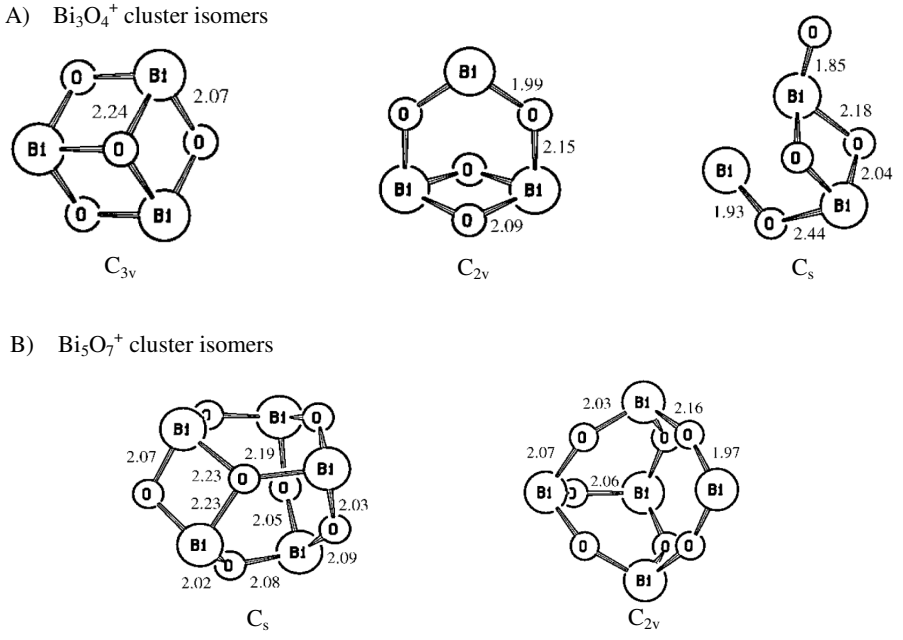

Figure 1.2. Rademann's optimized ORTEP structures of A) $Bi_3O_4^+$ and B) $Bi_5O_7^+$ cluster isomers showing the point group and bond distances [Å].[31]

Rademann et al. have also demonstrated that reactivity of oxygen and ethylene with $Bi_4O_6^+$ clusters is due to radical centers on bridging oxygen atoms.[32] These two observations support the oxo-bridged intermediates in the Graselli's proposed SOHIO mechanism.

The second series of homogeneous bismuth models for the SOHIO process were developed by our group. For several years now, we have been interested in modeling the role of the bismuth and molybdenum atoms in the SOHIO process. Motivated by this purpose, we have synthesized a series of bismuth complexes with hindered aryloxides using salt metathesis reactions. While preparing some of these compounds, we discovered that bismuth aryloxides of the type $[Bi(OAr)_3]$ (Ar = 2,6-RC_6H_3, R = ^{i}Pr, ^{t}Bu) readily decomposed to produce C-C coupled products (equation 1.3).[33]

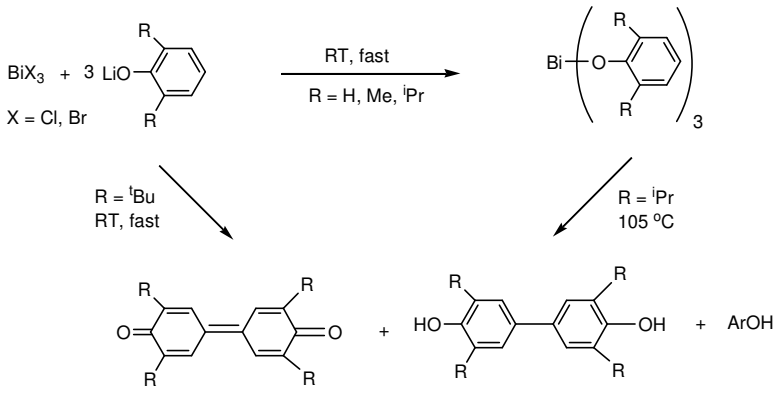

(1.3)

This was the first molecular bismuth compound to model the reactivity of the SOHIO catalyst. Equation 1.3 supports the proposal that propene activation occurs by a radical species formed by Bi^{III}-O bond homolysis. The proposed mechanism of oxidation in our bismuth model is illustrated in Scheme 1.2.

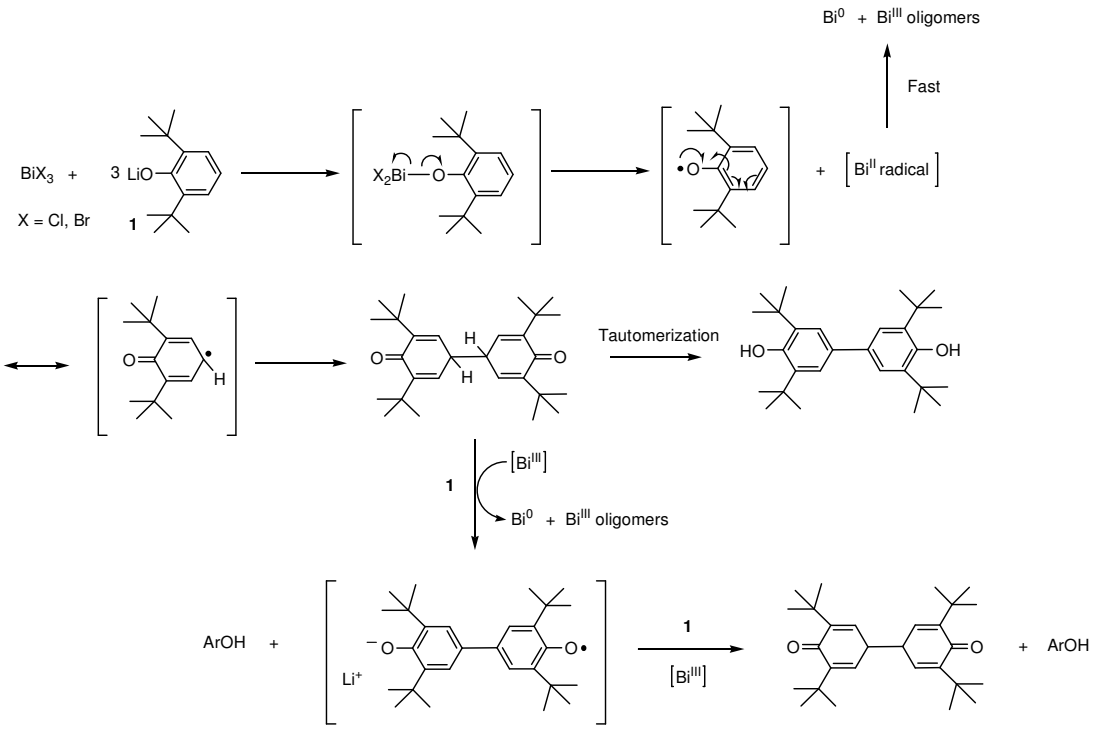

Scheme 1.2 Proposed mechanism of ligand oxidation in our molecular bismuth aryloxide model.[33]

More recently we have observed that the complex $Bi(OAr)_3$ (Ar = 2,6-^{i}Pr-4-BrC_6H_3) underwent an intramolecular C-H activation in the ligand to form an organometallic ladder Bi complex **2** (equation 1.4).[6] This result reinforces the linkage between this model and the SOHIO process, as Bi^{III} has activated allylic hydrogens similar to those involved in propene activation in the SOHIO rate determining step.

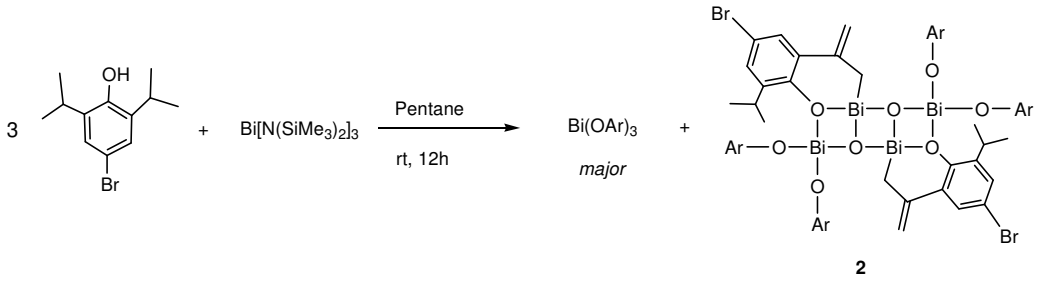

2 (1.4)

1.2.2 Heterometallic Bi/Mo models

The results obtained from the individual investigations with bismuth and molybdenum homogeneous models have shown similarity with the mechanistic steps proposed using the heterogeneous models. However, Bi/Mo heterogeneous systems have not been discussed so far.

The first soluble Bi/Mo heterometallic complex was reported by Klemperer and Liu in 1980.[34] The compound with formula $[^{t}Bu_4N]_2[Ph_3Bi(MoO_4)_2]\cdot 3H_2O$ contains the bismuth and molybdenum centers in their highest oxidation states, and it was only recently that Limberg et al. reported its X-ray structure (Figure 1.3a).[35] Villanneau et al. have also reported the synthesis and crystal structure of a Bi/Mo heterometallic cluster with formula $[NBu_4]_3[Bi^{III}\{Mo_5O_{13}(OMe)_4(NO)\}_2]\cdot 3H_2O$ (Figure 1.3b).[36] Both of these complexes contain Bi-O-Mo linkages, but no reactivity has been reported to date.

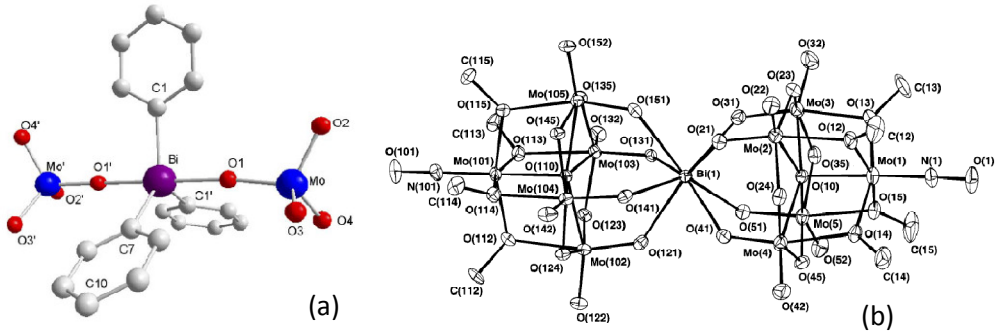

Figure 1.3 The first examples of soluble Bi/Mo heterometallic complexes.[35,36]

Limberg and coworkers recently reported a series of heterobimetallic alkoxide bridged complexes of the type Mo(μ-OR)Bi.[37] Complex $[Cp_2Mo(\mu\text{-}OEt)_2Bi(OEt)_2Cl]$ (Fig 1.4a) contains a molybdocene dialkoxide moiety bridged to a bismuth alkoxide by a Lewis acid/base interaction with the molybdenum alkoxy groups. Hoping to simulate the allymolybdenum surface intermediate suggested during the SOHIO process, Limberg's group also synthesized complexes

containing allylic ligands.[38] The first complex of this type was achieved by the reaction of $[(CH_3C_3H_4)Mo(CO)_2(CH_3CN)_2Cl]$ and $[Bi(OEt)_3]_x$ that produced a tetranuclear complex built of two $(CH_3C_3H_4)Mo(CO)_2(\mu\text{-}OEt)_3Bi$ units linked by two ethanolate ligands (Fig 1.4b). A second complex with a molecular structure of $[(CH_3C_3H_4)Mo(CO)_2(\mu\text{-}\kappa O,2\kappa O'\text{-}OCH_2CH_2OCH_3)_2(\mu\text{-}Cl)BiCl]$ (Fig 1.4c) was obtained from the reaction of $[Bi(OCH_2CH_2OCH_3)_3]_2$ and $[(CH_3C_3H_4)Mo(CO)_2(CH_3CN)_2Cl]$.[38] The bridging Cl ligand is found *trans* to the allyl group at the molybdenum center and to the terminal Cl ligand at the Bi center (Cl-Bi-Cl = 159.47(8)^o). The chloride free complex $[(CH_3C_3H_4)Mo(CO)_2(\mu\text{-}\kappa O,2\kappa O'\text{-}OCH_2CH_2OCH_3)_3Bi(THF)][BF_4]$ (Fig 1.4d) was prepared by treatment of $[(CH_3C_3H_4)Mo(CO)_2(CH_3CN)_2(THF)][BF_4]$ with one equivalent of $[Bi(OCH_2CH_2OCH_3)_3]_2$.[38] This compound contains a (π-allyl)Mo unit in an oxygen-rich coordination sphere, fulfilling some of the requirements for a structural model of the Bi/Mo propene oxidation catalyst.

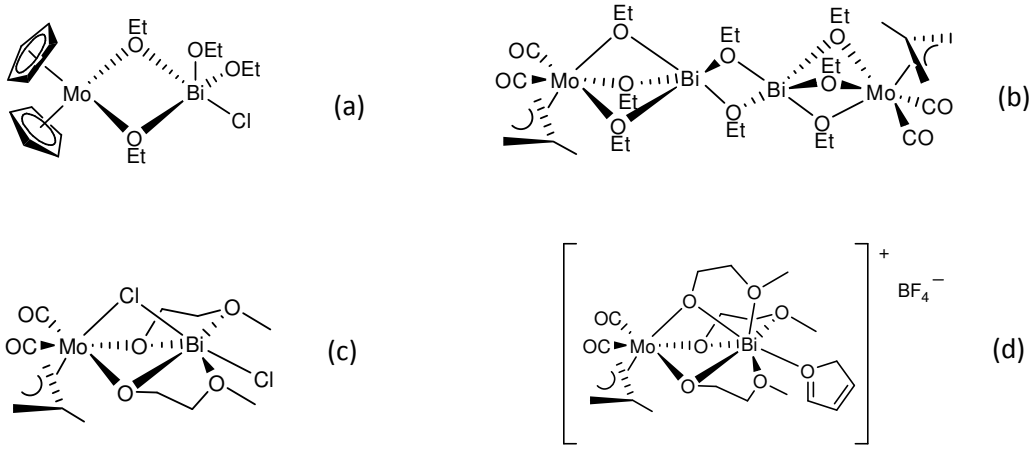

Figure 1.4 Alkoxide bridged [Mo](μ-OR)[Bi] complexes.[37-39]

Once Limberg and coworkers achieved the synthesis of soluble Bi/Mo alkoxides, they used a similar synthetic approach for the preparation of complexes containing Bi^{III}-O-Mo^{VI} moieties. The reaction between $[(o\text{-tolyl})_2Bi(OTf)(hmpa)_2]$ and one equivalent of

$[NBu_4][Cp^*MoO_3]$ afforded the complex $[\{(o\text{-tolyl})_2Bi\}(\mu\text{-}O)MoO_2Cp^*]_n$ (Fig. 1.5a).[35] The complex comprises Cp^*MoO_3 units linked by a bridging oxygen atom to the $(o\text{-tolyl})_2Bi$ fragment. The terminal Lewis basic Mo=O groups and Lewis acidic Bi^{III} center generate secondary interactions that led to the formation of a polymeric structure.

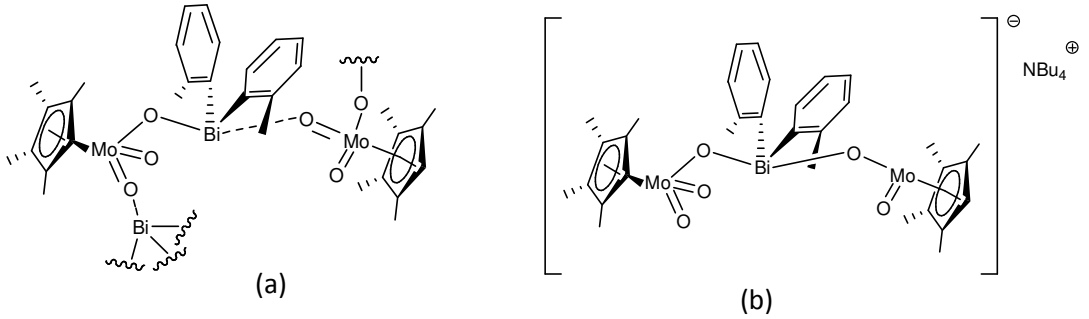

Figure 1.5 Heterobimetallic complexes containing Bi^{III}-O-Mo^{VI} linkages.[35,40]

The low solubility of $[\{(o\text{-tolyl})_2Bi\}(\mu\text{-}O)MoO_2Cp^*]_n$ is associated with its polymeric nature, and motivated Limberg et al. to synthesize analogous monomeric complexes. When $[\{(o\text{-tolyl})_2Bi\}(\mu\text{-}O)MoO_2Cp^*]_n$ was reacted with an extra equivalent of $[NBu_4][Cp^*MoO_3]$ a bright yellow solution was formed, and after workup the ionic compound $[NBu_4][(o\text{-tolyl})_2Bi(\mu\text{-}O)MoO_2Cp^*)_2]$ was isolated (Fig. 1.5b).[40] This monomeric complex contains two $Cp^*MoO_3^-$ moieties bound via oxygen atoms to an $(o\text{-tolyl})_2Bi^+$ fragment, forming a 10-electron 4-coordinate bismuth center. The coordination of a second equivalent of $Cp^*MoO_3^-$ saturates the Bi^{III} center, avoiding the formation of a polymeric structure.

Further syntheses of complexes containing oxygen linkages were achieved by the reaction of $BiPh_3Br_2$ with the molybdates $[NBu_4]_2MoO_4$ or $[NBu_4]_2Cp^*MoO_3$ to yield $[Ph_3Bi\{\mu\text{-}O\text{-}MoO_2Cp^*\}_2]$[35] (Fig 1.6a) or $[NBu_4]_2[Ph_3Bi(OMo_3O)_2]$[40] (Fig 1.6b), respectively.

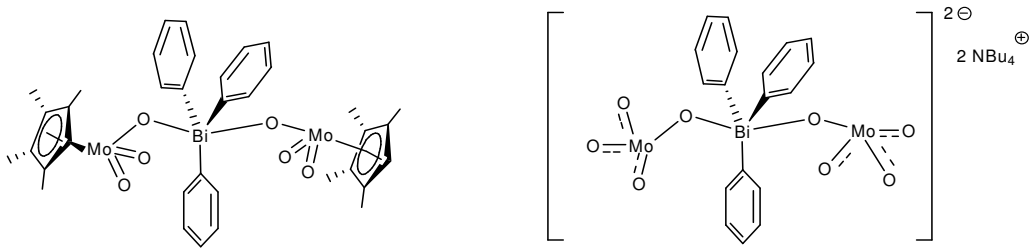

Figure 1.6 Monomeric heterobimetallic complexes containing Bi^{V}-O-Mo^{VI} linkages.[35,40]

While attempting to obtain a precursor for another Bi-O-Mo bridged complex, Limberg's group synthesized the Mo/Bi alkoxide $[Cp_2Mo\{Bi(O^tBu)_2\}_2]$[39] (equation 1.5) with direct Mo(IV)-Bi(III) bonds. Even though Mo-O-Bi linkages were absent, Limberg et al. demonstrated that the complex was able to catalyze the epoxidation of stilbene (equation 1.6).

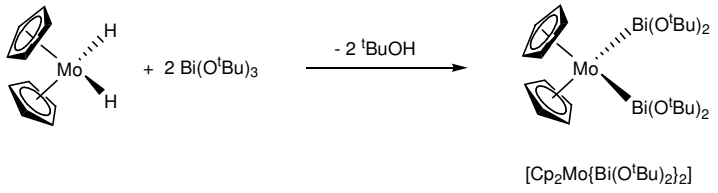

(1.5)

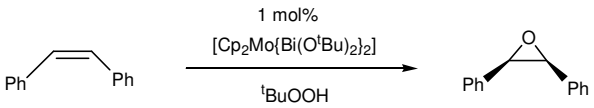

(1.6)

The authors suggest that the epoxidation takes place due to the formation of a transient complex with reactive Mo-O-Bi bonds.[39]

Further reactivity of the complex $[Cp_2Mo\{Bi(O^tBu)_2\}_2]$ with one equivalent of Cp_2MoH_2 allows the preparation of complex $[Cp_2Mo\{Bi(O^tBu)\}]_2$, that after loss of another two ^{t}BuOH molecules, undergoes intramolecular Bi-C bond formations (Scheme 1.3).

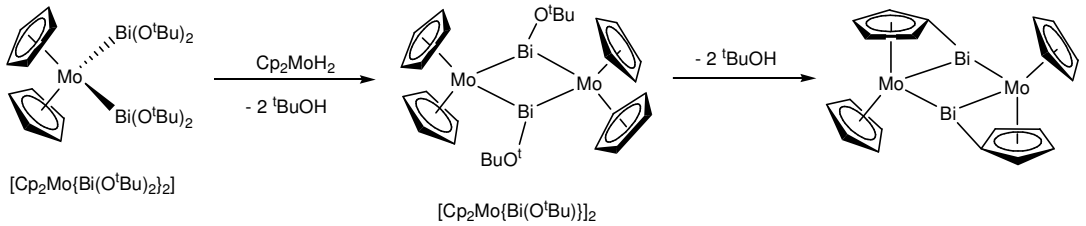

Scheme 1.3 Intramolecular C-H bond activation and Bi-C bond formation in covalently bonded Bi-Mo heterobimetallic alkoxides.[41,42]

The intramolecular activation in complex $[Cp_2Mo\{Bi(O^tBu)\}]_2$ is an interesting result since it demonstrates the potential of bismuth complexes for C-H activation, which is the rate determining step in the allylic oxidation of propene.

Overall, though a few soluble heterobimetallic Bi/Mo complexes have been made, there is still a need for more detailed investigations in order to achieve a better understanding of the mechanism in the SOHIO process. Considering that most of the SOHIO process investigations have been focused on understanding the action mode of the "simple" Bi_2O_3/MoO_3 oxide phase, it is an exciting challenge to aim for a deeper mechanistic knowledge in systems that mimic the real multicomponent catalysts used nowadays.

1.3 Our proposed Bi/Mo catalyst model

A current research project in Professor Hanna's lab is related to the synthesis and characterization of monometallic Bi^{III} and Mo^{VI} complexes with oxygen donor ligands. These monometallic complexes can be used as building blocks for the preparation of heterometallic Mo/Bi models that resemble the active site of the Bi_2O_3/MoO_3 heterogeneous catalyst used in the SOHIO process (Scheme 1.1, structure A). This section will present a compilation of the latest results of these studies and the future goals of the research project.

1.3.1 Bi^{III} and Mo^{VI} aryloxide complexes

Within the last few years our group has prepared a series of monometallic bismuth aryloxides obtained by simple metathesis or alcohol/amide exchange reactions. A 1:3 metal/aryloxide ratio is observed (Scheme 1.4) in most of these complexes.[43]

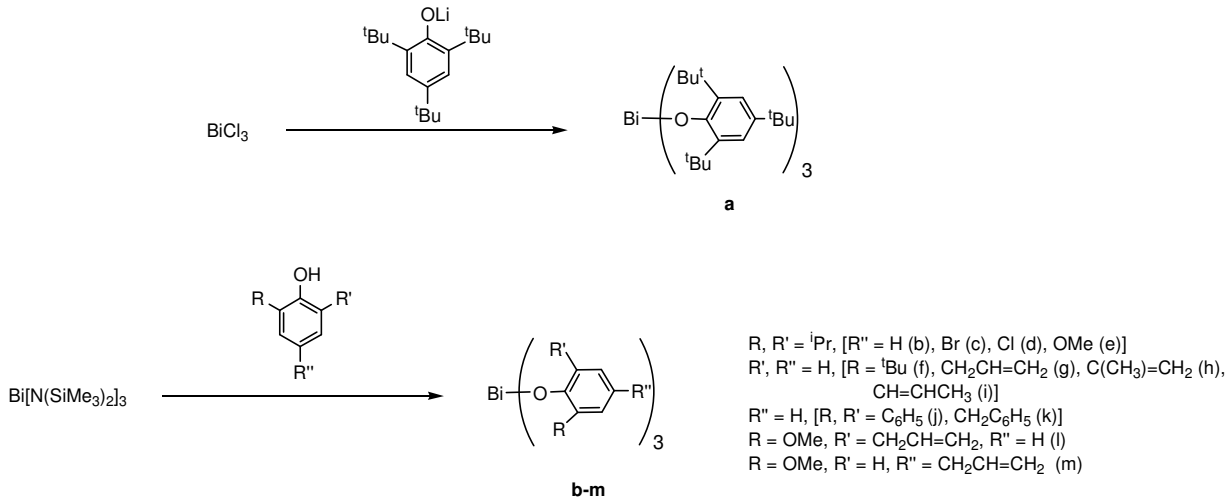

Scheme 1.4 Series of bismuth^{III} aryloxide complexes prepared by the Hanna group.[43]

Interestingly, while attempting the synthesis of bismuth complexes with bulky aryloxides, we observed unexpected oxidation reactions as previously depicted in equation 1.3. These results suggested that propene activation in the rate determining step in the SOHIO process most likely involves Bi^{III}-O homolysis giving a Bi^{II} radical species (Scheme 1.2).[33] We have also shown that during the synthesis of the complex $Bi(OAr)_3$ where Ar = 4-Br-2,6-$^{i}PrC_6H_3$ a side product with a ladder structure is formed by the C-H activation of the ^{i}Pr group (equation 1.4).[6] The importance of these results resides in the C-H activation promoted by the Bi^{III} center that supports the proposed slow step in the Graselli's SOHIO reaction mechanism (structure C, Scheme 1.1).

More recently a series of Mo^{VI} mono- and dioxo aryloxide complexes have been prepared by treating either the lithiated aryloxides or parent phenols with one equivalent of MoO_2Cl_2.[44-46] Some representative examples are depicted in Scheme 1.5. These Mo^{VI} complexes display very good solubility in most organic solvents and are isolable as crystalline monomeric units. The complexes display tetra-, penta- and hexacoordinate geometries. Some of them contain terminal chlorine groups that make them interesting building blocks for our bimetallic catalytic model.

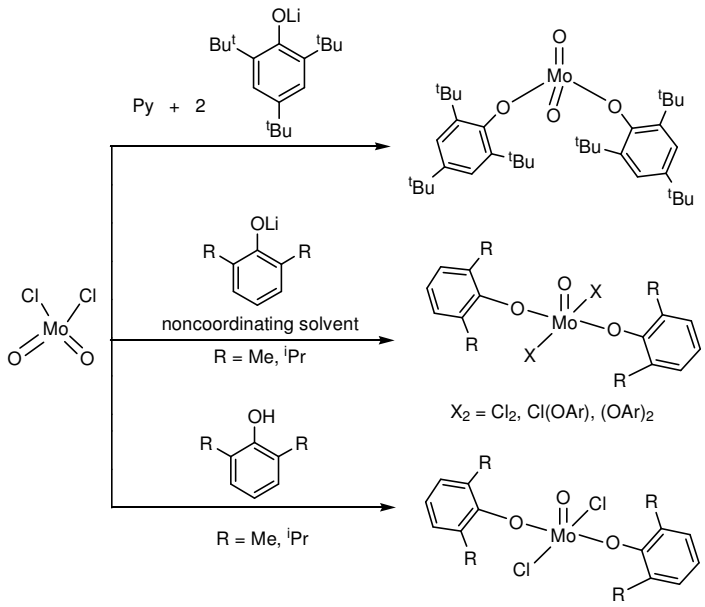

Scheme 1.5 Representative examples of Mo^{VI} aryloxide complexes synthesized in the Hanna lab.[44-46]

At this stage of our research, a fair amount of Bi or Mo monometallic precursors have been prepared and in some cases display interesting properties and reactivity. We are currently working on the development of synthetic pathways for joining these monometallic building blocks to afford our desired heterometallic Bi/Mo complexes.

Meanwhile, another route for the preparation of the Bi/Mo complexes in our lab is related to the use of organic frameworks that could mimic oxygen-rich surfaces. Such a modeling

approach requires a preorganized set of oxygen donor atoms located in a semi-planar arrangement, and the ability to coordinate two or more metallic centers simultaneously. The outstanding coordination capabilities and flexibility of the poly(dentate) calixarene ligands offer an excellent alternative for this purpose.

1.3.2 Calixarene ligands as oxo surfaces

Calixarenes (Scheme 1.6) are cyclic oligomers built from phenol units linked by methylene bridges.[47] Depending on the amount of base, and temperature used in their synthesis, several ring sizes can be synthesized. The calix[n]arene rings can be functionalized in the lower and/or upper rim by the addition of organic pendant arms, providing them with new properties that increase their selectivity and affinity toward specific ions or metal centers.[48] Some of their applications include catalysis, homogeneous modeling, enzyme mimics, host-guest chemistry, selective ion transport, sensors, and others.[49-51]

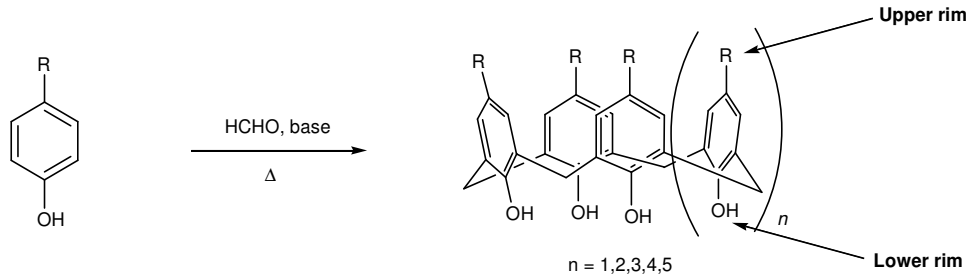

Scheme 1.6 Simplified synthesis and representation of the calix[n]arene ligands.

Our interest in calixarene ligands lies in their capabilities as host compounds and as platforms for attaching catalytic moieties. Floriani et al. have prepared a series of lower rim coordinated Mo^{VI} and W^{VI} dioxo complexes and have found that the reactivity of these compounds is very similar to that occurring on metal oxide surfaces.[52-54]

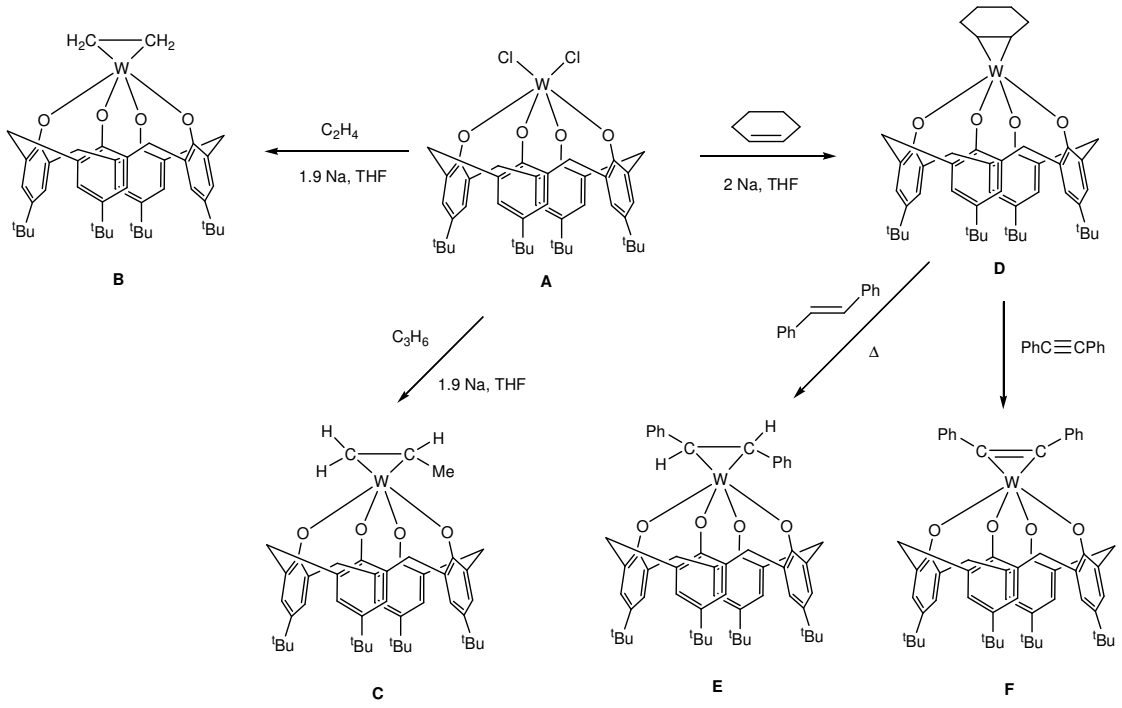

Scheme 1.7 M-C bond functionalities bonded to oxo surface modeled by calix[4]arenes.[55,56]

In one of their experiments, with the aid of a monometallic calix[4]arene [**HC4(H)$_4$**] tungsten complex (Scheme 1.7, **A**), a series of organometallic transformations permitted the formation of the η^2-olefin complexes **B** and **C**. A cyclohexene complex **D** was obtained by an analogous procedure. If **D** is further heated in toluene in the presence of a slight excess of a new olefin, the η^2-trans-stilbene complex **E** and diphenyl acetylene complex **F** can be obtained.[55,56] This interesting example of olefin rearrangement assisted by a calixarene metal oxo surface is similar to the SOHIO model system we wish to develop.

The first aim in our calixarene project was the preparation of bismuth and molybdenum monometallic precursors. If we could design monometallic complexes containing either reactive OH groups in the ligand or labile terminal groups attached to the first metal, further reactivity with an appropriate second metal substrate could afford the desired bimetallic complex (Scheme 1.8).

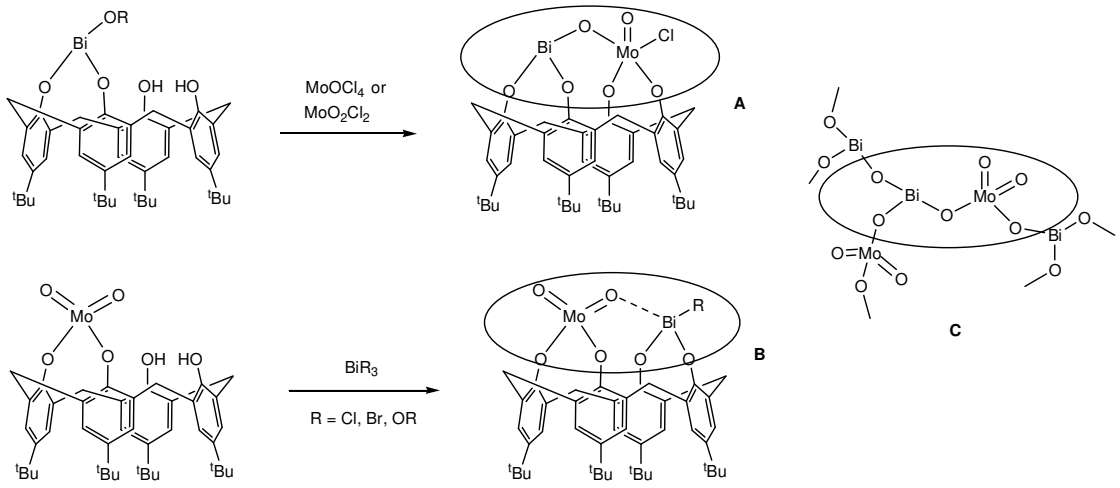

Scheme 1.8 Examples of proposed reactivity of calix[4]arene Bi^{III} and Mo^{VI} complexes for the preparation of models **A** and **B**, analogous to the SOHIO active site (**C**).

The models presented in Scheme 1.8 are only two of several possibilities that could take place when the calix[4]arene framework is utilized. It is expected that different synthetic pathways or different bismuth/molybdenum starting materials could allow the preparation of a constellation of structures. However, we expect that in all of these structural possibilities the proximity between the two metal centers in the lower rim of the calixarene will favor the formation of a dative or covalent metal-oxo-metal interaction (Scheme 1.8). Either of these metal oxo linkages could be useful for our mechanistic studies of the SOHIO process as they resemble the proposed catalyst active site (Scheme 1.8, **C**).

1.3.2.1 Bismuth and antimony complexes

In 2004 the Hanna group reported the synthesis of the first Sb^{III} and Bi^{III} calixarene complexes (Figure 1.7, **A** and **B**).[57] The reaction of the monosodium salt of *p-tert*-butylcalix[4]arene [Na·^{t}**BuC4(H)$_3$**] with two equivalents of $SbCl_3$ yielded the complex [Sb_2Cl_2{^{t}**BuC4**}] (**A**), while the treatment of *p-tert*-butylcalix[8]arene [^{t}**BuC8(H)$_8$**] with $Bi[N(SiMe_3)_2]_3$ afforded the [Bi_8O_4{^{t}**BuC8**}$_2$] cluster (**B**).

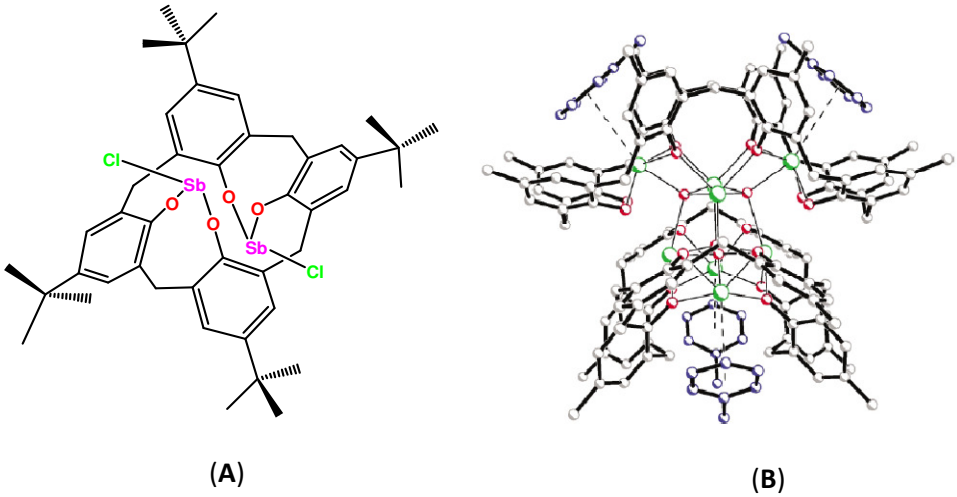

Figure 1.7 Structural representations of the first Sb^{III} and Bi^{III} calixarene complexes.[57]

Some interesting features are observed in these two complexes. In the antimony complex, for instance, the calixarene ring displays a 1,2-alternate conformation that allows the two Sb centers to adopt their normally observed trigonal pyramidal geometry. The antimony complex also contains two terminal Sb-Cl bonds that could be potential reactive groups for the synthesis of more extended structures. The Bi^{III} calix[8]arene complex, on the other hand, illustrates the ability of the ligand to resemble oxygen-rich surfaces by allowing the formation of a robust Bi_8O_{20} cluster. Both complexes saturate their respective calixarene lower rims with metal centers and have good solubility that facilitates their solution characterization.

In 2008 our group published a more general method for the synthesis of calix[4]arene bismuth and antimony complexes.[58] The preparation of a series of antimony complexes with the general formula $[Sb_2Cl_2\{\mathbf{RC4}\}]$ (R = H, ^{t}Bu, allyl) was achieved by the reaction of fully deprotonated calix[4]arenes with two equivalents of $SbCl_3$ (Scheme 1.9). The antimony complexes are air and moisture sensitive and have limited solubility in most organic solvents, but they can be analyzed in solution if DMSO is used.

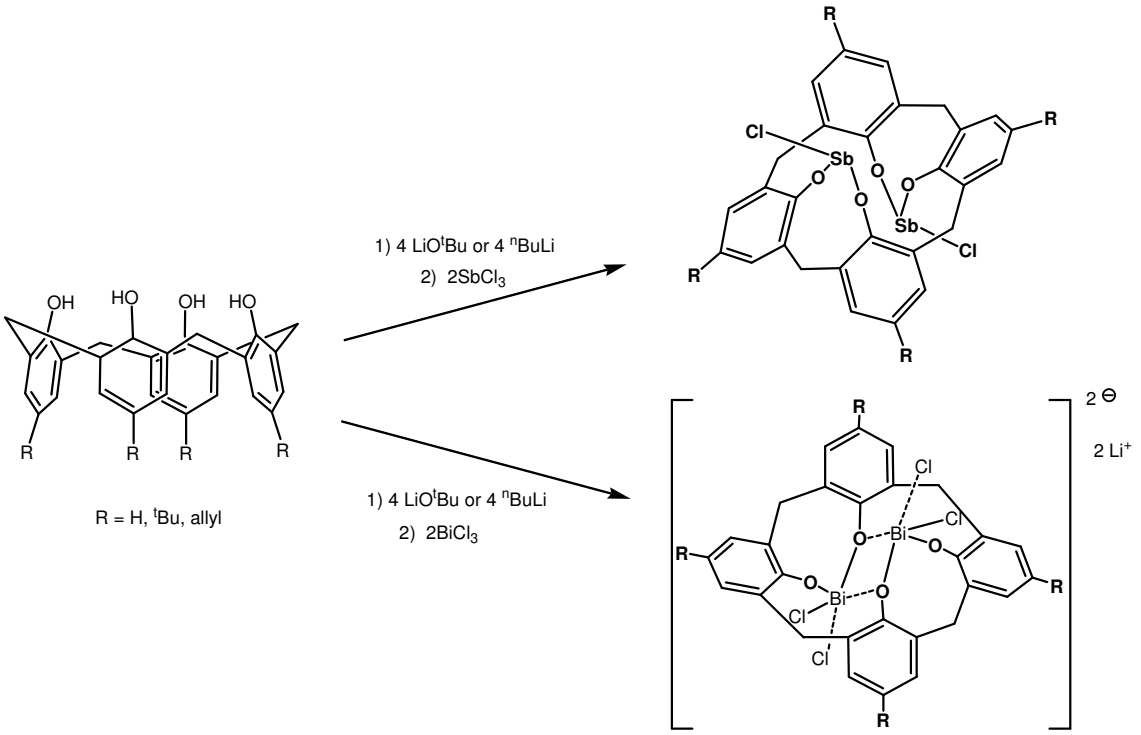

Scheme 1.9 Synthesis of calix[4]arene bismuth and antimony complexes.[58]

If the same synthetic pathway is applied to prepare the analogous bismuth complexes, the results are surprisingly different (Scheme 1.9). As in the case of the antimony complexes, the calixarene:metal ratio in the bismuth products is 1:2, but in this case no neutral complexes were obtained. Rather, the dianionic $[Bi_2Cl_4\{\mathbf{RC4}\}]^{2-}$ species are formed. The calixarene rings are in 1,2-alternate conformations and the bismuth centers contain two terminal Bi-Cl bonds. The overall neutrality of these complexes is maintained by the presence of two solvated lithium cations.

Our interest in preparing monometallic bismuth and antimony complexes led us to explore the chemistry of the alkyl-substituted calix[4]arenes. Based on the 1,2-disubstitution observed in the Bi^{III} and Sb^{III} calix[4]arene complexes above, we considered the 1,2-alkylsubstituted calix[4]arenes as possible ligands. When the 1,2-dibenzyl calix[4]arene [$\mathbf{HC4(Bn)_2(H)_2}$] was treated with two equivalents of NaO^tBu and one equivalent of $BiCl_3$ or

reacted with one equivalent of bismuth *tert*-butoxide, the monometallic [Bi(X){**HC4(Bn)$_2$**}] complex was obtained (equation 1.7).[58]

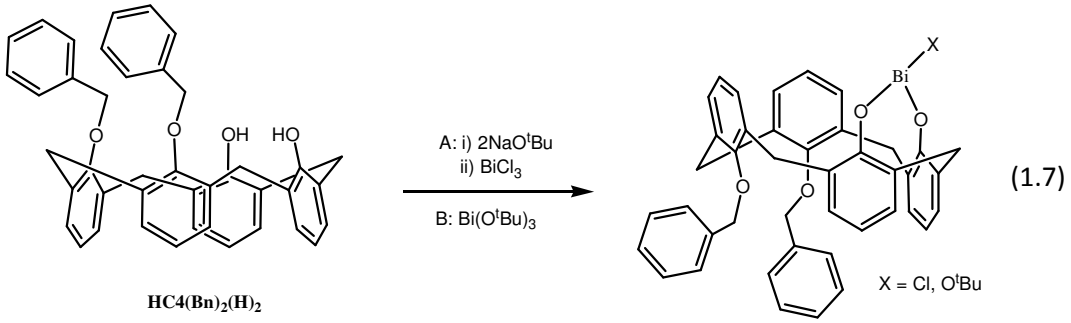

HC4(Bn)$_2$(H)$_2$ (1.7)

With the observation that in all the Bi^{III} and Sb^{III} complexes synthesized so far, the preferred ratio of oxygen atoms per metal center is 2:1, we decided to employed this synthetic strategy for the preparation of calix[8]arene complexes. Therefore, when the octalithium salt of **^{t}BuC8(H)$_8$** was reacted with four equivalents of $BiCl_3$ a complex with $[(BiCl_2)_4(\mu\text{–}Cl)_2\{Li_6\cdot$**^{t}BuC8**$\}]\cdot 4THF\cdot 7DME$ composition was obtained after recrystallization by diffusion of hexanes into a concentrated THF/DME (1:2 ratio) solution (Figure 1.8).[58]

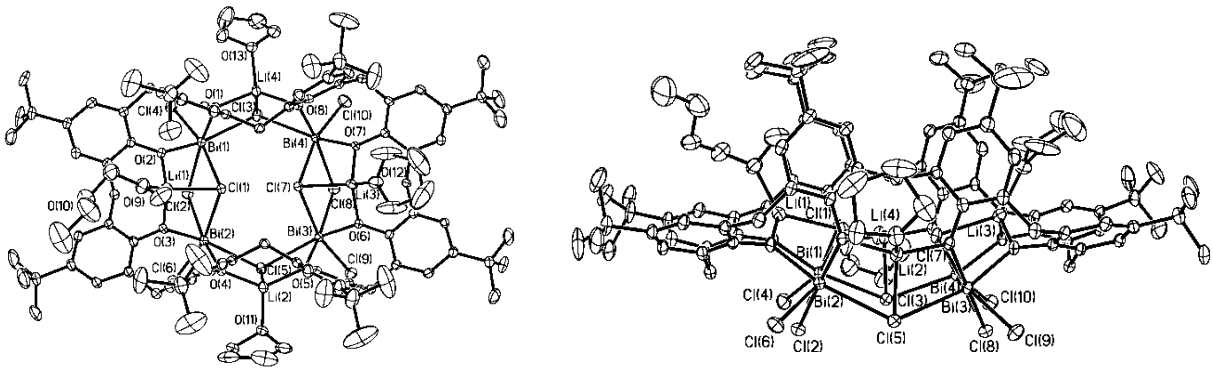

(A) (B)

Figure 1.8 ORTEP diagram of complex $[(Bi(\mu_3\text{-}Cl)Cl)_4(\mu\text{–}Cl)_2\{Li_4\cdot$**^{t}BuC8**$\}]^{2-}\cdot 3THF\cdot DME$ (anionic part). The ellipsoids are shown at 30% probability. Top view (A), side view (B).[58]

Complex $[(BiCl_2)_4(\mu\text{–}Cl)_2\{Li_6\cdot$ **^{t}BuC8**$\}]\cdot 4THF\cdot 7DME$ is extremely air and moisture sensitive.

1.3.2.2 Molybdenum complexes

The chemistry related to the synthesis of molybdenum(VI) calixarenes has been more developed in comparison to that for bismuth or antimony. Several research groups have been interested in the synthesis of such complexes due to their potential "as models of heterogeneous metal oxide catalyst surfaces, their capabilities of supporting organic transformations and their utility as building blocks for supramolecular structures."[59,60] The most common method for the preparation of molybdocalixarene complexes involves the reaction of parent calix[n]arenes (n = 4, 6, 8) with amino- or imido-molybdenum precursors.[51,61] Due to this synthetic pathway, a vast majority of molybdocalix[n]arene complexes found in literature often contain terminal Mo imido or Mo amino groups, while the number of reported oxomolybdenum calixarene complexes is still very limited.

Some interesting examples of terminal oxo complexes include the dioxomolybdenum(VI) dimethylcalixarene (**A**),[62] and other monooxomolybdenum(VI) calixarenes of the **B** type (Fig. 1.9).[52,63,64]

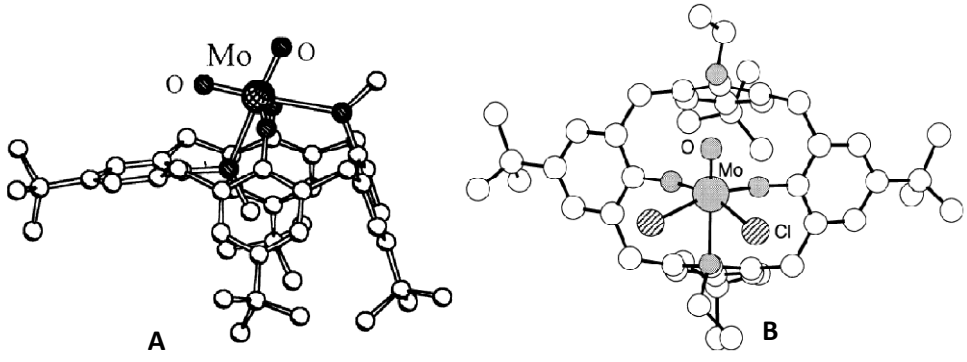

Figure 1.9 Examples of monometallic monooxo (**A**)[62] and dioxo molybdenum(VI) calix[4]arene complexes (**B**).[63]

Our interest in the preparation of monometallic molybdenum calixarene complexes containing terminal Mo=O groups prompted us to search for a methodology that could favor the presence of such moieties. As previously mentioned, we have shown that deprotonated calixarenes (calixanions) are excellent precursors for the synthesis of metallocalixarenes that were inaccessible by using the traditional parent calixarene as precursor (first reported calixarene antimony complex).[57] We therefore expected that the use of calixanions as precursors for the synthesis of oxomolybdocalixarenes could be an interesting alternate preparation.

When the Rcalix[4]arene monoanions (R = H, ^{t}Bu, allyl) were treated with one equivalent of MoO_2Cl_2, monooxo complexes of the type [MoO{**RC4**}]were obtained in moderate yields according to equation 1.8.[65]

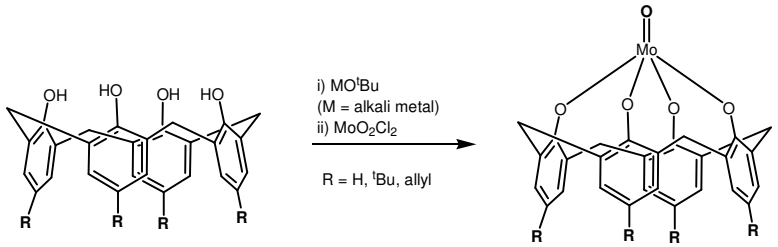

(1.8)

Complex [MoO{^{t}**BuC4**}] was previously synthesized by Floriani et al. using parent calixarene with $MoOCl_4$, but their methodology failed for the synthesis of the analogous [MoO{**HC4**}].[52]

When the Rcalix[4]arene ligands were treated with two or three equivalents of a strong alkali metal base followed by the addition of MoO_2Cl_2, a mixture of Mo monooxo, Mo dioxo, and unreacted calixarene was obtained. However, if 4 equivalents of the strong base and MoO_2Cl_2 were added, complexes of the type [MoO_2{M_2·**RC4**}] (M = alkali metal, R = H, ^{t}Bu) were obtained. During the synthesis of this large series of Mo dioxo complexes, it was observed that the alkali metal and the group in the *para* position of the ligand affected the structure of the final [MoO_2{M_2·**RC4**}] products.[65]

In the case of **HC4(H)$_4$**, the reaction of Li_4·**HC4** with MoO_2Cl_2 in THF produced the complex [MoO_2{Li_2·**HC4**}] in 58% yield (equation 1.9).

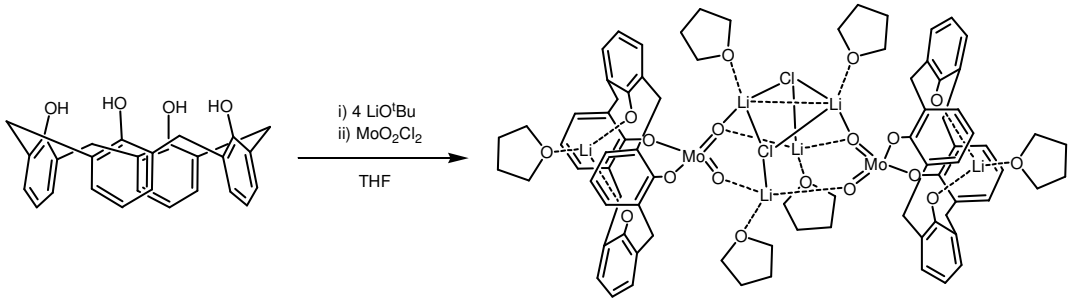

(1.9)

When the analogous reactions were carried out using M_4·**HC4** (M = Na, K) precursors (obtained from **HC4(H)$_4$** and 4MO^{t}Bu), the respective [MoO_2{Na_2·**HC4**}] complex was obtained only in 30% yield, while the isolation of the [MoO_2{K_2·**HC4**}] complex was unsuccessful. It was necessary to generate K_4·**HC4** by reacting **HC4(H)$_4$** with metallic K to produce the [MoO_2{K_2·**HC4**}] complex in 63% yield (equation 1.10).

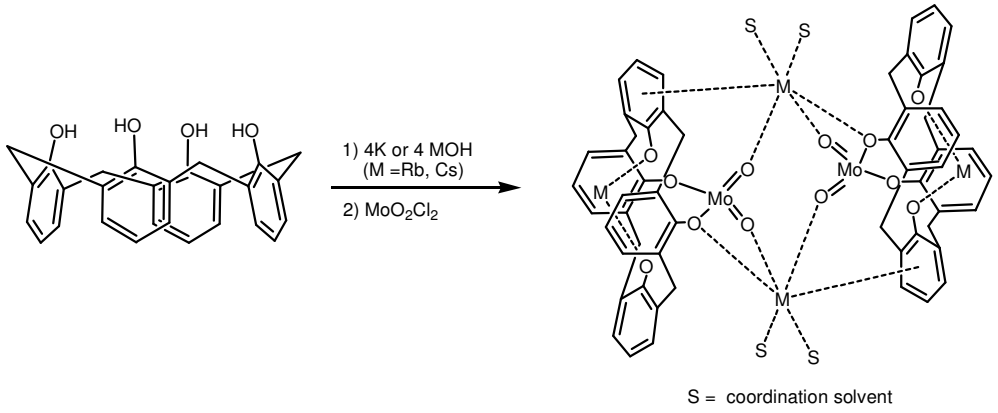

(1.10)

For the heavier Rb and Cs metals, the use of MO^{t}Bu for the preparation of the M_4·**HC4** precursor yielded, after the addition of MoO_2Cl_2, a mixture of at least three products that were hard to isolate. In this case, the [MoO_2{M_2·**HC4**}] complexes (M = Rb and Cs) were achieved by the treatment of **HC4(H)$_4$** with 4 equivalents of MOH·H_2O and MoO_2Cl_2 using a mixture of tetrahydrofuran (THF) and toluene (Eq. 1.10).

The reactivity of **^{t}BuC4(H)$_4$** is similar to that observed for **HC4(H)$_4$**. The [MoO_2{M_2·**^{t}BuC4**}] (M = Li, Na) complexes were obtained when **^{t}BuC4(H)$_4$** was treated with 4 equivalents of MO^{t}Bu and then with MoO_2Cl_2. Complex [MoO_2{K_2·**^{t}BuC4**}] can prepared following the method described above or by reacting the **^{t}BuC4(H)$_4$** with potassium metal and then with MoO_2Cl_2. For the preparation of the heavier [MoO_2{M_2·**^{t}BuC4**}] (M = Rb and Cs), the use of the MOH·H_2O base was only successful when M = Cs. In order to prepare the complex obtain [MoO_2{Rb_2·**^{t}BuC4**}] it was necessary to react **^{t}BuC4(H)$_4$** with 4 equivalents of Rb metal followed by the addition of MoO_2Cl_2.[65]

Most of the [MoO_2{M_2·**RC4**}] complexes described above are air and moisture sensitive and they usually have good solubility in most organic solvents.

From the discussion of section 1.3, it is evident that calixarenes are excellent ligands for the modeling of oxygen rich catalyst surfaces. It has been shown that bismuth or molybdenum can be attached to the calixarene either using the parent calixarene or calixanions as precursors, but we are still interested in improving some structural characteristics of our complexes. For example, all of our bismuth calix[4]arene complexes have a 2:1 metal/calixarene ratio, so the cavity is already saturated and unreacted OH groups are no longer present. The molybdenum Rcalix[4]arene complexes behave similarly by saturating the calixarene lower rim with one MoO_2^{2+} moiety and two alkali metals. These two series of complexes are interesting building blocks for our heterobimetallic model, but the lack of reactive OH groups makes it difficult to insert a second metal in the same calixarene framework. Our initial idea was to use the calixarene as a single oxo platform that could hold Bi and Mo simultaneously, but if the two metals cannot be attached to the same framework, the loss of the proximity between the two metals could affect the formation of M-O-M or M(μ–OR)M interactions.

The present dissertation work is focused on the design of mono- and bimetallic bismuth(III) and antimony(III) calixarene complexes that can be used as precursors for soluble Bi/Mo heterobimetallic models of the SOHIO process. Ideally the compounds should contain free OH groups on the ligand and/or labile terminal groups to facilitate the addition of oxo Mo^{VI} moieties to the same calixarene framework.

During our quest, we took advantage of the larger cavity size of the calix[n]arenes (n = 5-8) to prepare a series of Bi^{III} and Sb^{III} metallated complexes that displayed a broad structural diversity. We synthesized and used calix[n]anions (n = 5, 7) (Chapter 2) as metal precursors to obtain, for the first time, monometallic Bi^{III} and Sb^{III} calix[5]arene complexes containing free OH groups (Chapter 3). The use of parent calix[n]arenes (n = 6-8) as precursors led to the preparation of several complexes featuring mono- to tretranuclear structures (Chapter 4) while, with the aid of mono-silylated calix[5]arenes, highly soluble Bi^{III} and Sb^{III} compounds were achieved (Chapter 5).

The reactivity of the monometallic or silylated Bi^{III} and Sb^{III} calixarene complexes was tested and successfully utilized in the synthesis of the first soluble M/Mo (M = Sb, Bi) heterometallic models supported by calixarene ligands (Chapter 6). Finally, as part of our studies on C-H activation (the rate determining step in the SOHIO process) observed in Bi^{III} bisphenolates, we have synthesized the analogous Sb^{III} complexes and discovered that they are able to undergo C-H bond activations under similar reaction conditions (Chapter 7).

CHAPTER 2

ALKALI METALLATED CALIXARENES

2.1 Introduction

The base-induced condensation of *para*-substituted phenols and formaldehyde produces the calixarene series (Fig 2.1), macrocyclic compounds available in a variety of ring sizes.[66]

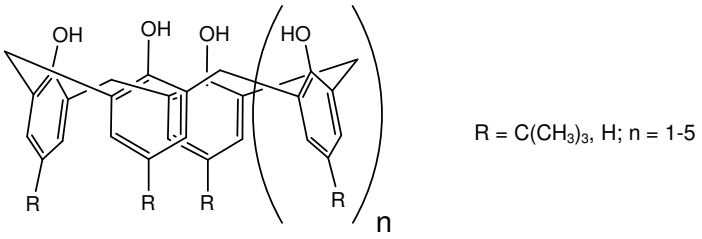

Figure 2.1 General representation of calix[4,5,6,7,8]arenes.

The cyclic framework of calixarenes, together with the presence of phenol oxygen donor atoms, promotes the complexation of metal atoms, while the hydrophobic cavity allows the inclusion of charged and neutral organic guests.[47,53,67,68] The relative facility with which calixarenes can be partially or totally functionalized at the upper or lower rims, coupled with their easy large-scale synthesis, at least for the even members of the series (n = 4, 6 or 8), has opened further perspectives for their use in supramolecular chemistry.[69] In particular, the hard acid character of the lower rim makes calixarenes interesting potential ligands for the complexation of transition metal elements.[61]

Deprotonated calixarene derivatives, "calixanions", have attracted interest in a number of fields. Calixanions, for example, have been utilized in organic and organometallic chemistry as precursors for functionalized complexes. Their extensive structural variety includes monomeric units and layered solid state structures, similar to clays.[49,50,70-72] The discovery that the parent

calixarenes effect the transport of alkali metal ions in water/organic solvent/water membrane systems has led to particular interest in mono-deprotonated calixanions.[68]

In the last two decades, considerable attention has been devoted to the chemical modification of the "major" even membered calix[n]arenes (n = 4,6,8), due to their ease and high yielding syntheses.[50,51,70,72,73] More recently, as a consequence of the improvements in their syntheses, significant progress has also been made in the odd membered calix[n]arenes (n = 5,7,9).[48,61,70]

Among the calix[*n*]arene anions reported in literature those for *n* = 4 are the most well represented.[74-77] In 2003 our group described the synthesis of a large series of mono- and dianionic calix[n]arene (n = 4, 6, 8) alkali metal salts,[74,75] observing that the size and nature of the alkali metal have a very important role in the conformation and the characteristics of the calixanions obtained. Solid state structures for monoanionic species [Li·**HC4(H)$_3$**, Na·**HC4(H)$_3$**, Rb·**HC4(H)$_3$**, and Cs·**HC4(H)$_3$**] exhibit the cone conformation while the dianionic species [e.g. M_2·**HC6(H)$_4$** (M = K, Rb, Cs)] contain calixarenes in a flattened 1,2,3-alternate conformation (Figure 2.2).

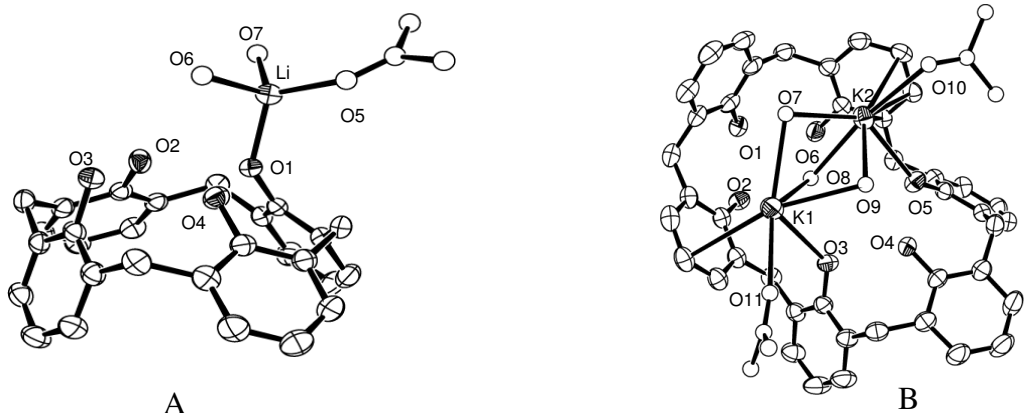

Figure 2.2 X-ray structures of [Li·**HC4(H)$_3$**]·2$(CH_3)_2$CO (**A**) and [K_2·**HC6(H)$_4$**] ·3H_2O·2$(CH_3)_2$CO (**B**) presenting cone and 1,2,3-alternate conformations, respectively.

We also demonstrated the utility of calix[4]anions as an entry into both main-group (the first antimony calixarene,[57] and transition metal calixarene complexes[65] that were inaccessible using the traditional parent calixarene as precursor.

Information about *para-tert*-butylcalix[5]arene [**^{t}BuC5(H)$_5$**] and *para-tert*-butylcalix[7]arene [**^{t}BuC7(H)$_7$**] anions, in contrast, is very limited. Titration of **^{t}BuC5(H)$_5$** with Et_3N in acetonitrile provided the spectrophotometric determination of the first two pK_a values of the calixarene ammonium salt (pK_{a1}= 11.5 ± 0.7; pK_{a2} = 15.4 ± 1.0).[78] This data led to the preparation of trianionic precursors and the further isolation of calix[5]arene lanthanide(III) complexes.[78] Gutsche and coworkers reacted **^{t}BuC5(H)$_5$** and $KHCO_3$ in a 1:1 ratio to generate the potassium monoanionic salt of **^{t}BuC5(H)$_5$** *in situ*. This K·**^{t}BuC5(H)$_4$** salt was used as precursor for the preparation of lower rim monosubstituted derivatives of **^{t}BuC5(H)$_5$**. No isolation or characterization of the monoanion salt was performed.[79] Pentaalkyl ester derivatives of *p*-benzylcalix[5]arene [**BnC5(H)$_5$**] were synthesized by Asfari and coworkers from the reaction of **BnC5(H)$_5$** with an excess of K_2CO_3 (to produce the anion precursor), followed by addition of the alkylating agent to yield the desired substituted calixarene.[80]

Some metallocalixarenes have been also obtained by the use of **^{t}BuC5(H)$_5$** anionic salt precursors in one-pot reactions. An unsymmetrical dimeric 1:1 K/Ti complex was achieved by the reaction of **^{t}BuC5(H)$_5$** with potassium followed by [Ti(acac)(OPr^{i})$_2$].[81] The solid state structure showed a central Ti-O-Ti core with an encapsulated K^+ ion on each calix[5]arene unit (Figure 2.3).

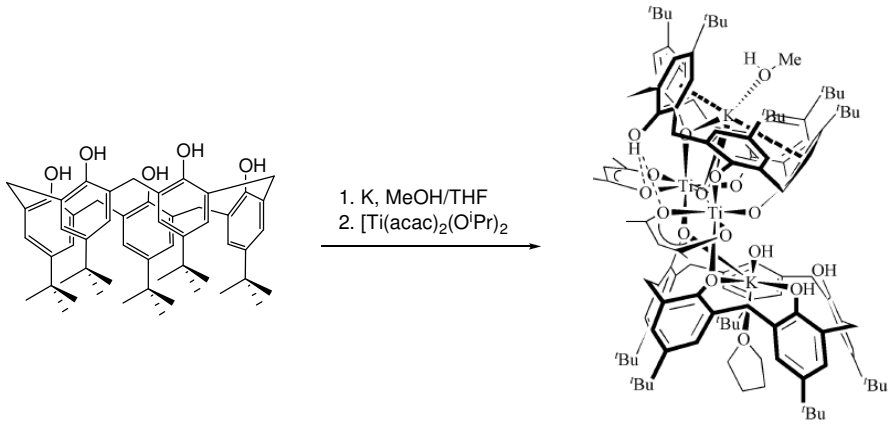

Figure 2.3 Synthesis of the heterobimetallic Ti/K calix[5]arene complex.

The crystal structures of the Na^+ and Rb^+ salts of a functionalized calix[5]arene were obtained by McKervey and coworkers during extraction studies of chemically modified calix[5]arenes.[82] No crystal structures of lithium or cesium salts of calix[5]arene have been reported.

The information related to deprotonated *p-tert*-butylcalix[7]arene [**^{t}BuC7(H)$_7$**] species is almost negligible. Neri and coworkers have *in situ* prepared alkali metallated calix[7]arene precursors employing K_2CO_3 as base, for the preparation of mono-, di-, tri-, tetra- and hepta-ether substituted compounds.[83] A similar procedure using KOH or Cs_2CO_3 allowed the preparation of doubly bridged calix[7]arene ligands.[84] (Scheme 2.1A).

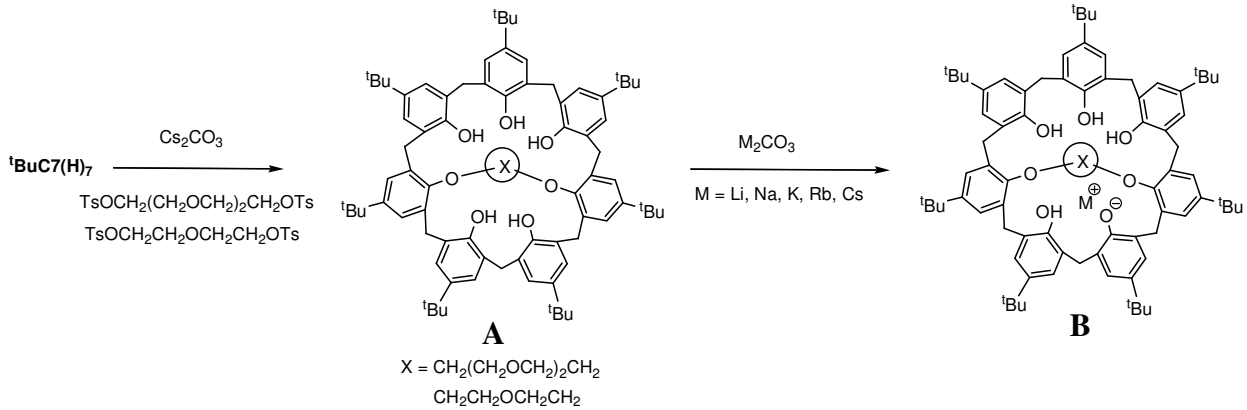

Scheme 2.1 Doubly bridged **^{t}BuC7(H)$_5$** ligands (**A**) and their alkali metallated complexes (**B**).

Gaeta and Neri reported the first examples of alkali metal salts of a 1,4-calix[7]-crown-4 obtained by the reaction of the ligand with M_2CO_3 (M = Li, Na, K, Rb and Cs). The complexes were characterized by ^{1}H NMR spectroscopy, however no X-ray structures were reported (Scheme 2.1B).[85] Hirata et al. performed some alkali metal extraction studies with the aid of ester derivatives of calix[n]arenes (n = 4-8) however no isolation of the products was achieved.[86]

Clearly the systematic isolation, study, and full characterization of the anionic salts of ^{t}**BuC5(H)$_5$** and ^{t}**BuC7(H)$_7$** are lacking. In most cases where ^{t}**BuC5** and ^{t}**BuC7** anions were prepared the level of deprotonation and conformation of the parent calix[n]arene remains ambiguous. We believe that if a controlled metallation in these calixarenes can be achieved, the affinity of the calixanion precursors to specific metal centers can be greatly enhanced. Therefore, in this chapter we describe the syntheses and characterization of the alkali metal salts of ^{t}**BuC5** mono-, di-, tri-, and pentaanions, and ^{t}**BuC7** mono- and dianions**.** The effects of base strength, alkali metal, and stoichiometry on the structure and deprotonation level of the calixarene ring will be discussed.

2.2 Results and discussion

2.2.1 Synthesis of *para-tert*-butylcalix[5]arene anions

2.2.1.1 Synthesis of monoanions

Alkali metal salts of monoanionic ^{t}**BuC5(H)$_5$** were obtained with several bases in 72-86% yields (Scheme 2.2). It is important to control the base stoichiometry and strength. Alkali salt monoanions are easily obtained from the reactions of ^{t}**BuC5(H)$_5$** with 1 equivalent of $MOC(CH_3)_3$ (M = Na, K), NaH, or with M_2CO_3 (M = Na, K). Reactions with $MOC(CH_3)_3$ and NaH are faster than the ones with M_2CO_3. The crude material is washed in pentane (or hexane)

and suitable X-ray quality crystals are obtained by the slow evaporation of the concentrated THF or MeCN solution.

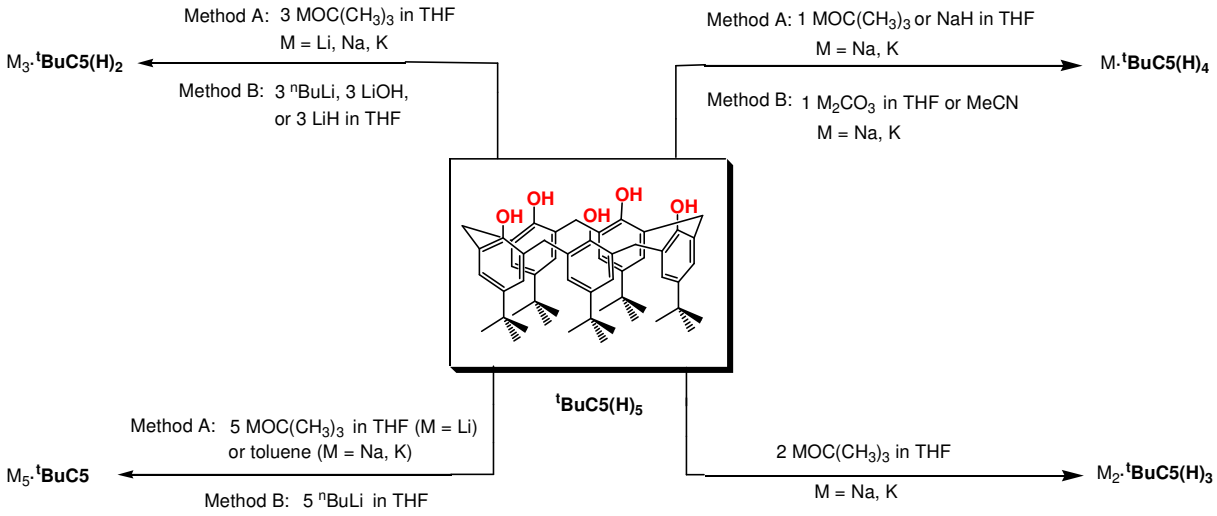

Scheme 2.2 Synthesis of *para-tert*-butylcalix[5]arene [^{t}**BuC5(H)$_5$**] anions.

As we previously reported, the reaction of calix[6]arene with one equivalent of M_2CO_3 leads to the preparation of calix[6]arene dianions.[74] For ^{t}**BuC5(H)$_5$**, when the reaction ratio of the M_2CO_3 (M = Na, K) salt was increased from 0.5 to 1-3 equivalents, the product obtained was surprisingly the monoanionic salt but in better yields. The best yield was obtained when using 1 equivalent of the carbonate salt (72-82% yield). These results could be due to the low solubility of the metal carbonates in THF or MeCN. In an attempt to produce the dianionic salts, we increased the solubility of the carbonates by using a mixture of C_6H_6/MeOH, however the reaction still yields the monoanionic salts of ^{t}**BuC5(H)$_5$**.

The synthesis of the lithium monoanion using Li_2CO_3 was unsuccessful due to its poor solubility (even in C_6H_6/MeOH). The use of 1 or two equivalents of LiH provides the monoanionic salt, however, we were able to reproduce this result only two times. Usually the reaction under those conditions yields a mixture of mono- and trianionic complexes and all our

attempts to optimize the reaction conditions failed. When present in mixture, the isolation of the monoanionic salt Li·^{t}**BuC5(H)$_4$** is unpractical because it decomposes readily in solution to the parent calixarene.

Most of the alkali metal salts of the ^{t}**BuC5(H)$_5$** monoanions are stable under air (no decomposition observed after two months) and they are moderately moisture stable. In all cases the preparation of the single crystals was performed under air.

2.2.1.2 Synthesis of dianions**.**

Although the treatment of ^{t}**BuC5(H)$_5$** with 1-3 equivalents of M_2CO_3 (M = Na, K) produced monoanions, we attempted to force the preparation of dianionic species by increasing the metal carbonate ratio from 4-5 equivalents. However, the results were unchanged yielding only monoanionic species. Alternatively, the use of 2 equivalents of stronger bases such as MH or MOH (M = Li, Na, K) yielded complex mixtures in all cases. It was necessary to treat ^{t}**BuC5(H)$_5$** with $MOC(CH_3)_3$ (M = Na, K) in a 1:2 ratio to produce the dianionic species M_2·^{t}**BuC5(H)$_3$** in good yields (92-96%) (Scheme 2.2). The products were purified by washing the crude product with pentane. X-ray quality crystals of the K_2·^{t}**BuC5(H)$_3$** salt could be obtained by slow evaporation of a THF and DMSO mixture (10:1 ratio). Stoichiometry in this reaction plays an important role since a small excess of the alkali *tert*-butoxide could afford a mixture of di- and trianionic salts. We attempted to synthesize the lithium dianion following the same strategy as for M_2·^{t}**BuC5(H)$_3$** (M = Na, K) using lithium *tert*-butoxide, however in all cases we observed the formation of the trianionic species Li_3·^{t}**BuC5(H)$_2$** in mixture with parent calixarene. Na_2·^{t}**BuC5(H)$_3$** and K_2·^{t}**BuC5(H)$_3$** are white powders, which after 4 days in air start to decompose to green powders (parent calixarene with insoluble alkali metal side products).

2.2.1.3 Synthesis of trianions**.**

The reported pK_a values of **^{t}BuC5(H)$_5$** (pK_{a1} = 11.5, pK_{a2} = 15.4),[78] suggested that the most suitable way to obtain the trianionic species would be the use of strong alkali metal bases. Indeed, we found that the use of alkali metal *tert*-butoxides easily yields the trianionic salts of **^{t}BuC5(H)$_5$** (Scheme 2.2)**.**

Reaction of **^{t}BuC5(H)$_5$** with $MOC(CH_3)_3$ or MOH (M = Li, Na, K) in a 1:3 ratio in THF at room temperature produces the respective trianionic salts. When $MOC(CH_3)_3$ was used, the products were easily isolated by crystallization of the crude material (71-97% yields); however isolation of the product was more difficult when MOH was used. LiH and ^{n}BuLi also produced the calixarene trianion even working with just 1 equivalent of base [the remaining product is unreacted **^{t}BuC5(H)$_5$**]. The use of 5 equivalents of LiH gave the best yield of Li_3·**^{t}BuC5(H)$_2$** (93%) while 3 equiv of Bu^{n}Li produced Li_3·**^{t}BuC5(H)$_2$** in 86% yield. The pure products are air stable white powders, but they start to decompose to parent **^{t}BuC5(H)$_5$** after 5 weeks in air.

2.2.1.3 Synthesis of pentaanions**.**

When **^{t}BuC5(H)$_5$** was treated in a 1:5 molar ratio with $MOC(CH_3)_3$ (M = Li, Na, K) or ^{n}BuLi the pentaanionic M_5·**^{t}BuC5** salts were obtained in 77-91% yields (Scheme 2.2). The selection of the right solvent is very important in these reactions. When **^{t}BuC5(H)$_5$** was treated with $MOC(CH_3)_3$ in THF, a mixture of Li_3·**^{t}BuC5(H)$_2$** and M_5·**^{t}BuC5** (M = Na, K) was obtained, however when the solvent was switched to toluene, pure M_5·**^{t}BuC5** was obtained. In a similar way when $LiOC(CH_3)_3$ was reacted with **^{t}BuC5(H)$_5$** in toluene a mixture of tri- and pentaanion was obtained. In this case THF was necessary for the preparation of pure product.

Attempts to synthesize tetraanionic salts $M_4 \cdot$ **^{t}BuC5(H)** by the reaction of **^{t}BuC5(H)$_5$** and $MOC(CH_3)_3$ (M = Li, Na, K) in a 1:4 ratio were unsuccessful, yielding a mixture of the tri- and pentaanionic salts of **^{t}BuC5(H)$_5$**.

2.2.2 Synthesis of *para-tert*-butylcalix[7]arene anions

2.2.2.1 Synthesis of mono- and dianions

The treatment of **^{t}BuC7(H)$_7$** with one equivalent of M_2CO_3 (M = Na, K, Rb, Cs) or MO^tBu (M = Na, K) yields the $M \cdot$ **^{t}BuC7(H)$_6$** anions in good yields (78-89%) (Scheme 2.3). The products are easily purified by washing the crude materials with 2x4 mL portions of pentane (or hexane) and single crystals can be obtained by slow evaporation of THF or MeCN solutions. Attempts to prepare the monoanions by using one equivalent of LiO^tBu or LiOH produced a mixture of several products (observed by ^{1}H NMR).

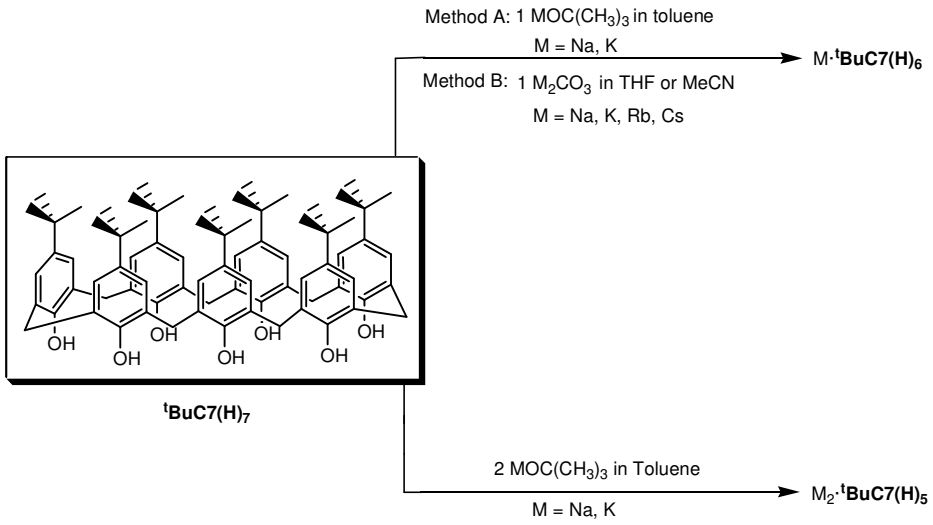

Scheme 2.3 Synthesis of *para-tert*-butylcalix[7]arene mono- and dianions.

The $M_2 \cdot$ **^{t}BuC6(H)$_4$** salts were obtained by reaction of the parent calixarene with one equivalent of M_2CO_3 (Na, K, Rb and Cs), however, for **^{t}BuC7(H)$_7$** the attempts to prepare $M_2 \cdot$ **^{t}BuC7(H)$_5$** salts utilizing 1-3 equivalents of M_2CO_3 were unsuccessful, yielding only

monoanions. It was necessary to treat **^{t}BuC7(H)$_7$** with two equivalents of MO^{t}Bu (M = Na, K) to obtain M_2·**^{t}BuC7(H)$_5$** in 82 and 76% yields, respectively. Dianions M_2·**^{t}BuC7(H)$_5$** (M = Na, K) were easily purified by washing the crude material with pentane or by diffusion of pentane into a concentrated THF solution. Attempts to prepare Li_2·**^{t}BuC7(H)$_5$** using 2 equivalents of LiO^{t}Bu produced a complex mixture. As already observed in **^{t}BuC5(H)$_5$**, the smaller lithium ion size probably favors the production of multi-deprotonated species (M > 2). Both calix[7]arene mono- and dianions are air stable in solid state, but they start to release the parent calixarene after three weeks in air.

The use of strong bases such as MO^{t}Bu or MOH (Li, Na, K) allowed us to prepare tri- and pentaanionic species for the **^{t}BuC5(H)$_5$** ligand. Following this methodology, we performed the reaction of **^{t}BuC7(H)$_7$** with three equivalents of MO^{t}Bu or MOH (M = Li, Na, K) at room temperature. The ^{1}H NMR spectra in all cases displayed more complex patterns than those observed for the calix[7]arene mono and dianionic species. This observation suggested multi-deprotonation in the lower rim; however, the isolation of the products was unpractical due to their fast decomposition in solution to parent **^{t}BuC7(H)$_7$**.

2.2.3 NMR spectroscopy

^{1}H NMR spectroscopy is a powerful tool for the study of the spectral patterns of the calixarene conformations while the VT NMR technique can be used to determine inversion rates.

The room temperature ^{1}H NMR spectra for the mono- (Figure 2.4) and dianionic salts (Figure 2.5) show similar patterns. The chemical shifts for aromatic protons in all mono- and dianionic salts shift upfield to 6.91-7.22 ppm in $CDCl_3$ as sharp singlets integrating to 10 and 14 protons for **^{t}BuC5(H)$_5$** and **^{t}BuC7(H)$_7$**, respectively. The methylene region shows two broad signals between 4.37 and 2.85 ppm in the case of Na·**^{t}BuC5(H)$_4$**, Na_2·**^{t}BuC5(H)$_3$** and

$M_2 \cdot$ **^{t}BuC7(H)$_5$** when M = Na, K. One broad signal between 3.86 and 3.76 ppm is observed for $K \cdot$ **^{t}BuC5(H)$_4$**, $K_2 \cdot$ **^{t}BuC5(H)$_3$** and $M \cdot$ **^{t}BuC7(H)$_6$** (M = Na, K, Rb, Cs). The broadness of the methylene signals indicates fluxionality of the complexes in solution.[87] The *tert*-butyl resonances in all mono- and dianionic salts appear as sharp singlets between 1.17 and 1.25 ppm.

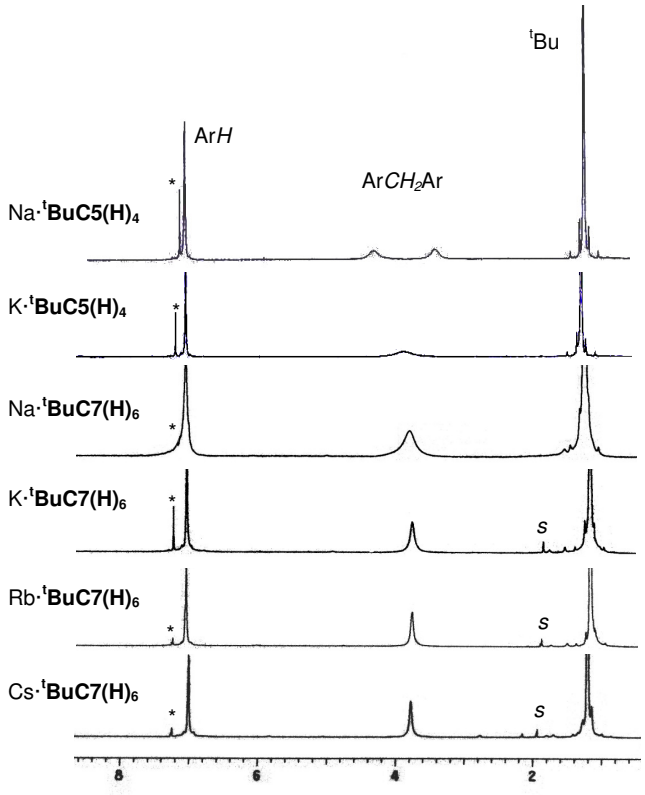

Figure 2.4 ^{1}H NMR spectra of alkali metal salts of the monoanionic **^{t}BuC5(H)$_4$** and **^{t}BuC7(H)$_6$** complexes in *$CDCl_3$. *s* = residual solvent.

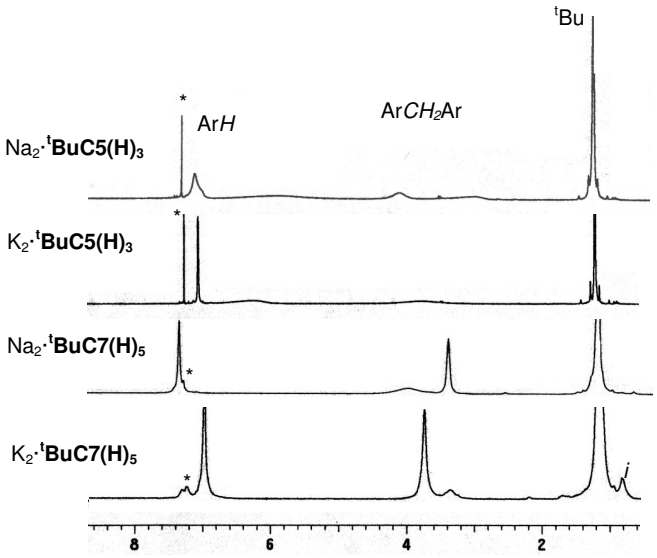

Figure 2.5 ^{1}H NMR spectra of alkali metal salts of the dianionic ^{t}**BuC5(H)$_3$** and ^{t}**BuC7(H)$_5$** complexes in *$CDCl_3$. *i* = impurity.

The behavior of the OH groups for the mono- and dianionic salts has strong dependence on the solvent, alkali metal and calixarene size. Signals for OH groups in the monoanions, for example, are only observed for the K·^{t}**BuC5(H)$_4$** salt (located at 8.66 ppm) when the NMR spectra are taken in $CDCl_3$ at room temperature. The OH groups for the Na·^{t}**BuC5(H)$_4$** and M·^{t}**BuC7(H)$_6$** (M = Na, K, Rb Cs) salts in this solvent are too broad to be observed at room temperature. In the case of the dianions, OH signals are only found for the K_2·^{t}**BuC5(H)$_3$** salt (at 13.6 ppm) when the solvent used is $CDCl_3$, however if we change the NMR solvent from $CDCl_3$ to DMSO-d_6, the OH signals for Na_2·^{t}**BuC5(H)$_3$** and K_2·^{t}**BuC5(H)$_3$** can be located at 15.38 and 15.15 ppm, respectively. This NMR behavior highlights the previously observed [in even numbered calix[n]arene salts (n = 4, 6, 8)] influence of the solvent polarity on the rate of conformational inversion of calixanions.[74]

^{13}C NMR spectra of all the mono and dianionic salts show four peaks for the aromatic carbons, one peak for the methylene groups and two peaks for *tert*-butyl groups. In the ^{13}C spectra the signals at about 34 ppm are assigned to the Ar*CH$_2$*Ar groups. The simplicity of the ^{1}H

NMR, and the single methylene peak in the ^{13}C spectra for the mono and dianionic salts, are typical of cone structures in the solution state, consistent with the solid state structures (*vide infra*).[79]

The ^{1}H NMR spectra of the trianionic salts of **^{t}BuC5(H)$_2$** (Figure 2.6) show patterns that are very different from those observed in the mono- and dianionic salts. In the case of the potassium trianion K_3·**^{t}BuC5(H)$_2$** the aromatic protons are present as a single peak at 7.69 ppm, while the Ar*CH*$_2$Ar protons show two doublet signals at 3.45 and 4.29 ppm. The presence of this pair of doublets indicates a loss in fluxionality of K_3·**^{t}BuC5(H)$_2$** in comparison with mono and dianionic salts. The *tert*-butyl group appears as a singlet at 1.51 ppm. The ^{13}C NMR spectrum shows four signals for aromatic carbons, one for methylene and two for *tert*-butyl groups. This NMR pattern is consistent with a cone conformation of K_3·**^{t}BuC5(H)$_2$** in solution.

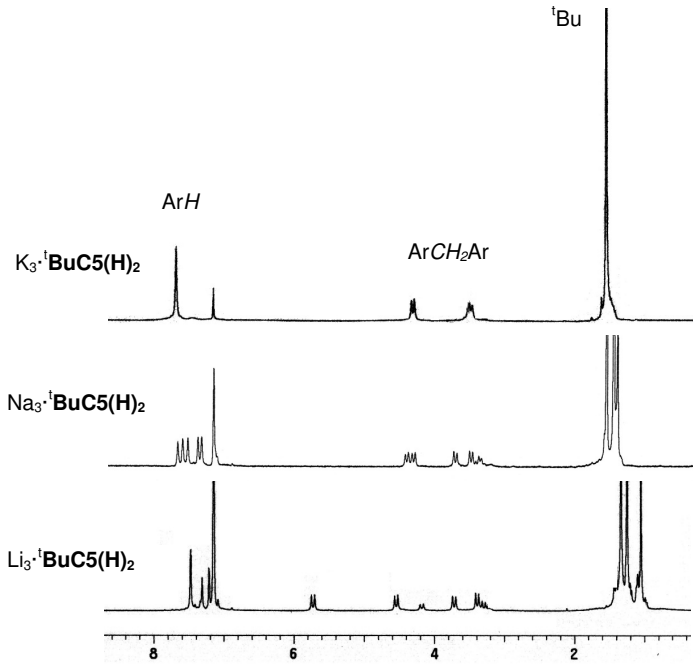

Figure 2.6 ^{1}H NMR spectra of alkali metal salts of the trianionic **^{t}BuC5(H)$_2$** complexes in C_6D_6.

The spectra of the lithium and sodium trianionic salts are more complex. The $Li_3 \cdot$ **^{t}BuC5(H)$_2$** salt shows three sharp singlets from 7.22-7.48 ppm in the aromatic area, while $Na_3 \cdot$ **^{t}BuC5(H)$_2$** exhibits five singlets from 7.33-7.67 ppm. Both the lithium and sodium salts produce six doublets (geminal coupling due to nonequivalent methylene hydrogens) for the methylene protons with two doublets being half the intensity of the others. This spectrum is a good indication of an overall C_s symmetry for the molecule and a probable 1,2 or 1,3-alternate, or partial cone conformation.[79] The *tert*-butyl area shows three singlet peaks in a 2:2:1 ratio probably due to the fact that the three alkali metals in the ring restrict the free rotation of phenolic groups in the annulus. ^{13}C spectra of reliable quality for $M_3 \cdot$ **^{t}BuC5(H)$_2$** (M = Li, Na) were not possible to aquire due to insufficient solubility.

The solution ^{1}H NMR spectra of pentaanionic **^{t}BuC5** salts are very similar (Figure 2.7). All of them show a single peak for aromatic protons, one *tert*-butyl peak and a pair of sharp doublets in the methylene area. The simplicity and sharp peaks in NMR permit the solution structures to be assigned as cone conformation.

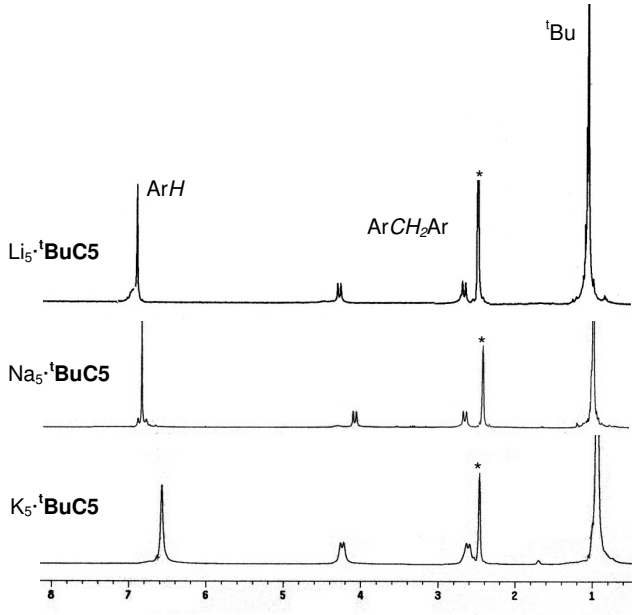

Figure 2.7 ^{1}H NMR spectra of the pentaanionic **^{t}BuC5** complexes in *DMSO-d_6.

2.2.4 Conformational studies.

^{t}BuC5(H)$_5$ resembles calix[4]arene with four basic conformations (cone, partial cone, 1,2-alternate, 1,3-alternate), but generally inverts more easily due to its wider annulus.[79] For the larger **^{t}BuC7(H)$_7$** the possibilities for conformational exchange increase notably, therefore the assignment of a ring conformation is less accurate.

Variable temperature ^{1}H NMR spectra for the salts M·**^{t}BuC5(H)$_4$** and M_2·**^{t}BuC5(H)$_3$** (M = Na, K,) led to their coalescence temperatures, and the energies ($\Delta G^{\pm}$) for the conformational interconversion were calculated (Table 2.1).

Table 2.1 Coalescence Temperatures at 300 MHz and Free Energies of Activation for the Conformational Inversion of M·**^{t}BuC5(H)$_4$** and M_2·**^{t}BuC5(H)$_3$** (M = Na, K) Anions.

Compound	T_c/^{o}K	$\Delta\nu$/ (±15) Hz	$\Delta G^{\pm}$/ (±0.4) kcal mol^{-1}
^{t}BuC5(H)$_5$	271		13.2
Na·**^{t}BuC5(H)$_4$**	276	280	12.6
K·**^{t}BuC5(H)$_4$**	278	184	12.9
Na_2·**^{t}BuC5(H)$_3$**	323	182	15.1
K_2·**^{t}BuC5(H)$_3$**	291	224	13.4

2.2.4.1 Inversion Energies.

The room temperature ^{1}H NMR spectrum of **^{t}BuC5(H)$_5$** exhibits a broad peak close to coalescence for the methylene groups that bridge the arene units (ArCH_2Ar), indicating that the two types of protons of the cone conformer are exchanging environments on the NMR time scale. We also observe a single broad signal in the room temperature NMR spectra of the salts K·**^{t}BuC5(H)$_4$** and K_2·**^{t}BuC5(H)$_3$**, but the spectra of Na·**^{t}BuC5(H)$_4$** and Na_2·**^{t}BuC5(H)$_3$** show a pair of broad signals. The calixanions are likewise in cone conformation, but the inversion is slightly less rapid in M·**^{t}BuC5(H)$_4$** and M_2·**^{t}BuC5(H)$_3$** (M = Na) than in the parent molecule.

The M·**^{t}BuC5(H)$_4$** salts (M = Na, K) have similar $\Delta G^{\pm}_{inv}$ values to that of the parent calixarene. This result is surprising since it was expected that the presence of an alkali metal in

the calixarene would increase the rigidity of the ring, as previously observed for **HC4(H)$_4$**, **HC6(H)$_6$** and **^{t}BuC6(H)$_6$**.[74]

Likewise, we expected that two metals in the cavity would lead to much higher $\Delta G^{\pm}_{inv}$ values for the dianionic salts compared to that of the parent calixarene. The data, however, show that the $K_2\cdot$**^{t}BuC5(H)$_3$** salt has a $\Delta G^{\pm}$ value similar to those of parent calix[5]arene and the monoanionic salts. The $Na_2\cdot$**^{t}BuC5(H)$_3$** salt is the only dianion showing a higher $\Delta G^{\pm}$ value (15.1±0.4 kcal mol^{-1}), indicating less conformational mobility and a probable dimeric structure (as observed in the solid state).

All of the energy differences are rather small, though, and we have noted other factors that influence the ^{1}H NMR patterns of the salts. Water or residual solvent leads to changes in the methylene area, probably due to interactions with either the cation or phenol groups of the calixarene. The high solvent sensitivity could be a reason for the unexpected values observed in our VT-NMR studies.

2.2.5 Crystal structures of the calixanions

The crystal structures of M·**^{t}BuC5(H)$_4$** (M = Na, K), M·**^{t}BuC7(H)$_6$** (M = K, Rb), $K_2\cdot$**^{t}BuC5(H)$_3$**, and $M_3\cdot$**^{t}BuC5(H)$_2$** (M = Li, Na) were obtained. To our knowledge these are the first reported examples of solid structural characterization for **^{t}BuC5(H)$_5$** and **^{t}BuC7(H)$_7$** anions. Bond distances and angles fall within normal parameters, as can be seen from Table 2.2.

Table 2.2 Selected M-O and M-C distances of Alkali Metal Salts of Calixanions

Compound	M-O (OAr)/ Å	M-O (solvate)/ Å	M-C/ Å[a]	Ref
Monoanions				
- ***Na*** *salts*				
[Na·^{t}**BuC5(H)$_4$**·THF]$_2$	2.336(2)-2.973(2)	2.332(3)		b
[Na·**HC4(H)$_3$**]$_2$·3Me$_2$CO	2.305(6)-2.359(6)	2.217(6)-2.441(7)		74
[Na·**HC4(H)$_3$**]$_2$·3Me$_2$CO	2.284(5)-2.337(5)	2.206(6)-2.394(5)		88
[Na·^{t}**BuC5(H)$_4$**·MeCN]$_2$	2.325(3)-2.696(3)			b
- ***K*** *salts*				
K·^{t}**BuC5(H)$_4$**·MeCN	2.670(2)-2.974(2)		3.355(3)-3.390(3)	b
K·^{t}**BuC5(H)$_4$**·2MeCN	2.751(6)-2.784(6)	2.750(8)	3.375(8)-3.505(8)	b
K·**HC4(H)$_3$**·1.5H$_2$O·THF	2.743(3)-2.893(2)	2.656(4)-2.845(3)	3.286(3)-3.515(3)	75
K·^{t}**BuC4(H)$_3$**·4THF	3.042(13)-3.160(12)	2.648(13)-2.728(11)		75
[K·^{t}**BuC4(H)$_3$**·2THF·H$_2$O]$_2$	2.737(2)-2.935(2)	2.694(2)-2.733(2)		75
- ***Rb*** *salts*				
Rb·^{t}**BuC7(H)$_6$**·2MeCN·H$_2$O	2.858(3)-2.893(3)	2.844(4)	3.476(4)-3.539(5)	b
Rb·^{t}**BuC4(H)$_3$**·4THF	3.124(2)	2.796(2)		74
Rb·**HC4(H)$_3$**·THF	2.943(3)	2.7770(17)	3.349(3)-3.579(3)	74
- ***Cs*** *salts*				
Cs·**HC4(H)$_3$**·Me$_2$CO	3.100(3)	2.959(3)	3.599(3)-3.840(3)	74
Cs·**HC4(H)$_3$**·pyridine	3.169(12)-3.704(16)		3.53(1)-4.17(1)	88
Cs·**HC4(H)$_3$**·H$_2$O	3.065(5)-3.673(5)	2.97(3)	3.530(7)	88
Cs·^{t}**BuC4(H)$_3$**·MeCN	~4.0		3.545(3)-3.961(3)	89
Cs·**HC6(H)$_5$**·Me$_2$CO	3.073(12)-3.535(15)	2.99(2)	3.416(15)-3.886(16)	74
Dianions				
[K$_2$·^{t}**BuC5(H)$_3$**·4DMSO]$_2$	2.655(8)- 2.838(8)	2.587(9)- 2.776(9)		b
K$_2$·**HC6(H)$_4$**·2Me$_2$CO	2.805(2)-3.056(3)	2.699(3)-2.981(3)	3.214(3)-3.713(3)	74
K$_2$·**HC6(H)$_4$**·5MeOH	2.64(1)-2.94(1)	2.74(1)-2.91(1)	3.28(2)-3.96(2)	90
Rb$_2$·**HC6(H)$_4$**·2Me$_2$CO	2.986(2)-2.999(3)	2.835(4)-3.095(4)	3.304(4)-3.731(4)	74
Cs$_2$·**HC6(H)$_4$**·2Me$_2$CO	2.975(12)-3.000(8)	2.853(10)-3.093(9)	3.301(13)-3.728(13)	74
Trianions				
[Li$_3$·^{t}**BuC5(H)$_2$**·3THF·H$_2$O]$_2$	1.887(10)-2.000(11)	1.836(16)-2.001(11)	2.700(17)	b
[Li$_3$·^{t}**BuC5(H)$_2$**·2THF·2H$_2$O]$_2$	1.905(7)- 2.064(8)	1.872(8)-1.995(10)	2.677(10)- 2.686(11)	b
[Na$_3$·^{t}**BuC5(H)$_2$**·2THF]$_2$	2.211(3)-2.995(4)	2.245(4)-2.262(6)	2.739(4)- 3.031(4)	b
Na$_3$·^{t}**BuC5(H)$_2$**·THF·4DMSO	2.290(4)-2.737(3)	2.251(3)- 2.409(3)	2.979(6)	b

[a]Distances for cation-π arene interactions. [b]This work.

2.2.5.1 Metal-oxygen versus metal-carbon (π-cation) interactions.

The ^{t}**BuC5(H)$_5$** and ^{t}**BuC7(H)$_7$** series allows us to examine the relative affinities of each metal for interaction with the phenolic oxygens on the calixarene lower rim versus π-cation interactions with the arene rings within the cavity. A combination of these effects determines the following structure types:

a) *Discrete monomeric units*. K·^{t}**BuC5(H)$_4$**·MeCN (Figure 2.8) exhibits a monomeric structure with coordination of the potassium atom to three phenolic oxygens in the calixarene

ring and one acetonitrile molecule. The conformation of the calixarene unit is flattened cone due to M-C π interactions. The M·^{t}**BuC7(H)$_6$**·2MeCN·H_2O (M = K, Rb) complexes also exhibit monomeric structures (Figures 2.9 and 2.10, respectively) with the calixarene ligand in distorted cone conformation and the metal centers displaying η^6-coordination with the ring **A**. The crystal structures are consistent with the ^{1}H NMR patterns observed in solution. In all these complexes the presence of bulky *tert*-butyl groups block the formation of polymeric structures.[88]

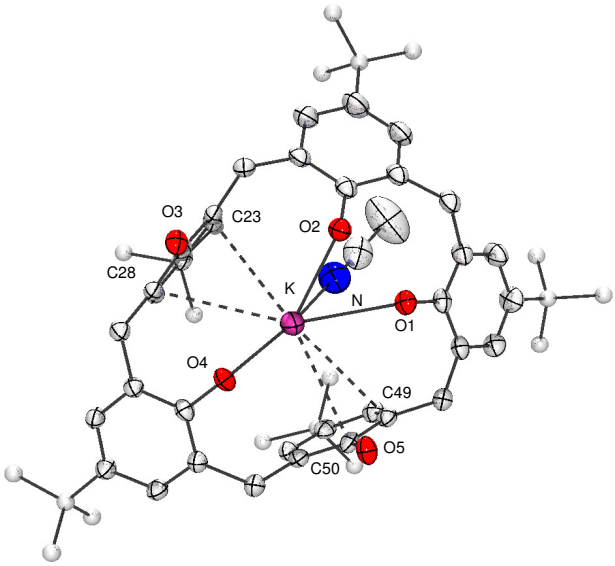

Figure 2.8 Crystal structure of K·^{t}**BuC5(H)$_4$**·MeCN. Thermal ellipsoids are shown at 50% probability; hydrogen atoms and noncoordinated solvent molecules are omitted for clarity.

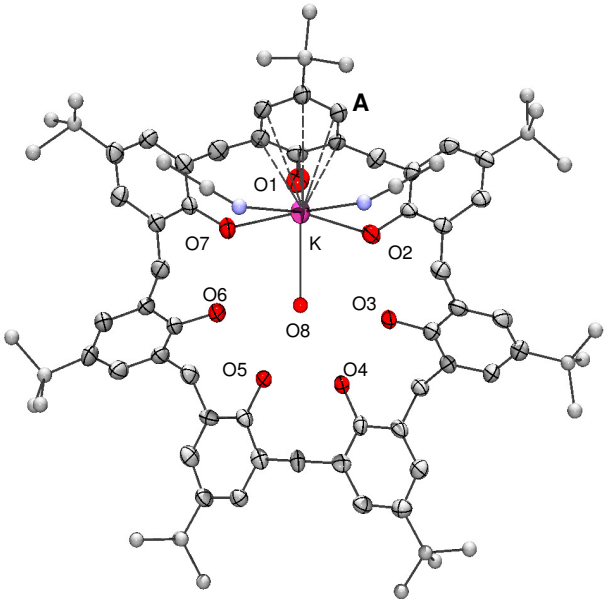

Figure 2.9 Crystal structure of K·^{t}**BuC7(H)$_6$**·2MeCN·H_2O. Thermal ellipsoids are shown at 50% probability; hydrogen atoms and noncoordinated solvent molecules are omitted for clarity.

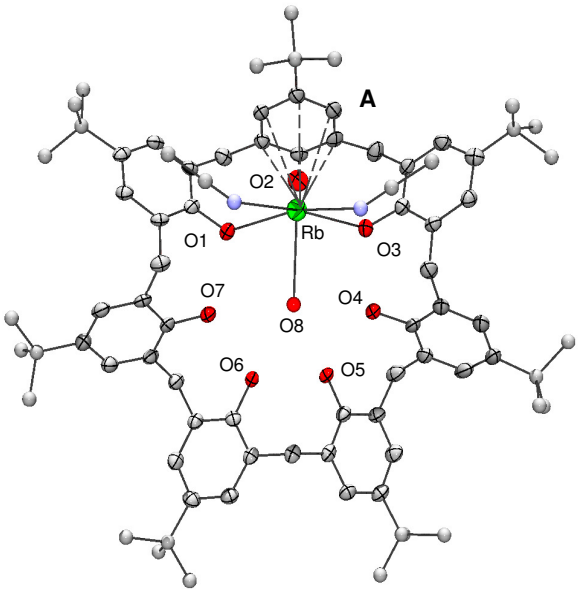

Figure 2.10 Crystal structure of monomeric Rb·^{t}**BuC7(H)$_6$**·2MeCN·H_2O. Thermal ellipsoids are shown at 50% probability; hydrogen atoms and noncoordinated solvent molecules are omitted for clarity.

The X-ray structure of $Na_3 \cdot {}^{t}$**BuC5(H)$_2$**$\cdot$THF$\cdot$4DMSO (Figure 2.11) shows a monomeric unit containing three sodium atoms located in the lower rim of the calixarene ring. A THF molecule was located inside the cavity, blocking the possible Na1-π arene interactions, while four DMSO solvate molecules are coordinated to the two exo sodium atoms (Na2 and Na3).

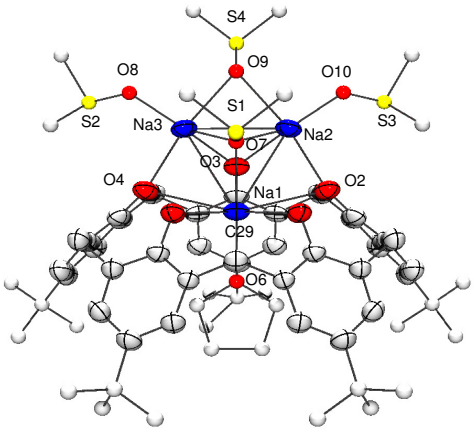

Figure 2.11 Crystal structure of monomeric $Na_3 \cdot {}^{t}$**BuC5(H)$_2$**$\cdot$THF$\cdot$4DMSO. Thermal ellipsoids are shown at 50% probability; hydrogen atoms are omitted for clarity.

b) *Discrete dimeric units*. The $Na \cdot {}^{t}$**BuC5(H)$_4$**$\cdot$S (S = THF, MeCN) dimer (Figure 2.12) contains an inversion center located halfway between the two sodium atoms. The structure does not show any π-cation interaction probably because of the small cation and its location on the lower rim, and the calixarene is in the cone conformation. Dimeric structures are also observed for $K_2 \cdot {}^{t}$**BuC5(H)$_3$** and $M_3 \cdot {}^{t}$**BuC5(H)$_2$** (M = Li, Na).

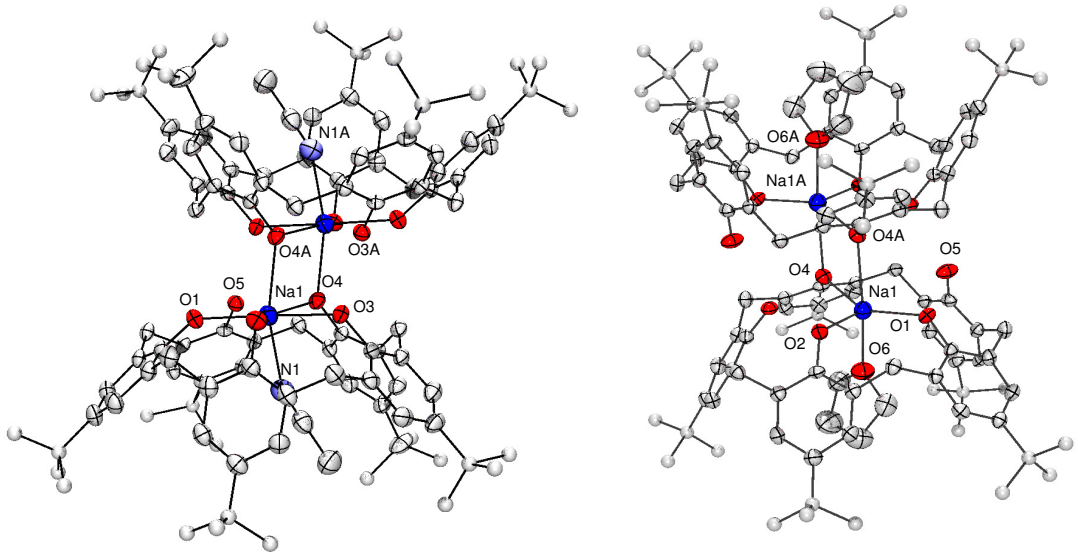

Na·^{t}**BuC5(H)$_4$**·MeCN Na·^{t}**BuC5(H)$_4$**·THF

Figure 2.12 Crystal structure of dimeric Na·^{t}**BuC5(H)$_4$**·S. Thermal ellipsoids are shown at 50% probability; hydrogen atoms and noncoordinated solvent molecules are omitted for clarity.

2.2.5.2 Core structures.

a) *Lithium*. Li aryloxides have a rich coordination chemistry with a predilection toward multinuclear clusters and Li-O-Li bridges.[91-93] The two Li$_3$·^{t}**BuC5(H)$_2$** complexes are quite similar; we will discuss only [Li$_3$·^{t}**BuC5(H)$_2$**·3THF·H$_2$O]$_2$ (Figure 2.13). The dimeric crystal structure of complex [Li$_3$·^{t}**BuC5(H)$_2$**·3THF·H$_2$O]$_2$ includes two different lithium atoms located in the lower rim of the calixarene unit (Li1 and Li2). The first lithium atom (Li1) is oxo bridged to a second one (Li1A) by one phenolic oxygen (O4A) from each calixarene unit, forming a four membered Li$_2$(μ-O)$_2$ core structure with Li-O distances of 1.973(11) Å and 1.993(11) Å. The Li-O-Li and O-Li-O angles are 80.7(5)^{o} and 99.3(5)^{o}, respectively. The second lower rim lithium atom (Li2) has a pseudo tetrahedral geometry with coordination to two phenolic oxygen atoms (O1 and O2) from the first ligand, one THF molecule and a phenolic oxygen (O4A) from the second calixarene. It can be observed that O4 triply bridges Li1, Li1A, and Li2, while O4A

bridges Li1, Li1A, and Li2A. The overall Li/O core structure in complex $[Li_3{\cdot}^{t}\mathbf{BuC5(H)_2}{\cdot}3THF{\cdot}H_2O]_2$ is similar to the one observed in the known dianionic $Li_2{\cdot}^{t}\mathbf{BuC4(H)_2}{\cdot}2Me_2CO$ salt.[74,94]

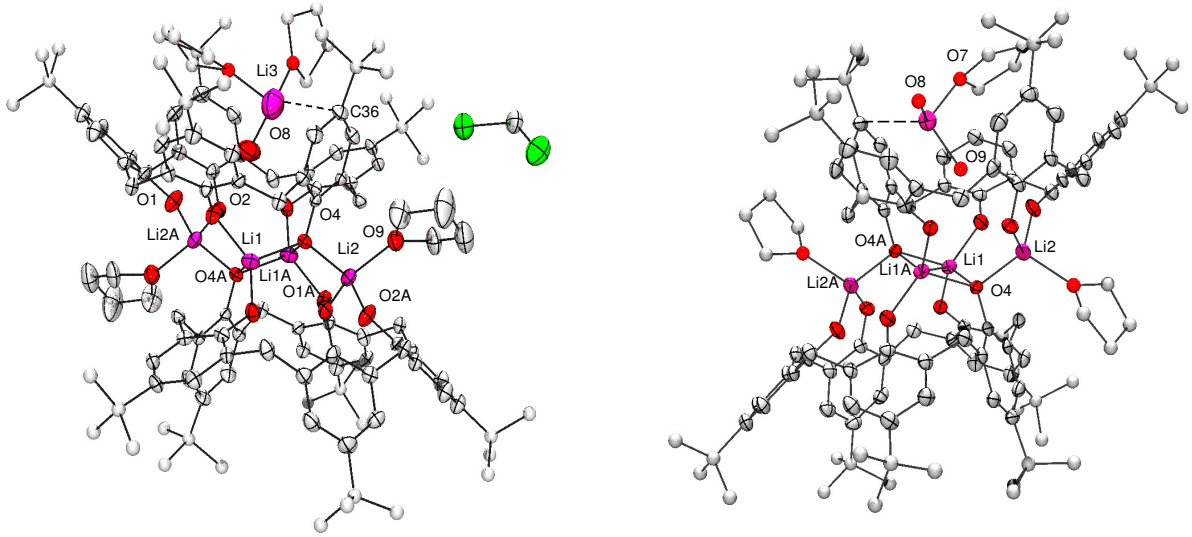

$[Li_3{\cdot}^{t}\mathbf{BuC5(H)_2}{\cdot}3THF{\cdot}H_2O]_2$ $[Li_3{\cdot}^{t}\mathbf{BuC5(H)_2}{\cdot}2THF{\cdot}2H_2O]_2$

Figure 2.13 Crystal structure of dimeric $[Li_3{\cdot}^{t}\mathbf{BuC5(H)_2}{\cdot}3THF{\cdot}H_2O]_2$ and $[Li_3{\cdot}^{t}\mathbf{BuC5(H)_2}{\cdot}2THF{\cdot}2H_2O]_2$. Thermal ellipsoids are shown at 50% probability; hydrogen atoms and third lithium of second ring are omitted for clarity.

An interesting feature of complex $[Li_3{\cdot}^{t}\mathbf{BuC5(H)_2}{\cdot}3THF{\cdot}H_2O]_2$ is the fact that the third lithium (Li3) atom is located in the hydrophobic cavity of the $^{t}\mathbf{BuC5(H)_2}$ rings rather than being coordinated to the harder oxygen lower rim. The Li3 atom is coordinated to two THF molecules, one water molecule, and has a long-range interaction with C36 [2.700(17) Å] to give an overall tetrahedral geometry.

While the ^{1}H NMR spectrum of $Li_3{\cdot}^{t}\mathbf{BuC5(H)_2}$ suggests a 1,2 or 1,3 alternate conformation, the calixarene rings in $[Li_3{\cdot}^{t}\mathbf{BuC5(H)_2}{\cdot}3THF{\cdot}H_2O]_2$ are in the flattened cone conformation. This conformation is adopted not because of M-C interactions but due to the steric hindrance of the solvent molecules and the number of alkali metals in the structure.

b) *Sodium.* The crystal structure of compound Na·^{t}**BuC5(H)$_4$**·S (S = THF or MeCN) is shown in Figure 2.12. The Na1 and Na1A atoms in Na·^{t}**BuC5(H)$_4$**·THF display a distorted trigonal bipyramidal geometry. Each Na atom is coordinated to three aryloxides from the first calixarene ring, one aryloxide from the second ring (O4 or O4A), and a THF molecule. In addition, a weak Na-O3 interaction is observed with a distance of 2.973(2) Å. For Na·^{t}**BuC5(H)$_4$**·MeCN, the Na1 and Na1A are coordinated to four oxygen atoms from the first calixarene ring, a single oxygen (O4 or O4A) from the second ring, and a strongly bonded MeCN [Na1-N1, 2.372(5) Å] to give a pseudo-octahedral geometry. Similar Na geometries are observed in Na·^{t}**BuC4(H)$_3$** monoanions[76,88] and some sodium atoms in the core cluster of Floriani's Na$_4$·^{t}**BuC4**.[95] All the Na-O bond distances fall within normal ranges (see Table 2.2). The structures Na·^{t}**BuC5(H)$_4$**·S exhibit a four membered Na$_2$(μ-O)$_2$ core with the two sodium atoms bridged by O4 and O4A. The Na$_2$(μ-O)$_2$ core forms a rectangle with Na1-O4 and Na1-O4A distances of 2.696(3) and 2.407(3) Å, respectively, when S = MeCN, and distances of 2.461(2) and 2.681(2) Å, respectively when S = THF.

The dimer Na$_3$·^{t}**BuC5(H)$_2$**·2THF (Figure 2.14) shows an architecture similar to that of the lithium trianion (Figure 2.13). Two oxo-bridged tetracoordinated sodium atoms (Na1 and Na1A) link the two calixarene rings and the cone conformation is observed. A four membered Na$_2$(μ–O)$_2$ core is observed with Na-O distances of 2.298(3) and 2.346(3) Å. The O(5)-Na(1)-O(5A) and Na(1)-O(5)-Na(1A) angles are 96.49(10) and 83.51(10)^{o}, respectively. The main distinction of the sodium trianion structure is the fact that the third sodium atom (Na3) apparently has a higher O-bridging affinity than the lithium. The Na3 cation is located inside the cavity (like Li3) but it is also bonded to O1 and O4 from the calixarene ring. This coordination environment for Na3 is similar to that observed in the tetraanion Na$_4$·^{t}**BuC4** reported by Floriani

and coworkers.[95] The Na-C interactions range between 2.739(4) and 3.031(4) Å. All sodium atoms in $Na_3 \cdot {}^{t}$**BuC5(H)$_2$**$\cdot$2THF are four-coordinate with geometry close to tetrahedral.

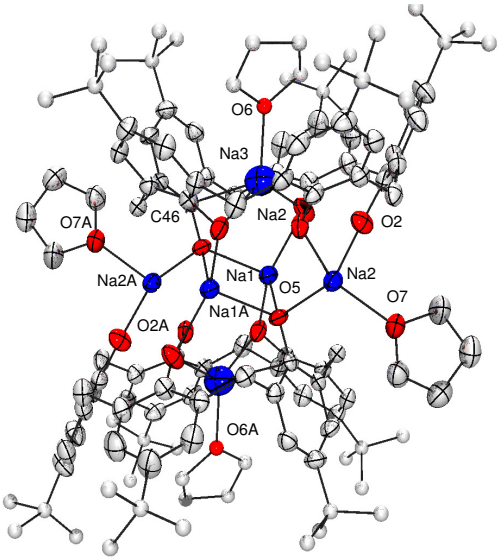

Figure 2.14 Crystal structure of dimeric $Na_3 \cdot {}^{t}$**BuC5(H)$_2$**$\cdot$2THF. Thermal ellipsoids are shown at 50% probability and *t*-Bu groups shown at arbitrary size due to disorder; hydrogen atoms are omitted for clarity.

The crystal structure of $Na_3 \cdot {}^{t}$**BuC5(H)$_2$**$\cdot$THF$\cdot$4DMSO (Figure 2.11) includes one sodium atom (Na1) centered between the five phenolic oxygens of the calixarene, one THF, and one DMSO molecule in a geometry close to pentagonal bipyramidal. The other two sodium atoms (Na2 and Na3) are coordinated to four DMSO molecules on one side, and three calixarene phenolic oxygen atoms on the other. The calixarene oxygen O3 and DMSO oxygen O7 triply bridge the 3 sodium atoms in the core structure with Na-OAr distances of 2.293(3) to 2.532(4) Å. There is just one possible weak M-C interaction, Na1-C29 [2.979(6) Å], allowing the calixarene ring to retain the cone conformation. This particular example points out the importance of the solvate in the solid structure of the calixanions, because the terminal DMSO molecules on Na2 and Na3 atoms block the possible formation of a dimeric structure.

c) Potassium. The monomeric crystal structures of K·**^{t}BuC5(H)$_4$** (Fig 2.9) and K·**^{t}BuC7(H)$_6$** (Figure 2.8) contain the potassium atoms located inside the calixarene cavity with coordination to three contiguous aryloxides. The K-(OAr) bond distances range from 2.670(2)-2.974(2) Å, in the normal range (Table 2.2). **^{t}BuC5(H)$_4$** allows the potassium center to interact with two arene rings through η^2 interactions, while only one η^6 coordination with the metal center is observed in the larger **^{t}BuC7(H)$_6$** ligand.

The overall structure of K_2·**^{t}BuC5(H)$_3$**·4DMSO can be viewed as a dimer (Figure 2.15) containing two different types of potassium atoms. The dimeric unit shows K2 and K2A atoms occupying the central position of the lower rim of the calixarene ligands despite the fact that the oxygen atom in ring E does not participate in binding. The K1 and K1A atoms are coordinated to O4 and O5 from different calixarene ligands and to O6, O7, and O8 from three different DMSO molecules (DMSO containing O6 omitted for clarity). The calixarene oxygen atoms O4 and O5 μ^2-bridge K2 with K1 and K1A, respectively, while O5A and O4A μ^2-bridge K2A with K1 and and K1A, respectively. The overall K_4O_8 core structure of K_2·**^{t}BuC5(H)$_3$**·4DMSO contains a central $K_4(\mu\text{–}O)_4$ eight membered ring (formed by K1, K2, K1A, K2A, O4, O5, O5A, and O4A) that adopts a pseudo chair conformation, with K-O distances in the range of 2.654(8) to 2.823(8) Å. A DMSO molecule is in the calixarene cavity.

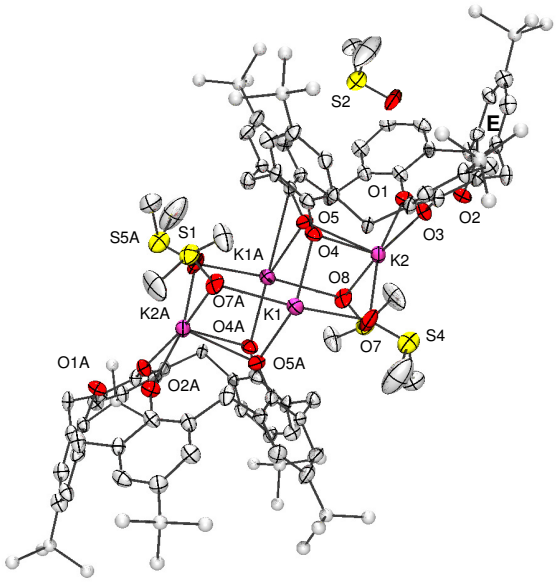

Figure 2.15 Crystal structure of dimeric K_2·^{t}**BuC5(H)$_3$**·4DMSO. Thermal ellipsoids are shown at 50% probability; hydrogen atoms and noncoordinated DMSO molecules are omitted for clarity.

d) Rubidium. The crystal structure of Rb·^{t}**BuC7(H)$_6$** is isostructural to that of K·^{t}**BuC7(H)$_6$**. The rubidium atom displays a seven coordinate geometry similar to those observed in calixarene and aryloxide complexes.[92] A special feature of the structure is the bonding of two acetonitrile and one H_2O molecules to the Rb atom through the hydrophobic cavity of the calixarene. This combination of coordination to the metal ion and inclusion in the calixarene is similar to that reported for the coordination of pyridine N-oxide in the $Na_8[Tb_4(C_5H_5NO)_4(H_2O)_{18}L'_4]$ (L' = *p*-sulfonatocalix[5]arene) complex.[96]

Table 2.3 Crystallographic Data and Summary of Data Collection and Structure Refinement

	[Na·^{t}**BuC5(H)$_4$**·THF]$_2$·C_5H_{12}	[Na·^{t}**BuC5(H)$_4$**·MeCN]$_2$·3MeCN	[K·^{t}**BuC5(H)$_4$**·MeCN]·MeCN	[K·^{t}**BuC7(H)$_6$**·2MeCN·H_2O] ·MeCN	[Rb·^{t}**BuC7(H)$_6$**·2MeCN·H_2O] ·MeCN
Formula	$C_{123}H_{166}Na_2O_{12}$	$C_{120}H_{153}N_5Na_2O_{10}$	$C_{59}H_{75}KN_2O_5$	$C_{83}H_{108}O_8KN_3$	$C_{83}H_{108}O_8RbN_3$
Fw	1882.61	1871.51	931.34	1314.86	1361.23
cryst syst	Triclinic	Triclinic	Triclinic	Monoclinic	Monoclinic
space group	*P*-1	*P*-1	*P*-1	$P2_1$/n	$P2_1$/c
T, K	213(2)	218(2)	218(2)	218(2)	213(2)
a, Å	12.6599(13)	13.5128(10)	12.333(3)	16.777(9)	16.768(10)
b, Å	16.0093(16)	18.0249(13)	13.352(4)	23.555(12)	23.650(15)
c, Å	16.8202(17)	24.6368(18)	17.870(5)	20.771(11)	23.290(11)
α, deg	103.727(2)	91.401(2)	81.001(5)	90	90
β, deg	103.495(2)	94.0300(10)	76.788(5)	104.181(10)	120.29(3)
γ, deg	106.933(2)	110.029(2)	84.162(4)	90	90
V, A^3	2995.6(5)	5616.3(7)	2822.9(13)	7958(7)	7975(8)
Z	1	2	2	4	4
$d_{calcd.}$ g·cm^{-3}	1.004	1.099	1.092	1.087	1.124
μ, mm^{-1}	0.069	0.0760	0.140	0.120	0.674
Refl collected	12957	15760	16891	49636	45041
T_{min}/ T_{max}	0.986	0.985	0.973	0.989	0.941
N_{measd}	11128	14297	9838	11438	11465
[R_{int}]	[0.0476]	[0.0403]	[0.0823]	[0.0884]	[0.0685]
R [I>2sigma(I)]	0.0687	0.0778	0.0725	0.1340	0.0600
R_w[I>2sigma(I)]	0.1872	0.2251	0.2134	0.3571	0.1646
GOF	0.867	1.066	0.922	1.123	1.013

	[K_2·^{t}**BuC5(H)$_3$**·4DMSO]$_2$·8DMSO	[Li_3·^{t}**BuC5(H)$_2$**·3THF·H_2O]$_2$ ·$2CH_2Cl_2$	[Li_3·^{t}**BuC5(H)$_2$**·2THF·$2H_2O$]$_2$ ·2THF	[Na_3·^{t}**BuC5(H)$_2$** · 2THF]$_2$·3.5THF	[Na_3·^{t}**BuC5(H)$_2$**·THF·4DMSO]·2THF
Formula	$C_{142}H_{232}K_4O_{26}S_{16}$	$C_{136}H_{190}Cl_4Li_6O_{18}$	$C_{134}H_{190}Li_6O_{20}$	$C_{140}H_{194}Na_6O_{17.5}$	$C_{75}H_{115}Na_3O_{12}S_4$
Fw	3024.81	2296.41	2162.58	2294.96	1405.88
cryst syst	Monoclinic	Monoclinic	Triclinic	Triclinic	Monoclinic
space group	$P2_1$/n	$P2_1$/c	*P*-1	*P*-1	*C*2/m
T, K	213(2)	213(2)	213(2)	213(2)	213(2)
a, Å	14.440(4)	17.7408(16)	12.5244(10)	18.031(6)	25.352(8)
b, Å	17.897(4)	24.315(2)	15.3805(14)	18.856(6)	18.019(5)
c, Å	32.661(8)	17.1428(17)	18.6388(16)	23.754(7)	20.226(6)
α, deg	90	90	99.127(2)	108.640(5)	90
β, deg	94.166(5)	117.360(2)	96.553(2)	93.571(6)	119.548(4)
γ, deg	90	90	103.382(2)	111.761(5)	90
V, A^3	8418(4)	6567.7(11)	3405.9(5)	6956(4)	8038(4)
Z	2	2	1	2	4
$d_{calcd.}$ g·cm^{-3}	1.193	1.159	1.050	0.975	1.162
μ, mm^{-1}	0.364	0.152	0.068	0.078	0.189
Refl collected	53275	18144	8451	43727	30637
T_{min}/ T_{max}	0.93	0.970	0.987	0.985	0.994
N_{measd}	14831	10894	8376	24370	9723
[R_{int}]	[0.2382]	[0.0934]	[0.0324]	[0.0404]	[0.0764]
R [I>2sigma(I)]	0.1134	0.0795	0.0824	0.1038	0.1082
R_w[I>2sigma(I]	0.2276	0.1855	0.2609	0.2929	0.3249
GOF	1.012	0.903	1.109	1.110	1.205

2.3 Experimental section

2.3.1 General Information

Unless otherwise noted, all manipulations were carried out in a nitrogen filled glove-box or using standard Schlenk techniques. Starting materials were obtained from commercial suppliers and used without further purification.

para-tert-Butylcalix[5]arene [**^{t}BuC5(H)$_5$**] was prepared by the literature procedure[97] and *para-tert*-butylcalix[7]arene [**^{t}BuC7(H)$_7$**] was recovered as a side product from the **^{t}BuC5(H)$_5$** synthesis. Both calix[n]arene ligands were dried at 110 ^{0}C at least 24 hrs under vacuum before use. Tetrahydrofuran was freshly distilled from Na/benzophenone. Methanol was passed through a column of dried 4Å molecular sieves, kept over 4Å sieves for 15 days, then the solvent was distilled and stored over 4Å molecular sieves. Benzene was dried by refluxing over Na/benzophenone and stored over 4Å molecular sieves. Other anhydrous solvents were purchased from Aldrich and stored over molecular sieves under nitrogen before using. Deuterated benzene, dimethyl sulfoxide, and chloroform were dried over CaH_2. The melting points of all the compounds were taken in capillary tubes on a Mel-temp apparatus (Laboratory devices, Cambridge, MA) using a 500 ^{o}C thermometer. ^{1}H NMR and ^{13}C spectra were recorded at room temperature on a Varian XL-300 spectrometer at 300 and 75 MHz, respectively. Analytical samples were dried under vacuum for at least 24 hrs (for M = Li, Na, K salts only). Microanalyses were performed by Atlantic Microlab, Inc, Norcross, GA. IR and UV/Vis spectra were obtained with an Infinity Gold^{TM} FTIR spectrometer and Agilent 8453 spectrophotometer, respectively. Filtrations used a medium sintered glass filter. X-ray data for [Na_2·**^{t}BuC5(H)$_3$** ·2THF]$_2$·3.5THF and [K_2·**^{t}BuC5(H)$_3$**·4DMSO]$_2$·8DMSO were collected on a Bruker SMART APEX CCD diffractometer at low temperature using Mo Kα radiation by Professors Arnold L. Rheingold and James A. Golen at the University of California San Diego. All other X-ray

diffraction experiments were performed on a Bruker SMART 1000 CCD detector at variable low temperature using Mo Kα radiation. In some cases the positions of the phenolic hydrogens have been located in the crystal structures, while in other cases the positions may be inferred by comparison of O-O distances and/or M-O bond lengths.

2.3.2 Preparation of compounds

2.3.2.1 Monoanion synthesis

Na·^{t}**BuC5(H)$_4$**: Method A: $NaOC(CH_3)_3$ (0.0490 g, 0.509 mmol) in THF (5 mL) was added dropwise to a solution of ^{t}**BuC5(H)$_5$** (0.412 g, 0.508 mmol) in THF (10 mL). The colorless solution was allowed to stir for 24 hrs at room temperature with no visible change. The solvent was removed by vacuum yielding a white powder. The powder was washed with pentane (5 mL) and allowed to settle. The remaining pentane was removed using a pipette. This washing procedure was repeated. Recrystallization of the powder was performed either by pentane diffusion into its THF solution or by slow evaporation in air of a concentrated acetonitrile solution to give colorless crystals of Na·^{t}**BuC5(H)$_4$** in 83% yield (0.349 g, 0.422 mmol). Single crystals were obtained from the slow evaporation in air of a concentrated THF/acetonitrile/pentane (2:1:1 ratio) solution of the product.

Method B: A suspension of NaH (0.0120 g, 0.510 mmol) in THF (5 mL) was added to a solution of ^{t}**BuC5(H)$_5$** (0.412 g, 0.508 mmol) in THF (10 mL). The white suspension was allowed to stir for 24 hrs at room temperature. The mixture was filtered and the remaining solid NaH was removed. The filtrate was dried under reduced pressure yielding a white-yellowish mixture [mixture of ^{t}**BuC5(H)$_5$** and Na·^{t}**BuC5(H)$_4$**]. This crude material was washed twice with pentane (5 mL portions). Filtration and vacuum drying for 2 hrs at room temperature led to the product as a white powder. The solid was recrystallized either by slow evaporation of solvent

(THF) or by pentane diffusion in a THF solution yielding colorless crystals of Na·**^{t}BuC5(H)$_4$** in 81% yield (0.346 g, 0.411 mmol).

Method C: Under air, a suspension of Na_2CO_3 (0.0540 g, 0.510 mmol) in MeCN or THF (10 mL) was added to a solution of **^{t}BuC5(H)$_5$** (0.412 g, 0.508 mmol) in MeCN or THF (20 mL). The white suspension was refluxed under nitrogen for 24 hrs. The mixture was filtered and the remaining solid Na_2CO_3 was removed. The filtrate was dried under reduced pressure yielding a white-yellowish mixture [mixture of **^{t}BuC5(H)$_5$** and Na·**^{t}BuC5(H)$_4$**]. This crude material was washed twice with pentane (5 mL portions). Filtration and vacuum drying for 2 hrs at room temperature led to the product as a white powder. The solid was recrystallized either by slow evaporation of solvent (THF) or by pentane diffusion in a THF solution yielding colorless crystals of Na·**^{t}BuC5(H)$_4$** in 72% yield (0.306 g, 0.366 mmol). Single crystals were obtained by the slow evaporation in air of a concentrated acetonitrile solution of the product. M.p. 444-446 ^{o}C; ^{1}H NMR ($CDCl_3$, TMS): δ = 1.23 (s, 45H, C(C*H*$_3$)$_3$), 3.47 (b, 5H, Ar*CH*$_2$ Ar), 4.37 (b, 5H, ArC*H*$_2$ Ar), 7.18 ppm (s, 10H, Ar*H*). OH peaks were too broad to be observed at rt; ^{13}C NMR ($CDCl_3$, TMS): δ = 31.7 (C(*C*H$_3$)$_3$), 31.9 (*C*(CH$_3$)$_3$), 34.1 (Ar*C*H$_2$ Ar), 125.9, 127.4, 143.1, 149.2 ppm (aromatic carbons); IR (KBr): *v* = 3431m (OH), 3306m (OH), 3052w, 2961vs, 2911w, 2868w, 1607w, 1483vs, 1389w, 1362m, 1294m, 1248w, 1204s, 1196w, 874m, 818 cm^{-1}(w); UV/Vis (THF) λ_{max}/nm (ε/dm^{3}mol^{-1}cm^{-1}): 286 (7.84 x 10^4), 280 (7.83 x 10^3), 241 (4.43 x 10^3); elemental analysis calcd (%) for $C_{55}H_{69}O_5Na\cdot C_2H_3N$: C 78.30, H 8.33; found C 78.49, H 8.56.

Na·**^{t}BuC7(H)$_6$**: Method A: $NaOC(CH_3)_3$ (0.0244 g, 0.254 mmol) in toluene (5 mL) was added dropwise to a solution of **^{t}BuC7(H)$_7$** (0.288 g, 0.254 mmol) in toluene (10 mL). The light-yellow solution was allowed to stir for 24 hrs at room temperature with no visible change. The solvent was removed by vacuum yielding a white-yellowish powder. The powder was washed

twice with pentane/hexane (4 mL) and filtered (or centrifuged) to yield the crude product. Recrystallization of the powder was performed either by pentane diffusion into its THF solution or by slow evaporation in air of a concentrated acetonitrile solution to give colorless crystals of Na·^{t}**BuC7(H)$_6$** in 86% yield (0.253 g, 0.218 mmol). Single crystals were obtained from the slow evaporation in air of a concentrated THF or acetonitrile solution of the product.

Method B: Under air, a suspension of Na_2CO_3 (0.0269 g, 0.254 mmol) in THF or MeCN (5 mL) was added to a solution of ^{t}**BuC7(H)$_7$** (0.288 g, 0.254 mmol) in THF or MeCN (10 mL). The white suspension was refluxed under nitrogen for 24 hrs. The mixture was filtered and the remaining solid Na_2CO_3 was removed. The filtrate was dried under reduced pressure yielding a white-yellowish mixture [mixture of ^{t}**BuC7(H)$_7$** and Na·^{t}**BuC7(H)$_6$**]. This crude material was washed twice with pentane/hexane (4 mL portions). Filtration and vacuum drying for 4 hrs at room temperature led to the product as a white powder. The solid was recrystallized either by slow evaporation of solvent (THF) or by pentane diffusion in a THF solution yielding colorless crystals of Na·^{t}**BuC7(H)$_6$** in 83% yield (0.244 g, 0.210 mmol). Single crystals were obtained by the slow evaporation in air of a concentrated acetonitrile solution of the product; however they were too low quality for X-ray analyses. M.p. 348-350 ^{o}C; ^{1}H NMR ($CDCl_3$, TMS): δ = 1.23 (s, 63H, C(C*H*$_3$)$_3$), 3.81 (b, 14H, ArC*H*$_2$ Ar), 7.08 (s, 14H, Ar*H*). No OH peaks were observed at room temperature.

K·^{t}**BuC5(H)$_4$**: Method A: A solution of $KOC(CH_3)_3$ (0.0571 g, 0.517 mmol) in THF (5 mL) was added dropwise to a solution of ^{t}**BuC5(H)$_5$** (0.412 g, 0.508 mmol) in THF (10 mL) and the resulting clear solution was allowed to stir for 24 hrs at rt. The solvent of the final colorless solution was removed by vacuum yielding a white-yellowish powder. This crude material was washed twice with pentane (5 mL portions). Filtration and vacuum drying for 2 hrs at room

temperature led to the product as a white powder. The solid was recrystallized by either pentane diffusion into its THF solution or by slow evaporation in air of an acetonitrile solution to give colorless crystals of K·**^{t}BuC5(H)$_4$** in 86% yield (0.369 g, 0.437 mmol).

Method B: Under air, a suspension of K_2CO_3 (0.0591 g, 0.519 mmol) in MeCN or THF (10 mL) was added to a solution of **^{t}BuC5(H)$_5$** (0.412 g, 0.508 mmol) in MeCN or THF (20 mL). The white suspension was refluxed under nitrogen for 24 hrs. At the end of the reaction the white mixture was filtered and the remaining solid K_2CO_3 was removed. The filtrate was dried under reduced pressure yielding a white-yellowish mixture [mixture of **^{t}BuC5(H)$_5$** and K·**^{t}BuC5(H)$_4$**]. This crude material was washed twice with pentane (5 mL portions). Filtration and vacuum drying led to the product as a white powder. The solid was recrystallized either by slow evaporation of a THF solution or by pentane diffusion in a THF solution yielding white crystalline needles of K·**^{t}BuC5(H)$_4$** in 82% yield (0.357 g, 0.417 mmol). Single crystals were obtained after two weeks by diffusion of pentane in a THF/DMSO (5:1) solution of the product. M.p. 303-305 ^{o}C; ^{1}H NMR ($CDCl_3$, TMS): δ = 1.21 (s, 45H, C(C*H*$_3$)$_3$), 3.86 (b, 10H, ArC*H*$_2$ Ar), 7.11 (s, 10H, Ar*H*), 8.66 ppm (b, 4H, O*H*); ^{13}C NMR ($CDCl_3$, TMS): δ = 31.6 (C(*C*H$_3$)$_3$), 32.7 (*C*(CH$_3$)$_3$), 33.8 (Ar*C*H$_2$ Ar), 125.6, 128.7, 140.9, 151.9 ppm (aromatic carbons); IR (KBr): *v* = 3298s (OH), 3052w, 2961vs, 2911w, 2869w, 1599w, 1482s, 1393w, 1362m, 1292m, 1236w, 1199s, 1117m, 881w, 819 cm^{-1} (w); UV/Vis (THF) λ_{max}/nm (ε/dm^{3}mol^{-1}cm^{-1}): 287 (4.152 x 10^3), 241 (4.255 x 10^3); elemental analysis calcd (%) for $C_{55}H_{69}O_5K \cdot C_2H_3N$: C 76.86, H 8.15; found C 76.47, H 8.13.

K·**^{t}BuC7(H)$_6$**: Method A: KOC(CH$_3$)$_3$ (0.0285 g, 0.254 mmol) in toluene (5 mL) was added dropwise to a solution of **^{t}BuC7(H)$_7$** (0.288 g, 0.254 mmol) in toluene (10 mL). The light-yellow solution was allowed to stir for 24 hrs at room temperature with no visible change. The

solvent was removed by vacuum yielding a white-yellowish powder. The powder was washed twice with pentane/hexane (4 mL) and filtered (or centrifuged) to yield the crude product. Recrystallization of the powder was performed either by hexane diffusion into its THF solution or by slow evaporation in air of a concentrated acetonitrile solution to give colorless crystals of K·^{t}**BuC7(H)$_6$** in 89% yield (0.0265 g, 0.226 mmol). Single crystals were obtained from the slow evaporation in air of a concentrated THF or acetonitrile solution of the product.

Method B: Under air, a suspension of K_2CO_3 (0.0351 g, 0.254 mmol) in THF or MeCN (5 mL) was added to a solution of ^{t}**BuC7(H)$_7$** (0.288 g, 0.254 mmol) in THF or MeCN (10 mL). The white suspension was refluxed under nitrogen for 24 hrs. The mixture was filtered and the remaining solid K_2CO_3 was removed. The filtrate was dried under reduced pressure yielding a white-yellowish mixture [mixture of ^{t}**BuC7(H)$_7$** and K·^{t}**BuC7(H)$_6$**]. This crude material was washed twice with pentane/hexane (4 mL portions). Filtration and vacuum drying for 4 hrs at room temperature led to the product as a white powder. The solid was recrystallized either by slow evaporation of solvent MeCN (or THF) or by pentane diffusion in a THF solution yielding colorless crystals of K·^{t}**BuC7(H)$_6$** in 84% yield (0.0250 g, 0.213 mmol). Single crystals were obtained by the slow evaporation in air of a concentrated acetonitrile solution of the product. M.p. 376-378 ^{o}C; ^{1}H NMR ($CDCl_3$, TMS): δ = 1.21 (s, 63H, C(C*H*$_3$)$_3$), 3.76 (b, 14H, ArC*H*$_2$ Ar), 7.05 (s, 14H, Ar*H*). No OH peaks were observed at room temperature.

Rb·^{t}**BuC7(H)$_6$**: Under air, a suspension of Rb_2CO_3 (0.0587 g, 0.254 mmol) in THF or MeCN (5 mL) was added to a solution of ^{t}**BuC7(H)$_7$** (0.288 g, 0.254 mmol) in THF or MeCN (10 mL). The final yellowish solution was dried under reduced pressure yielding a white-yellowish solid [mixture of ^{t}**BuC7(H)$_7$** and Rb·^{t}**BuC7(H)$_6$**]. This crude material was washed twice with pentane/hexane (4 mL portions). Filtration and vacuum drying for 4 hrs at room

temperature led to the product as a white powder. The solid was recrystallized by slow evaporation in air of a concentrated acetonitrile solution to yield block colorless crystals of Rb·**^{t}BuC7(H)$_6$** in 78% yield (0.241 g, 0.198 mmol). M.p. 326 ^{o}C (decomp); ^{1}H NMR ($CDCl_3$, TMS): δ = 1.25 (s, 63H, C(CH_3)$_3$), 3.81 (b, 14H, ArCH_2 Ar), 7.06 ppm (s, 14H, Ar*H*). The OH peaks were not observed at rt. ^{13}C NMR ($CDCl_3$, TMS): δ = 31.8 (C(*C*H_3)$_3$), 33.6 (*C*(CH$_3$)$_3$), 34.2 (Ar*C*H$_2$ Ar), 125.8, 128.5, 142.7, 150.5 ppm (aromatic carbons).

Cs·**^{t}BuC7(H)$_6$**: The same procedure as the one performed for Rb·**^{t}BuC7(H)$_6$** was followed, using Cs_2CO_3 (0.0827 g, 0.254 mmol). The product was purified by slow evaporation of a concentrated THF (or MeCN) solution to obtain Cs·**^{t}BuC7(H)$_6$** as block colorless crystals in 86% yield (0.276 g, 0.218 mmol). M.p. 319 ^{o}C (decomp); ^{1}H NMR ($CDCl_3$, TMS): δ = 1.20 (s, 63H, C(CH_3)$_3$), 3.78 (b, 14H, ArCH_2 Ar), 7.00 (s, 14H, Ar*H*). No OH peaks were observed at rt. ^{13}C NMR ($CDCl_3$, TMS): δ = 31.9 (C(*C*H_3)$_3$), 34.1 (*C*(CH$_3$)$_3$), no Ar*C*H$_2$Ar peak observed, 125.7, 128.7, 141.8, 151.2 ppm (aromatic carbons); elemental analysis calcd (%) for $C_{55}H_{69}O_5Cs$: C 69.58, H 7.89; found C 69.23, H 7.90.

2.3.2.2 Dianion Synthesis

Na_2·**^{t}BuC5(H)$_3$**: NaOC(CH$_3$)$_3$ (0.0980 g, 1.01 mmol) in THF (5 mL) was added dropwise to a solution of **^{t}BuC5(H)$_5$** (0.412 g, 0.508 mmol) in THF (15 mL). The light yellow solution was allowed to stir at rt for 24 hrs, then was dried under vacuum yielding a white solid. Hexane (10 mL) was added to the solid and the mixture was stirred for 15 min. Pure Na_2·**^{t}BuC5(H)$_3$** was obtained in 92% yield as a white powder after filtration (0.400 g, 0.467 mmol). M.p. 450 ^{o}C (decomp); ^{1}H NMR ([D$_6$]DMSO, TMS): δ = 1.16 (s, 45H, C(CH_3)$_3$), 3.09 (b, 5H, ArCH_2 Ar), 4.22 (b, 5H, ArCH_2 Ar), 6.96 (s, 10H, Ar*H*), 15.38 ppm (b, 3H, O*H*); ^{1}H NMR ($CDCl_3$, TMS): δ = 1.22 (s, 45H, C(CH_3)$_3$), 2.85 (b, 5H, ArCH_2Ar), 4.03 (s, 5H, ArCH_2Ar), 6.97 ppm (s, 10H,

Ar*H*). OH peaks were too broad to be observed at rt. ^{13}C NMR ([D_6]DMSO, TMS): δ = 32.3 (C(*C*H_3)$_3$), 33.3 (*C*(CH$_3$)$_3$), 34.0 (Ar*C*H_2 Ar), 124.9, 127.9, 137.8, 154.7 ppm (aromatic carbons); IR (KBr): *v* = 3415m (OH), 3048w, 2961vs, 2904s, 2863s, 2356w, 1607w, 1482vs, 1393m, 1362s, 1295s, 1240m, 1204vs, 115w, 874m, 817m, 794 cm^{-1} (m); UV/Vis (THF) λ_{max}/nm (ε/dm^{3}mol^{-1}cm^{-1}): 242 (1.682 x 10^4), 286 (1.586 x 10^4); elemental analysis calcd(%) for $C_{55}H_{68}O_5Na_2 \cdot 2.5(C_4H_8O)$: C 75.40, H 8.57; found C 75.09, H 8.76.

$Na_2 \cdot$**^{t}BuC7(H)$_5$**: NaOC(CH$_3$)$_3$ (0.0488 g, 0.508 mmol) in toluene (5 mL) was added dropwise to a solution of **^{t}BuC7(H)$_7$** (0.288 g, 0.254 mmol) in THF (15 mL). The light yellow solution was allowed to stir at rt for 24 h, then dried under vacuum yielding a yellowish solid. Hexane (10 mL) was added to the solid and the mixture was stirred for 3 hrs. The mixture was filtered and the solid recovered was dried under vacuum to give the crude material as a white solid. Pure $Na_2 \cdot$**^{t}BuC7(H)$_5$** was obtained in 82% yield as a white powder after diffusion of pentane into its concentrated THF solution (0.246 g, 0.208 mmol). M.p. 411-413 ^{o}C; ^{1}H NMR (C_6D_6, TMS): δ = 1.25 (s, 63H, C(C*H*$_3$)$_3$), 3.38 (b, 7H, Ar*CH*$_2$ Ar), 3.97 (b, 7H, ArC*H*$_2$ Ar), 7.22 (s, 14H, Ar*H*). No OH peaks were observed at rt.

$K_2 \cdot$**^{t}BuC5(H)$_3$**: A solution of KOC(CH$_3$)$_3$ (0.114 g, 1.01 mmol) in THF (5 mL) was added dropwise to a solution of **^{t}BuC5(H)$_5$** (0.412 g, 0.508 mmol) in THF (15 mL). The light yellow solution was allowed to stir at rt for 24 hrs, then was dried under vacuum yielding a white solid. Hexane (10 mL) was added to the solid and the mixture was stirred for 15 min. Pure $K_2 \cdot$**^{t}BuC5(H)$_3$** in 96% yield was obtained as a white powder after filtration (0.434 g, 0.488 mmol). Crystals suitable for X-ray analysis were obtained by slow evaporation of a concentrated THF/DMSO (10:1 ratio) solution of $K_2 \cdot$**^{t}BuC5(H)$_3$**. M.p. 353-355 ^{o}C; ^{1}H NMR ([D_6]DMSO, TMS): δ = 1.16 (s, 45H, C(C*H*$_3$)$_3$), 3.06 (b, 5H, ArC*H*$_2$ Ar), 4.27 (b, 5H, ArC*H*$_2$ Ar), 6.94 (s,

10H, Ar*H*), 15.15 ppm (b, 3H, O*H*); ^{1}H NMR ($CDCl_3$, TMS): δ = 1.20 (s, 45H, C(CH_3)$_3$), 3.77 (b, 10H, ArCH_2Ar), 7.06 ppm (s, 10H, Ar*H*). OH peaks were too broad to be observed at rt. ^{13}C NMR ([D_6]DMSO, TMS): δ = 32.4 (C(*C*H_3)$_3$), 33.2 (*C*(CH$_3$)$_3$), 33.9 (Ar*C*H$_2$ Ar), 124.9, 127.9, 136.9, 155.4 ppm (aromatic carbons); IR (KBr): *ν* = 3411m (OH), 3053w, 2960vs, 2094s, 2871m, 1603w, 1482vs, 1393w, 1362m, 1295m, 1232w, 1203s, 1124w, 874w, 818 cm^{-1} (w); UV/Vis (THF) λ_{max}/nm (ε/dm^{3}mol^{-1}cm^{-1}): 277 (8.154 x 10^5), 287 (8.90 x 10^5); elemental analysis calcd (%) for $C_{55}H_{68}O_5K_2 \cdot C_2H_6SO$: C 70.90, H 7.73; found C 71.09, H 7.76.

$K_2 \cdot$**^{t}**$BuC7(H)_5$**: KOC(CH$_3$)$_3$ (0.0570 g, 0.508 mmol) in toluene (5 mL) was added dropwise to a solution of **^{t}**$BuC7(H)_7$** (0.288 g, 0.254 mmol) in THF (15 mL). The light yellow solution was allowed to stir at rt for 24 hrs, then was dried under vacuum yielding a yellowish solid. Hexane (10 mL) was added to the solid and the mixture was stirred for 1 h. The mixture was filtered and the solid recovered was dried under vacuum to give the crude material as a white solid. Pure $K_2 \cdot$**^{t}**$BuC7(H)_5$** was obtained in 76% yield as a white powder after diffusion of pentane into its concentrated THF solution (0.234 g, 0.193 mmol). M.p. < 454 ^{o}C (decomp); ^{1}H NMR ($CDCl_3$, TMS): δ = 1.17 (s, 63H, C(CH_3)$_3$), 3.22 (b, 2H, Ar*C*H_2 Ar), 3.97 (b, 12H, ArCH_2 Ar), 6.91 (s, 14H, Ar*H*), 13.6 (b, 5H, OH).

2.3.2.3 Trianion synthesis

$Li_3 \cdot$**^{t}**$BuC5(H)_2$**: Method A: Under air, a suspension of LiH (0.0130 g, 1.55 mmol) in THF (7 mL) was added to a solution of **^{t}**$BuC5(H)_5$** (0.418 g, 0.515 mmol) in THF (10 mL). The white suspension was placed into a 100 mL round bottom flask, and then kept in reflux under nitrogen for 24 hrs. The final colorless solution was vacuum dried yielding a white solid. The solid was redissolved in THF (5 mL) and then recrystallized by the diffusion of pentane into the solution. After three days at rt colorless crystals appeared. The remaining solvent was removed and the

crystals were dried under vacuum yielding Li_3·**^{t}BuC5(H)$_2$** as a white solid in 71% yield (0.303 g, 0.366 mmol). Single crystals of the product were obtained by diffusion of dichloromethane into its THF solution.

The same procedure, but increasing the number of equivalents to 4 and 5 mmol of LiH, increased the yield of Li_3·**^{t}BuC5(H)$_2$** to 82% (0.350 g, 0.422 mmol) and 93% (0.396 g, 0.479 mmol), respectively.

Method B: The same procedure of method A was performed using a solution of 0.0378 g (1.57 mmol) of LiOH (instead of LiH) in dry methanol (5 mL). The product was recrystallized from diffusion of pentane into THF solution to obtain 0.380 g (0.458 mmol, 89% yield). In this case increasing the equivalents of LiOH to 4 and 5 increased the yields to 92% (0.392 g, 0.474 mmol) and 94% (0.401 g, 0.484 mmol), respectively.

Method C: A 2.0 M solution of n-BuLi in pentane (0.0931 g, 1.55 mmol) was added dropwise to a solution of **^{t}BuC5(H)$_5$** (0.420 g, 0.518 mmol) in THF (10 mL) to give a yellowish solution. The reaction mixture was allowed to stir for 24 hrs at rt. The solvent was removed under vacuum to give a yellowish solid. Pentane (5 mL) was added to the solid and allowed to stir for 5 min. The mixture was filtered to give 0.369 g of a white crystalline powder of pure Li_3·**^{t}BuC5(H)$_2$** (0.443 mmol, 86% yield). Single crystals of the product were obtained by pentane diffusion into a concentrated THF solution of the product.

Method D: The same procedure as method C was performed using 1.58 mmol (0.126 g) of $LiOC(CH_3)_3$ (instead of n-BuLi) in THF (5 mL), to give Li_3·**^{t}BuC5(H)$_2$** in 97% yield (0.413 g, 0.500 mmol). M.p. 422-424 ^{o}C; ^{1}H NMR (C_6D_6, TMS): δ = 1.05 (s, 9H, C(CH_3)$_3$), 1.25 (s, 18H, C(CH_3)$_3$), 1.34 (s, 18H, C(CH_3)$_3$), 3.30 (d, 1H, J=14 Hz, ArCH_2Ar), 3.39 (d, 2H, J=13 Hz, ArCH_2Ar), 3.72 (d, 2H, J= 14 Hz, ArCH_2Ar), 4.18 (d, 1H, J=14 Hz, ArCH_2Ar), 4.54 (d, 2H, J= 13 Hz, ArCH_2Ar), 5.73 (d, 2H, J= 14 Hz, ArCH_2Ar), 7.22 (b, 2H, ArH), 7.32 (b, 2H, ArH), 7.48

ppm (b, 6H, Ar*H*). OH peaks were not observed at rt. ^{13}C NMR (C_6D_6, TMS): δ = 25.0 (Ar*C*H_2Ar), 31.3, 31.7, 31.8 (C(*C*H_3)$_3$), 32.5 (Ar*C*H_2Ar), 33.5, 33.7, 33.8 (*C*(CH_3)$_3$), 36.4 (Ar*C*H_2Ar), 125.5, 125.8, 126.4, 126.7, 130.3, 130.5, 130.7, 138.6, 140.6, 152.8, 154.1, 158.7 ppm (aromatic carbons); IR (KBr): *v* = 3519m (OH), 3423m (OH), 3049w, 2960vs, 2904m, 2871m, 1611w, 1482vs, 1446s, 1362m, 1291m, 1204w, 1112w, 877w, 817 cm^{-1} (w); UV/Vis (THF) λ_{max}/nm (ε/dm^{3}mol^{-1}cm^{-1}): 289 (9.089 x 10^3); elemental analysis calcd (%) for $C_{55}H_{67}O_5Li_3 \cdot 4(C_4H_8O) \cdot CH_2Cl_2$: C 71.93, H 8.47; found C 71.54, H 8.27.

$Na_3 \cdot$**^{t}BuC5(H)$_2$**: A suspension of $NaOC(CH_3)_3$ (0.92 g, 2.02 mmol) in toluene (10 mL) was added dropwise to a solution of **^{t}BuC5(H)$_5$** (0.412 g, 0.508 mmol) in toluene (20 mL). The mixture was stirred at rt. After the first 2 hrs of stirring the starting yellowish mixture became a yellow-white mixture, and then it was allowed to stir for another 22 hrs. The yellowish mixture was dried under reduced pressure producing a yellowish solid. To the solid was added pentane (10 mL) and the mixture was stirred for 10 min. Filtration and vacuum drying of the solid led to the crude product as a white powder. Recrystallization of the powder was performed either by slow evaporation of solvent (THF) or by pentane diffusion into a THF solution yielding 0.423 g of $Na_3 \cdot$**^{t}BuC5(H)$_2$** (0.472 mmol, 93% yield). The slow evaporation of a concentrated THF/DMSO (10:1) solution of the product gave block colorless single crystals suitable for X-ray analysis. M.p 434-436 ^{o}C; ^{1}H NMR (C_6D_6, TMS): δ = 1.33 (s, 9H, C(C*H*$_3$)$_3$), 1.39 (s, 18H, C(C*H*$_3$)$_3$), 1.49 (s, 18H, C(C*H*$_3$)$_3$), 3.27 (d, 1H, *J* =12 Hz, ArC*H*$_2$Ar), 3.35 (d, 1H, *J* = 12 Hz, ArC*H*$_2$Ar), 3.44 (d, 2H, *J* =13 Hz , ArC*H*$_2$Ar), 3.67 (d, 2H, *J* = 14 Hz , ArC*H*$_2$Ar), 4.27 (d, 2H, *J* =14 Hz , ArC*H*$_2$Ar), 4.37 (d, 2H, *J* = 13 Hz , ArC*H*$_2$Ar), 7.33 (s, 2H, Ar*H*), 7.38 (s, 2H, Ar*H*), 7.53 (s, 2H, Ar*H*), 7.60 (s, 2H, Ar*H*), 7.67 ppm (s, 2H, Ar*H*); OH peaks were not observed at rt. ^{13}C NMR could not be obtained due to insufficient solubility; IR (KBr): *v* = 3542m (OH), 3352m

(OH), 3054w, 2960vs, 2906s, 2867s, 1609w, 1481vs, 1391m, 1363s, 1293s, 1206s, 1164m, 1002m, 904m, 885m, 819 cm^{-1} (m); UV/Vis (THF) λ_{max}/nm (ε/$dm^3mol^{-1}cm^{-1}$): 298 (1.267 x 10^4); elemental analysis calcd (%) for $C_{55}H_{67}O_5Na_3 \cdot 3(C_2H_6SO)$: C 65.92, H 7.71; found C 66.17, H 7.47.

$K_3 \cdot$ **^{t}BuC5(H)$_2$**: $KOC(CH_3)_3$ (0.173 g, 1.54 mmol) in THF (10 mL) was added dropwise to a solution of **^{t}BuC5(H)$_5$** (0.416 g, 0.509 mmol) in THF (20 mL). The colorless solution was stirred at rt for 24 hrs. The final yellowish solution was dried under reduced pressure producing a yellowish solid. The solid was redissolved in THF (5 mL), and hexane diffusion caused the precipitation of white solid. Filtration and vacuum drying of the solid led to the crude product as a white powder. The powder was washed twice with pentane (5 mL) to give 0.458 g of pure $K_3 \cdot$ **^{t}BuC5(H)$_2$** (0.494 mmol, 97% yield). Single colorless crystals were obtained after two weeks by the slow evaporation of a concentrated THF/DMSO (5:1 ratio) solution of the product. M.p. 383-384 ^{o}C; ^{1}H NMR (C_6D_6, TMS): δ = 1.51 (s, 45H, C(C*H*$_3$)$_3$), 3.45 (b, 5H, ArC*H*$_2$Ar), 4.29 (b, 5H, ArC*H*$_2$Ar), 7.69 ppm (s, 10H, Ar*H*). No OH peaks were observed at rt. ^{13}C NMR (C_6D_6, TMS): δ = 31.9 (C(*C*H$_3$)$_3$), 33.9 (*C*(CH$_3$)$_3$), 40.3 (Ar*C*H$_2$Ar), 125.5, 129.2, 140.0, 153.6 ppm (aromatic carbons). IR (KBr): *v* = 3413m, 2858vs, 2906s, 2868m, 2360m, 1642m, 1477vs, 1401s, 1362m, 1299s, 1202m, 1123w, 1030s, 953m, 881m, 815 cm^{-1} (m). UV/Vis (THF) λ_{max}/nm (ε/$dm^3mol^{-1}cm^{-1}$): 307 (9.041 x 10^3); elemental analysis calcd (%) for $C_{55}H_{67}O_5K_3$: C 71.38, H 7.30; found C 71.00, H 7.58.

2.3.2.4 Pentaanion synthesis

$Li_5 \cdot$ **^{t}BuC5**: A solution of $LiOC(CH_3)_3$ (0.206 g, 2.58 mmol) in THF (5 mL) was added to a solution of **^{t}BuC5(H)$_5$** (0.418 g, 0.515 mmol) in THF (15 mL). The yellow solution obtained was stirred at rt for 24 hrs. The final yellow-orange solution was vacuum dried yielding a white-

yellow solid. The solid was washed twice with hexane (5 mL portions) and filtered. The white solid obtained gave 0.398 g of $Li_5 \cdot$ **^{t}BuC5** (77% yield).

Method B: A 2 M solution of n-BuLi in pentane (0.0840 g, 1.40 mmol) was added dropwise to a solution of **^{t}BuC5(H)$_5$** (0.214 g, 0.254 mmol) in THF (10 mL) and the reaction mixture was allowed to stir for 24 hrs at rt. The solvent was vacuum evaporated yielding a yellowish powder. Pure $Li_5 \cdot$ **^{t}BuC5** in 78% yield (0.168 g, 0.402 mmol) was obtained after washing the crude material twice with pentane (5 mL portions). Single crystals could be obtained from the slow evaporation of a concentrated THF: DMSO (10:1) solution of product, however the crystals did not diffract well. M.p. 436 ^{o}C; ^{1}H NMR ([D_6]DMSO, TMS): δ = 1.07 (s, 45H, C(CH_3)$_3$), 2.69 (d, 5H, *J* =12 Hz, ArC*H*$_2$Ar), 4.30 (d, 5H, *J* =13 Hz, ArC*H*$_2$Ar), 6.94 ppm (s, 10H, Ar*H*); ^{1}H NMR (C_6D_6, TMS): δ = 1.41 (s, 45H, C(C*H*$_3$)$_3$), 3.57 (b, 5H, Ar*CH*$_2$ Ar), 4.02 (b, 5H, ArC*H*$_2$ Ar), 7.47 ppm (s, 10H, Ar*H*); ^{13}C NMR (C_6D_6): δ = 25.3 (C(*C*H$_3$)$_3$), 31.9 (*C*(CH$_3$)$_3$), 33.7 (Ar*C*H$_2$Ar), 125.6, 129.7, 137.9, 157.7 ppm (aromatic carbons). IR (KBr): *v* = 3048w, 2959vs, 2904s, 2867s, 1606w, 1481vs, 1456s, 1392s, 1361s, 1295vs, 1204m, 1044w, 906w, 875w, 820m, 804 cm^{-1} (m). UV/Vis (THF) λ_{max}/nm (ε/dm^{3}mol^{-1}cm^{-1}): 283 (3.95 x 10^4); elemental analysis calcd (%) for $C_{55}H_{65}0_5Li_5 \cdot 3(C_2H_6SO)$: C 68.14, H 7.78; found C 67.94, H 7.91.

$Na_5 \cdot$ **^{t}BuC5**: A suspension of NaOC(CH_3)$_3$ (0.247 g, 2.58 mmol) in toluene (5 mL) was added to a solution of **^{t}BuC5(H)$_5$** (0.418 g, 0.515 mmol) in toluene (15 mL). The white cloudy solution obtained was stirred at rt for 24 hrs. The final white mixture was vacuum dried yielding a white-yellowish solid. The solid was washed twice with hexane (5 mL portions) and filtered. The white solid obtained gave 0.435 g of $Na_5 \cdot$ **^{t}BuC5** (0.469 mmol, 91% yield). M.p. 466 ^{o}C (decomp); ^{1}H NMR ([D_6]DMSO, TMS): δ = 1.07 (s, 45H, C(C*H*$_3$)$_3$), 2.69 (d, 5H, *J* =13 Hz,

ArC*H*$_2$Ar), 4.14 (d, 5H, *J* =13 Hz, ArC*H*$_2$Ar), 6.79 ppm (s, 10H, *ArH*); ^{13}C NMR could not be obtained due to insufficient solubility; IR (KBr): *v* = 3042w, 2959vs, 2905s, 2867s, 1557w, 1478vs, 1392s, 1361s, 1294vs, 1237w, 1202m, 882 cm^{-1} (w). UV/Vis (THF) λ_{max}/nm (ε/dm^{3}mol^{-1}cm^{-1}): 287 (2.511 x 10^4); elemental analysis calcd (%) for $C_{55}H_{67}O_5Na_5$: C 71.72, H 7.11; found C 71.43, H 7.43.

K_5·**^{t}BuC5**: The same procedure as the one performed for Na_5·**^{t}BuC5** was followed, using **^{t}BuC5(H)$_5$** (0.418 g, 0.515 mmol) and $KOC(CH_3)_3$ (0.291 g, 2.59 mmol). Filtration gave 0.451 g of K_5·**^{t}BuC5** as a white crystalline powder (0.448 mmol, 87% yield). M.p. 465 ^{o}C; ^{1}H NMR ([D$_6$]DMSO, TMS): δ = 0.97 (s, 45H, C(C*H*$_3$)$_3$), 2.51 (d, 5H, *J* =16 Hz, ArC*H*$_2$Ar), 4.18 (d, 5H, *J* =13 Hz, ArC*H*$_2$Ar), 6.55 ppm (s, 10H, *ArH*). ^{13}C NMR ([D$_6$]DMSO, TMS) δ = 31.9 (C(*C*H$_3$)$_3$), 32.7 (*C*(CH$_3$)$_3$), 33.5 (Ar*C*H$_2$ Ar), 123.5, 127.9, 130.2, 163.9 ppm (aromatic carbons). IR (KBr): *v* = 2961vs, 2904s, 2866s, 2342w, 1601m, 1479vs, 1392s, 1317s, 1297vs, 1235m, 1200s, 1127s, 882 cm^{-1} (m). UV/Vis (THF) λ_{max}/nm (ε/dm^{3}mol^{-1}cm^{-1}): 290 (4.191 x 10^4), 261 (3.844 x 10^4); elemental analysis calcd (%) for $C_{55}H_{67}O_5K_5$·$(C_4H_8O)_3$·CH_2Cl_2: C 62.69, H 7.04; found C 62.73, H 7.28.

2.3.3 Solubility and Air-sensitivity of Calixanions

All calixarene salts are very soluble in $CHCl_3$ and DMSO but less soluble in benzene or toluene. Most of the mono-, di- and trianionic salts are air stable, so it is easy to purify them by recrystallization. Their crystals readily lose solvent molecules to become powder. The salts Na·**^{t}BuC5(H)$_4$**, K·**^{t}BuC5(H)$_4$**, and M·**^{t}BuC7(H)$_6$** (M = K, Rb, Cs) were initially obtained as white powders. When they were left for one month in air they become green-brown and the ^{1}H NMR showed a significant increase in the amount of parent calixarene. Most of the

crystallizations were done in air, except for the air-sensitive pentaanions; their manipulation was performed under inert atmosphere.

2.3.4 VT-NMR studies

Temperature-dependent ^{1}H NMR spectra were recorded in a Varian XL-300 spectrometer at 300 MHZ, and the coolant was liquid nitrogen. The rate constants (k_c in s^{-1}) for conformational interconversion at the coalescence temperature were calculated from the equation $k_c = 2.22[(\Delta\nu^2 + 6J^2_{AB})^{1/2}]$.[87,98-100] The free energy barrier to conformational interconversion in kcal·mol^{-1} was calculated from the equation $\Delta G^{\pm} = 4.58T_c(10.32 + \log T_c/k_c)/1000$. As in previous work, we assume an accuracy of ±5 ^{o}C for the value of T_c, an accuracy of ±15 Hz for the value of Δν, and an accuracy of ±2 Hz for the value of J_{AB}, and estimate that the values should be accurate to ±0.4 kcal·mol^{-1}.[87,98,99] The value of Δν was taken as the difference in Hz between the frequencies of the methylene doublets undergoing coalescence (observed at a sufficiently low temperature that the peaks are sharp).[87,98-100]

2.3.5 General X-ray crystal structure information

All crystal samples were colorless. X-ray data for Na_3**^{t}BuC5(H)$_2$**·2THF and **[**K_2·**^{t}BuC5(H)$_3$**·4DMSO]$_2$ were collected on a Bruker SMART APEX CCD diffractometer (UCSD) while all other data were collected on a Bruker SMART 1000 CCD detector. Both diffractometers used variable low temperature and Mo Kα radiation, and SADABS[101] absorption corrections were applied. The crystals used in the experiments were coated with mineral oil, and data were collected under a variable low-temperature nitrogen stream. Crystallographic data are summarized in Table 3. All structures were solved by direct methods and subsequent difference Fourier syntheses and refined by full matrix least-squares methods against F^2 (SHELX 97).[102] Most solvent molecules as well as some *tert*-butyl groups are positionally disordered. Disorder

for some *tert*-butyl groups was due to 2-fold axis, and was modeled using partial occupancies (PART instruction).[102] Some other disordered molecules and solvents were refined using a combination of restraints on the distances while keeping the disordered parts similar (use of the SADI and SAME instructions).[102] All non-hydrogen atoms were refined anisotropically except for atoms of disordered fragments which were refined with isotropic thermal parameters. H atoms were constrained with a riding model. In the crystal structures of $[Na\cdot\mathbf{^tBuC5(H)_4}\ THF]_2$, and $[Na_3\mathbf{^tBuC5(H)_2}\cdot 2THF]_2$, disordered solvent molecules (7 THF molecules in $[Na_3\mathbf{^tBuC5(H)_2}\cdot 2THF]_2$ and one pentane molecule in $[Na\cdot\mathbf{^tBuC5(H)_4}\ THF]_2$) were treated with the program SQUEEZE.[103] Corrections of the X-ray data for $[Na_3\mathbf{^tBuC5(H)_2}\cdot 2THF]_2$ and $[Na\cdot\mathbf{^tBuC5(H)_4}\ THF]_2$ by SQUEEZE (290 and 54 electron cell, respectively), were close to the required values (280 and 42 electron cell, respectively), similar to the results described previously.[74] The programs ORTEP32[104] and POV-RAY[105] were used to generate the X-ray structural diagrams pictured in this chapter.

2.4 Conclusions

We have reported the high-yield synthesis and complete characterization for a comprehensive series of *p-tert*-butylcalix[5]arene mono-, di-, tri-, and pentaanions and *p-tert*-butylcalix[7]arene mono- and dianions. The synthesis consists of the simple addition of base to the parent calixarene, but the choices of the base, stoichiometry, and solvent are very important.

NMR and X-ray structural studies show that the complexes with lithium and sodium are in their cone conformations and the structures with potassium, rubidium and cesium contain the flattened cone conformation due to their M-C π-arene interactions. The degree of flexibility of the ring depends mainly on the cavity size, nature of the metal and the deprotonation level of the complex.

We have illustrated the variety of structural types available to alkali metal salts of *p-tert*-butylcalix[5]arene and *p-tert*-butylcalix[7]arene in the solid state. These include monomeric and dimeric units. Bulky *tert*-butyl groups in the upper rim of the **^{t}BuC5(H)$_5$** and **^{t}BuC7(H)$_7$** appear to block polymer formation in the solid state. Alkali metal atoms were found to bind the calixarene ring in the *endo* and *exo* positions. Alkali metal cation-π interactions can be observed for most alkali metals, and these interactions become progressively more important as the size of the alkali metal increases.

CHAPTER 3

CALIX[5]ARENE BISMUTH(III) AND ANTIMONY(III) COMPLEXES

3.1 Introduction

Calixarenes have found numerous applications in many fields, including catalysis[106] and complexation of ions[107,108] and cations[109,110] for sensing and waste remediation. Recently, interest has focused on the synthesis of metallocalixarenes due to their potential for modeling heterogeneous oxygen-rich surfaces.[70]

In the last two decades most of the research on metallocalixarenes has focused on complexes containing transition and f block metals, while the number of main group metallocalixarenes is very limited.[51,61] In particular, relatively few bismuth and antimony calixarene complexes have been reported despite their potential as precursors for material, devices for high-tech applications, and building blocks for supramolecular structures.[6,111]

Main group calixarene complexes reported in the literature (M = B, As, Al, Ga, Zn, Ge, Sn) are usually prepared by either parent or ether-substituted calixarenes in reactions with organometals, metal amides or metal alkoxides.[112-119] Most of these complexes are supported by even numbered calix[n]arene (4 and 8) ligands and the cavity is usually fully metallated. Our group, on the other hand, has described the synthesis and characterization of a large series of mono-, di-, tri-, and pentaanionic calixarene alkali metal salts,[74,75,120] and has already demonstrated their utility as an entry into both main group and transition metallocalixarenes (including the first reported antimony calixarene) that were inaccessible using the traditional parent calixarene as precursor.[57,65]

Our group was the first to report bismuth(III) and antimony(III) calixarene complexes,[57] and we recently published a more general procedure for the preparation of bismuth **RC4(H)$_4$** (R

= H, ^{t}Bu, allyl) complexes.[58] Most of these complexes are bimetallic with the calixarene ligands fully saturated and featuring $M_2(\mu\text{–}O)_2$ central cores.

We are currently interested in forming partially metallated calixarenes that may be used as precursors for heterobimetallic calixarene complexes. In the bismuth/antimony calix[4]arene complexes, however, no partially metallated complexes with free OH groups were achieved. We therefore decided to explore the coordination chemistry of larger calix[n]arene (n = 5-8) ligands in order to take advantage of the larger cavity size and flexibility in comparison to those of calix[4]arenes.

In this chapter, we describe the synthesis and characterization of mono- and bimetallic bismuth(III) and antimony(III) complexes of calix[5]arenes achieved by the use of the triply deprotonated calix[5]anions as precursors or by the use of parent calixarenes in reaction with strong bases. This is the first part of two investigations involving Bi and Sb complexation to calix[n]arenes (n = 5-8). The second part will be presented in Chapter 4 where the reactivity of Bi and Sb with calix[n]arenes (n = 6-8) and the description of the coordination changes upon increase of flexibility and conformational exchange will be discussed.[121]

For the bismuth and antimony calix[5]arene complexes, we will discuss here the synthetic and structural trends encountered upon changing the nature of the group in the para position, the substitution level in the calixarene cavity, and the strength of the base used in the synthesis. Some of the preliminary reactivity of the free OH groups present in monometallic calixarenes will be addressed as well.

3.2 Results and discussion.

3.2.1 Synthesis of *p-tert*-butylcalix[5]arene [^{t}**BuC5(H)$_5$**] complexes.

The reaction of the trianionic calix[5]arene salts M'$_3$·^{t}**BuC5(H)$_2$** (M' = Li, Na, K)[120] with one equivalent of MCl_3 (M = Sb and Bi) in THF or toluene for 48 hrs at room temperature, produces complexes [Bi{^{t}**BuC5(H)$_2$**}] **3.1** and [Sb{^{t}**BuC5(H)$_2$**}] **3.2** (Scheme 3.1). In general, the reaction gives a mixture of the [M{^{t}**BuC5(H)$_2$**}] monometallic product and parent calixarene. Purification of the products from the reaction mixture by successive toluene washing cycles (to remove parent calixarene impurity) yields complexes **3.1** and **3.2** in yields of 81% and 65%, respectively (when Li$_3$·^{t}**BuC5(H)$_2$** is used). Both complexes are partially soluble in benzene at room temperature and highly soluble in hot toluene, but they are completely insoluble in any saturated hydrocarbon solvent. Both complexes are air sensitive and stable in solid state (up to three months under inert atmosphere) but they start to decompose to parent calixarene in solution after 4 days. We also prepared complexes **3.1** and **3.2** by the 1:1 reaction of parent calixarene with M(O^{t}Bu)$_3$ (M = Bi, Sb) at room temperature or with Bi[N(SiMe$_3$)$_2$]$_3$ at 95 ^{o}C (Scheme 3.1), however in both cases purification is more difficult and the yields are lower than 50%.

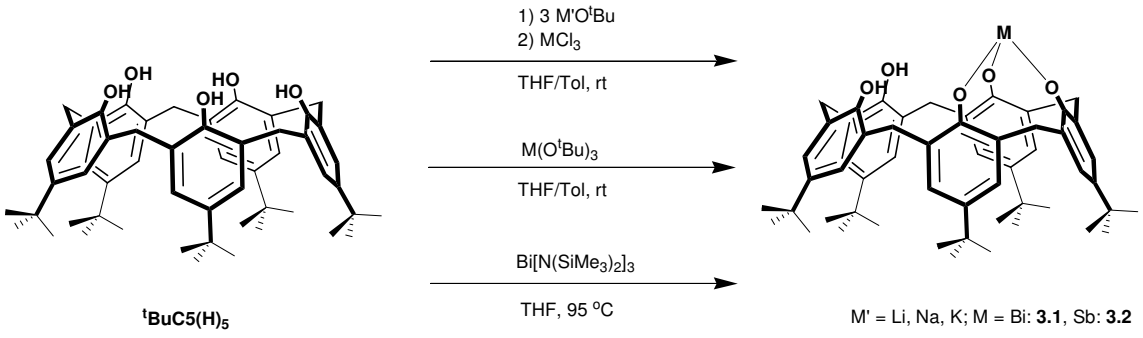

Scheme 3.1 Preparation of ^{t}**BuC5(H)$_5$** monometallic bismuth and antimony complexes.

In reactivity studies of the smaller main group elements such as Si, P and As with calix[4]arene **RC4(H)$_4$** (R = H, ^{t}Bu) and *para-tert*-butylcalix[5]arene [^{t}**BuC5(H)$_5$**] ligands,

Lattman et al. prepared mono- and dinuclear complexes by changing the calixarene/main group element reaction ratio from 1:1 to 1:2, respectively.[114,122-126] However, for the heavier Sb and Bi atoms the reaction of M'$_4$·**RC4** tetraanions (M' = Li, Na) with either 1 or 2 equivalents of MCl_3 (M = Bi, Sb) produces complexes in a 1:2 calix/metal ratio.[58] The only way to prepare monometallic complexes with **RC4(H)$_4$** ligands is to block the 1,2 or 1,3 phenol positions of the cavity.[95,113,116] Complexes **3.1** and **3.2** are the first examples of monometallic bismuth and antimony complexes with calixarene ligands that still contain free OH groups. The ability to prepare complexes **3.1** and **3.2** in good yield can be attributed to the use of a true trianionic precursor and the appropriate cavity size and flexibility of the **^{t}BuC5(H)$_5$** ligand.

3.2.2 Synthesis of substituted calix[5]arene complexes

Previous VT-NMR measurements of the monobenzyl lower rim substituted **^{t}BuC5(Bn)(H)$_4$** ligand showed that over a temperature range of 20-95 ^{o}C the only conformer present in solution was the "cone-in."[79] The four remaining OH groups on the cone-in **^{t}BuC5(Bn)(H)$_4$** are oriented in the same direction and are closer to each other than the OH groups in parent **^{t}BuC5(H)$_5$**, offering a good environment for the complexation of multivalent ions. When **^{t}BuC5(Bn)(H)$_4$** was treated with one equivalent of Bi(O^{t}Bu)$_3$ in pentane, yellow needles were obtained. X-ray and elemental analyses showed that a monometallic complex [Bi{**^{t}BuC5(Bn)(H)**}] **3.3** featuring a free OH group was obtained (see Scheme 3.2). We find that even though **^{t}BuC5(Bn)(H)$_4$** resembles the calix[4]arenes in the fact that 4 OH groups are available for reactivity, its larger cavity size and flexibility favors the preparation of the monometallic complex **3.3** instead of a bimetallic complex with the $Bi_2(\mu\text{–}O)_2$ core usually observed in calix[4]arene complexes.[58]

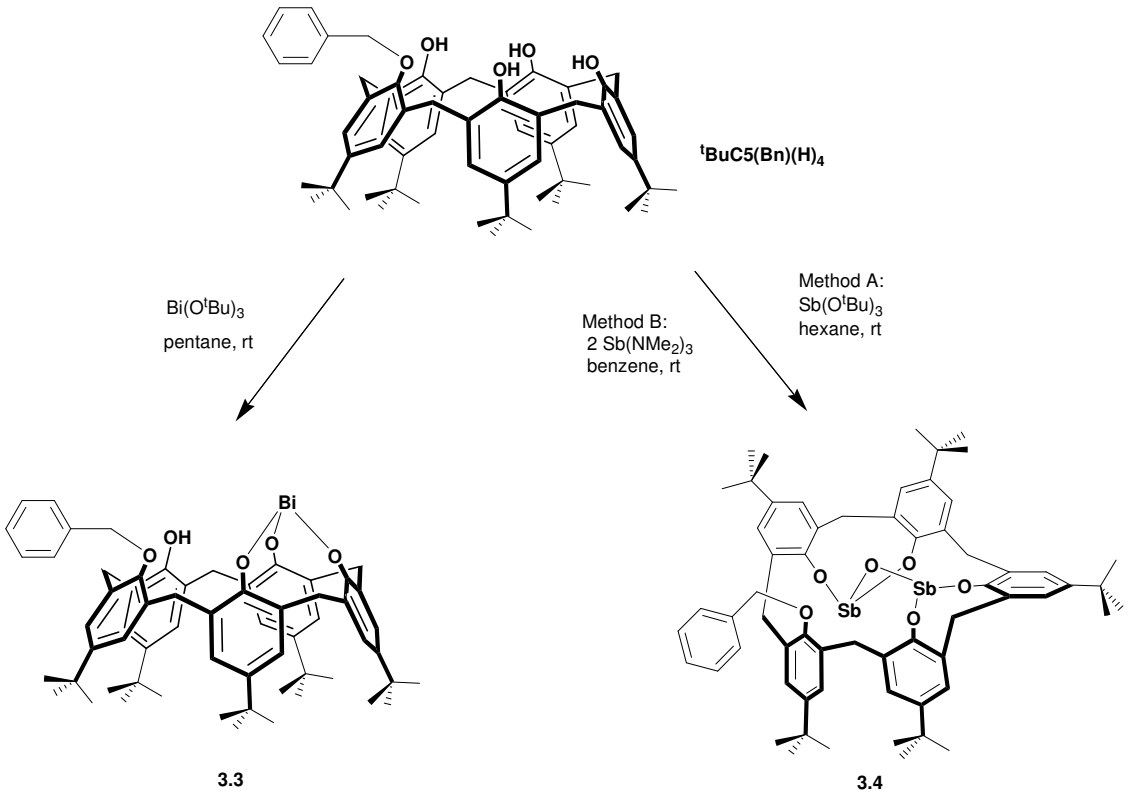

Scheme 3.2 Preparation of **^{t}BuC5(Bn)(H)$_4$** bismuth and antimony complexes.

Treatment of **^{t}BuC5(Bn)(H)$_4$** with SbR_3 (R = NMe_2, O^tBu) in a 1:1 ratio results in the precipitation of colorless needles with composition [Sb_2O{**^{t}BuC5(Bn)**}] **3.4**, as illustrated in Scheme 3.2. The bimetallic complex contains an oxygen bridge between the two antimony atoms, featuring an overall [$(ArO)_2Sb]_2(\mu–O)$ core. The presence of the extra bridging oxygen in complex **3.4** inhibits the formation of the $Sb_2(\mu–O)_2$ core observed in the [Sb_2Cl_2{**RC4**}] antimony complexes reported by our group.[57,58]

Complex **3.4** can also be obtained by the reaction of **^{t}BuC5(Bn)(H)$_4$** and $Sb(NMe_2)_3$ in a 1:2 ratio for 48 hrs in benzene (Scheme 2). In this case the product, obtained in high purity, exhibits better solubility so it can be analyzed by ^{1}H NMR spectroscopy. Attempts to prepare a monometallic antimony complex of **^{t}BuC5(Bn)(H)$_4$** by decreasing the $Sb(O^tBu)_3$ or $Sb(NMe_2)_3$

amount to 0.5 equivalents were unsuccessful, yielding only the bimetallic complex **3.4** in lower yields.

Complex **3.4** contains a bridging oxygen that does not belong to the calixarene. From previous reports on preparation of bismuth or antimony oxo clusters it has been observed that the use of $Bi(OSiR_3)_3$, $Bi(O^tBu)_3$, or $Sb(O^tBu)_3$ can lead to the elimination of R-O-R molecules (R = ^{t}Bu, $OSiMe_3$) allowing the formation of bridging oxygen atoms within the core structures.[127-129]

This precedent suggested that the -O^{t}Bu moiety could be the source of the bridging oxygen atom in complex **3.4**, however $Sb(NMe_2)_3$ (Scheme 3.2) also allowed the formation of complex **3.4**. When we performed the reaction of **^{t}BuC5(Bn)(H)$_4$** with $Sb(O^tBu)_3$ (1:2 ratio) in deuterated benzene, the product **3.4** was obtained but no ^{t}BuO^{t}Bu was observed. We therefore believe that rather than the -O^{t}Bu moiety, moisture in the calixarene is the most probable source for the bridging oxygen. Lattman and coworkers also observed the formation of [As_2O{**RC4**}] complexes similar to **3.4** when they used $As(NMe_2)_3$ and calixarene ligands that contained moisture.[114]

3.2.3 Synthesis of *p*-benzylcalix[5]arene [**BnC5(H)$_5$**] complexes

The first synthetic approach we used to prepare monometallic Bi and Sb complexes of **BnC5(H)$_5$** involved the use of calixanion precursors.[120] To date no alkali metal salts of **BnC5(H)$_5$** have been reported, however, Asfari and coworkers prepared **BnC5(H)$_5$** alkali metal salts *in situ* as precursors for the preparation of pentaalkyl ester derivatives of **BnC5(H)$_5$**.[80] Their results suggested that we could prepare trianionic **BnC5(H)$_5$** precursors for our metallic complexes, analogous to our trianionic **^{t}BuC5(H)$_5$** precursors.[120] Indeed, when **BnC5(H)$_5$** was reacted with 3 equivalents of M'O^{t}Bu (M' = Li, Na) in THF, trianionic salts of **BnC5(H)$_5$** were achieved in high yields. Unfortunately the attempts to obtain monometallic Bi and Sb complexes

by the reaction of the M'$_3$·**BnC5(H)$_2$** precursors with MCl_3 yielded mainly parent calixarene and only a trace of new complexes.

Our second approach used parent calixarene as precursor. When **BnC5(H)$_5$** was reacted in a 1:1 molar ratio with $Bi(O^tBu)_3$ a new product, together with unreacted parent calixarene, was observed by ^{1}H NMR. The increase of the reaction ratio to 1:2.5 **BnC5(H)$_5$**:$Bi(O^tBu)_3$ allowed the complete consumption of parent calixarene and the preparation of cleaner product. After crystallization by diffusion of hexanes into a concentrated THF/DME/DMSO (1:2:0.1) solution we obtained the bimetallic complex $[Bi_2O\{$**BnC5(H)**$\}]_2$ **3.5** in 68 % yield (Scheme 3.3). The attempts to increase the yield of complex **3.5** by reacting **BnC5(H)$_5$** with 2 or 3 equivalents of $Bi[N(SiMe_3)_2]_3$ in toluene or THF were unsuccessful, yielding intractable yellow solids in all cases.

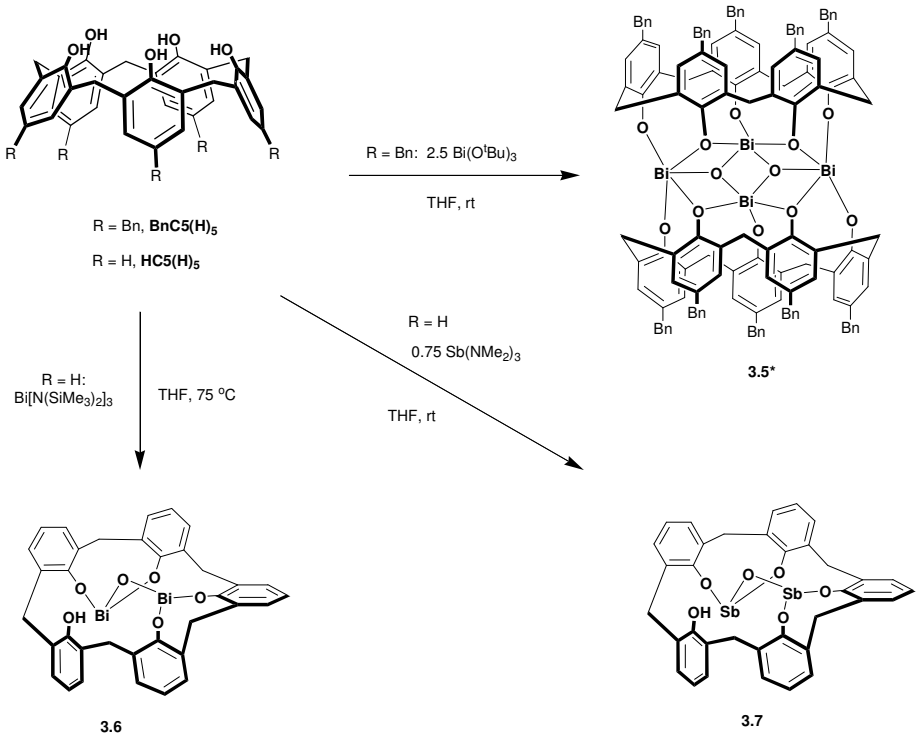

Scheme 3.3 Preparation of **BnC5(H)$_5$** and **HC5(H)$_5$** bismuth and antimony complexes. *Each calixarene unit in complex **3.5** contains an OH group (not located).

In order to obtain the analogous **BnC5(H)$_5$** antimony complexes, we treated the parent calixarene with Sb(O^{t}Bu)$_3$ or Sb(NMe$_2$)$_3$ in 1:1 or 1:2 [**BnC5(H)$_5$**:Sb(NMe$_2$)$_3$] ratios, however, all attempts proved unsuccessful, yielding insoluble white solids in all cases.

3.2.4 Synthesis of *p*-H-calix[5]arene [**HC5(H)$_5$**] complexes

HC5(H)$_5$ is less reactive than **^{t}BuC5(H)$_5$** and **BnC5(H)$_5$**. Attempts to synthesize monometallic complexes by the reaction of **HC5(H)$_5$** with M(O^{t}Bu)$_3$ (M = Sb, Bi) or by the reaction of trianionic precursors M'$_3$·**HC5(H)$_5$** (M' = Li, Na) with MCl$_3$ were unsuccessful, yielding either insoluble solids or parent calixarene. Based on the precedent of the successful preparation of a large series of bismuth aryloxides[43] and the first **^{t}BuC8(H)$_8$** bismuth cluster[57] by the exchange reaction of Bi[N(SiMe$_3$)$_2$]$_3$ and the appropriate aryloxide, we reacted **HC5(H)$_5$** with one equivalent of Bi[N(SiMe$_3$)$_2$]$_3$ at 75 ^{o}C for 16 hrs (Scheme 3.3). After washing the crude material with ether and recrystallizing from DME, a single product was isolated (**3.6**). This complex **3.6** is very soluble in DMSO, less soluble in benzene, and completely insoluble in any saturated hydrocarbon solvent. Single crystals of complex **3.6** were obtained by the slow evaporation of a concentrated DME solution; however the quality of the crystals was insuficient for X-ray diffraction. We suggest **3.6** as the structure of this new complex (see Scheme 3.3), based on the ^{1}H NMR spectrum and the elemental analysis data.

In order to prepare the analogous antimony complex, we proceeded to react **HC5(H)$_5$** with Sb(NMe$_2$)$_3$ in a 1:1 or 1:2 ratio in THF. An insoluble white precipitate was obtained in both cases. However, when the ratio of the Sb(NMe$_2$)$_3$ was decreased to 0.75, the ^{1}H NMR spectrum showed a new complex in mixture with unreacted **HC5(H)$_5$**. Single crystals of pure product were obtained by hexane diffusion into a concentrated benzene solution of crude material. The X-ray structure of the product shows a bimetallic complex [Sb$_2$O{**HC5(H)**}] **3.7** containing a similar

core as the one observed for complex **3.4** (Scheme 3.3). Attempts to prepare the monometallic complex [Sb{**HC5(H)$_2$**}] by decreasing the ratio of the Sb(NMe$_2$)$_3$ to 0.5 equivalents or using Sb(O^{t}Bu)$_3$ were unsuccessful, yielding the bimetallic complex [Sb$_2$O{**HC5(H)**}] **3.7** in lower yields. Complexes **3.6** and **3.7** are air and moisture sensitive and start to decompose after five days in solution.

3.2.5 Reactivity of monometallic complexes

It has already been demonstrated that the cavity size of **^{t}BuC5(H)$_5$** presents an ideal balance between constraint and flexibility to allow the preparation of complexes with more than one heteroatom in the lower rim.[130,131] We therefore expected complexes **3.1** and **3.2** to be highly reactive; the mobility of the calixarene and the two remaining OH groups could facilitate the addition of a second metal in the cavity. Indeed, when complex **3.1** is reacted in a 1:1 ratio with Bi(O^{t}Bu)$_3$ in benzene, a bimetallic complex **3.8** is produced (Equation 3.1). Pure product can be isolated in 41% yield after slow evaporation from an ether solution of crude material. X-ray quality crystals of complex **3.8** were obtained by recrystallization from an Et$_2$O/DMSO mixture (5:1). The crystal structure of complex **3.8** shows a dimer with a Bi$_4$O$_2$(OR)$_4$ core similar to the one observed in complex **3.5**.

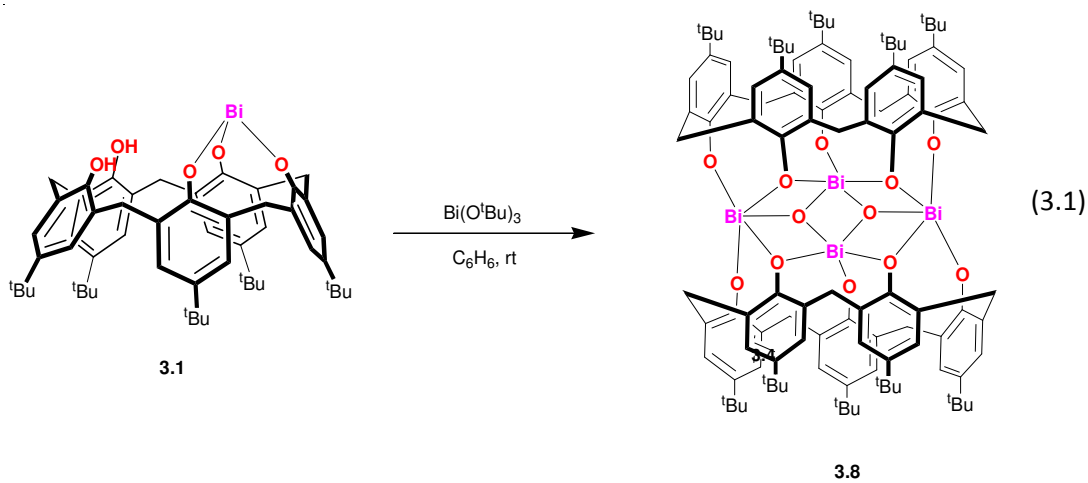

3.1 3.8

(3.1)

The reactivity of complex **3.2** is similar to that observed for complex **3.1**. Reaction of **3.2** with $Sb(O^tBu)_3$ in a 1:1 ratio at rt led to the bimetallic complex **9** (Scheme 3.4). Alternatively complex **3.9** can be obtained from the reaction of **^{t}BuC5(H)$_5$** with two equivalents of $Sb(O^tBu)_3$ in hexanes or $Sb(NMe_2)_3$ in benzene with 43% and 48% yields, respectively. X-ray quality crystals of **3.9** can be obtained by slow evaporation of a hexane/benzene (1:2) solution to give **3.9**·$3C_6H_6$ or by the slow evaporation of a concentrated hexane/DMSO (4:1) solution to give **3.9**·2DMSO. NMR characterization of the two crystalline forms of complex **3.9** was not possible due to their very poor solubility after recrystallization. Complexes **3.8** and **3.9** are quite air and moisture sensitive.

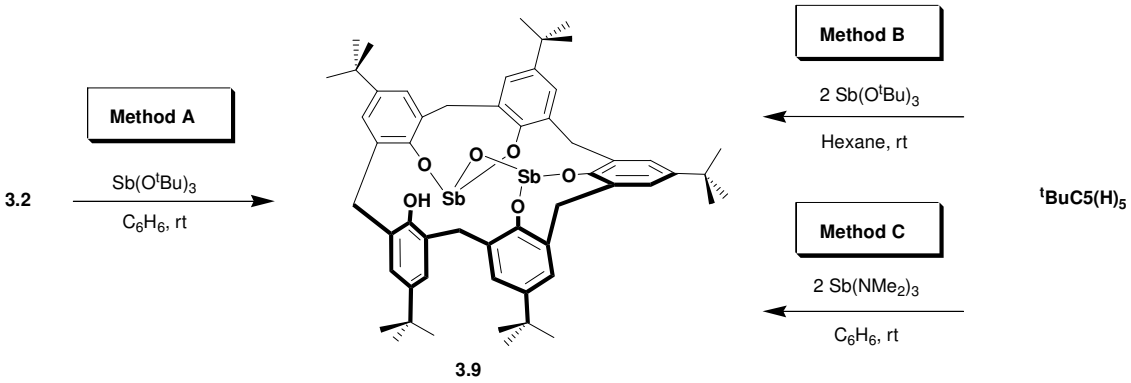

Scheme 3.4 Different pathways for the synthesis of complex [Sb_2O{**^{t}BuC5(H)**}] **3.9**.

We attempted to prepare heterobimetallic Sb/Bi complexes by reacting **3.1** or **3.2** with one equivalent of the respective $M(O^tBu)_3$ in benzene or toluene. The best results were obtained using benzene when stirring for 2 h as two products were observed. However, the products were never isolated due to their poor stability in solution.

3.3 Spectral data

^{1}H NMR spectroscopy is an important tool for the conformational analysis of the calix[n]arenes (n = 4, 5).[79] These two ligands show mainly four up/down conformations (Figure

3.1) that can be designated as cone, partial cone, 1,2-alternate and 1,3-alternate, though in calix[5]arene the conformational assignations are less accurate due to the larger cavity size and flexibility.

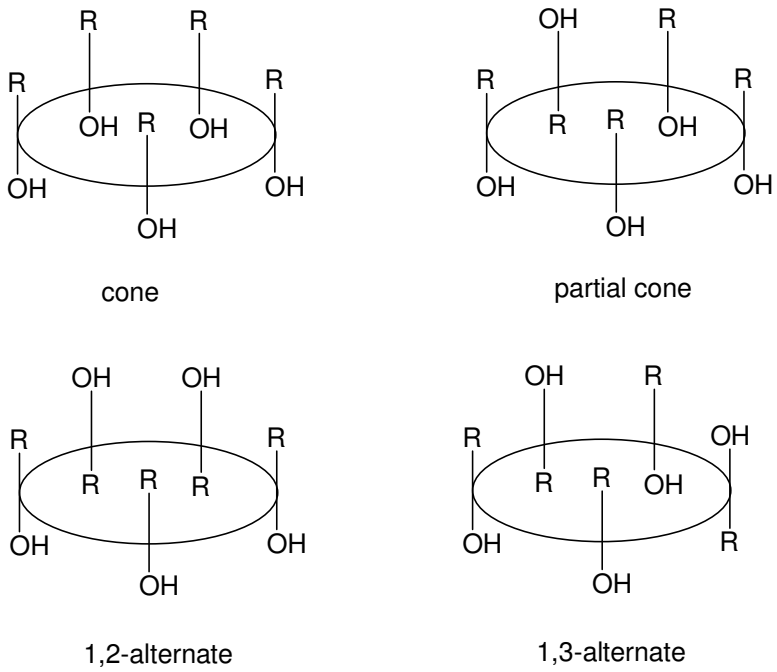

Figure 3.1 Idealized conformations of calix[5]arenes.

The two monometallic complexes **3.1** and **3.2** display very different solution behavior. The ^{1}H NMR spectrum of complex **3.1**, for example, shows three pairs of doublets and five broad signals for the $ArCH_2Ar$ groups, and also three signals each for the ^{t}Bu and aromatic groups (Figure 3.2). This NMR pattern is unusual, and the broad peaks indicate that complex **3.1** is fluxional at room temperature. In contrast, the ^{1}H NMR spectrum for complex **3.2** shows ten well defined pairs of doublets for methylene groups, integrating to one proton each, and five singlets for the ^{t}Bu groups (Figure 3.2). This spectrum is a clear indication of C_1 symmetry.[79] Monometallic complexes **3.1** and **3.2** both have two sharp singlets for OH groups in the downfield range of 9.51-11.97 ppm (OH for **^{t}BuC5(H)$_5$** is at 8.66 ppm).

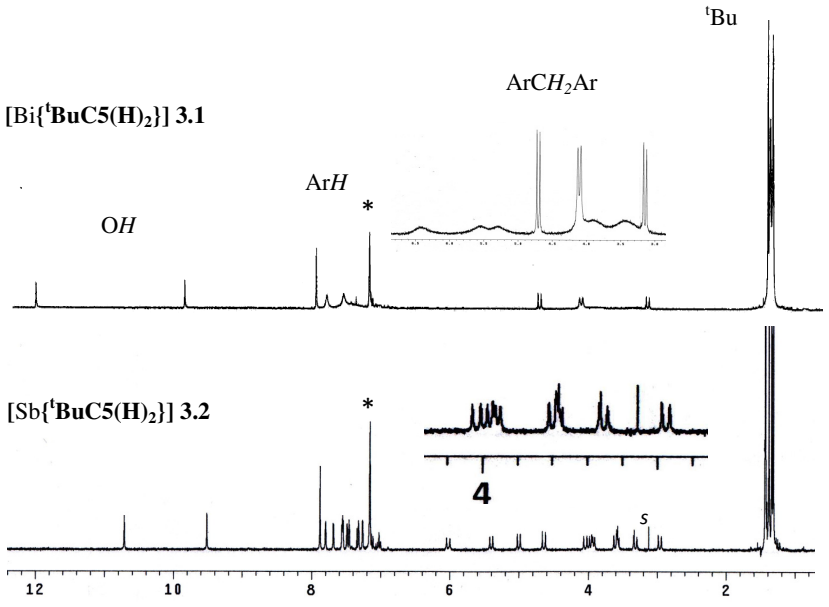

Figure 3.2 ^{1}H NMR spectra of complexes [Bi{^{t}**BuC5(H)$_2$**}] **3.1** and [Sb{^{t}**BuC5(H)$_2$**}] **3.2** in *C_6D_6. *s* = toluene.

Bimetallic antimony complexes **3.4** and **3.7** display complicated ^{1}H NMR spectral patterns (Figure 3.3). Complex **3.4** produces ten pairs of doublets for methylene protons and five singlets for ^{t}Bu groups, while complex **3.7** displays eight doublets in the methylene area. Both complexes show a C_1 symmetry in solution.[79] Complex **3.7** has an OH peak that is quite downfield, at 10.58 ppm.

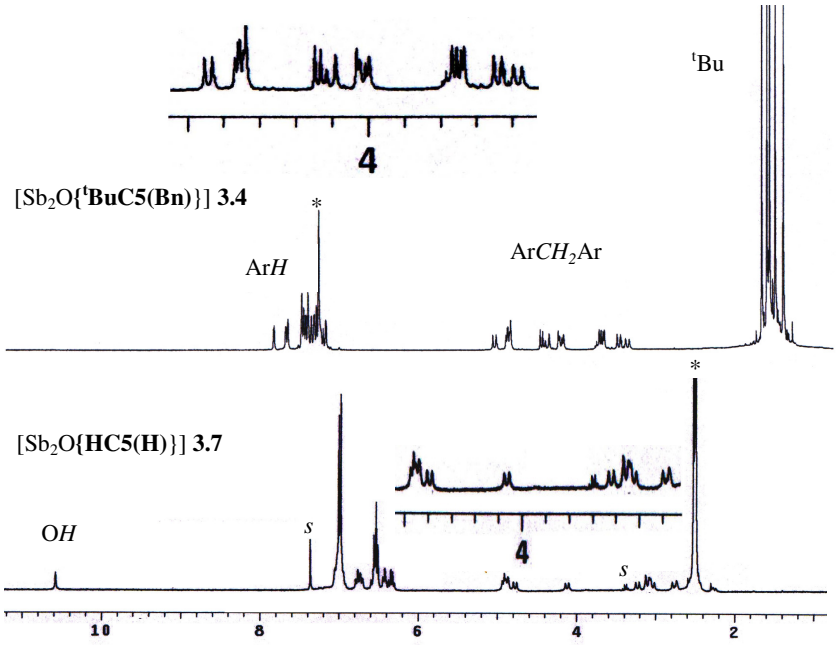

Figure 3.3 ^{1}H NMR spectra of complexes [$Sb_2O\{^{t}$**BuC5(Bn)**$\}$] **3.4** in $^{*}C_6D_6$ and [$Sb_2O\{$**HC5(H)**$\}$] **3.7** in *DMSO-d_6. *s* = residual solvent.

The ^{1}H NMR spectra of bimetallic bismuth complexes **3.5** and **3.8** differ from the antimony analogues (Figure 3.4). Complex **3.5** gives two pairs of doublets for $ArCH_2Ar$ groups at 3.02 and 4.36 ppm (J = 13.2 Hz), one singlet for the CH_2Ph moiety at 3.73 ppm, and a multiplet for the aromatic protons. Complex **3.8** shows two broad signals at 3.43 and 4.71 (each integrating to 5), one singlet for aromatic protons, and one singlet for ^{t}Bu groups. The remaining OH groups for **3.5** and **3.8** were not observed at room temperature. The presence of two signals in the methylene region and the single peaks for aromatic and ^{t}Bu groups, indicate that the average conformation of the calixarene ring in both complexes is the cone. The broad peaks also suggest that both complexes are fluxional at room temperature.[132]

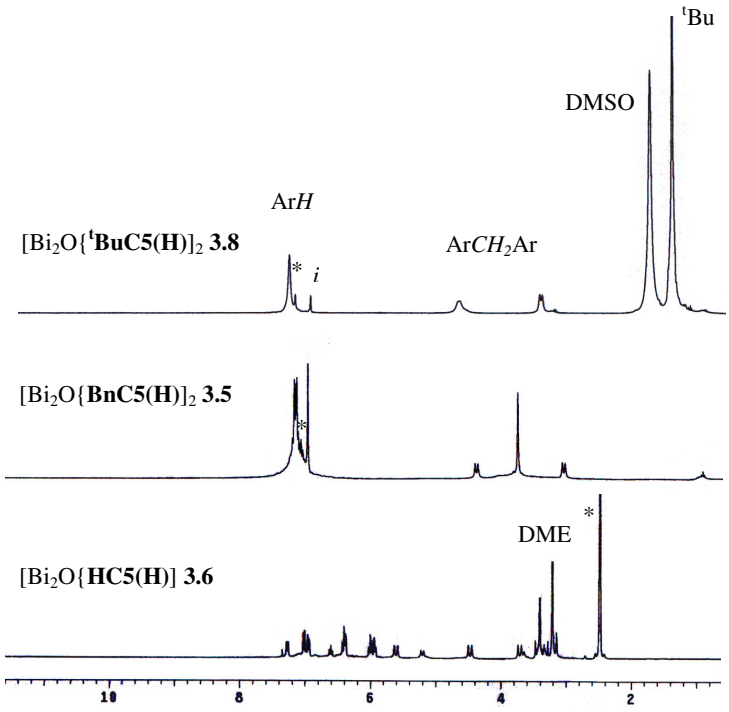

Figure 3.4 ^{1}H NMR spectra of complexes [$Bi_2O\{^{t}$**BuC5(H)**$\}]_2$ **3.8**, and [$Bi_2O\{$**BnC5(H)**$\}]_2$ **3.5** in *C_6D_6, and [$Bi_2O\{$**HC5(H)**$\}]_2$ **3.6** in *DMSO-d_6. *i* = impurity.

Assuming that all the bimetallic bismuth complexes will contain a similar core structure, we expected complex **3.6** to display similar methylene patterns to those observed for complexes **3.5** and **3.8**. However, the ^{1}H NMR spectrum of complex **3.6** displays six doublets for methylene protons (geminal coupling due to nonequivalent methylene hydrogens), with two of the doublets being half the intensity of the others (Figure 3.4). These smaller doublets, due to the unique methylene bridging group, are separated by about 1 ppm. This is usually a good indication of an overall C_s symmetry. The noticeable change of the methylene patterns, and the fact that an OH peak is located at 13.3 ppm, suggested that the conformation of complex **3.6** had changed from the expected cone (as observed in **3.5** and **3.8**) to 1,2-alternate. It is possible that complexes **3.5** and **3.8** are in dimeric form in solution and can retain cone conformations while complex **3.6** is monomeric and adopts the 1,2-alternate conformation (Scheme 3.4).

3.4 Crystal and molecular structures.

3.4.1 Calixarene antimony complexes

Crystal structures of **3.4**, **3.7**, **3.9**·$3C_6H_6$ and **3.9**·2DMSO are shown in Figures 3.5-3.8, respectively, and selected bond distances and angles are listed in Table 3.1. Complexes **3.4**, **3.7**, **3.9**·$3C_6H_6$ and **3.9**·2DMSO all have a $[(RO)_2Sb]_2(\mu\text{-}O)$ core with two oxygen bridged antimony atoms, similar to the cores observed in $[As_2O\{\mathbf{RC4}\}]$ bimetallic complexes reported by Lattman and coworkers.[114] The Sb-O-Sb angles are close to 134° and are slightly larger than those observed for $Sb_2(\mu\text{-}O)_2$ and other organometallic $M_2(\mu\text{-}O)_2$ cycles supported by calixarene ligands [100.1(8)-130.1(4)°].[115,116,133-135]

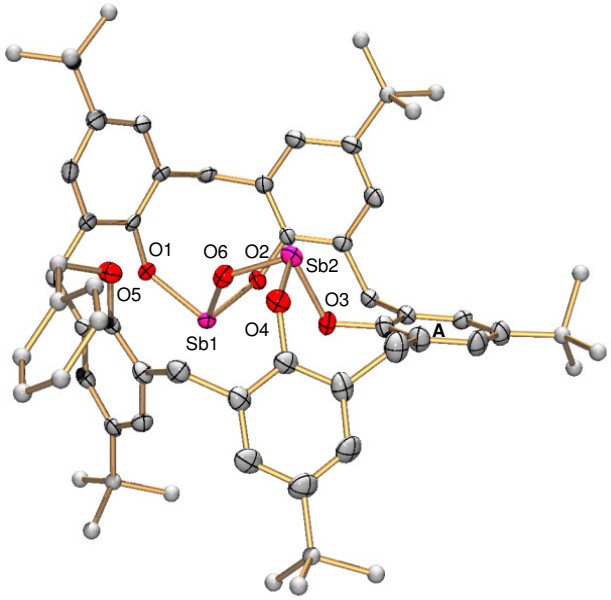

Figure 3.5 ORTEP diagram of complex **3.4** with thermal ellipsoids at the 50% probability level. H atoms and non-coordinated solvents are omitted for clarity.

In complexes **3.4**, **3.7**, and **3.9**·$3C_6H_6$ the Sb-(μ-O) bond lengths range from 1.922(4) to 1.946(6) Å. In **9**·2DMSO the solvent coordination apparently causes a larger variation, with Sb-(μ-O) distances of 1.890(6) and 1.986(6) Å. All these Sb-O distances are shorter than those

observed in the $Sb_2(\mu\text{-}O)_2$ rings of the $[Sb_2Cl_2\{\mathbf{RC4}\}]$ calixarene complexes reported by our group [2.0274(16)-2.4574(17)].[57,58] (see Table 3.2). All of the X-ray structures show monomeric calixarene units in a distorted 1,2-alternate conformation (with the ring A located in the central plane) despite the fact that complex **3.4** is mono-substituted with a benzyl group in the lower rim and that complex **3.5** lacks *tert*-butyl groups in the *para* positions. This conformation is similar to the one observed in some phosphorus and silicon-based $^{t}\mathbf{BuC5(H)_5}$ ligands,[126,136] but different from the flattened cone conformation observed in $[As_2O\{\mathbf{RC4}\}]$ complexes.[114]

Table 3.1 Selected bond lengths (Å) and angles (º) of complexes **3.4**, **3.7**, **3.9**·$3C_6H_6$ and **3.9**·2DMSO

	3.4	**3.7**	**3.9**·$3C_6H_6$	**3.9**·2DMSO
Sb(1)-O(1)	1.979(6)	2.005(4)	1.978(3)	1.980(6)
Sb(1)-O(2)	2.025(6)	2.009(4)	1.986(3)	2.006(6)
Sb(1)-O(6)	1.944(7)	1.946(4)	1.934(3)	1.986(6)
Sb(2)-O(3)	1.983(6)	1.992(4)	2.024(3)	2.027(6)
Sb(2)-O(4)	1.982(6)	2.007(4)	1.979(3)	1.992(6)
Sb(2)-O(6)	1.928(6)	1.922(4)	1.942(3)	1.890(6)
Sb-O(DMSO)	----------	----------	----------	2.503(7), 2.548(8)
Sb(1)-O(6)-Sb(2)	134.9(3)	134.3(2)	134.85(18)	134.5(3)
O(1)-Sb(1)-O(2)	91.9(2)	94.52(16)	92.78(13)	93.8(3)
O(3)-Sb(2)-O(4)	91.8(3)	89.31(15)	95.06(13)	89.6(3)
O(6)-Sb(1)-O(1)	92.3(3)	91.35(15)	97.41(14)	91.9(3)
O(6)-Sb(2)-O(3)	88.6(3)	90.23(16)	94.68(13)	89.5(3)
OAr-Sb-O(DMSO)	----------	----------	----------	75.5(3)-161.5(3)

Table 3.2 Comparison between distances in Sb-O-Sb bridges

	Sb-O_{bridge} / Å	Ref.
3.4	1.928(6) , 1.944(7)	This work
3.7	1.922(4) , 1.946(4)	This work
3.9·$3C_6H_6$	1.934(3) , 1.942(3)	This work
3.9·2DMSO	1.890(6) , 1.986(6)	This work
[Sb_2Cl_2{^{t}**BuC4**}]	2.0274(16), 2.4574(17)	[57]
[Sb_2Cl_2{**HC4**}]	2.027(2), 2.447(2)	[58]
$(Ph_2Sb)_2O$	1.971(3), 1.978(3)	[137]
$(o\text{-}Tol_2Sb)_2O$	1.967(2), 1.978(2)	[137]
$(p\text{-}Tol_2Sb)_2$º	1.967(4), 1.986(4)	[137]
{{[η^3-N(o-C_6H_4OH)(o-$C_6H_4O)_2$]Sb}$_2$(μ_2-O)}$_2$	1.976(2)-2.912(2)	[138]
{[η^3-PhN(o-$C_6H_4O)_2$]Sb}$_4$(μ_3-O)$_2$	1.989(6)-2.538(6)	[138]

In the X-ray structures for complexes **3.4**, **3.7** and **3.9**·$3C_6H_6$ (Figures 3.5-3.7), the Sb(1) and Sb(2) atoms are each coordinated to two aryloxide groups from the calixarene ligand and to the oxygen bridge to provide an overall trigonal pyramidal geometry. The pyramidal geometry is common for antimony(III) aryloxides and alkoxides reported in literature.[57,138,139] The antimony centers each form an eight-membered ring by coordination of the two aryloxide groups from the calixarene ligand. The conformation in the eight membered rings could be described as twisted boat (TB),[140] similar to the conformations observed in silicon and phosphorus **^{t}BuC5(H)$_5$** complexes.[126,136] The Sb-OAr bond lengths are in the range of 1.978(3) to 2.027(6) Å and O-Sb-O angles are in the range of 88.6(3)º to 97.41(14)º. These fall within the normal ranges for antimony(III) alkoxide and aryloxide complexes.[138,139]

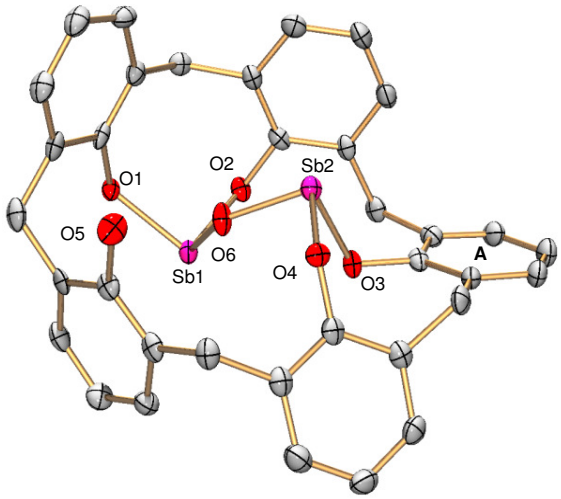

Figure 3.6. ORTEP diagram of complex **3.7** with thermal ellipsoids at the 50% probability level. H atoms and non-coordinated solvents are omitted for clarity.

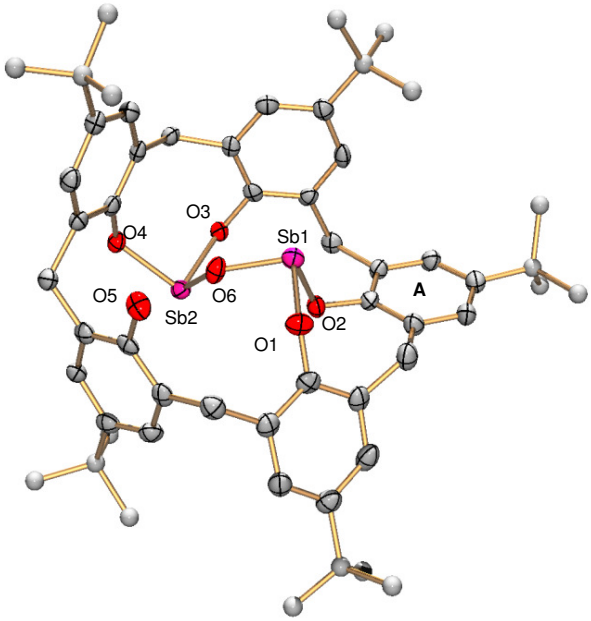

Figure 3.7. ORTEP diagram of complex **3.9**·$3C_6H_6$ with thermal ellipsoids at the 50% probability level. H atoms and non-coordinated solvents are omitted for clarity.

Complex **3.9**·2DMSO is a different crystalline form of [$Sb_2O\{^tBuC5(H)\}$] **3.9**, that differs only by the extra solvent coordination to the antimony centers (Figure 3.8). This solvent

coordination is responsible for the change of unit cell from triclinic *P*-1 in **3.9**·3C_6H_6 to tetragonal $I4_1/a$ for **3.9**·2DMSO. The two antimony atoms in **3.9**·2DMSO are tetracoordinate, with O(1) and O(2) from the calixarene unit, O(6) from the bridge, and O(7) from the DMSO solvent. In the same fashion Sb(2) is coordinated to O(3) and O(4) from calixarene, bridge O(6), and O(8) from DMSO. The three primary Sb-O bonds form a pyramidal structure around the Sb atom, whereas the much longer secondary interaction with DMSO lies across from one of the primary Sb-O bonds. The Sb(1)-O(1) and Sb(1)-O(2) distances are 1.980(6) and 2.006(6) Å, while Sb(2)-O(3) and Sb(2)-O(4) distances are 2.027(6) and 1.992(6) Å, respectively. All of these distances are similar to the Sb-O distances reported for **RC4(H)$_4$** (R = H, ^{t}Bu) calixarene antimony complexes and to Sb(III) amino- and oxo aryloxide complexes.[57,138,139] The Sb-DMSO bond distances Sb(1)-O(7) and Sb(2)-O(8) are 2.548(8) and 2.503(7) Å, respectively, which are noticeably longer than the Sb-aryloxide bond lengths but similar to the distances observed in DMSO coordination in other antimony aryloxide complexes [2.305(2), 2.405(2) Å].[58,138]

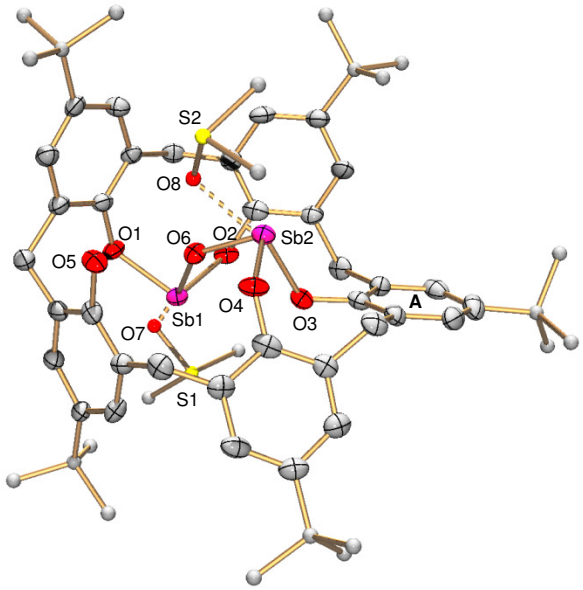

Figure 3.8. ORTEP diagram of complex **3.9**·2DMSO with thermal ellipsoids at the 50% probability level. H atoms and non-coordinated solvents are omitted for clarity.

It is important to notice that structures **3.7**, **3.9**·$3C_6H_6$ and **3.9**·2DMSO contain an available OH group that is located far away from the metal-containing core structure. These OH groups make complexes **3.7**, **3.9**·$3C_6H_6$ and **3.9**·2DMSO suitable functional precursors for the preparation of more complex entities.

The conformation of the $[(ArO)_2Sb]_2O$ fragment in complexes **3.4**, **3.7**, **3.9**·$3C_6H_6$ and **3.9**·2DMSO is similar to the ones observed in some diarylantimony oxide $(Ar_2Sb)_2O$ derivatives (Figure 3.9).[137] In the terminology used by Breunig et al.,[137] it can be described as *syn-anti* with respect to the Sb-OAr interactions. Tanski and coworkers found a similar $[(ArO_2)Sb]_2O$ fragment in their oxo aryloxide complexes, but they also observed that an aryloxide group attached to one of the antimony centers interacted weakly with the other antimony center to form a central $Sb_2(\mu\text{–}O)_2$ four membered ring [Sb···O 2.912(2) Å].[138] In our antimony calixarene complexes the 1,2-alternate conformation adopted by the ligands separates the aryloxides of each antimony center, inhibiting any bridging interaction. The Lewis acidity of the antimony center is, however, evidenced by the Sb-DMSO coordination in **3.9**·2DMSO.

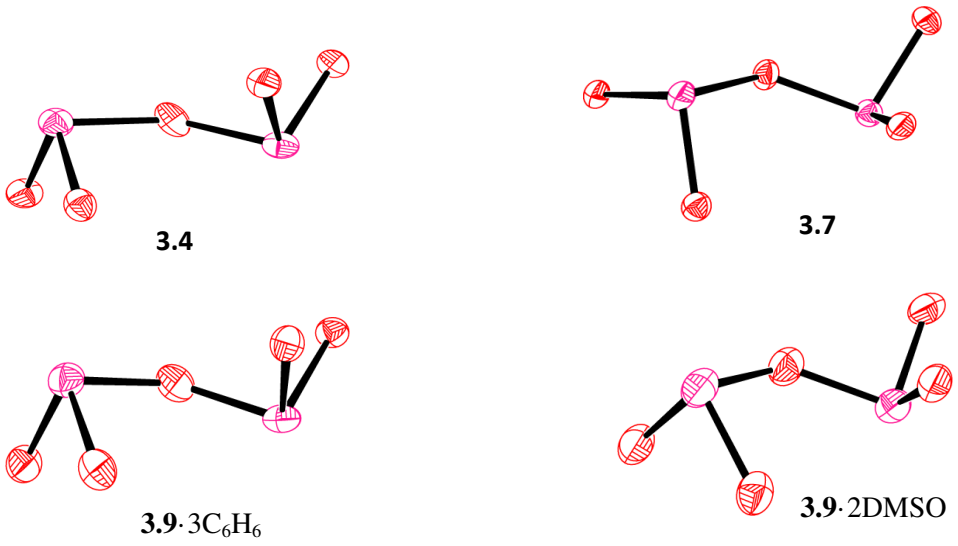

Figure 3.9. *Syn-anti* Sb-OAr conformations for the dinuclear moiety in the antimony complexes **3.4**, **3.7**, **3.9**·$3C_6H_6$ and **3.9**·2DMSO.

3.4.2 Calixarene bismuth complexes

The crystal structures of **3.1** and **3.3** are illustrated in Figures 3.10 and 3.11, respectively, and selected bond distances and angles are listed in Table 3.3.

Table 3.3 Selected bond lengths (Å) and angles (º) of complexes **3.1** and **3.3**

3.1				**3.3**	
Bi(1)-O(2)	2.891(7)	O(2)-Bi(1)-O(3)	81.7(2)	Bi(1)-O(2)	2.096(7)
Bi(1)-O(3)	2.120(6)	O(3)-Bi(1)-O(4)	87.9(2)	Bi(1)-O(1)	2.119(7)
Bi(1)-O(4)	2.134(6)	O(3)-Bi(1)-O(5A)	92.5(2)	Bi(1)...O(4)	3.520(9)
Bi(1)-O(5A)	2.142(5)	O(5)-Bi(1)-O(5A)	74.72(19)	Bi(1)-O(4A)	2.112(7)
Bi(1)-O(5)	2.733(5)	O(4)-Bi(1)-O(5A)	83.8(2)	O(1)-Bi(1)-O(2)	89.9(3)
Bi(1)-O(5)-Bi(1A)	105.28(19)	O(4)-Bi(1)-O(5)	77.82(19)	O(1)-Bi(1)-O(4A)	91.6(3)
				O(2)-Bi(1)-O(4A)	94.1(3)

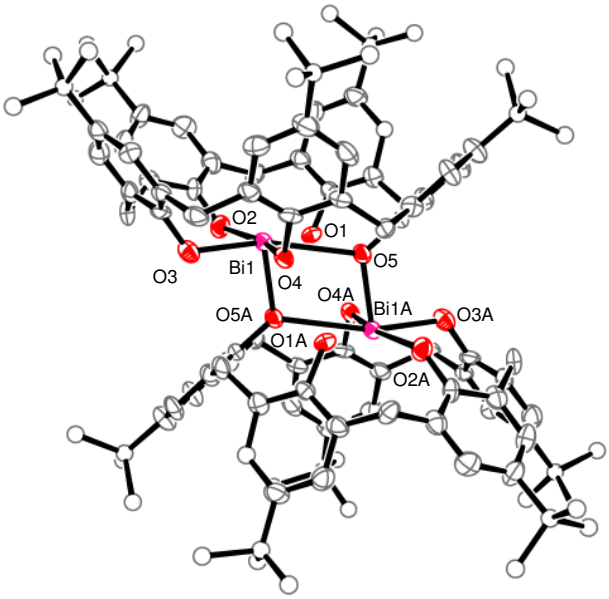

Figure 3.10. ORTEP diagram of complex **3.1** with thermal ellipsoids at the 50% probability level. H atoms and non-coordinated solvents are omitted for clarity.

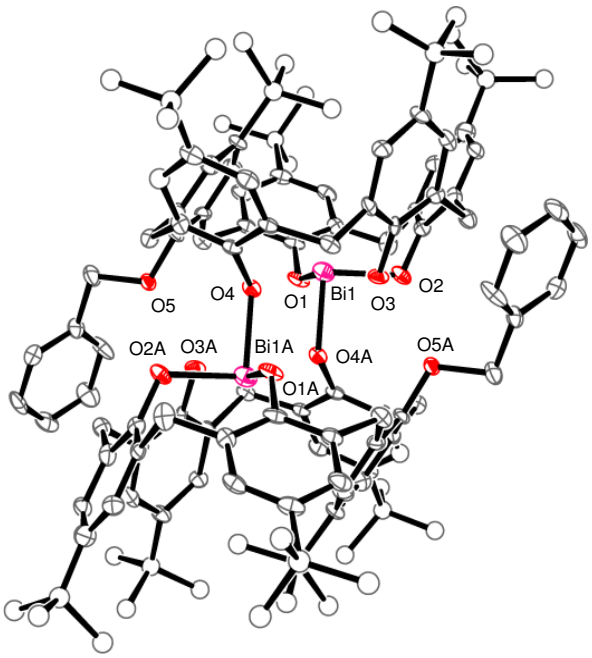

Figure 3.11. ORTEP diagram of complex **3.3** with thermal ellipsoids at the 50% probability level. H atoms are omitted for clarity.

The structures of **3.1** and **3.3** are both dimeric units with a bismuth atom coordinated to each calixarene and containing an inversion center located halfway between the two bismuth atoms. Complex **3.1** contains a central planar $Bi_2(\mu\text{-}O)_2$ four-membered ring, similar to the ones observed in other $M_2(\mu\text{-}O)_2$ (M = Al, Sn, Ga and Ge) rings of calix[4]arene main group organometallic complexes.[112,116,133] The Bi-(μ–O) distances in the $Bi_2(\mu\text{-}O)_2$ central ring are [2.142(5) Å] and [2.733(5) Å], the shorter one being the interaction of Bi(1) with an aryloxide from the second calixarene [O(5A)]. The O-Bi-O angles in the $Bi_2(\mu\text{-}O)_2$ four-membered ring are 74.72(19)^o while the Bi(1)-O(5)-Bi(1A) angles are 105.28(19)^o. The bismuth center displays a trigonal pyramidal geometry defined by the primary bonds Bi(1)-(O3), Bi(1)-O(4) and Bi(1)-O(5A), while the Bi(1) secondary interactions with O(2) and O(5) have bond lengths of 2.891(7) and 2.733(5), respectively. The primary Bi-O bond lengths range from 2.120(6) to 2.142(5) Å,

within the normal range for bismuth(III) calixarene, alkoxide and aryloxide complexes.[57,141-145] The two calixarene rings in complex **3.1** display slightly flattened cone conformations.

In a similar fashion to **3.1**, complex **3.3** contains bismuth atoms that are covalently bound to two aryloxides from the first calixarene ring [e.g. Bi(1)-O(1) and Bi(1)-O(2)] and to one aryloxide from the second one [Bi(1)-O(4A)] in a trigonal pyramidal geometry. The presence of the monobenzyl group in **^{t}BuC5(Bn)(H)$_4$** affects the secondary interactions in the bismuth atoms of complex **3.3** since only a weak Bi(1)-O(3) interaction with a distance of 2.769(7) Å is observed. The possible second interaction with O(4) (that could form a $Bi_2(\mu\text{-}O)_2$ central ring) is avoided because of the bulkiness of the benzyl group. The calixarene ring adopts a distorted "paco (partial cone) in" conformation, and O(4) is forced to be far away from the bismuth center. The covalent Bi-O distances range from 2.096(7) to 2.119(7) Å and O-Bi-O angles range from 89.9(3) to 94.1(3)^o. No bismuth π-arene interactions were observed.

The X-ray structures of complexes **3.5** and **3.8** are illustrated in Figures 3.12 and 3.13 and selected bond distances and angles are listed in Table 3.4. Each calixarene unit in complexes **3.5** and **3.8** contains an $[(ArO)_2M]_2(\mu\text{–}O)$ fragment similar to the one observed in the monomeric antimony structures described above. However, in **3.5** and **3.8** the larger size of bismuth and the conformation adopted by the calixarene rings allow two of these $[(ArO)_2Bi]_2(\mu\text{–}O)$ fragments to form bridging Bi···O interactions [e.g. Bi(1)-O(6A)] and thereby form dimeric structures (Figures 3.12 and 3.13). The dimeric **3.5** and **3.8** now contain five fused $Bi_2(\mu\text{-}O)_2$ four membered rings in an overall $Bi_4O_2(OR)_8$ core. The $Bi_4O_2(OR)_8$ core (see Figure 3.14) has emerged as a common subunit in bismuth oxo alkoxide clusters, such as the calixarene cluster $[Bi_8O_4\{$**^{t}BuC8**$\}_2]$ reported previously by our group.[57,127,146-149]

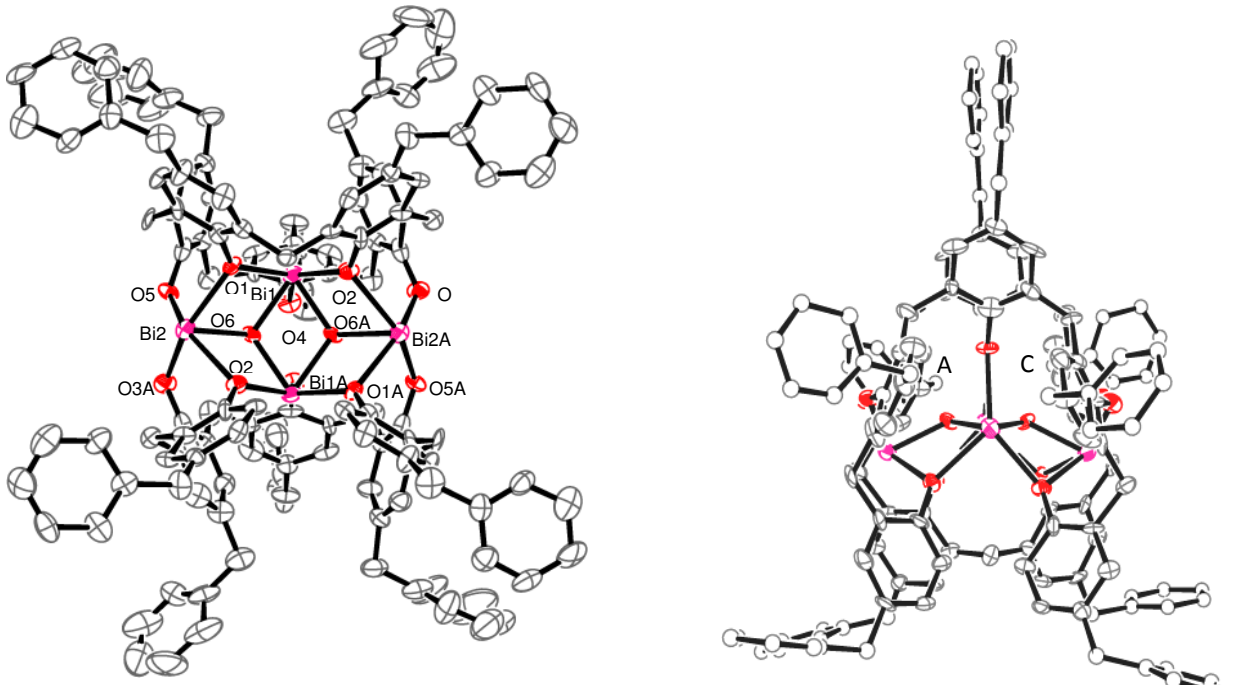

A: Side view **B.** Top view

Figure 3.12. ORTEP diagram of complex **3.5** with thermal ellipsoids at the 50% probability level. H atoms and non-coordinated solvents are omitted for clarity.

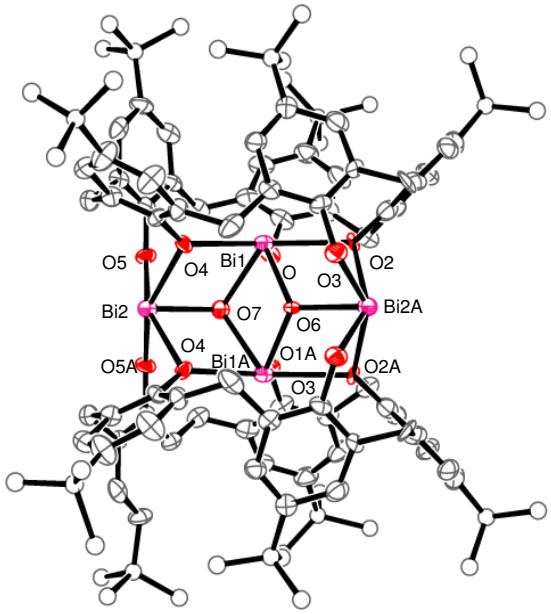

Figure 3.13. ORTEP diagram of complex **3.8** with thermal ellipsoids at the 50% probability level. H atoms and non-coordinated solvents are omitted for clarity.

Table 3.4. Selected bond lengths (Å) and angles (°) of complexes **3.5** and **3.8**

5				**8**			
Bi(1)-O(1)	2.392(11)	O(6)-Bi(1)-O(6A)	68.3(5)	Bi(1)-O(1)	2.238(8)	O(6)-Bi(1)-O(7)	70.0(3)
Bi(1)-O(2)	2.368(12)	O(2)-Bi(1)-O(6)	68.4(4)	Bi(1)-O(2)	2.491(7)	O(2)-Bi(1)-O(6)	67.4(3)
Bi(1)-O(4)	2.382(12)	O(1)-Bi(2)-O(6A)	69.1(4)	Bi(1)-O(4)	2.481(7)	O(4)-Bi(2)-O(7)	74.6(2)
Bi(1)-O(6)	2.166(1)	O(2A)-Bi(2)-O(6A)	66.6(4)	Bi(1)-O(6)	2.127(6)	O(2)-Bi(2A)-O(6)	68.9(2)
Bi(1)-O(6A)	2.142(12)	O(3)-Bi(2A)-O(6)	87.1(5)	Bi(1)-O(7)	2.271(6)	Bi(1)-O(4)-Bi(2)	100.3(3)
Bi(2)-O(1)	2.391(12)	Bi(1)-O(1)-Bi(2)	100.7(4)	Bi(2)-O(4)	2.328(7)	Bi(1)-O(7)-Bi(2)	114.4(3)
Bi(2)-O(5)	2.182(12)	Bi(1)-O(7)-Bi(2)	118.1(5)	Bi(2)-O(5)	2.245(8)	Bi(1)-O(2)-Bi(2A)	100.0(3)
Bi(2)-O(6A)	2.127(11)	Bi(1)-O(2)-Bi(2A)	99.1(4)	Bi(2)-O(7)	2.122(10)	Bi(1)-O(6)-Bi(2A)	119.1(3)
Bi(2)-O(2A)	2.476(12)	Bi(1)-O(6)-Bi(2A)	119.4(5)	Bi(2A)-O(6)	2.189(10)	Bi(1)-O(6)-Bi(1A)	114.3(5)
Bi(2)-O(3A)	2.206(13)	Bi(1)-O(6)-Bi(1A)	111.4(5)	Bi(1)-Bi(1A)	3.5733(8)	Bi(1)-O(7)-Bi(1A)	103.8(4)
Bi(1)-Bi(1A)	3.5583(16)	O(1)-Bi(1)-O(2)	90.5(4)	Bi(1A)-Bi(2)	3.6937(7)	O(1)-Bi(1)-O(2)	89.5(3)
Bi(1)-Bi(2)	3.6820(12)	O(1)-Bi(1)-O(4)	129.1(4)	Bi(2A)-Bi(1)	3.7212(8)	O(1)-Bi(1)-O(4)	122.0(3)
Bi(1)-Bi(2A)	3.6868(11)	O(1)-Bi(2)-O(5)	86.4(4)			O(4)-Bi(2)-O(5)	84.8(3)
		O(2)-Bi(2A)-O(3)	89.0(4)			O(2)-Bi(2A)-O(3)	85.4(3)

Each dimeric structure contains the calixarene framework in a flattened cone conformation with the rings A and C close to each other. The $Bi_4O_2(OR)_8$ cores of both complexes contain two μ_3-O atoms [O(6), O(6A) in **3.5** and O(6), O(7) in **3.8**] that do not belong to calixarene phenolates.

In complexes **3.5** and **3.8** (Figures 3.12 and 3.13), the central $Bi_2(\mu\text{-}O)_2$ four membered rings **I**, formed by Bi(1), Bi(1A), O(6) and O(6A) atoms in complex **3.5** and Bi(1), Bi(1A), O(6) and O(7) in complex **3.8**, contain Bi-O bond lengths ranging from 2.127(6) to 2.271(6) Å. These distances are comparable to the Bi-OAr distances [2.182(12)-2.491(7) Å]. The O-Bi-O angles in the central ring **I** are 68.3(5) and 70.0(3)^o for **3.5** and **3.8**, respectively, and the Bi(1)-O-Bi(1A) angles range from 103.8(4)^o to 114.3(5)^o. Both distances and angles are similar to planar $M_2(\mu$-

$O)_2$ rings found in calixarene, alkoxide and aryloxide complexes reported in literature.[57,112,116,133] Torsion angles from the central ring **I** in complexes **3.5** and **3.8** are 6.82(9)° and 11.51(8)°, respectively. The larger torsion angle indicates that the central $Bi_2(\mu\text{-}O)_2$ four membered ring in complex **3.8** is more deviated from planarity.

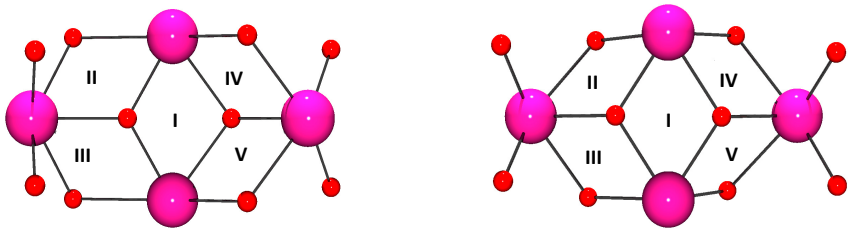

3.5 **3.8**

Figure 3.14 POV-ray diagram of the $Bi_4O_2(OR)_8$ core structures of complexes **3.5** and **3.8** showing the five fused $Bi_2(\mu\text{-}O)_2$ rings (I-V).

The other four $Bi_2(\mu\text{-}O)_2$ rings in the $Bi_4O_2(OR)_8$ core structure of complexes **3.5** and **3.8** (**II-V**, see Figure 3.14) contain Bi-O bond lengths and torsion angles similar to those observed for the central ring **I**. They possess individual planarity, but they are not coplanar with the central $Bi_2(\mu\text{-}O)_2$ ring. In this regard, the outer **II-V** rings behave like the rings found on the twisted framework in Uchiyama's ladder complex.[150] Metal-metal distances within the $Bi_4O_2(OR)_8$ core for complex **3.5** are Bi(1)-Bi(2) 3.6820(12), Bi(1)-Bi(2A) 3.6868(11), and Bi(1)-Bi(1A) 3.5583(16) Å, while metal-metal distances in the complex **3.8** core are Bi(1A)-Bi(2) 3.6937(7), Bi(1)-Bi(2A) 3.7212(8), and Bi(1)-Bi(1A) 3.5733(8) Å. All these distances are similar to those found in the dimeric units of $Bi(OCH_2CH_2OMe)_3$.[151] Bi-OAr bond lengths in complexes **3.5** and **3.8** fall in the range of 2.182(12)-2.491(7) Å, which are typical for Bi(III) aryloxide/alkoxide complexes.[57,141-145] The bismuth atoms Bi(1) and Bi(2) in complexes **3.5** and **3.8** are both five-coordinate but display different geometries. Bi(1) and Bi(1A) are coordinated to three oxygen atoms from the phenolates and to μ_3-bridging O(6) and O(7) atoms to give a trigonal prismatic

geometry with a vacant coordination site that points into to the calixarene cavity (Figures 3.12 and 3.13). The geometry around the Bi(1) and Bi(1A) is quite similar to that described as intermediate in the mechanism for interchanging apical and equatorial atoms in square pyramidal molecules.[152] On the other hand the Bi(2) and Bi(2A) atoms reside in a distorted square-based pyramidal geometry with the basal plane formed by four oxygen atoms from the calixarene ligand and the apical position occupied by one oxygen [O(6) or O(7)] from the central bridge **I**. The geometries around the bismuth atoms in complexes **3.5** and **3.8** are similar to the ones observed in some bismuth aryl alkoxides and heterobimetallic bismuth oxo clusters.[146-148] No bismuth π-arene interactions are observed for **3.5** and **3.8**.

3.5 Experimental section

3.5.1 General information

Unless otherwise noted, all manipulations were carried out in a nitrogen filled glovebox. Starting materials were obtained from commercial suppliers and used without further purification. *p-tert*-Butylcalix[5]arene,[97] *p*-benzylcalix[5]arene,[153] *p*-H-calix[5]arene,[154] monobenzyl-*p-tert*-butylcalix[5]arene,[79] $Bi(O^tBu)_3$,[145] $Bi[N(SiMe_3)_2]_3$,[155] and $Sb(O^tBu)_3$[156] were prepared by the literature procedures. $Sb(NMe_2)_3$ was purchased from Strem Chemicals and used as received. All calixarene starting materials were dried at 110 ^oC for at least 24 hrs. Tetrahydrofuran was freshly distilled from Na/benzophenone; other anhydrous solvents were purchased from Aldrich and stored over molecular sieves under nitrogen before using. Deuterated benzene and dimethyl sulfoxide were dried over CaH_2. The melting points of all the compounds were taken in capillary tubes on a Mel-temp apparatus (Laboratory devices, Cambridge, MA) using a 500 ^oC thermometer. A melting temperature proceeded by a ">" sign indicates that the compound starts to decompose at that temperature but appears to actually melt

at some higher temperature. ^{1}H NMR and ^{13}C spectra were recorded on a Varian XL-300 spectrometer at 300 and 75 MHz, respectively. Analytical samples were dried under vacuum for at least 24 hrs. Microanalyses were performed by Atlantic Microlab, Inc, Norcross, GA. IR and UV/Vis spectra were obtained with an Infinity Gold™ FTIR spectrometer and Agilent 8453 spectrophotometer, respectively. Filtrations used a medium sintered glass filter. All X-ray diffraction experiments were performed in a Bruker SMART 1000 CCD detector at low temperature using Mo Kα radiation.

3.5.2 Synthesis of complexes

[Bi{^{t}**BuC5(H)$_2$**}] (**3.1**): Method A: LiO^{t}Bu (0.121 g, 1.52 mmol) in THF (3 mL) was added to a solution of ^{t}**BuC5(H)$_5$** (0.412 g, 0.507 mmol) in THF (5 mL) and the reaction mixture was allowed to stir for 24 hrs at room temperature. $BiCl_3$ (0.160 g, 0.507 mmol) in THF (4 mL) was then added to the resulting colorless solution of Li_3·^{t}**BuC5(H)$_2$** salt,[120] immediately yielding a yellow solution. After two hrs of stirring a yellow precipitate was formed and the reaction mixture was allowed to stir for another 46 hrs. The mixture was vacuum filtered to give the crude product as yellow powder. Purification of the product was performed by stirring the crude product in 15 mL of toluene for 24 hrs and centrifuging (procedure repeated 2 times) to give 0.419 g of [Bi{^{t}**BuC5(H)$_2$**}] (0.412 mmol, 81% yield). Single crystals were obtained from slow evaporation of a concentrated solution in benzene/DME (1:2 ratio). [Bi{^{t}**BuC5(H)$_2$**}] can also be obtained by the reaction of the sodium or potassium trianionic salts[120] with $BiCl_3$. The yields obtained are 35% (0.180 g, 0.177 mmol) and 60% (0.309 g, 0.304 mmol), respectively.

Method B: Bi(O^{t}Bu)$_3$ (0.0220 g, 0.0512 mmol) in 3 mL of toluene was added dropwise to a colorless solution of ^{t}**BuC5(H)$_5$** (0.0412 g, 0.0507 mmol) in 5 mL of toluene, immediately yielding a yellow solution. The reaction mixture was allowed to stir for 48 hrs producing a

yellow mixture. The crude product was obtained as yellow solid after centrifugation. Purification of product was performed by adding 10 mL of benzene to the crude material and warming the mixture at 45 ^{o}C until the solid was totally dissolved. The solution was placed in the freezer at −2 ^{o}C for three days to give 0.0255 g of pure [Bi{^{t}**BuC5(H)$_2$**}] (0.0251 mmol, 49% yield).

Method C: A mixture of solutions of ^{t}**BuC5(H)$_5$** (0.0824 g, 0.101 mmol) and $Bi[N(SiMe_3)_2]_3$ (0.0693 g, 0.102 mmol) in 5 and 3 mL of THF, respectively, were placed in a solvent bomb and allowed to heat in an isotemp bath at 95 ^{o}C for 12 hrs. The reaction mixture was vacuum dried to yield the crude material as yellow solid. Purification of the product was performed by stirring the crude product in 10 mL of toluene for 24 hrs and centrifuging (procedure repeated 2 times) to give 0.0431 g of [Bi{^{t}**BuC5(H)$_2$**}] (0.0424 mmol, 42% yield). Mp**:** 378-380 ^{o}C. ^{1}H NMR (C_6D_6): δ 1.35 (s, 18H, C(C*H*$_3$)$_3$), 1.39 (s, 9H, C(C*H*$_3$)$_3$), 1.42 (s, 18H, C(C*H*$_3$)$_3$), 3.14 (d, *J* = 12.9 Hz, 1H, ArC*H*$_2$Ar), 3.32 (b, 1H, ArC*H*$_2$Ar), 3.86 (b, 2H, ArC*H*$_2$Ar), 4.11 (d, *J* = 14.0 Hz, 2H, ArC*H*$_2$Ar), 4.71 (d, *J* = 12.9 Hz, 1H, ArC*H*$_2$Ar), 5.25 (b, 1H, ArC*H*$_2$Ar), 5.54 (b, 1H, ArC*H*$_2$Ar), 6.38 (b, 1H, ArC*H*$_2$Ar), 7.52 (b, 4H, Ar*H*), 7.76 (b, 4H, Ar*H*), 7.92 (s, 2H, Ar*H*), 9.82 (s, 1H, O*H*), 11.97 (s, 1H, O*H*). ^{13}C{^{1}H} NMR (C_6D_6): δ 150.4, 148.4, 146.0, 144.0, 135.9, 129.1, 128.4, 126.3, 125.7, 126.3, 125.5, 125.4 (aromatic carbons), 34.1, 34.0, 33.5 (*C*(CH$_3$)$_3$), 31.8 (Ar*C*H$_2$Ar), 31.7, 31.5, 30.3 (C(*C*H$_3$)$_3$), 28.2, 21.3 (Ar*C*H$_2$Ar). IR (KBr, cm^{-1}): 3291m, 2954vs, 2905m, 2871m, 2353w, 1644w, 1605w, 1472vs, 1394m, 1364m, 1292m, 1241m, 1196vs, 1119m, 1302w, 900w, 869w. UV/vis λ_{max}/nm (THF) (ε/dm^{3}mol^{-1}cm^{-1}): 281 (1.52 x 10^4), 322 (8.22 x 10^3). Anal. Calcd for $C_{55}H_{67}O_5Bi \cdot 0.5C_7H_8$: C 66.09, H 6.73. Found: C 65.98, H 6.92.

[Sb{^{t}**BuC5(H)$_2$**}] (**3.2**): A colorless solution of $SbCl_3$ (0.115 g, 0.504 mmol) in 3 mL of THF (or toluene) was added dropwise to a colorless solution of 0.500 mmol of M'$_3$·^{t}**BuC5(H)$_2$**

(M' = Li, Na or K)[120] in 5 mL of THF. The mixture was allowed to stir for 48 hrs yielding a white mixture. The crude material is obtained as white solid after filtration. Pure product can be obtained by stirring the crude material with 15 mL of toluene for 12 hrs and centrifuging (procedure repeated 2 times) to yield [Sb{^{t}**BuC5(H)$_2$**}] in 65% (0.326 mmol, 0.303 g), 43% (0.215 mmol, 0.200 g) and 18% (0.0904 mmol, 0.0837 g) yields, respectively.

Method B: A colorless solution of Sb(O^{t}Bu)$_3$ (0.0174 g, 0.0510 mmol) in 3 mL of THF was added to a solution of ^{t}**BuC5(H)$_5$** (0.0412 g, 0.0507 mmol) in 5 mL of THF (or toluene), immediately yielding a cloudy solution. The reaction was allowed to stir for 48 hrs with the production of a white mixture. Crude material was obtained as white powder after centrifugation. Purification of product was performed by adding 10 mL of benzene to the crude material and warming the mixture at 45 ^{o}C until the solid was totally dissolved. The solution was placed in the freezer at −2 ^{o}C for 3 days to give 0.0212 g of [Sb{^{t}**BuC5(H)$_2$**}] (0.0228 mmol, 45% yield). Mp: 374-376 ^{o}C. ^{1}H NMR (C_6D_6): δ 1.31 (s, 9H, C(C*H*$_3$)$_3$), 1.34 (s, 9H, C(C*H*$_3$)$_3$), 1.38 (s, 9H, C(C*H*$_3$)$_3$), 1.43 (s, 9H, C(C*H*$_3$)$_3$), 1.44 (s, 9H, C(C*H*$_3$)$_3$), 2.96 (d, *J* = 13.2 Hz, 1H, ArC*H*$_2$Ar), 3.31 (d, *J* = 13.5 Hz, 1H, ArC*H*$_2$Ar), 3.61 (d, *J* = 13.2 Hz, 1H, ArC*H*$_2$Ar), 3.91 (d, *J* = 13.2 Hz, 1H, ArC*H*$_2$Ar), 3.96 (d, *J* = 13.5 Hz, 1H, ArC*H*$_2$Ar), 4.04 (d, *J* = 13.5 Hz, 1H, ArC*H*$_2$Ar), 4.64 (d, *J* = 13.2 Hz, 1H, ArC*H*$_2$Ar), 5.00 (d, *J* = 13.2 Hz, 1H, ArC*H*$_2$Ar), 5.39 (d, *J* = 13.2 Hz, 1H, ArC*H*$_2$Ar), 6.02 (d, *J* = 13.5 Hz, 1H, ArC*H*$_2$Ar), 7.26 (d, *J* = 2.4 Hz, 1H, Ar*H*), 7.32 (d, *J* = 2.1 Hz, 1H, Ar*H*), 7.46 (d, *J* = 2.4 Hz, 1H, Ar*H*), 7.49 (d, *J* = 2.1 Hz, 1H, Ar*H*), 7.55 (d, *J* = 2.1 Hz, 1H, Ar*H*), 7.56 (d, *J* = 2.4 Hz, 1H, Ar*H*), 7.68 (d, *J* = 2.4 Hz, 1H, Ar*H*), 7.79 (d, *J* = 2.4 Hz, 1H, Ar*H*), 7.88 (s, 2H, Ar*H*), 9.51 (s, 1H, O*H*)**,** 10.71 (s, 1H, O*H*). ^{13}C{^{1}H} NMR (C_6D_6) δ = 151.6, 150.7, 149.1, 148.7, 147.9, 147.5, 146.2, 145.5, 144.9, 143.0, 137.7, 135.4, 135.2, 135.1, 134.9, 134.2, 133.7, 130.4, 126.5, 126.2 (aromatic carbons), 35.2, 34.3, 34.2 (Ar*C*H$_2$Ar), 34.1, 34.0,

33.96, 33.91, 31.8 *C*$(CH_3)_3$, 31.7, 31.64, 31.61, 31.57, 31.5 C(*C*$H_3)_3$, 25.6, 21.3 (Ar*C*H_2Ar). IR (KBr, cm^{-1}): 3397s, 3059w, 2950vs, 2909s, 2868m, 2360m, 1640w, 1475vs, 1394w, 1363m, 1293m, 1239m, 1190vs, 1117s, 987w, 876w, 815w. UV/vis (THF) λ_{max}/nm (ε/$dm^3mol^{-1}cm^{-1}$): 278 (2.76 x 10^5). Anal. calcd for $C_{55}H_{67}O_5Sb \cdot 0.5C_7H_8$: C 71.99, H 7.33. Found: C 72.25, H 7.62.

[Bi{^{t}**BuC5(Bn)(H)**}]$_2$ (**3.3**): A colorless solution of Bi($O^tBu)_3$ (0.0216 g, 0.0504 mmol) in pentane (3 mL) was added to a colorless solution of ^{t}**BuC5(Bn)(H)$_4$** (0.0452 g, 0.0502 mol) in pentane (5 mL). The reaction mixture was allowed to stand and slowly diffuse for 48 hrs to yield crude product as yellow crystalline powder. Vacuum filtration of crude material and two successive 5 mL pentane washing cycles produced 0.0483 g of pure [Bi{^{t}**BuC5(Bn)(H)**}]$_2$ (0.0218 mmol, 87% yield). Due to poor solubility of the product no NMR characterization was available. X-ray quality yellow needles of [Bi{^{t}**BuC5(Bn)(H)**}]$_2$ were obtained when ^{t}**BuC5(Bn)(H)$_4$** in 4 mL of benzene and Bi($O^tBu)_3$ in 2 mL of hexane (same amounts as above) are allowed to slowly diffuse over a period of two weeks. Mp: > 320 ^oC. IR (KBr, cm^{-1}): 3423w, 3177w, 3053w, 2961vs, 2904s, 2868m, 2360w, 1591w, 1463vs, 1393w, 1361m, 1293m, 1243m, 1194vs, 1122s, 974w, 873w, 822w. UV/vis (THF) λ_{max}/nm (ε/$dm^3mol^{-1}cm^{-1}$): 218 (Absorption coefficient ε is not available due to the limited solubility). Anal Calcd for $C_{124}H_{146}O_{10}Bi_2$: C 67.26, H 6.65. Found: C 67.17, H 6.76.

[Sb_2O\{^{t}**BuC5(Bn)**\}] (**3.4**): A colorless solution of Sb($O^tBu)_3$ (0.0176 g, 0.0516 mmol) in 3 mL of pentane was added to a colorless solution of ^{t}**BuC5(Bn)(H)$_4$** (0.0452 g, 0.0502 mol) in 5 mL of pentane. The reaction mixture was allowed to stand and slowly diffuse for 48 hrs. White needles precipitated out from the reaction mixture. Filtration and two successive 5 mL pentane washing cycles yielded 0.0231 g of pure [Sb_2O\{^{t}**BuC5(Bn)**\}] needles (0.0200 mmol, 40% yield). If two equivalents of Sb($O^tBu)_3$ are used (0.0351g, 0.103 mmol), 0.0441 g of pure

[Sb_2O{**^{t}BuC5(Bn)**}] needles are obtained (0.0381 mmol, 76% yield). X-ray quality crystals of [Sb_2O{**^{t}BuC5(Bn)**}] were obtained when hexane was used as reaction solvent (using same amounts as above).

Method B: A colorless solution of $Sb(NMe_2)_3$ (0.0262 g, 0.103 mmol) in 3 mL of benzene was added dropwise to a colorless solution of **^{t}BuC5(Bn)(H)$_4$** (0.0452 g, 0.0502 mmol) in 4 mL of benzene and the reaction mixture was allowed to stir for 48 hrs at rt. The solvent was evacuated to yield the crude product as a light beige solid. Crystallization by hexanes diffusion into a concentrated benzene solution of crude product yielded 0.0517 g of [Sb_2O{**^{t}BuC5(Bn)**}] as colorless block crystals (0.0447 mmol, 89% yield). Mp = 328-330 ^oC. ^1H NMR (C_6D_6): δ 1.17 (s, 9H, C(CH_3)$_3$), 1.27 (s, 9H, C(CH_3)$_3$), 1.35 (s, 9H, C(CH_3)$_3$), 1.38 (s, 9H, C(CH_3)$_3$), 1.45 (s, 9H, C(CH_3)$_3$), 3.18 (d, *J* = 14.1 Hz, 1H, ArCH_2Ar), 3.29 (d, *J* = 13.5 Hz, 1H, ArCH_2Ar), 3.49 (d, *J* = 13.5 Hz, 1H, ArCH_2Ar), 3.52 (d, *J* = 15.6 Hz, 1H, ArCH_2Ar), 4.03 (d, *J* = 13.5 Hz, 1H, ArCH_2Ar), 4.05 (d, *J* = 14.7 Hz, 1H, ArCH_2Ar), 4.21 (d, *J* = 15.6 Hz, 1H, ArCH_2Ar), 4.29 (d, *J* = 13.5 Hz, 1H, ArCH_2Ar), 4.70 (s, 2H, OCH_2Ar), 4.72 (d, *J* = 14.7 Hz, 1H, ArCH_2Ar), 4.89 (d, *J* = 14.1 Hz, 1H, ArCH_2Ar), 7.07 (d, *J* = 2.4 Hz, 2H, CH_2Ar*H*), 7.10 (s, 1H, Ar*H*), 7.19 (s, 1H, Ar*H*), 7.22 (d, *J* = 2.7 Hz, 1H, Ar*H*), 7.26 (d, *J* = 2.7 Hz, 1H, Ar*H*), 7.30 (t, *J* = 2.4 Hz, 3H, CH_2Ar*H*), 7.33 (d, *J* = 2.4 Hz, 1H, Ar*H*), 7.36 (s, 1H, Ar*H*), 7.38 (s, 1H, Ar*H*), 7.56 (d, *J* = 2.7 Hz, 1H, Ar*H*), 7.59 (d, *J* = 2.1 Hz, 1H, Ar*H*), 7.74 (d, *J* = 2.1 Hz, 1H, Ar*H*). $^{13}C\{^1H\}$ NMR (C_6D_6) δ = 153.6, 152.7, 151.8, 149.7, 146.8, 143.2, 142.7, 142.2, 136.9, 135.8, 135.4, 133.3, 133.1, 131.7, 130.7, 130.2, 129.7, 128.9, 126.6, 126.1, 125.5, 125.4, 124.3, 124.1 (aromatic carbons), 75.8 (O*C*H_2Ar), 39.8, 36.0, 34.5 (Ar*C*H_2Ar), 34.5, 34.1, 33.99, 33.95, 32.2 *C*(CH_3)$_3$, 31.9, 31.80, 31.78, 31.76, 31.6 C(*C*H_3)$_3$, 30.1, 28.9 (Ar*C*H_2Ar). IR (KBr, cm^{-1}): 3391w, 3218m, 3053w, 2960vs, 2903s, 2867s, 2360w, 1748w, 1591w, 1466vs, 1415w, 1393w, 1375w, 1362s, 1296m,

1239s, 1193vs, 1122s, 981m, 914w, 873m. UV/vis (THF) λ_{max}/nm (ε/dm^{3}mol^{-1}cm^{-1}): 279 (1.68 x 10^4). Anal Calcd for $C_{62}H_{72}O_6Sb_2 \cdot 1.5C_6H_{14}$: C 66.31, H 7.29. Found: C 66.26, H 6.94.

$[Bi_2O\{$**BnC5(H)**$\}]_2$ (**3.5**): A colorless solution of $Bi(O^tBu)_3$ (0.0215 g, 0.0502 mmol) in 3 mL of THF was added dropwise to a colorless solution of **BnC5(H)$_5$** (0.0493 g, 0.0502 mmol) in 5 mL of THF. The reaction mixture was allowed to stir for 24 hrs. A ^{1}H NMR spectrum of the crude mixture allowed the observation of the product $[Bi_2O\{$**BnC5(H)**$\}]_2$ in mixture with starting material. Addition of 1.5 more equivalents of $Bi(O^tBu)_3$ (0.0323 g, 0.0754 mmol) to the reaction mixture and stirring for another 24 hrs permitted all the starting material to be consumed. Recrystallization by diffusion of hexanes into a concentrated THF/DME/DMSO (1:2:0.1) solution of the crude product yielded 0.0482 g of yellow block single crystals of $[Bi_2O\{$**BnC5(H)**$\}]_2$ (0.0171 mmol, 68% yield). Mp: > 282 ^{o}C. ^{1}H NMR (C_6D_6) δ = 3.02 (d, *J* = 13.2 Hz, 5H, ArC*H*$_2$Ar), 3.73 (s, 10H, C*H*$_2$Ar), 4.36 (d, *J* = 13.2 Hz, 5H, ArC*H*$_2$Ar), 6.95 (s, 10H, Ar*H*), 7.02-7.18 (m, 25H, CH$_2$Ar*H*). No OH peak was observed at room temperature. No ^{13}C spectrum is available due to insufficient solubility. IR (KBr, cm^{-1}): 3427w, 3049w, 3064w, 3024w, 2908s, 2839w, 1602s, 1493s, 1446vs, 1246m, 1224v, 1145s, 1123w, 1067w, 1023w, 906w, 799s. UV/vis (THF) λ_{max}/nm (ε/dm^{3}mol^{-1}cm^{-1}): 262 (2.70 x 10^4). Anal Calcd for: $C_{140}H_{112}Bi_4O_{12} \cdot 2C_4H_{10}O_2 \cdot 4C_2H_6SO$: C 56.52, H 4.74. Found C 56.57, H 4.64.

$[Bi_2O\{$**HC5(H)**$\}]$ (**3.6**): A mixture of solutions of **HC5(H)$_5$** (0.0539 g, 0.102 mmol) and $Bi[N(SiMe_3)_2]_3$ (0.0697 g, 0.101 mmol) in 5 and 2 mL of THF, respectively, were placed in a solvent bomb and allowed to heat in an isotemp oil bath at 75 ^{o}C for 16 hrs. The little solid from the reaction was removed by centrifugation and the supernatant was vacuum dried to yield a yellow solid. Washing the yellow solid with 3 mL of ether and vacuum filtering yielded the crude product as a yellow powder. Recrystallization by slow evaporation of a concentrated DME

solution gave 0.0412 g of [Bi_2O\{**HC5(H)**\}] as yellow block crystals (0.0429 mmol, 42% yield). Mp: > 290 ^oC. ^1H NMR (DMSO-d_6) δ = 3.20 (d, *J* = 15.0 Hz, 2H, ArC*H*$_2$Ar), 3.48 (d, *J* = 12.6 Hz, 1H, ArC*H*$_2$Ar), 3.74 (d, *J* = 15.3 Hz, 2H, ArC*H*$_2$Ar), 4.51 (d, *J* = 15.3 Hz, 2H, ArC*H*$_2$Ar), 5.24 (d, *J* = 12.6 Hz, 1H, ArC*H*$_2$Ar), 5.64 (d, *J* = 15.0 Hz, 2H, ArC*H*$_2$Ar), 5.93 (d, *J* = 6.3 Hz, 2H, Ar*H*), 6.00 (t, *J* = 7.5 Hz, 2H, Ar*H*), 6.38 (d, *J* = 7.2 Hz, 2H, Ar*H*), 6.43 (t, *J* = 7.5 Hz, 2H, Ar*H*), 6.61 (t, *J* = 6.9 Hz, 1H, Ar*H*), 6.95 (d, *J* = 7.2 Hz, 2H, Ar*H*), 7.01 (d, *J* = 7.5 Hz, 2H, Ar*H*), 7.27 (d, *J* = 7.5 Hz, 2H, Ar*H*), 13.3 (s, 1H, O*H*). No ^{13}C NMR was obtained due to limited solubility. IR (KBr, cm^{-1}): 3347w, 3053w, 3004w, 2916m, 1913w, 1699w, 1586ss, 1454vs, 1438vs, 1307w, 1291m, 1243vs, 1208vs, 1196w, 1083s, 1027w, 950w, 898m, 845s, 817m, 757vs. UV/vis (THF) λ_{max}/nm (ε/$dm^3mol^{-1}cm^{-1}$): 259 (5.46 x 10^4), 293 (2.02 x 10^4). Anal Calcd for $C_{35}H_{26}O_6Bi_2$·0.75 $C_4H_{10}O_2$: C 44.39, H 3.28. Found: C 44.04, H 3.55.

[Sb_2O\{**HC5(H)**\}] (**3.7**): A colorless solution of $Sb(NMe_2)_3$ (0.0193 g, 0.0760 mmol) in 2 mL of THF was added dropwise to a colorless solution of **HC5(H)$_5$** (0.0539 g, 0.102 mmol) in 5 mL of THF and the reaction mixture was allowed to stir for 16 hrs. The solvent of the colorless solution was evacuated to yield a white solid. Recrystallization by diffusion of hexane into a concentrated benzene solution of the crude material allowed the formation of pure product as colorless needles in 44% yield (0.0449 mmol, 0.0352 g). Mp: 222-224 ^oC. ^1H NMR (DMSO-d_6) δ = 2.76 (d, *J* = 15.3 Hz, 1H, ArC*H*$_2$Ar), 3.04 (d, *J* = 15.3 Hz, 1H, ArC*H*$_2$Ar), 3.10 (d, *J* = 14.1 Hz, 2H, ArC*H*$_2$Ar), 3.23 (d, *J* = 13.8 Hz, 1H, ArC*H*$_2$Ar), 4.12 (d, *J* = 12.6 Hz, 1H, ArC*H*$_2$Ar), 4.77 (d, *J* = 12.6 Hz, 1H, ArC*H*$_2$Ar), 4.88 (d, *J* = 14.1 Hz, 2H, ArC*H*$_2$Ar), 4.91 (d, *J* = 13.8 Hz, 1H, ArC*H*$_2$Ar), 6.32-6.44 (m, 3H, Ar*H*), 6.53 (t, *J* = 7.5 Hz, 4H, Ar*H*), 6.71 (d, *J* = 6.6 Hz, 1H, Ar*H*), 6.77 (d, *J* = 6.6 Hz, 1H, Ar*H*), 6.99 (d, *J* = 7.5 Hz, 6H, Ar*H*), 10.58 (s, 1H, O*H*). The ^{13}C spectrum is not available due to insufficient solubility. IR (KBr, cm^{-1}): 3346w, 3182m, 3030w,

2956w, 2916m, 2853w, 2364w, 1588s, 1462s, 1448vs, 1373w, 1301w, 1251vs, 1210vs, 1084s, 1019ws, 958w, 852s, 818m, 756vs, 679m. UV/vis (THF) λ_{max}/nm (ε/$dm^3mol^{-1}cm^{-1}$): 280 (2.07 x 10^4). Anal Calcd for $C_{35}H_{26}O_6Sb_2 \cdot 1.5C_6H_6$: C 58.51, H 3.91. Found: C 58.19, H 3.86.

$[Bi_2O\{^tBuC5(H)\}]_2$ (**3.8**): A colorless solution of $Bi(O^tBu)_3$ (0.0215 g, 0.0502 mmol) in 3 mL of benzene was added dropwise to a yellow suspension of compound **3.1** (0.0508 g, 0.0500 mmol) in 5 mL of benzene, immediately resulting in a yellow solution. The reaction mixture was allowed to stir for 24 hrs and the solvent was removed to yield a yellow solid. This solid was redissolved in a mixture of 2 mL of THF, 1 mL of acetonitrile, and 0.3 mL of DMSO and allowed to stand for 1 day. The small amount of solid obtained was removed by centrifugation and the solution was vacuum dried to yield the crude product as a light yellow solid. Pure product in 41% yield (0.0101 mmol, 0.0251 g) was obtained by slow evaporation of an ether solution of the crude product. Single crystals were obtained by the slow evaporation of a concentrated Et_2O/DMSO (5:1) solution over several weeks. Mp: > 268 °C. ^{1}H NMR (C_6D_6) δ = 1.40 (s, 45H, $C(CH_3)_3$), 1.76 (b, 30H, coordinated DMSO), 3.43 (b, 5H, $ArCH_2Ar$), 4.71 (b, 5H, $ArCH_2Ar$), 7.48 (s, 10H, Ar*H*). No OH peak was observed at room temperature. $^{13}C\{^1H\}$ NMR (C_6D_6) δ = 153.5, 141.2, 128.4, 124.1 (aromatic carbons), 40.4 ($C(CH_3)_3$), 33.8 ($ArCH_2Ar$), 31.9 ($C(CH_3)_3$). IR (KBr, cm^{-1}): 3290w, 3056w, 3029w, 2961vs, 2904m, 2867m, 2356w, 1595w, 1480vs, 1461vs, 1393w, 1361s, 1291s, 1241s, 1191vs, 1126s, 1039w, 906w, 872.6w, 818w. UV/vis (THF) λ_{max}/nm (ε/$dm^3mol^{-1}cm^{-1}$): 277 (2.32 x 10^4). Anal. calcd for $C_{110}H_{132}O_{12}Bi_4 \cdot 5C_2H_6SO$: C 50.17, H 5.68. Found: C 50.24, H 5.48.

$[Sb_2O\{^tBuC5(H)\}]$ (**3.9**)**:** A colorless solution of $Sb(O^tBu)_3$ (0.0171 g, 0.0501 mmol) in 2 mL of benzene was added dropwise to a white suspension of compound **3.2** (0.0465 g, 0.0500 mmol) in 3 mL of benzene. The reaction mixture was allowed to stir for 24 hrs. A second

equivalent of $Sb(O^tBu)_3$ (0.0171 g, 0.0501 mmol) in 2 mL of benzene was added to the reaction mixture and it was allowed to stir for another 24 hrs. The solvent was evacuated and crude product was extracted with hexanes. X-ray quality crystals of **3.9**·2DMSO were obtained by slow evaporation of a hexane/DMSO solution (4:1) over 2 days (0.0341 mmol, 0.0417 g, 68% yield).

Method B: To a colorless solution of **^{t}BuC5(H)$_5$** (0.0412 g, 0.0507 mol) in 3 mL of hexanes was added $Sb(O^tBu)_3$ (0.0342 g, 0.100 mmol) in 2 mL of hexanes. The solution was allowed to stand and slowly diffuse for 48 hrs. At the end of this time colorless X-ray quality needles were obtained. Filtration and two 5 mL pentane washing cycles allowed [$Sb_2O\{^t$**BuC5(H)**$\}$] **3.9** to be obtained as white crystalline needles in 43% yield (0.0218 mmol, 0.0233 g).

Method C: A colorless solution of $Sb(NMe_2)_3$ (0.0259 g, 0.102 mmol) in 2 mL of benzene was added dropwise to a colorless solution of **^{t}BuC5(H)$_5$** (0.0412 g, 0.0507 mol) in 3 mL of benzene and the reaction mixture was allowed to stir for 48 hrs. The solvent was reduced to half volume and 2 mL of hexane were added. The mixture was allowed to slowly evaporate to give 0.0319 g of **9**·$3C_6H_6$ as X-ray quality colorless crystals (0.0245 mmol, 48% yield). Mp: 176-178 ^oC. No NMR data are available due to insufficient solubility. IR (KBr, cm^{-1}): 3500w, 3047w, 2961vs, 2903vs, 2863s, 2360w, 1755w, 1575w, 1478vs, 1435s, 1414m, 1392m, 1316s, 1290s, 1245s, 1202vs, 1119s, 1103m, 1060m, 1011s, 946s, 916m, 877m, 767s, 741s, 675w, 538s. UV/vis (DMSO) λ_{max}/nm (ε/$dm^3mol^{-1}cm^{-1}$): 262 (3.38×10^4). Anal Calcd for $C_{55}H_{66}O_6Sb_2 \cdot 2C_2H_6SO$: C 57.95, H 6.43. Found C 57.57, H, 6.49.

Table 3.5 Crystallographic Data and Summary of Data Collection and Structure Refinement

	3.1	**3.3**	**3.4**	**3.5**
Formula	$C_{110}H_{134}Bi_2O_{10}$	$C_{124}H_{146}Bi_2O_{10}$	$C_{62}H_{72}O_6Sb_2$	$C_{140}H_{112}Bi_4O_{12}$
Fw	2034.13	2214.37	1156.72	2822.30
cryst syst	Monoclinic	Triclinic	Triclinic	Orthorhombic
space group	*C2/c*	*P*-1	*P*-1	*Pnna*
T, K	223(2)	213(2)	213(2)	213(2)
a, Å	28.586(5)	12.142(2)	14.411(4)	34.222(7)
b, Å	18.566(3)	14.819(3)	16.183(4)	19.487(4)
c, Å	26.834(5)	18.082(4)	16.211(4)	19.805(4)
α, deg	90	86.083(3)	94.706(5)	90
β, deg	122.108(9)	74.457(4)	109.515(5)	90
γ, deg	90	69.430(3)	105.495(5)	90
V, A^3	12063(4)	2933.5(10)	3372.4(16)	13208(5)
Z	4	1	2	4
d_{calcd} g·cm^{-3}	1.120	1.253	1.139	1.418
μ, mm^{-1}	2.960	3.049	0.842	5.369
Refl collected	34359	15173	18324	66832
T_{min}/T_{max}	0.845	0.902	0.953	0.839
N_{measd}	10608	8360	9667	9516
[R_{int}]	[0.1373]	[0.0677]	[0.0772]	[0.1882]
R [I>2sigma(I)]	0.0617	0.0649	0.0634	0.0714
R (all data)	0.1075	0.0782	0.1003	0.1314
R_w [I>2sigma(I)]	0.1391	0.2041	0.1993	0.1992
R_w (all data)	0.1521	0.2146	0.2224	0.2388
GOF	0.958	1.098	1.064	1.060
	3.7·C_6H_6	[**3.8**·2DMSO]· 3.5 DMSO	**3.9**·$3C_6H_6$	[**3.9**·2DMSO]· 1.5DMSO
Formula	$C_{41}H_{32}O_6Sb_2$	$C_{121}H_{165}Bi_4O_{17.5}S_{5.5}$	$C_{73}H_{84}O_6Sb_2$	$C_{62}H_{87}O_{9.5}S_{3.5}Sb_2$
Fw	864.17	2911.87	1300.90	1340.1
cryst syst	Monoclinic	Monoclinic	Triclinic	Tetragonal
space group	*C2/c*	$P2_1/m$	*P*-1	$I\text{-}4_1/a$
T, K	213(2)	223(2)	213(2)	223(2)
a, Å	14.538(2)	18.6628(13)	14.965(3)	29.948(4)
b, Å	18.489(2)	33.463(2)	15.239(3)	29.948(4)
c, Å	25.417(3)	22.8640(16)	16.261(4)	31.765(8)
α, deg	90	90	72.976(5)	90
β, deg	105.258(3)	109.8140(10)	68.079(4)	90
γ, deg	90	90	70.384(4)	90
V, A^3	6590.7(15)	13433.4(16)	3180.5(12)	28489(9)
Z	8	4	2	16
d_{calcd} g·cm^{-3}	1.742	1.304	1.358	1.140
μ, mm^{-1}	1.690	5.304	0.901	0.859
Refl collected	15662	91378	12994	100086
T_{min}/T_{max}	0.921	0.473	0.929	0.937
N_{measd}	4735	24057	8992	17255
[R_{int}]	[0.0965]	[0.1009]	[0.0464]	[0.1260]
R [I>2sigma(I)]	0.0425	0.0703	0.0406	0.1081
R (all data)	0.0533	0.0917	0.0625	0.1921
R_w [I>2sigma(I)]	0.1075	0.1915	0.1004	0.2801
R_w (all data)	0.1144	0.1999	0.1097	0.3185
GOF	1.018	1.126	0.941	0.938

3.5.3 General X-ray information

X-ray data for **3.1**, **3.3**, **3.4**, **3.5**, **3.7**, **3.8**, **3.9**·$3C_6H_6$ and **3.9**·2DMSO were collected on a SMART Bruker 1000 CCD detector diffractometer at low temperature using Mo Kα radiation. The crystallographic data and some details of the data collection and refinement of the structures are given in Table 3.5. Absorption corrections in all cases were applied by SADABS.[101] All structures were solved by direct methods and subsequent difference Fourier syntheses and refined by full matrix least-squares methods against F^2 (SHELX 97).[102] Disorder for some *tert*-butyl groups was due to 2-fold axis, and was modeled using partial occupancies (PART instruction).[102] Some other disordered molecules and solvents were refined using a combination of restraints on the distances while keeping the disordered parts similar (use of the SADI and SAME instructions).[102] All non-hydrogen atoms were refined with anisotropic displacement coefficients, except atoms of disordered fragments which were refined with isotropic thermal parameters. The H atoms in structures were taken in calculated positions. In the crystal structures of **3.8**·2DMSO and **3.9**·2DMSO**,** highly disordered molecules (14 DMSO molecules in **3.8** and 24 DMSO molecules in **3.9**·2DMSO) were treated with the program SQUEEZE.[103] Corrections of the X-ray data for **3.8**·2DMSO and **3.9**·2DMSO by SQUEEZE (587 and 1021 electron cell, respectively), were close to the required values (588 and 1008 electron cell, respectively). The program ORTEP32 was used to generate the X-ray structural diagrams pictured in this chapter.[104]

3.6 Conclusions

We have synthesized and fully characterized a series of calix[5]arene bismuth(III) and antimony(III) mono- and bimetallic complexes. The use of calixanions as precursors for the preparation of monometallic complexes was only successful when using the **^{t}BuC5(H)$_5$** ligand.

For the other **RC5(H)$_5$** (R = H, Bn) ligands the use of metal alkoxides or metal amides yielded the desired products. We have shown that the odd numbered calix[5]arenes are excellent ligands for the preparation of partially metallated complexes that feature free OH groups. Reaction of complexes **3.1** and **3.2** with M(O^{t}Bu)$_3$ allowed the addition of a second metal into the cavity verifying that the free OH groups are available for reactivity. All bimetallic complexes contain [(ArO)$_2$M]$_2$(μ-O) fragments but the antimony complexes **3.4**, **3.7**, **3.9**·3C$_6$H$_6$ and **3.9**·2DMSO are monomeric with the calixarenes in 1,2-alternate conformations, while the bismuth complexes **3.1**, **3.3**, **3.5** and **3.8** are dimeric units with the calixarene in cone-like conformations and displaying an overall (ArO)$_8$Bi$_4$O$_2$ motif. This trend may be due to the larger Lewis acidity, and/or the larger size of the bismuth atoms.

CHAPTER 4

CALIX[n]ARENE (n = 6-8) BISMUTH(III) AND ANTIMONY(III) COMPLEXES

4.1 Introduction

In the last three decades several bismuth and antimony alkoxides have been synthesized and studied as precursors for MOCVD or sol-gel synthesis of high purity metal oxides.[111,157] However, the number of bismuth and antimony aryloxides (including calixarenes) is small in comparison to transition metal and f block complexes.[51,61] Our interest in bismuth and antimony calixarene complexes lies in the development of bimetallic model molecules analogous to the SOHIO Bi-Mo catalyst for the study of the chemistry related to the oxidation and ammoxidation of propene.[6,111]

We described in Chapter 3 the synthesis and characterization of a series of bismuth and antimony complexes of the calix[n]arenes (n = 4, 5) obtained by the use of calixanion precursors[74] in reaction with MCl_3 (M = Bi, Sb) or reacting parent calixarene with strong bases.[57,58] Most of these metallocalix[n]arenes (n = 4,5) exist as mono- or binuclear complexes and they sometimes contain reactive moieties (such as terminal M-Cl) or unreacted phenolic OH groups, which enhance their capabilities as building blocks.

The coordination chemistry of the larger calix[n]arenes (n = 6-8) towards metallic centers has been studied during last decade. Reactions of the larger calixarenes with metal precursors tend to produce multi-metallic complexes with oxo environments.[61] The enhanced flexibility and conformational exchange of the larger calixarenes in comparison to that of the smaller membered calix[n]arenes (n = 4, 5) offers an extensive range of coordination modes, but it is very challenging to control the metallation.

In extension of our studies on the potential of bismuth and antimony aryloxides as assembling units for heterometallic complexes, we decided to explore the coordination capabilities of the larger calix[n]arenes (n = 6-8).[61] We believe that the large cavity size and availability of oxygen donor atoms in their lower rim offer considerable potential for platforms that could emulate aspects of heterogeneous catalyst surfaces. [70,158] In this Chapter we describe the synthesis and full characterization of a series of bismuth and antimony calix[n]arene (n = 6-8) complexes. We will highlight the level of metallation and the calixarene conformation after complexation. Aspects such as reactivity variation depending on the ring size and solid state structural features will also be discussed.

4.2 Results and discussion

We have found that the metal to calixarene ratio is variable, but there are pronounced similarities in the core structures. The core structures follow motifs that we have observed both in other calixarene complexes[57,58,159] as well as in non-calixarene complexes.[6]

Overall, it appears that the core structure is defined by the metal's preferred environment together with the availability of bridging oxygens, and the organic ligand(s) conform to the preferred core structures.

4.2.1. Monometallic complexes

Complex [Bi{^{t}**BuC6(H)$_3$**}]$_2$ **4.1** was prepared in 33% yield by the reaction of ^{t}**BuC6(H)$_6$** with one equivalent of Bi[N(SiMe$_3$)$_2$]$_3$ at 45 ^{o}C in ethyl ether. The product was obtained as yellow needles suitable for X-ray analysis. The reaction was slow under these conditions, but attempts to optimize the yield or accelerate the generation of **4.1** by increasing the reaction temperature produced a complex mixture. When the analogous reaction of **HC6(H)$_6$** with one equivalent of Bi[N(SiMe$_3$)$_2$]$_3$ or Bi(O^{t}Bu)$_3$ was performed, the crude ^{1}H NMR spectrum showed

a mixture of at least three products that were hard to isolate. It was necessary to react **HC6(H)$_6$** in a 1:2 ratio with Bi(O^{t}Bu)$_3$ to produce [Bi{**HC6(H)$_3$**}] **4.2** in 72% yield (Scheme 4.1). The solvent in this reaction is critical. If THF is used, [Bi{**HC6(H)$_3$**}] **4.2** is the only product obtained; however if toluene is used, complexes [Bi$_2${**HC6**}] **4.3** and [Bi{**HC6(H)$_3$**}] are obtained in 23 and 57% yields, respectively. The groups in the *para* position have a strong effect on the solubility of the **RC6(H)$_6$** bismuth complexes. Complex **4.1** has very low solubility in most solvents, while complexes **4.2** and **4.3** are moderately soluble in DMSO and THF. Complex **4.1-4.3** are moderately is air stable. Parent calixarene begins to appear in the ^{1}H NMR after one week for complex **4.1** and after 2 days for **4.2** and **4.3**.

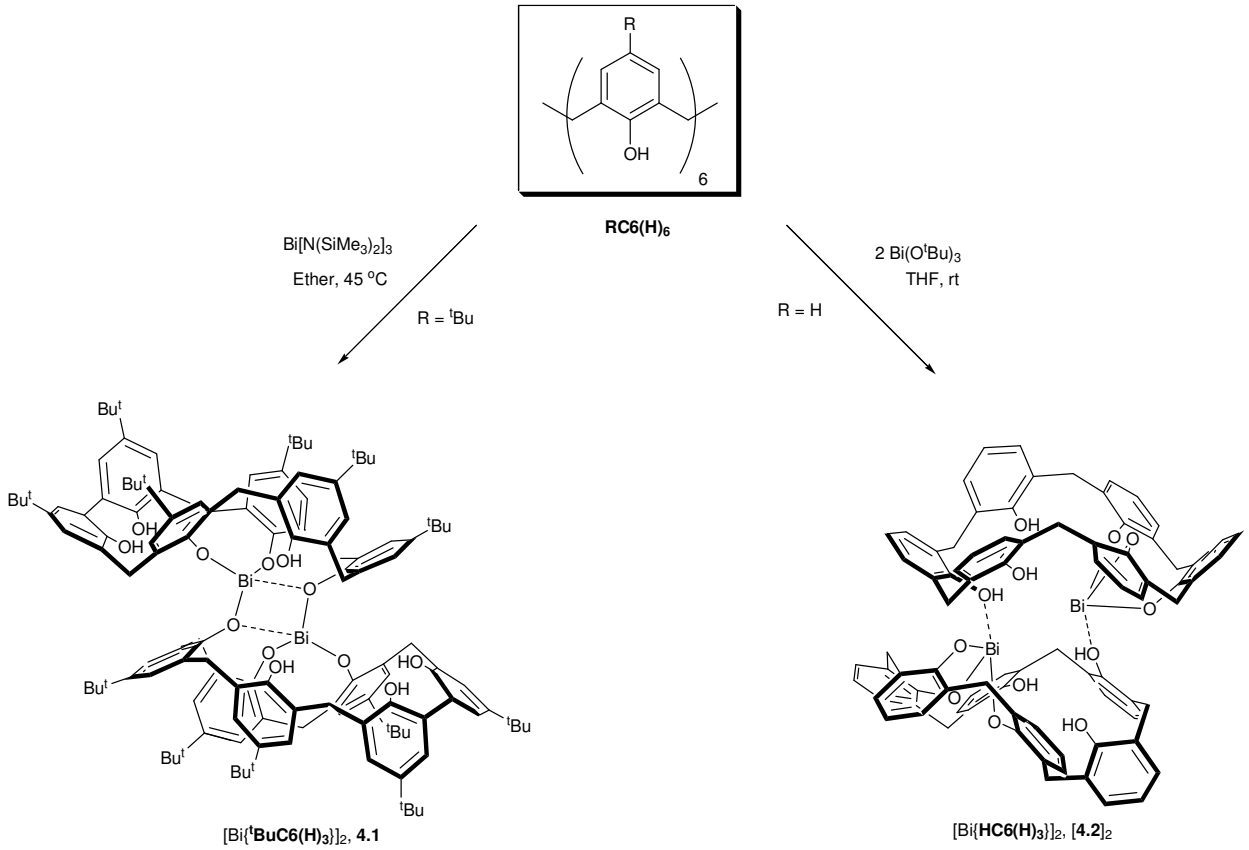

Scheme 4.1. Synthesis of monometallic complexes **4.1** and **4.2**.

The synthesis of mononuclear complexes of **RC6(H)$_6$** with transition metals or heavy main group elements is difficult, as evidenced by the few complexes of this kind reported in literature. [Ti(Cp){^{t}**BuC6(H)$_3$**}][160] and [Mo=NR{**HC6(H)$_2$**}] [161] are the only monometallic calix[6]arene complexes containing the metal center coordinated directly to the calixarene lower rim. Some other mononuclear complexes with metals such as Cu(I),[162] Cu(II),[163] Zn(II),[164] Pd(II), and Pt(II)[165] were obtained with the aid of nitrogen or phosphorus lower rim substituted **RC6(H)$_6$** ligands.

^{1}H NMR studies were only possible for complex **4.2** (Figure 4.1) since complex **4.1** had very low solubility. Complex **4.2** produced six methylene doublets (integrating to 2 hydrogens each) and two sharp peaks at 13.75 and 14.61 ppm (1:2 ratio) for the unreacted OH groups. As expected the complex displays highly unsymmetrical NMR patterns due to the partial metallation.

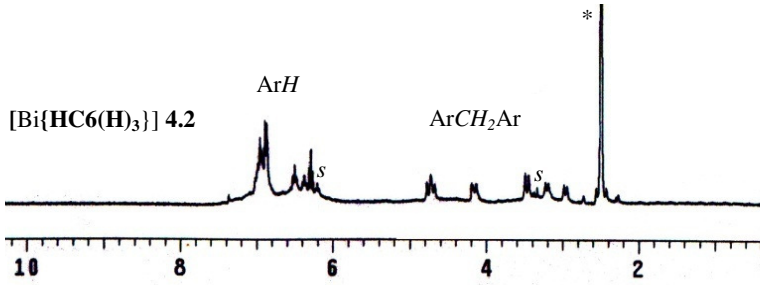

Figure 4.1. ^{1}H NMR spectra of complex [Bi{**HC6(H)$_3$**}] **4.2** in *DMSO-d$_6$. *s* = residual solvent (OH region not shown).

The crystal structures of **4.1** and **4.2** are illustrated in Figures 4.2 and 4.3, respectively, and selected bond distances and angles are listed in Table 4.1. Complexes **4.1** and **4.2** display very similar features and are structurally analogous to our calix[5]arene complex [Bi{^{t}**BuC5(H)$_2$**}].[121] Both complexes exhibit a dimeric structure with a bismuth atom

coordinated to each calixarene lower rim, and contain an inversion center located halfway between the two bismuth atoms. Each bismuth atom in complexes **4.1** and **4.2** is tetracoordinated with three aryloxides from a first calixarene unit and one aryloxide from the second unit.

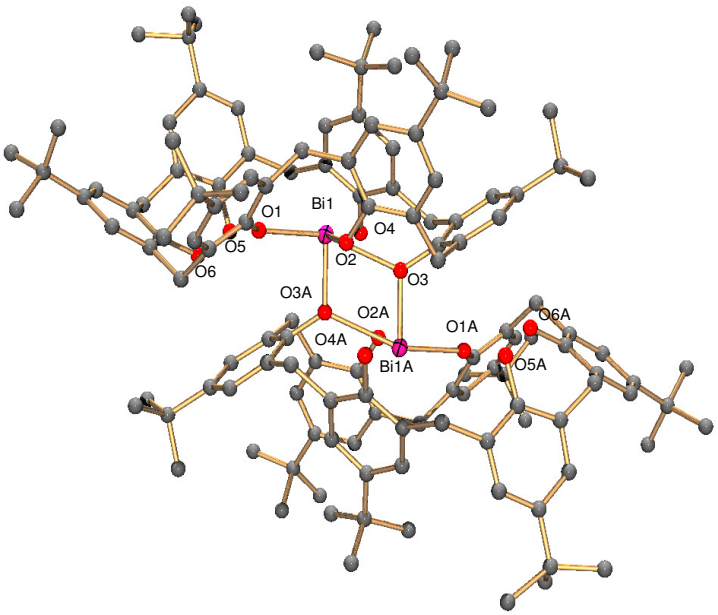

Figure 4.2. Crystal structure of complex **4.1**. Hydrogen atoms are omitted for clarity.

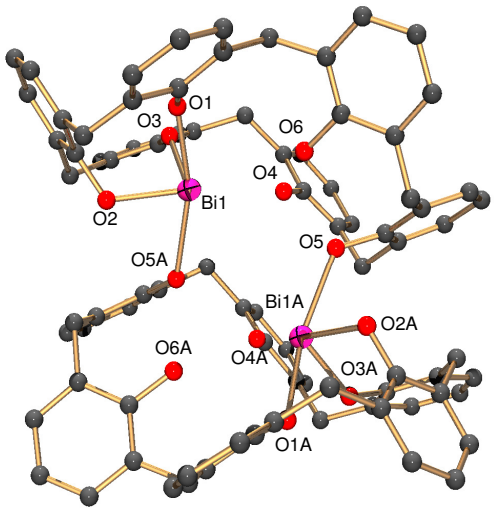

Figure 4.3. Crystal structure of complex **4.2.** Hydrogen atoms and uncoordinated solvents are omitted for clarity.

Table 4.1 Selected bond lengths (Å) and angles (º) of complexes **4.1** and **4.2**

4.1				**4.2**			
Bi(1)-O(1)	2.188(5)	O(1)-Bi(1)-O(3)	154.9(19)	Bi(1)-O(1)	2.210(6)	O(2)-Bi(1)-O(3)	87.4(3)
Bi(1)-O(2)	2.063(6)	O(1)-Bi(1)-O(3A)	93.9(2)	Bi(1)-O(2)	2.116(7)	O(1)-Bi(1)-O(5A)	163.5(2)
Bi(1)-O(3)	2.529(5)	O(2)-Bi(1)-O(3A)	87.9(2)	Bi(1)-O(3)	2.095(7)	O(2)-Bi(1)-O(5A)	79.2(3)
Bi(1)-O(3A)	2.141(5)	O(3)-Bi(1)-O(3A)	67.3(2)	Bi(1)-O(5A)	2.429(7)	O(3)-Bi(1)-O(5A)	104.0(3)
O(1)-Bi(1)-O(2)	86.6(2)	Bi(1)-O(3)-Bi(1A)	112.7(2)	O(1)-Bi(1)-O(2)	84.3(3)		
O(2)-Bi(1)-O(3)	76.64(18)			O(1)-Bi(1)-O(3)	74.5(3)		

The bismuth atoms in complex **4.1** contain primary Bi-O bonds with two aryloxides from the first calixarene [Bi(1)-O(1), Bi(1)-O(2) or Bi(1A)-O(1A), Bi(1A)-O(2A)] and with one aryloxide from the second ligand unit [Bi(1)-O(3A) or Bi(1A)-O(3)] in an overall pyramidal structure around the Bi center. The much longer secondary interaction [Bi(1)-O(3) or Bi(1A)-O(3A)] lies across from one of the primary Bi-O bonds with a distance of 2.529(5) Å. The primary Bi(1)-O(3A) and Bi(1A)-O(3) interactions link the two calixarene units and form a central planar $Bi_2(\mu\text{-}O)_2$ four-membered ring similar to the ones observed in other $M_2(\mu\text{-}O)_2$ rings of calix[n]arene (n = 4, 5) main group organometallic complexes (M = Al, Sn, Ga and Zn)[112,115,116,133] and in the $[U_2Cl_2\{\mathbf{HC6}\}(3THF)]_2$ complex.[166] The O-Bi-O and Bi-O-Bi angles in the $Bi_2(\mu\text{-}O)_2$ ring are 67.3(2)^o and 112.7(2)^o, respectively.

The bismuth atoms in complex **4.2** contain three primary Bi-O bonds with aryloxides from the same calixarene [Bi(1)-O(1), Bi(1)-O(2), Bi(1)-O(3)] and a secondary interaction with an aryloxide from the second calixarene unit [Bi(1)-O(5A)]. The primary Bi-O bonds provide a pyramidal geometry around the bismuth center, while the longer secondary interaction [2.429(7) Å] links the two calixarenes. The O(5) and O(5A) atoms are still protonated, leading to a long Bi(1)-O(5A) bond, and possibly the reason that the $Bi_2(\mu\text{-}O)_2$ ring is not formed in complex **4.2**.

The primary Bi-OAr bond distances and ArO-Bi-OAr angles in **4.1** and **4.2** range from 2.063(6) to 2.210(6) Å and 67.3(2)^{o} to 163.5(2)^{o}, respectively, and fall within normal ranges for other bismuth(III) calixarene, alkoxide and aryloxide complexes.[57,58,121,141-145] The two calixarene backbone units in the structures of **4.1** and **4.2** are in distorted cone conformations and no bismuth π-arene interactions were observed.

4.2.2 Bimetallic complexes

The syntheses of binuclear complexes **4.3**, **4.4**, **4.5**, and **4.6** and the trinuclear side product **4.4a** are illustrated in Scheme 4.2. Complexes **4.3-4.5** are monomeric whereas complex **6** is dimeric in order to allow formation of the trademark $Bi_4O_2(OAr)_8$ core structure.[6,57,58,159] We will see this same $Bi_4O_2(OAr)_8$ core supported by a single calix[8]arene ring in the next section (tetranuclear complexes).

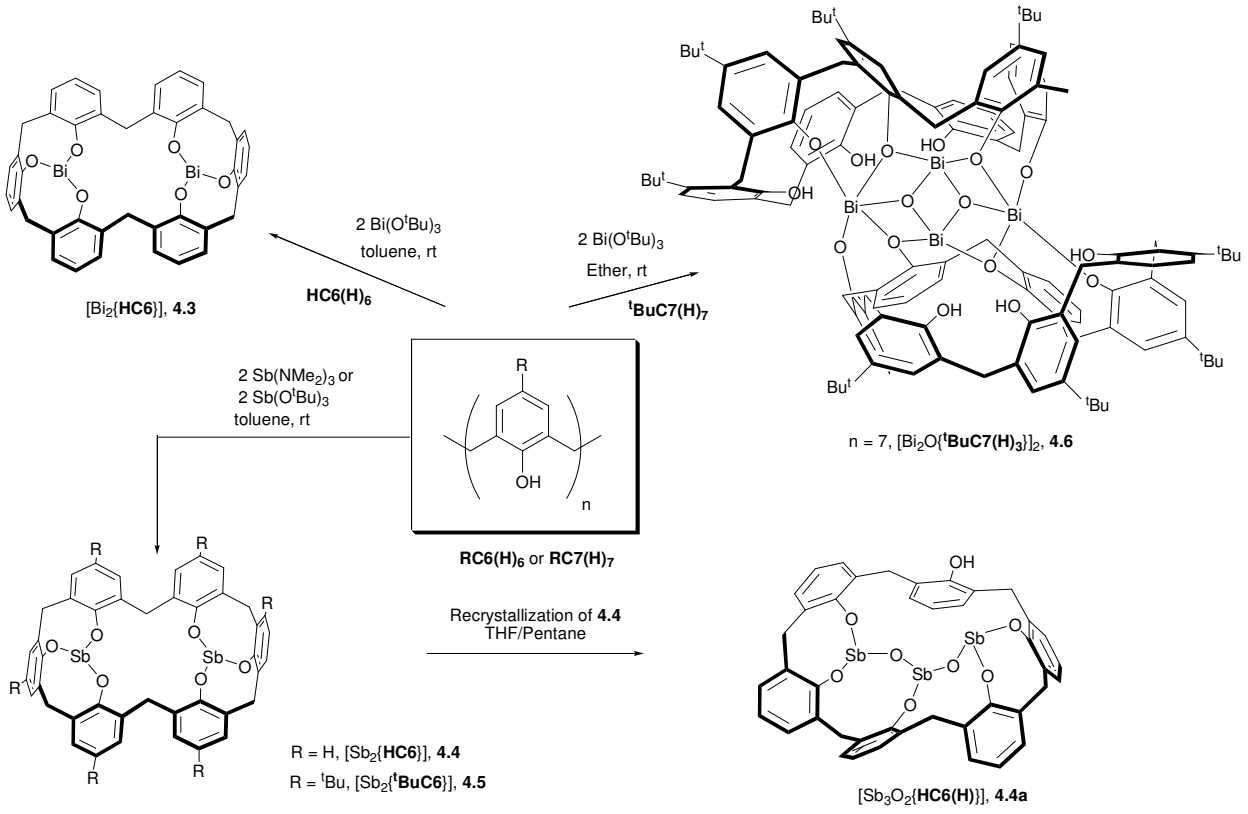

Scheme 4.2. Synthesis of dinuclear bismuth and antimony calix[n]arene (n = 6, 7) complexes.

4.2.2.1 Calix[6]arene complexes

As described above the bimetallic complex [Bi_2{**HC6**}] **4.3** is obtained by the reaction of **HC6(H)$_6$** and 2 equivalents of $Bi(O^tBu)_3$ in toluene. The low solubility of **HC6(H)$_6$** in toluene presumably favors the preparation of the bimetallic complex. Complex **4.3** has very low solubility in most solvents and is highly air and moisture sensitive.

In order to prepare **RC6(H)$_6$** (R = H, ^{t}Bu) monometallic antimony complexes we treated the *in situ* prepared trianionic calixarene precursors Li_3·**RC6(H)$_3$** with 1 equiv of $SbCl_3$. The reaction in both cases yielded either complex mixtures or uncharacterizable solids. On the other hand, when **RC6(H)$_6$** reacted with one or two equivalents of SbX_3 (X = O^tBu, NMe_2) in toluene or benzene, clean products with composition [Sb_2{**HC6**}] **4.4** and [Sb_2{**^{t}BuC6**}] **4.5** were obtained. These results are not surprising since **RC6(H)$_6$** usually favours the formation of dinuclear coordination complexes.[61]

While preparing complex **4.5** we noticed that traces of moisture in the calixarene ligand affected the outcome of the reaction. For example, when SbR_3 was reacted with oven-dried **^{t}BuC6(H)$_6$**, a mixture of **4.5** and an unknown complex was obtained. However, if the reaction was carried out using calixarene ligand that had been dried under vacuum at 120 ^{o}C for 3 days, pure complex **4.5** was obtained after workup.

Complexes **4.3**, **4.4** and **4.5** contain very similar ^{1}H NMR spectra (Figure 4.4). The three complexes show two doublets and a singlet in the methylene area and in case of complex **4.5** two *tert*-butyl peaks in 2:1 ratio are observed. These patterns are characteristic of calix[6]arene in 1,2,3-alternate conformation, as described previously for various alkali and transition metal complexes.[60,74,160]

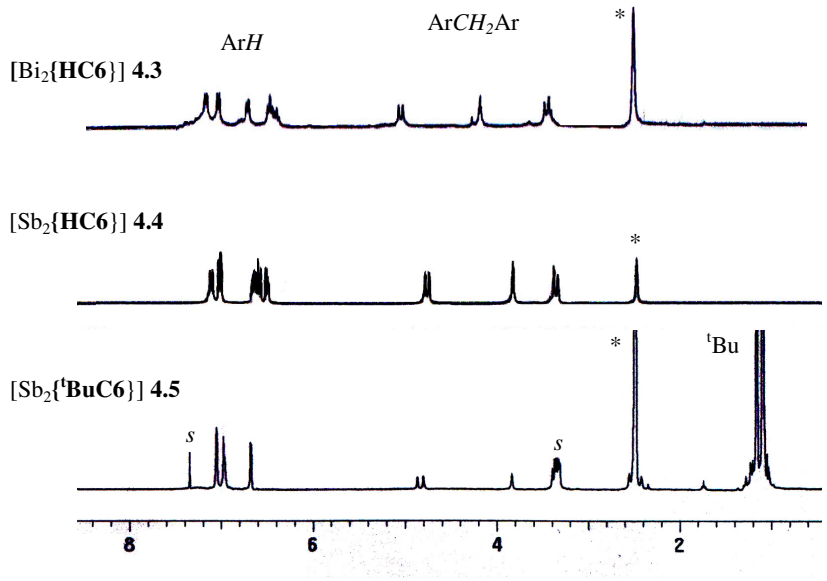

Figure 4.4. ^{1}H NMR spectra in *DMSO-d_6 for binuclear complexes **4.3**, **4.4** and **4.5**. *s* = residual solvent.

We obtained needle-like single crystals of complex **4.4** by diffusion of pentane into a dilute THF solution. The crystal structure is depicted in Figure 4.5 and selected bonds and angles are shown in Table 4.2. In the solid state complex **4.4** crystallizes in the *P*-1 space group as a monomeric bimetallic complex with each Sb atom coordinated to three contiguous aryloxide oxygens in a trigonal pyramidal geometry. An overall C_{2v} plane of symmetry is observed between the two antimony centers and the calixarene ligand displays a distorted 1,2,3-alternate conformation in agreement with the symmetry observed in the ^{1}H NMR spectrum. The crystal structure of **4.4** is similar to that of other dinuclear calix[6]arene complexes reported in literature.[60,160,165,167] The Sb-OAr bond distances range from 1.940(3) to 1.988(3) Å and the O-Sb-O angles range from 90.36(14) to 97.52(13)^{o}, comparable to the distances and angles observed in previous antimony calixarene complexes reported by our group.[57,58,121]

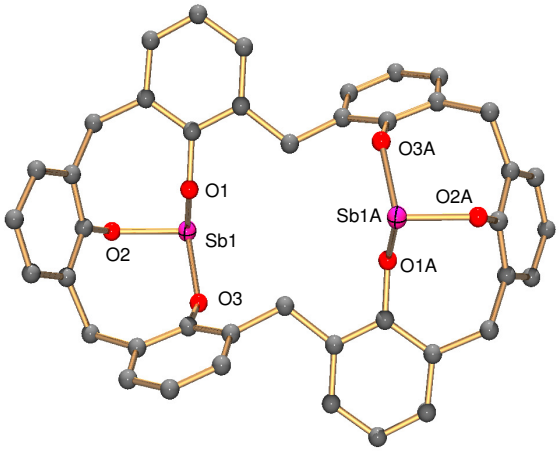

Figure 4.5. Crystal structure of the complex [Sb_2{**HC6**}] **4.4**. Hydrogen atoms and non-coordinated solvents are omitted for clarity.

Table 4.2 Selected bond lengths (Å) and angles (°) of complexes **4.4** and **4.4a**

4.4		**4.4a**			
Sb(1)-O(1)	1.940(3)	Sb(1)-O(1)	1.977(4)	Sb(3)-O(8)	1.946(4)
Sb(1)-O(2)	1.988(3)	Sb(1)-O(2)	2.021(4)	O(1)-Sb(1)-O(7)	93.79(19)
Sb(1)-O(3)	1.975(3)	Sb(1)-O(7)	1.918(4)	O(2)-Sb(1)-O(7)	86.76(16)
O(1)-Sb(1)-O(2)	97.52(13)	Sb(1)-O(9)	2.548(4)	O(3)-Sb(2)-O(8)	95.42(19)
O(2)-Sb(1)-O(3)	90.36(14)	Sb(2)-O(3)	1.989(4)	O(7)-Sb(2)-O(8)	86.17(16)
O(1)-Sb(1)-O(3)	92.51(14)	Sb(2)-O(7)	2.017(4)	O(4)-Sb(3)-O(8)	93.9(2)
		Sb(2)-O(8)	1.948(4)	O(5)-Sb(3)-O(8)	90.26(18)
		Sb(3)-O(4)	2.001(5)	Sb(1)-O(7)-Sb(2)	123.0(2)
		Sb(3)-O(5)	2.012(4)	Sb(2)-O(8)-Sb(3)	123.3(2)

While attempting the crystallization of complex **4.4** prepared from the reaction of oven-dried **HC6(H)$_6$** and Sb(O^{t}Bu)$_3$, we obtained a white precipitate together with a few colorless crystalline blocks. We analyzed the crystals and were surprised to find a different unit cell than the one recorded for complex **4.4**. The crystal structure showed a new complex with composition [Sb_3O_2{**HC6(H)**}] **4.4a**. The structure of complex **4.4a** is illustrated in Figure 4.6 and selected

bond distances and angles are listed in Table 4.2. Complex **4.4a** displays a monomeric structure containing an overall $Sb_3(\mu\text{-}O)_2(OAr)_5$ core. Complex **4.4a** is the second example of a trimetallated complex supported by a calix[6]arene ligand reported in the literature to date.[167]

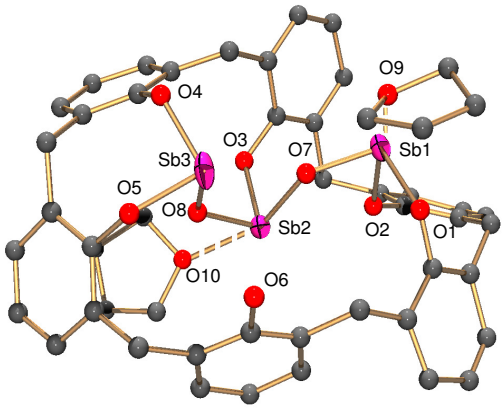

Figure 4.6. Crystal structure of the trimetallated complex $[Sb_3O_2\{\mathbf{HC6(H)}\}]$ **4.4a**. Hydrogen atoms are omitted for clarity.

Complex **4.4a** contains different coordination environments around the three antimony atoms. The Sb(1) atom is covalently coordinated to two aryloxides and a bridging oxygen, while the Sb(2) is covalently coordinated to one aryloxide and two bridging oxygens with an overall trigonal pyramidal geometry around the antimony center. Both Sb(1) and Sb(2) have secondary Sb-O(THF) interactions [Sb(1)-O(9) and Sb(2)-O(10)] with distances of 2.548(4) and 2.600(4) Å, respectively. These distances are similar to other Sb-O(THF) interactions found in literature.[138] The Sb(3) atom, on the other hand, is coordinated to two aryloxides and a bridging oxygen in a trigonal pyramidal geometry. The Sb-OAr bond distances range from 1.977(4) to 2.021(4) Å, in the normal range for Sb(III) aryloxide and alkoxide complexes.[57,121,138,139]

The Sb(1)-O(7) and Sb(2)-O(7) bond distances are 1.918(4) and 2.017(4) Å, respectively, while Sb(2)-O(8) is 1.948(6) and Sb(3)-O(8) is 1.946(4) Å. All of these distances are similar to the Sb-OAr distances, indicating covalent bonding with the bridging oxygens. The Sb(1) and

Sb(3) atoms are part of eight membered rings formed by coordination of the two aryloxide groups from the calixarene. The conformation in both rings could be described as twisted boat (TB), similar to the conformations observed in other main group calixarene complexes.[126,136] The zig-zag arrangement of the metallic core forces the calixarene ligand to adopt a distorted partial cone conformation.

Bridging oxygens. In complex **4.4a** the three antimony atoms are linked by two bridging oxygens [O(7) and O(8)] that do not belong to the calixarene ligand. Similarly, we have observed bridging oxygens appearing in calix[5]arene[159] and even-numbered calixarene complexes[57,58] of both bismuth and antimony. Bismuth complexes **4.6**, **4.7**, and **4.8** (*vide infra*) will also feature bridging oxygens of unknown source. In previous discussions,[6,57,58,159] we have concluded that the most likely source of oxygen in all of these cases is the calixarene starting material. It is well known that the lower rim OH groups of parent calixarene form a hydrogen bonding network, and that water is relatively strongly associated to solid calixarene.

Although it is difficult to definitively remove all water from calixarene starting materials, we did find that a more thorough drying of **HC6(H)$_6$** starting material eliminated the appearance of the oxygen-bridged byproduct **4.4a**. We were not successful in forming complex **4.4a** from complex **4.4** by addition of stoichiometric water; parent calixarene was formed instead. Likewise, the use of "dried" calixarene in the synthesis of oxygen-bridged bismuth complex **4.6** led only to complex mixtures; undried calixarene is necessary in order to produce pure product.

4.2.2.2 Calix[7]arene complexes

Within the "larger" calix[n]arenes (n = 6-8), the **RC7(H)$_7$** ligand is the most scarcely investigated due to its difficult and low yielding synthesis.[87,168] Only few papers concerning lower rim metal complexes of **RC7(H)$_7$** can be found in the literature.[85,169-171] We expected the

selective synthesis of **^{t}BuC7(H)$_7$** complexes to be a challenge due to its greater coordination and conformational flexibility in comparison to the **RC6(H)$_6$** ligand. Indeed, when **^{t}BuC7(H)$_7$** was reacted with 3 equivalents of LiO^{t}Bu (to produce the trianionic salt) a mixture of at least 4 products was observed by ^{1}H NMR spectroscopy. This result indicated that calixanions might not be selective precursors for the synthesis of Bi or Sb complexes. However, when **^{t}BuC7(H)$_7$** was treated with one equivalent of Bi(O^{t}Bu)$_3$ in diethyl ether one new complex was observed together with unreacted **^{t}BuC7(H)$_7$**. The ^{1}H NMR spectrum of the reaction mixture showed three OH peaks, eleven different doublets for the methylene protons, and seven *tert*-butyl peaks (all integrating in a 1:1 ratio) (see Figure 4.7). The low symmetry suggests partial metallation of the calixarene. When a second equivalent of Bi(O^{t}Bu)$_3$ was added to the reaction mixture, the parent calixarene was totally consumed, yielding only the new complex **4.6** (Scheme 4.2). The stepwise addition of Bi(O^{t}Bu)$_3$ to **^{t}BuC7(H)$_7$** is very important since the single addition of 2 equivalents of Bi(O^{t}Bu)$_3$ produced a complex mixture. Single crystals were obtained by slow evaporation of a DME/benzene/DMSO (1:1:1) solution of the product.

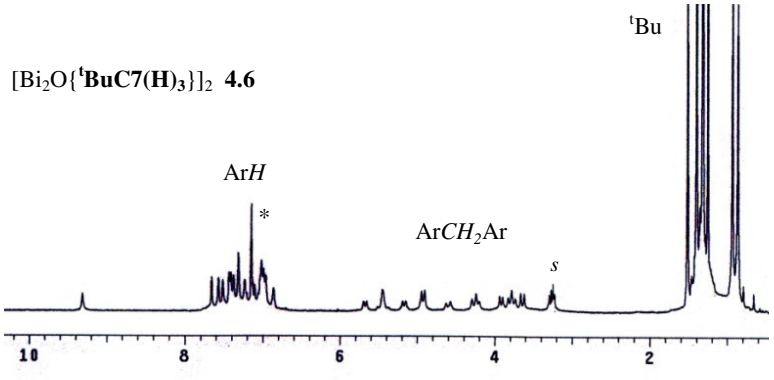

Figure 4.7. ^{1}H NMR spectra of complex [$Bi_2O\{^{t}$**BuC7(H)$_3$**$\}]_2$ **4.6** in *C_6D_6. *s* = residual solvent (OH region not shown).

The crystal structure of complex **4.6** is shown in Figure 4.8 and selected bond distances and angles are listed in Table 4.3. Complex **4.6** crystallizes in the space group $P2_1/n$ and displays

a dimeric structure with each calixarene ligand containing two bismuth atoms in the lower rim. The X-ray structure of complex **4.6** represents the first of its kind since only structures of **RC7(H)$_7$** with lanthanides[169,171] are found in the literature. The core structure of **4.6** can be described as five fused $Bi_2(\mu\text{-}O)_2$ four-membered rings in a overall $Bi_4O_2(OR)_8$ motif. The $Bi_4O_2(OR)_8$ core has emerged as a common subunit in bismuth oxo alkoxide clusters, such as the calixarene complexes [Bi_4O_2{^{t}**BuC8**}], [Bi_4O_2{^{t}**BuC5(H)**}$_2$], and [Bi_4O_2{**BnC5(H)**}$_2$] reported previously by our group.[57,121] Two bridging oxygens [O(15) and O(16)] that do not belong to the calixarene ring are observed in the $Bi_4O_2(OAr)_8$ core structure. Similar to our other Bi and Sb calixarene complexes,[57,159] they probably originate from moisture in the calixarene ligands.

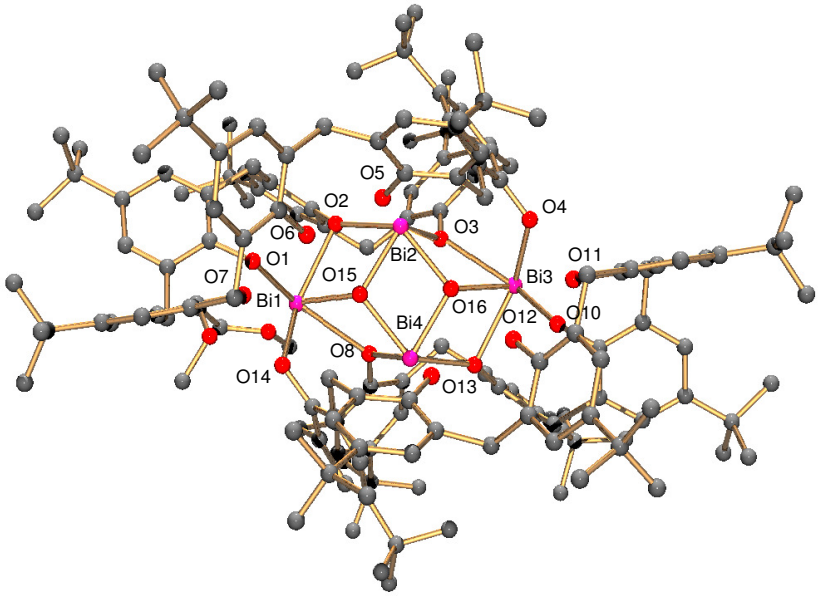

Figure 4.8. Crystal structure of complex **4.6**. Hydrogen atoms and DME molecules coordinated to Bi(1) and Bi(3) are omitted for clarity.

Table 4.3 Selected bond distances (Å) and angles (º) of complex **4.6**

4.6					
Bi(1)-O(1)	2.188(6)	Bi(3)-O(9)	2.459(7)	Bi(2)-O(3)-Bi(3)	98.6(2)
Bi(1)-O(2)	2.439(6)	Bi(3)-O(10)	2.194(6)	Bi(2)-O(16)-Bi(3)	113.4(3)
Bi(1)-O(8)	2.655(6)	Bi(3)-O(16)	2.174(6)	Bi(2)-O(16)-Bi(4)	106.3(3)
Bi(1)-O(14)	2.151(6)	Bi(4)-O(8)	2.190(7)	Bi(3)-O(9)-Bi(4)	102.6(2)
Bi(1)-O(15)	2.172(6)	Bi(4)-O(9)	2.270(6)	O(15)-Bi(2)-O(16)	71.5(2)
Bi(2)-O(2)	2.251(6)	Bi(4)-O(15)	2.214(6)	O(15)-Bi(4)-O(16)	71.8(2)
Bi(2)-O(3)	2.209(6)	Bi(4)-O(16)	2.174(6)	Bi(1)-Bi(2)	3.6821(5)
Bi(2)-O(15)	2.180(6)	Bi(1)-O(2)-Bi(2)	103.4(2)	Bi(2)-Bi(3)	3.6720(5)
Bi(2)-O(16)	2.220(6)	Bi(1)-O(15)-Bi(2)	115.5(3)	Bi(3)-Bi(4)	3.6928(5)
Bi(3)-O(3)	2.622(6)	Bi(1)-O(15)-Bi(4)	114.4(3)	Bi(2)-Bi(4)	3.5162(6)
Bi(3)-O(4)	2.157(6)	Bi(1)-O(8)-Bi(4)	98.7(2)		

The central $Bi_2(\mu\text{-}O)_2$ four membered ring **I,** formed by Bi(2), Bi(4), O(15) and O(16) atoms (Figure 4.9), contains Bi-O bond lengths in the range from 2.174(6) to 2.220(6) Å. These distances are similar to those for Bi-OAr primary bonds, indicating covalent bonding to the triply bridging oxygens.

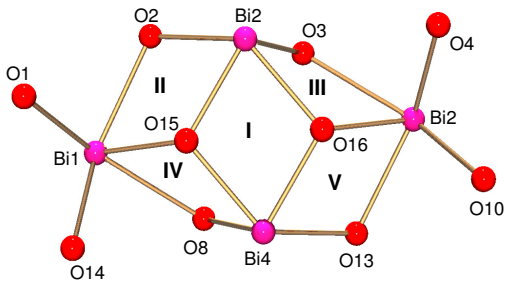

Figure 4.9. $Bi_4O_2(OR)_8$ structure of complex **4.6** showing the five $Bi_2(\mu\text{-}O)_2$ fused rings.

The O-Bi-O angles in the central ring **I** are 71.5(2)^{o} and 71.8(2)^{o} and the Bi-O-Bi angles are 106.3(3)^{o}. Both distances and angles are similar to those found in the $M_2(\mu\text{-}O)_2$ rings found in calixarene, alkoxide or aryloxide complexes reported in literature.[112,115,116,133] The torsion angle for the central ring **I** in complex **4.6** is 15.76(8)^{o}, indicating deviation from planarity.

The four outer rings in the $Bi_4O_2(OR)_8$ core structure of complex **4.6** (**II-V**, see Figure 4.9) contain Bi-O bond lengths and torsion angles similar to those observed for the central ring **I**. Metal-metal distances within the $Bi_2O_2(OR)_8$ core for complex **4.6** are Bi(1)-Bi(2) 3.6821(5), Bi(2)-Bi(3) 3.6720(5), Bi(3)-Bi(4) 3.6928(5), Bi(2)-Bi(4) 3.5162(6) and Bi(4)-Bi(1) 3.6882(5) Å. All these distances are similar to those found in our previously reported [Bi_4O_2{**RC5(H)**}$_2$] complexes.[159]

The Bi(1) and Bi(3) metal centers are coordinated to four aryloxides, one bridging oxygen and a DME molecule (not shown in Figure 4.8), to form a distorted octahedral geometry. The four aryloxide groups occupy the equatorial positions while the bridging oxygen and DME define the apical positions. The O-Bi-O angle for the apical positions is around 161^{o}, showing deviation to the expected 180^{o}. The Bi(2) and Bi(4) atoms are coordinated to two aryloxides and two bridging oxygens in a overall distorted square-based pyramidal geometry. The calixarene ligands display a distorted cone conformation and three OH groups can be located in agreement with the NMR spectrum. No bismuth π-arene interactions are observed for **4.6**.

4.2.3. Tetranuclear complexes

The synthesis of tetranuclear complexes **4.7** and **4.8** is illustrated in Scheme 4.3. The cavity of calix[8]arene is the first to be sufficiently spacious to support the entire $Bi_4O_2(OAr)_8$ core with a single calixarene ligand, leading to a 4:1 metal to ligand ratio. The accessibility of the $Bi_4O_2(OAr)_8$ core is illustrated by an overall dimeric structure of complexes [**4.7**]$_2$ and [**4.8**]$_2$

(Scheme 3), in which a larger central cluster is composed of two $Bi_4O_2(OAr)_8$ ladders linked together in a perpendicular fashion.

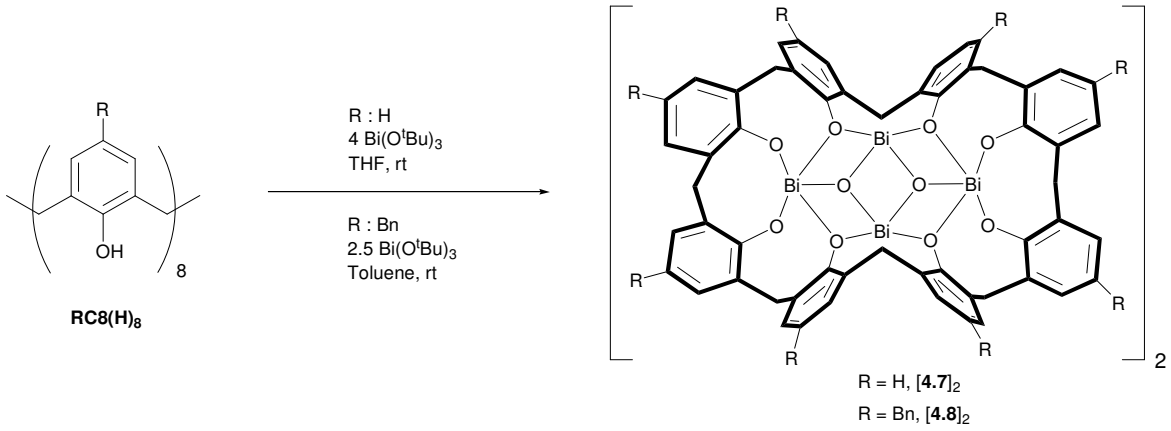

Scheme 4.3. Synthesis of tetranuclear calix[8]arene bismuth complexes.

The Rcalix[8]arene (R = H, Bn) ligands have very similar reactivity. Treatment of **RC8(H)$_8$** with 1 equivalent of $Bi(O^tBu)_3$ resulted in a mixture of unreacted **RC8(H)$_8$** and $[Bi_4O_2\{$**HC8**$\}]$ **4.7** or $[Bi_4O_2\{$**BnC8**$\}]$ **4.8**. The ^{1}H NMR spectrum of the reaction mixture in both cases displayed only a single OH peak belonging to the parent **RC8(H)$_8$** ligand, suggesting that the new complex was fully metallated. We noticed that the stepwise addition of 4 equivalents of $Bi(O^tBu)_3$ to **HC8(H)$_8$** in THF and the stepwise addition of 2.5 equivalents of $Bi(O^tBu)_3$ to **BnC8(H)$_8$** in toluene yielded pure complexes $[Bi_4O_2\{$**HC8**$\}]$ **4.7** and $[Bi_4O_2\{$**BnC8**$\}]$ **4.8**, respectively (Scheme 4.3). It is very important to use stepwise addition of the $Bi(O^tBu)_3$ in order to avoid side products. The ^{1}H NMR spectra for complexes **4.7** and **4.8** (Figure 4.10) displayed three pairs of doublets for the methylene area (2:1:1 intensity) and no OH groups were observed. The ^{1}H NMR patterns are similar to those observed for our previously synthesized $[Bi_4O_2\{$**^{t}BuC8**$\}]$ complex[57] and are consistent with the preparation of the analogous tetranuclear complexes **4.7** and **4.8**. Attempts to produce partially metallated complexes by decreasing the

equivalents of $Bi(O^tBu)_3$ to 0.75 or 0.5 resulted in the production of the tetranuclear complexes in poor yields.

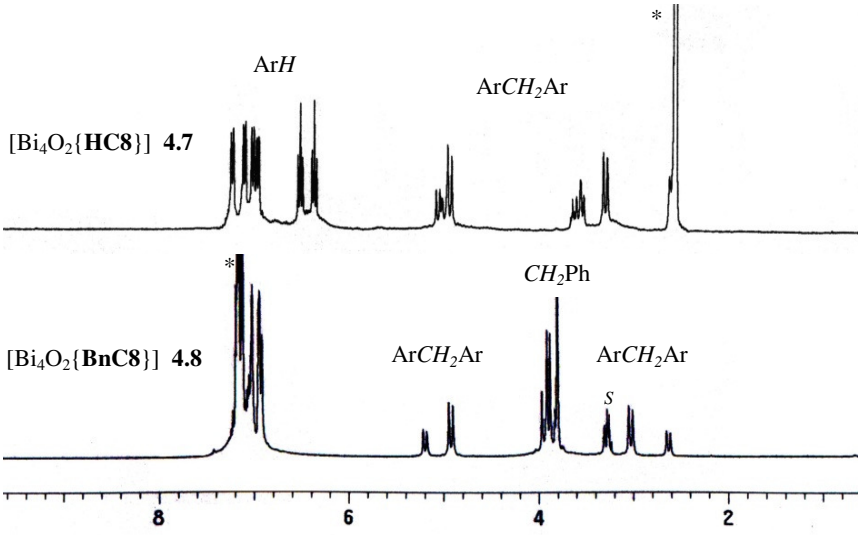

Figure 4.10. ^{1}H NMR spectra of tetranuclear complexes **4.7** in *DMSO-d_6 and **4.8** in *C_6D_6**.** *s* = residual solvent.

Single crystals of complex [**4.7**]$_2$ were obtained by diffusion of hexane into a toluene/benzene/MeCN (1:1:1) solution and single crystals of complex [**4.8**]$_2$ were obtained by hexane diffusion into a THF/toluene/DME (1:1:1) solution. The X-ray structures of complexes **[4.7]**$_2$ and [**4.8**]$_2$ are illustrated in Figures 4.11-4.13 and selected bond distances and angles for complex [**4.8**]$_2$ are listed in Table 4.4. The structure of complex [**4.7**]$_2$ could not be well refined due to the poor quality of the crystal; however the atom connectivity is clear and allows its comparison with complex [**4.8**]$_2$. The crystal structures of complexes [**4.7**]$_2$ and [**4.8**]$_2$ display very similar features. Each calixarene ligand in both structures is tetrametallated and contains five fused $Bi_2(\mu\text{-}O)_2$ four-membered rings in an overall $Bi_4O_2(OAr)_8$ core system similar to that observed in complex **4.6** and other calixarene complexes prepared in our lab (see Figure 4.11).[57,58,121]

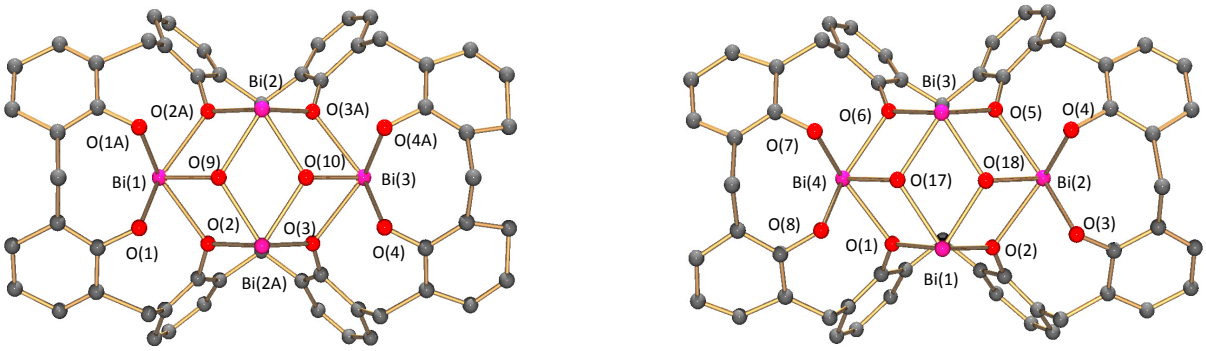

4.7 **4.8**

Figure 4.11. Monomeric representation of complexes [**4.7**]$_2$ and [**4.8**]$_2$ displaying the $Bi_4O_2(OAr)_8$ motif.

As in case of complex **4.6,** the five fused four-membered rings feature individual planarity, but they are not coplanar with each other. The calixarene ligands are in a pinched cone conformation with a C_{2v} symmetry consistent with the NMR patterns. The monomeric representation of complexes [**4.7**]$_2$ and [**4.8**]$_2$ (Figure 4.11) resembles the structure of the complex ion $[(Bi(\mu_3\text{-}Cl)Cl)_4(\mu\text{–}Cl)_2\{Li_4\cdot\mathbf{^tBuC8}\}]^{2-}\cdot 3THF\cdot DME$ synthesized in our lab with the aid of calixanion precursors.[58] All Bi-O bond distances, Bi-O-Bi angles, and O-Bi-O angles in complex [**4.8**]$_2$ fall in the normal range for bismuth calixarene complexes (Table 4.4).

The overall structure of complex [**4.7**]$_2$ (Figure 4.12) has S_4 symmetry and consists of two **HC8** units linked by a Bi_8O_4 core similar to the one found in the complex $[Bi_8O_4\{\mathbf{^tBuC8}\}_2]$ reported by our group.[57] If the oxygen atoms of the calixarene are considered, complex [**4.7**]$_2$ contains a robust Bi_8O_{20} oxo cluster (Figure 4.13) that contains two different types of bismuth atoms. The first type includes the bismuth atoms Bi(1), Bi(3), Bi(5) and Bi(5A), that are coordinated to four calixarene oxygens and to one bridging oxygen in a distorted square-based pyramidal geometry. The basal plane is formed by four calixarene oxygens and the apical position is occupied by the bridging oxygen. The second type of bismuth atom includes Bi(2),

Bi(2A), Bi(4) and Bi(6), with coordination to two oxygens from the calixarene ligand and to three bridging oxygens.

Table 4.4 Selected bond lengths (Å) and angles (º) for complex [**4.8**]$_2$

			[4.8]$_2$		
Bi(1)-O(1)	2.294(9)	Bi(5)-O(9)	2.287(9)	O(17)-Bi(1)-O(18)	69.1(3)
Bi(1)-O(2)	2.294(9)	Bi(5)-O(16)	2.248(10)	O(2)-Bi(2)-O(17)	70.5(3)
Bi(1)-O(17)	2.263(8)	Bi(5)-O(18)	2.540(9)	O(17)-Bi(3)-O(18)	66.8(3)
Bi(1)-O(18)	2.218(9)	Bi(5)-O(19)	2.257(9)	O(1)-Bi(4)-O(18)	69.5(3)
Bi(1)-O(19)	2.556(9)	Bi(5)-O(20)	2.290(9)	O(19)-Bi(5)-O(20)	68.3(4)
Bi(2)-O(2)	2.394(9)	Bi(6)-O(9)	2.447(10)	O(9)-Bi(6)-O(19)	69.9(3)
Bi(2)-O(3)	2.156(10)	Bi(6)-O(10)	2.200(10)	O(19)-Bi(7)-O(20)	67.8(3)
Bi(2)-O(4)	2.210(10)	Bi(6)-O(11)	2.173(11)	O(13)-Bi(8)-O(20)	69.6(4)
Bi(2)-O(5)	2.552(10)	Bi(6)-O(12)	2.436(10)	O(1)-Bi(1)-O(2)	86.2(3)
Bi(2)-O(17)	2.115(8)	Bi(6)-O(19)	2.112(9)	O(3)-Bi(2)-O(4)	82.1(4)
Bi(3)-O(5)	2.227(10)	Bi(7)-O(12)	2.239(10)	O(5)-Bi(3)-O(6)	85.1(3)
Bi(3)-O(6)	2.266(9)	Bi(7)-O(13)	2.219(10)	O(7)-Bi(4)-O(8)	77.5(4)
Bi(3)-O(17)	2.294(10)	Bi(7)-O(19)	2.300(9)	O(10)-Bi(6)-O(11)	79.3(4)
Bi(3)-O(18)	2.322(8)	Bi(7)-O(20)	2.275(11)	O(12)-Bi(7)-O(13)	84.8(4)
Bi(3)-O(21)	2.609(10)	Bi(7)-O(21)	2.621(10)	O(14)-Bi(8)-O(15)	81.5(5)
Bi(4)-O(1)	2.414(9)	Bi(8)-O(13)	2.547(11)	Bi(1)-O(18)-Bi(3)	112.0(3)
Bi(4)-O(6)	2.414(9)	Bi(8)-O(14)	2.197(11)	Bi(1)-O(17)-Bi(3)	111.4(4)
Bi(4)-O(7)	2.187(10)	Bi(8)-O(15)	2.148(11)	Bi(5)-O(19)-Bi(7)	111.7(4)
Bi(4)-O(8)	2.182(10)	Bi(8)-O(16)	2.446(9)	Bi(5)-O(20)-Bi(7)	111.4(4)
Bi(4)-O(18)	2.138(9)	Bi(8)-O(20)	2.116(10)		
Bi(7)-O(17)	2.842(9)	O(9)-Bi(5)-O(16)	87.2(3)		

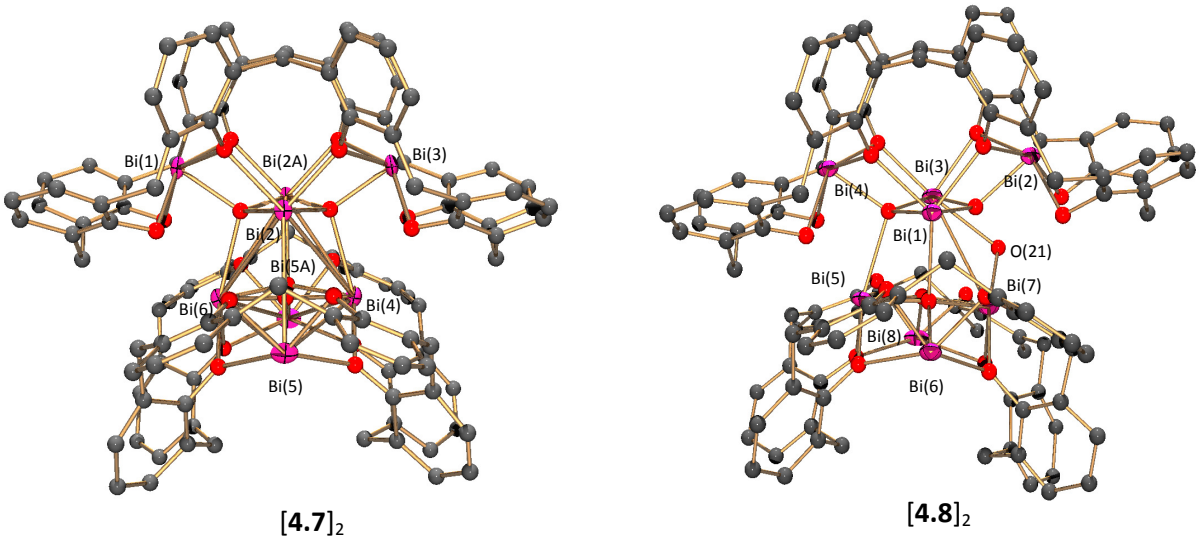

Figure 4.12. Crystal structures of the dimeric $[Bi_8O_4\{\mathbf{HC8}\}_2]$ $[\mathbf{4.7}]_2$ and $[Bi_8O_4\{\mathbf{BnC8}\}_2]\cdot H_2O$ $[\mathbf{4.8}]_2$ complexes. Hydrogen atoms, benzyl groups in $[\mathbf{4.8}]_2$, and uncoordinated solvent molecules are omitted for clarity.

The Bi_8O_{20} cluster in $[\mathbf{4.7}]_2$ can be more easily viewed as two Bi_4O_{10} cores that are linked by the interaction between Bi(2)-O(11), Bi(2A)-O(11A) and Bi(4)-O(10), Bi(6)-O(9) (see Figure 4.13). It can be noticed that a cubane-like cage is formed in the middle of the cluster by the interactions between the Bi(2), Bi(2A), Bi(4), and Bi(6) atoms and the μ_4-oxygens O(9), O(10), O(11), and O(11A). The Bi-O-Bi and O-Bi-O angles in the cubane range from 67.29° to 112.24°, far from the ideal 90°, indicating high distortion in the cage.

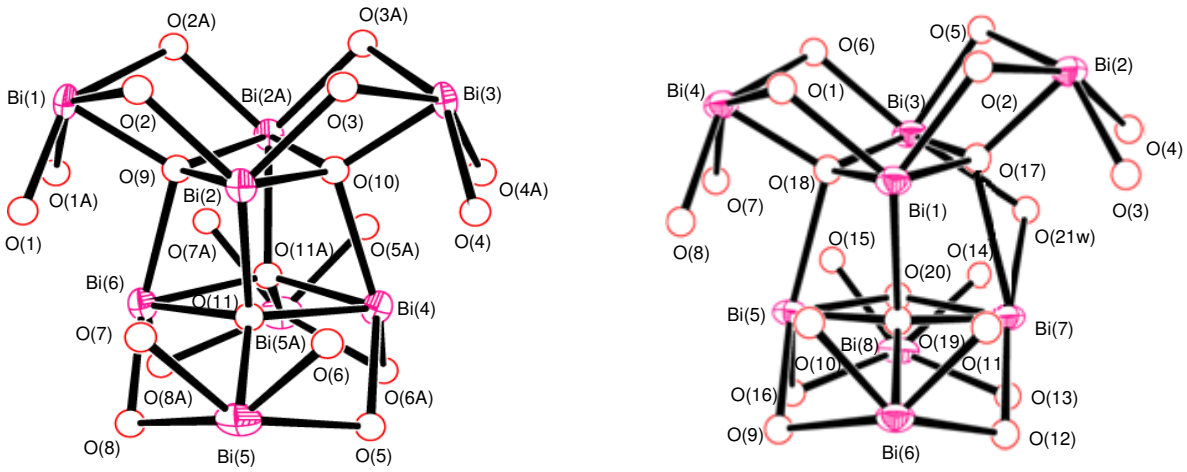

$[\mathbf{4.7}]_2$ $[\mathbf{4.8}]_2$

Figure 4.13. Core structures of complexes $[\mathbf{4.7}]_2$ and $[\mathbf{4.8}]_2$.

The overall structure of complex $[\mathbf{4.8}]_2$ is dimeric, with two calixarene units joined by a $Bi_8O_4 \cdot H_2O$ core. The inclusion of O(21w) (from coordinated H_2O) makes the overall Bi_8O_{21} cluster in $[\mathbf{4.8}]_2$ less symmetric than that of complex $[\mathbf{4.7}]_2$. The Bi_8O_{21} cluster can be viewed as two Bi_4O_{10} half-cores and one H_2O molecule, linked by the interactions of Bi(1)-O(19), Bi(3)-O(20), Bi(5)-O(18), Bi(7)-O(17), Bi(3)-O(21w) and Bi(7)-O(21w) (Figure 4.13). The presence of O(21w) (w = H_2O) makes the Bi(7)-O(17) and Bi(3)-O(20) interactions [2.842(9) and 2.827(10) Å, respectively] much longer than the other bridging interactions that link the two half-cores [2.540(9) and 2.556(9) Å]. The Bi(3)-O(21w) and Bi(7)-O(21w) interactions have bond distances of 2.609(10) and 2.621(10) Å, respectively, and are comparable to other Bi-O(w) bond distances found in literature [2.57(1) - 2.784(10) Å].[172-175]

The $Bi_4O_{20} \cdot H_2O$ metallic core displays two different coordination environments around the bismuth atoms. The Bi(2), Bi(4), Bi(6), and Bi(8) atoms are pentacoordinated with a distorted square-based pyramidal geometry. Each Bi atom is bonded to four aryloxides and one bridging oxygen. The Bi(5) and Bi(1) atoms are coordinated to four aryloxides and to three bridging

oxygens while the Bi(3) and Bi(7) are bonded to three bridging oxygens, two aryloxides, one water molecule and one MeCN (not shown in Figure 4.12) in a distorted capped trigonal prismatic geometry around the bismuth centers.

The high coordination numbers displayed by the bismuth atoms in **4.6**, [**4.7**]$_2$ and [**4.8**]$_2$ are characteristic for bismuth oxo clusters found in literature,[111] while the Bi–(μ–O) and Bi…Bi distances in **4.6** and [**4.8**]$_2$ are similar to those observed in di- and tetrametallated calixarene bismuth complexes (Table 4.5).

Table 4.5 Selected Structural Parameters for **4.6** and **[4.8]**$_2$

	Bi...Bi/Å	**Bi–(μ_3–O,μ_4–O)/ Å**	**Reference**
[Bi_4O_2{^{t}**BuC5(H)**}$_2$]	3.5733(8)-3.7212(8)	2.122(10)-2.271(6)	[159]
[Bi_4O_2{**BnC5(H)**}$_2$]	3.5583(16)-3.6868(11)	2.142(12)-2.127(11)	[159]
[Bi_4O_2{^{t}**BuC8**}]$_2$	3.6985(3)-3.7670(3)	2.148(3)-2.482(4)	[57]
4.6	3.5162(6)-3.6928(5)	2.172(6)-2.655(6)	[b]
[**4.8**]$_2$	3.6836(10)-3.8887(11)	2.112(9)-2.842(9)	[b]

[b] This work

The robust structure of complexes **4.7** and **4.8** causes relatively good air and moisture stability; no decomposition was observed after exposure to air for a period of 3 days.

4.3 Experimental section

4.3.1 General Information

All manipulations were carried out in a nitrogen-filled glovebox. *para-tert*-Butylcalix[6]arene,[176] *p*-H-calix[6]arene,[177] *para-tert*-butylcalix[7]arene,[87] *p*-H-calix[8]arene,[177] *p*-benzylcalix[8]arene,[153] Bi(O^{t}Bu)$_3$,[145] Bi[N(SiMe$_3$)$_2$]$_3$[155] and Sb(O^{t}Bu)$_3$[156] were prepared by the literature procedures. Sb(NMe$_2$)$_3$ was purchased from Strem Chemicals and used as received. All calixarene starting materials were oven-dried at 110 ^{o}C for at least 24 hrs. For the synthesis of

complex [Sb_2{^{t}**BuC6**}] **4.5**, the calixarene was vacuum-dried at 120 ^oC for three days. Tetrahydrofuran was freshly distilled from Na/benzophenone; other anhydrous solvents were purchased from Aldrich and stored over molecular sieves under nitrogen before using. Deuterated benzene and dimethyl sulfoxide were dried over CaH_2. Other starting materials were obtained from commercial suppliers and used without further purification.

The melting points of all compounds were taken in sealed and evacuated capillary tubes on a Mel-temp apparatus (Laboratory devices, Cambridge, MA) using a 500 ^oC thermometer. A melting temperature proceeded by a ">" sign indicates that the compound starts to decompose at that temperature but appears to actually melt at some higher temperature. ^1H NMR and ^{13}C spectra were recorded on a Varian XL-300 spectrometer at 300 and 75 MHz, respectively. Microanalyses were performed by Atlantic Microlab, Inc, Norcross, GA. IR and UV/vis spectra were obtained with an Infinity Gold^{TM} FTIR spectrometer and Agilent 8453 spectrophotometer, respectively. Filtrations used a medium sintered glass filter. In most cases the crystals for X-ray diffraction included solvents of crystallization, as shown in Table 4.6. For analytical samples the crystals were dried under vacuum at room temperature for 24 hrs.

4.3.2 Synthesis of compounds

[Bi{^{t}**BuC6(H)$_3$**}]$_2$ (**4.1**)**:** A suspension of ^{t}**BuC6(H)$_6$** (0.0487 g, 0.0500 mmol) in 20 mL of diethyl ether and a solution of $Bi[N(SiMe_3)_2]_3$ (0.0355 g, 0.0515 mmol) in 10 mL of diethyl ether were placed in a solvent bomb. The resulting yellowish suspension was allowed to heat in an isotemp oil bath at 45 ^oC for 3 days. Yellow X-ray quality needles were formed in the bottom of the solvent bomb. Filtration of the mixture and further washing with 2x3 mL portions of ethyl ether yielded 0.0198 g of pure [Bi{^{t}**BuC6(H)$_3$**}]$_2$ (0.0084 mmol, 33% yield) as yellow needles. Mp**: >** 355 ^oC. No NMR characterization was possible due to limited solubility. IR (KBr, cm^{-1}):

3258m (OH), 3048w, 2963vs, 2904s, 2868m, 2361w, 1756w, 1602w, 1479vs, 1460vs, 1393m, 1362s, 1295s, 1251s, 1201vs, 1121s, 944m, 907s, 874m, 842s. UV/vis (DMSO-d_6) λ_{max}/nm (ε/dm^{3}mol^{-1}cm^{-1}): 291 (1.92 x 10^4). Anal. Calcd for $C_{132}H_{162}O_{12}Bi_2 \cdot 2C_4H_{10}O$: C 67.07, H 7.32. Found: C 66.88, H 7.42.

[Bi{**HC6(H)$_3$**}] (**4.2**)**:** A colorless solution of Bi(O^{t}Bu)$_3$ (0.0445 g, 0.104 mmol) in THF (3 mL) was added dropwise to a white suspension of **HC6(H)$_6$** (0.0319 g, 0.0501 mol) in THF (5 mL). The reaction mixture turned yellow and was allowed to stir for 48 hrs to yield a yellow solution. Filtration of the small amount of solid and vacuum removal of the solvent gave the crude product as a yellow solid. Pure [Bi{**HC6(H)$_3$**}] in 72% yield (0.0304 g, 0.0361 mmol) was obtained after washing the crude material with 2x3 mL of benzene. Single crystals were obtained after cooling a concentrated THF/toluene/benzene (2:1:1) solution of the product outside the glovebox at 2 ^{o}C for several weeks. Mp: > 302 ^{o}C. ^{1}H NMR (DMSO-d_6) δ = 2.97 (d, *J* = 12.6 Hz, 2H, ArC*H*$_2$Ar), 3.21 (d, *J* = 11.7 Hz, 2H, ArC*H*$_2$Ar), 3.47 (d, *J* = 13.8 Hz, 2H, ArC*H*$_2$Ar), 4.15 (d, *J* = 12.6 Hz, 2H, ArC*H*$_2$Ar), 4.67-4.77 (two doublets overlapping, 4H, ArC*H*$_2$Ar), 6.29-6.50 (three overlapping triplets, 6H, Ar*H*), 6.87-6.89 (three doublets overlapping, 6H, Ar*H*), 6.94-7.02 (three doublets overlapping, 6H, Ar*H*), 13.75 (s, 1H, O*H*), 14.61 (s, 2H, O*H*). ^{13}C NMR spectrum not available due to limited solubility. IR (KBr, cm^{-1}): 3449w (OH), 3054m, 3016m, 2950m, 2914m, 1585s, 1494w, 1444vs, 1298s, 1249vs, 1207vs, 1084vs, 952w, 892m, 841vs, 808m, 757vs, 731s, 694m. UV/vis (DMSO-d_6) λ_{max}/nm (ε/dm^{3}mol^{-1}cm^{-1}): 286 (1.87 x 10^4). Anal. Calcd for $C_{42}H_{33}O_6Bi \cdot C_4H_8O$: C 60.40, H 4.52. Found: C 60.71, H 4.61.

[Bi$_2${**HC6**}] (**4.3**)*:* A colorless solution of Bi(O^{t}Bu)$_3$ (0.0218 g, 0.0509 mmol) in toluene (3 mL) was added dropwise to a white suspension of **HC6(H)$_6$** (0.0160 g, 0.0251 mol) in toluene (5 mL). The reaction mixture turned yellow and was allowed to stir for 48 hrs to yield a yellow

mixture. Filtration of the mixture gave a yellow solid and a light yellow supernatant.* Pure [Bi_2{**HC6**}] in 23% yield (0.00605 g, 0.00577 mmol) can be obtained after washing the yellow solid with 2x3 mL toluene. Mp: > 280 ^oC. ^1H NMR (DMSO-d_6) δ = 3.42 (d, *J* = 13.2 Hz, 4H, ArC*H*$_2$Ar), 4.12 (s, 4H, ArC*H*$_2$Ar), 4.95 (d, *J* = 13.2 Hz, 4H, ArC*H*$_2$Ar), 6.25 (t, *J* = 7.2 Hz, 2H, Ar*H*), 6.32 (t, *J* = 7.5 Hz, 4H, Ar*H*), 6.55 (d, *J* = 6.9 Hz, 4H, Ar*H*), 6.86 (d, *J* = 7.2 Hz, 4H, Ar*H*), 6.99 (d, *J* = 6.9 Hz, 4H, Ar*H*). Due to low solubility no ^{13}C NMR could be obtained. IR (KBr, cm^{-1}): 3055w, 3019w, 2970vs, 2916vs, 1586s, 1494w, 1461s, 1444vs, 1301m, 1250vs, 1208vs, 1085s, 841m, 821w, 756vs, 731m. UV/vis (THF) λ_{max}/nm (ε/$dm^3mol^{-1}cm^{-1}$): 284 (1.78 x 10^4), 486 (2.30 x 10^2). Anal Calcd for $C_{42}H_{30}O_6Bi_2 \cdot 1.5C_7H_8$: C 53.13, H 3.57. Found: C 53.39, H 3.86.

*If the light-yellow supernatant is vacuum dried and the yellow solid obtained is washed with 3x2 mL of benzene, 0.0120 g of [Bi{**HC6(H)$_3$**}] **4.2** (0.0143 mmol, 57% yield) can be obtained.

[Sb_2{**HC6**}] (**4.4**)*:* Method A: A solution of Sb(O^{t}Bu)$_3$ (0.0515 g, 0.151 mmol) in 2 mL of toluene was added dropwise to a suspension of **HC6(H)$_6$** (0.0319 g, 0.0501 mmol) in 4 mL of toluene. The reaction mixture turned into a clear solution after 2 hrs of stirring and after 4 hrs it became a white mixture. The final white suspension was allowed to stir for 48 hrs. The crude product was obtained as a white solid after centrifugation. Pure **HC6**$(Sb)_2$ in 81% yield (0.0355 g, 0.0406 mmol) was obtained after washing the crude material 3 times with 4 mL portions of toluene. When [Sb_2{**HC6**}] was recrystallized by diffusion of hexanes into a concentrated THF solution white powder of [Sb_2{**HC6**}] **4.4** and a few X-ray quality colorless block crystals of the side product [Sb_3O_2{**HC6(H)**}] **4.4a** were obtained.

(**4.4a**)*:* Mp: 368-370 ^{o}C. Due very low solubility of **4.4a** no NMR characterization was possible. IR (KBr, cm^{-1}): 3470w (OH), 3054w, 3013w, 2953w, 2926m, 1919w, 1584s, 1494w, 1448vs, 1324m, 1287m, 1251vs, 1193vs, 1193vs, 1174vs, 1085vs, 910s, 886w, 851vs, 818s, 796m, 757vs, 736s, 701s, 678m, 651m. UV/vis (THF) λ_{max}/nm (ε/dm^{3}mol^{-1}cm^{-1}): 219 (3.44 x 10^4). Anal Calcd for $C_{42}H_{31}O_8Sb_3 \cdot 3C_4H_8O$: C 52.08, H 4.45. Found: C 51.87, H 4.52.

Method B: A colorless solution of $Sb(NMe_2)_3$ (0.0383 g, 0.151 mmol) in 3 mL of toluene was added dropwise to a white suspension of **HC6(H)$_6$** (0.0319 g, 0.0501 mmol) in 7 mL of toluene. The reaction turned immediately into a colorless solution and was allowed to stir for 48 hrs. The final white mixture was filtered (or centrifuged) to yield the crude product as a white solid. Pure [Sb_2{**HC6**}] was obtained in 83% yield (0.0364 g, 0.0416 mmol) after washing the crude material twice with 4 mL portions of toluene. Single crystals of [Sb_2{**HC6**}] were obtained by diffusion of pentane into a diluted THF solution of the product. Mp: > 444 ^{o}C. ^{1}H NMR (DMSO-d$_6$): 3.37 (d, *J* = 12.9 Hz, 4H, ArC*H*$_2$Ar), 3.83 (s, 4H, ArC*H*$_2$Ar), 4.75 (d, *J* = 12.9 Hz, 4H, ArC*H*$_2$Ar), 6.46 (d, *J* = 7.5 Hz, 4H, Ar*H*), 6.56 (t, *J* = 7.5 Hz, 4H, Ar*H*), 6.61 (t, *J* = 7.5 Hz, 2H, Ar*H*), 6.97 (d, *J* = 7.5 Hz, 4H, Ar*H*), 7.06 (d, *J* = 7.5 Hz, 4H, Ar*H*). Due to low solubility no ^{13}C NMR spectrum could be obtained. IR (KBr, cm^{-1}): 3055w, 3012w, 2954w, 2927m, 2855w, 2358w, 2339w, 1919w, 1584m, 1447vs, 1324w, 1288w, 1253vs, 1242vs, 1205vs, 1192vs, 1173vs, 1048vs, 909m, 892w, 851vs. UV/vis (THF) λ_{max}/nm (ε/dm^{3}mol^{-1}cm^{-1}): 258 (3.23 x 10^4), 264 (3.01 x 10^4). Anal Calcd for $C_{42}H_{30}O_6Sb_2 \cdot 1.5C_4H_8O \cdot 1.5C_5H_{12}$: C 61.12, H 5.55. Found: C 61.46, H 5.23.

[Sb_2{^{t}**BuC6**}] (**4.5**)*:* Method A: A colorless solution of $Sb(O^tBu)_3$ (0.0342 g, 0.100 mmol) in 4 mL of benzene was added dropwise to a white suspension of vacuum-dried (at 120^o C) ^{t}**BuC6(H)$_6$** (0.0489 g, 0.0502 mmol) in 6 mL of benzene. The mixture became colorless after

10 min and was allowed to stir for 48 hrs. The final white mixture was filtered (or centrifuged) to give the crude product as a white powder. The solid was washed twice with 5 mL of benzene to yield [Sb_2{**^{t}BuC6**}] as a white solid in 68% yield (0.0413g, 0.0341 mmol).

Method B: [Sb_2{**^{t}BuC6**}] can also be obtained in 71% yield (0.0431 g, 0.0356 mmol) following the same procedure described above but using $Sb(NMe_2)_3$ (0.0257 g, 0.101 mmol). Mp: 428-430 ^{o}C. ^{1}H NMR (DMSO-d_6): δ = 1.10 (s, 36H, C(CH_3)$_3$), 1.17 (s, 18H, C(CH_3)$_3$), 3.39 (d, *J* = 12.6 Hz, 4H, ArCH_2Ar), 3.87 (s, 4H, ArCH_2Ar), 4.83 (d, *J* = 12.6 Hz, 4H, ArCH_2Ar), 6.67 (d, *J* = 2.4 Hz, 4H, Ar*H*), 6.96 (bs, 4H, Ar*H*), 7.05 (bs, 4H, Ar*H*). No ^{13}C spectrum could be obtained due to limited solubility. IR (KBr, cm^{-1}): 3063w, 3031w, 2959vs, 2866s, 1594w, 1467vs, 1414w, 1393w, 1361s, 1295s, 1196vs, 1118s, 1109s, 913w, 870w, 840m, 813m, 823w, 802w, 750vs, 680s. UV/vis (THF) λ_{max}/nm (ε/dm^{3}mol^{-1}cm^{-1}): 218 (6.39 x10^4), 279 (1.07 x 10^3). Anal. calcd for $C_{66}H_{78}O_6Sb_2$: C 65.47, H 6.49. Found: C 65.73, H 6.41.

[Bi_2O{**^{t}BuC7(H)$_3$**}]$_2$ (**4.6**)***:*** A colorless solution of Bi(O^{t}Bu)$_3$ (0.0218 g, 0.0509 mmol) in 3 mL of diethyl ether was added dropwise to a colorless solution of **^{t}BuC7(H)$_7$** (0.0570 g, 0.0502 mmol) in 5 mL of diethyl ether. The reaction mixture was allowed to stir for 24 hrs. A ^{1}H NMR spectrum of the crude mixture allowed the observation of the product [Bi_2O{**^{t}BuC7(H)$_3$**}]$_2$ **4.6** in mixture with parent calixarene. Addition of 1 more equivalent of Bi(O^{t}Bu)$_3$ (0.0218 g, 0.0509 mmol) to the reaction mixture and stirring for another 24 hrs permitted all the starting material to be totally consumed. Pure [Bi_2O{**^{t}BuC7(H)$_3$**}]$_2$ in 81% yield (0.0203 g, 0.0407 mmol) was obtained after washing the crude material with 3 mL portions of hexane. Single crystals were obtained by slow evaporation of a concentrated THF/DME/DMSO (1:2:0.5) solution of crude product. Mp: 310-312 ^{o}C. ^{1}H NMR (C_6D_6) δ = 0.87 (s, 9H, C(CH_3)$_3$), 0.94 (s, 9H, C(CH_3)$_3$), 1.26 (s, 9H, C(CH_3)$_3$), 1.32 (s, 9H, C(CH_3)$_3$), 1.33 (s, 9H, C(CH_3)$_3$), 1.41 (s, 9H, C(CH_3)$_3$), 1.52 (s,

9H, C(CH_3)$_3$), 3.64 (d, *J* = 13.2 Hz, 2H, ArCH_2Ar), 3.73-3.82 (two doublets overlapping, 2H, ArCH_2Ar), 3.92 (d, *J* = 12.6 Hz, 1H, ArCH_2Ar), 4.20-4.29 (two doublets overlapping, 2H, ArCH_2Ar), 4.60 (d, *J* = 16.2 Hz, 1H, ArCH_2Ar), 4.93 (d, *J* = 12.6 Hz, 2H, ArCH_2Ar), 5.17 (d, *J* = 13.2 Hz, 1H, ArCH_2Ar), 5.45 (s, 2H, ArCH_2Ar), 5.67 (d, *J* = 12.3 Hz, 1H, ArCH_2Ar), 6.86 (s, 1H, Ar*H*), 6.96-7.03 (m, 4H, Ar*H*), 7.24 (s, 1H, Ar*H*), 7.32 (s, 2H, Ar*H*), 7.38 (s, 1H, Ar*H*), 7.42 (s, 1H, Ar*H*), 7.44 (s, 1H, Ar*H*), 7.51 (s, 1H, Ar*H)*, 7.57 (s, 1H, Ar*H*), 7.66 (s, 1H, Ar*H*), 9.32 (s, 1H, O*H*), 11.49 (s, 1H, O*H*), 12.13 (s, 1H, O*H*). $^{13}C\{^1H\}$ NMR (C_6D_6) δ = 153.8, 150.9, 150.6, 150.3, 149.3, 148.2, 146.6, 145.8, 144.6, 144.2, 143.4, 142.9, 138.7, 138.1, 135.7, 135.6, 134.6, 134.5, 133.3, 132.1, 126.8, 126.5, 126.2, 125.9, 125.5, 125.2, 123.8, 123.1 (aromatic carbons), 34.5, 34.2, 34.12, 34.09, 33.9, 33.85 (two signals overlapping), 33.79, 33.4, 32.1, 31.8, 31.7, 31.6, 31.4, 31.0 (two signals overlapping), 30.0, 25.6, 22.5, 21.2, 15.4. IR (KBr, cm^{-1}): 3180m (OH), 3050w, 2961vs, 2906vs, 2867s, 1753w, 1602m, 1479vs, 1461vs, 1393s, 1362s, 1293s, 1243s, 1199vs, 1120s, 911m, 872m, 819s. UV/vis (C_6H_6) λ_{max}/nm (ε/$dm^3mol^{-1}cm^{-1}$): 278 (3.98 x 10^4). Anal Calcd for $C_{154}H_{188}O_{16}Bi_4 \cdot 6C_2H_6SO$: C 55.38, H 6.27. Found C 55.11, H 5.95.

[Bi_4O_2{**HC8**}] (**4.7**): A colorless solution of Bi(O^{t}Bu)$_3$ (0.0434 g, 0.101 mmol) in 2 mL of THF was added dropwise to a white suspension of **HC8(H)$_8$** (0.0424 g, 0.0500 mmol) in 4 mL of THF yielding a yellow mixture. The reaction mixture was allowed to stir for 24 hrs. Dropwise addition of two more equivalents of Bi(O^{t}Bu)$_3$ (0.0434 g, 0.101 mmol) to the yellow mixture resulted in the production of a yellow solution after 24 hrs of stirring. The solvent was removed under vacuum to yield the crude product as a yellow solid. Pure [Bi_4O_2{**HC8**}] in 64% yield (0.0547 g, 0.0320 mmol) was obtained after recrystallization of the crude material by hexane diffusion into a THF/benzene/toluene (1:1:1) solution. X-ray quality crystals were obtained by hexane diffusion into a THF/toluene/DME (1:1:1) solution of the crude product. Mp: > 302 ^{o}C.

^{1}H NMR (DMSO-d_6) δ = 3.25 (d, *J* = 12.9 Hz, 4H, ArC*H*$_2$Ar), 3.51 (two doublets overlapping, 4H, ArC*H*$_2$Ar), 4.92 (d, *J* = 12.9 Hz, 4H, ArC*H*$_2$Ar), 5.02 (two doublets overlapping, 4H, ArC*H*$_2$Ar), 6.36 (t, *J* = 7.2 Hz, 4H, Ar*H*), 6.52 (t, *J* = 7.5 Hz, 4H, Ar*H*), 6.97 (d, *J* = 7.5 Hz, 4H, Ar*H*), 7.02 (d, *J* = 7.5 Hz, 4H, Ar*H*), 7.11 (d, *J* = 7.2 Hz, 4H, Ar*H*), 7.24 (d, *J* = 7.2 Hz, 4H, Ar*H*). ^{13}C{^{1}H} NMR (DMSO-d_6) δ = 156.2, 156.0, 137.5, 135.9, 135.1, 134.6, 129.7, 129.6, 129.0, 128.9, 128.3, 127.9, 127.8, 126.0, 119.9, 119.5 (aromatic carbons), 32.0, 31.4, 25.8, 21.8 (Ar*C*H$_2$Ar). IR (KBr, cm^{-1}): 3051w, 3016w, 2960w, 2913w, 1586m, 1462w, 1446vs, 1428vs, 1385w, 1245vs, 1206s, 1088m, 901m, 838m, 818w, 759s, 694w, 852s. UV/vis (C_6H_6) λ_{max}/nm (ε/dm^{3}mol^{-1}cm^{-1}): 277 (3.15 x 10^4). Anal Calcd for $C_{56}H_{40}O_{10}Bi_4 \cdot 3C_6H_6$: C 45.74, H 3.01, Found: C 45.45, H 3.37.

[Bi_4O_2{**BnC8**}] (**4.8**)**:** A colorless solution of Bi(O^{t}Bu)$_3$ (0.0218 g, 0.0509 mmol) in 3 mL of toluene was added dropwise to a white suspension of **BnC8(H)$_8$** (0.0789 g, 0.0503 mmol) in 5 mL of toluene and the reaction mixture was allowed to stir for 24 hrs. A second equivalent of Bi(O^{t}Bu)$_3$ (0.0218 g, 0.0509 mmol) was added to the reaction mixture and allowed to stir for 24 hrs. A ^{1}H NMR spectrum of the reaction mixture showed the product in mixture with parent calixarene. Removal of the small amount of solid from the yellow mixture and addition of 0.5 equivalents of Bi(O^{t}Bu)$_3$ (0.0109 g, 0.0254 mmol) permitted all the starting material to be consumed. Recrystallization by diffusion of hexane into a concentrated benzene/toluene/acetonitrile (1:1:1) solution of the crude material allowed the formation of [Bi_4O_2{**BnC8**}] as yellow block crystals in 52% yield (0.0635 g, 0.0261 mmol). Mp: > 290 ^{o}C. ^{1}H NMR (C_6D_6) δ = 2.63 (d, *J* = 13.2 Hz, 2H, ArC*H*$_2$Ar), 3.02 (d, *J* = 13.5 Hz, 4H, ArC*H*$_2$Ar), 3.28 (d, *J* = 14.1 Hz, 2H, ArC*H*$_2$Ar), 3.80 (s, 8H, OC*H*$_2$Ph), 3.88 (s, 4H, OC*H*$_2$Ph), 3.91 (s, 4H, OC*H*$_2$Ph), 3.95 (d, *J* = 13.2 Hz, 2H, ArC*H*$_2$Ar), 4.92 (d, *J* = 13.5 Hz, 4H, ArC*H*$_2$Ar), 5.19 (d, *J* =

14.1 Hz, 2H, ArC*H*$_2$Ar), 6.91 (bd, *J* = 2.1 Hz, 4H, Ar*H*), 6.53 (bd, *J* = 2.1 Hz, 8H, Ar*H*), 7.02 (b, 8H, Ar*H*), 7.12 (b, 12H, Ar*H*), 7.14 (b, 12H, Ar*H*), 7.18-7.20 (m, 12H, Ar*H*). $^{13}C\{^1H\}$ NMR (C_6D_6) δ = 153.0, 148.9, 142.3, 142.0, 140.3, 136.9, 136.8, 136.7, 135.8, 133.5, 129.3, 129.1, 128.6, 128.5, 126.2, 126.1 (aromatic carbons), 41.9, 41.3, 34.3, 34.1, 31.1, 30.2 (Ar*C*H$_2$Ar) (two peaks are missing, probably overlapping with DMSO-d_6). IR (KBr, cm^{-1}): 3081w, 3062w, 3024m, 2990w, 2909m, 2841w, 1601m, 1550w, 1493s, 1451vs, 1431vs, 1274s, 1220vs, 1143vs, 1131vs, 1074s, 1029s, 901s, 790s, 730s, 698vs. UV/vis (DMSO) λ_{max}/nm (ε/$dm^3mol^{-1}cm^{-1}$): 262 (6.96 x 10^4), 293 (4.53 x 10^4). Anal Calcd for $C_{112}H_{88}O_{10}Bi_4 \cdot C_6H_6 \cdot C_2H_3N$: C 56.54, H 3.84, Found: C 56.59, H 4.14.

4.3.3 General X-ray structure information

X-ray data of **4.1**, [**4.2**]$_2$, **4.4**, **4.4a**, [**4.7**]$_2$, and [**4.8**]$_2$ were collected on a SMART Bruker 1000 CCD detector diffractometer using Mo Kα radiation. Data for **4.6** were collected in a Bruker D8 diffractometer with an APEX CCD detector. The crystallographic data and some details of the data collection and refinement of the structures are given in Table 4.6. Absorption corrections in all cases were applied by SADABS.[101] All structures were solved by direct methods and subsequent difference Fourier syntheses and refined by full matrix least-squares methods against F^2 (SHELX 97).[102] Disorder for some *tert*-butyl groups was due to 2-fold axis, and was modeled using partial occupancies (PART instruction).[102] Some other disordered molecules and solvents were refined using a combination of restraints on the distances while keeping the disordered parts similar (use of the SADI and SAME instructions).[102]

Table 4.6 Crystallographic Data and Summary of Data Collection and Structure Refinement

	4.1·$2C_4H_{10}O$	[**4.2**]$_2$·7THF·$2H_2O$	**4.4**·2THF	**4.4a**·4THF
Formula	$C_{140}H_{182}Bi_2O_{14}$	$C_{112}H_{126}Bi_2O_{21}$	$C_{50}H_{46}Sb_2O_8$	$C_{58}H_{63}Sb_3O_{12}$
Fw	2506.9	2226.15	1018.37	1317.39
cryst syst	Triclinic	Orthorhombic	Triclinic	Triclinic
space group	*P*-1	*P*ccn	*P*-1	*P*-1
T, K	223(2)	213(2)	213(2)	213(2)
a, Å	14.536(3)	13.940(3)	13.122(7)	13.617(2)
b, Å	16.592(3)	24.307(5)	13.766(8)	13.864(2)
c, Å	17.299(3)	29.061(7)	14.418(8)	15.698(2)
α, deg	117.870(3)	90	94.090(10)	69.825(3)
β, deg	107.174(3)	90	115.115(8)	79.972(2)
γ, deg	94.819(3)	90	114.994(8)	69.980(3)
V, A^3	3399.9(11)	9847(4)	2035.2(19)	2608.3(7)
Z	1	4	2	2
d_{calcd} g·cm^{-3}	1.224	1.499	1.662	1.494
μ, mm^{-1}	2.636	3.642	1.386	1.594
Refl collected	23002	38534	8268	14392
T_{min}/T_{max}	0.794	0.865	0.904	0.934
N_{measd}	11845	7102	5779	7451
[R_{int}]	[0.0723]	[0.1790]	[0.0510]	[0.0607]
R [I>2sigma(I)]	0.0612	0.0475	0.0343	0.0422
R_w[I>2sigma(I)]	0.1375	0.0876	0.0840	0.1006
GOF	0.945	0.858	0.952	0.921
	4.6·5.5DME·$2C_6H_{14}$	[**4.7**]$_2$	[**4.8**]$_2$·$4C_6H_6$·2MeCN·H_2O	
Formula	$C_{188}H_{271}Bi_4O_{27}$	$C_{112}H_{80}Bi_8O_{20}$	$C_{252}H_{208}Bi_8N_2O_{21}$	
Fw	3799.07	3417.60	5272.19	
cryst syst	Monoclinic	Orthorhombic	Triclinic	
space group	$P2_1/n$	*P*nma	*P*-1	
T, K	100(2)	213(2)	223(2)	
a, Å	17.5399(13)	30.287(6)	19.468(4)	
b, Å	30.330(2)	21.769(4)	22.096(4)	
c, Å	34.753(3)	22.432(4)	27.093(6)	
α, deg	90	90	92.148(4)	
β, deg	102.4290(10)	90	90.463(4)	
γ, deg	90	90	112.019(3)	
V, A^3	18055(2)	14790(5)	10794(4)	
Z	4	4	2	
d_{calcd} g·cm^{-3}	1.380	1.535	1.593	
μ, mm^{-1}	3.951	9.531	6.560	
Refl collected	154751	97048	51430	
T_{min}/T_{max}	0.828	0.691	0.878	
N_{measd}	42061	10925	30715	
[R_{int}]	[0.0954]	[0.1938]	[0.1229]	
R [I>2sigma(I)]	0.0775	0.1159	0.0649	
R_w[I>2sigma(I)]	0.1625	0.2590	0.1617	
GOF	1.114	1.038	0.936	

All non-hydrogen atoms were refined with anisotropic displacement coefficients, except atoms of disordered fragments which were refined with isotropic thermal parameters. In the crystal structures of **4.1, 4.4a** and **4.6,** highly disordered solvent molecules (2 Et_2O molecules in **1**, 4 THF molecules in **4.4a** and 2 DME molecules in **4.6**) were treated with the program SQUEEZE.[103] Corrections of the X-ray data for **4.1**, **4.4a** and **4.6** by SQUEEZE (80, 163 and 109 electron cell, respectively) were close to the required values (84, 160 and 100 electron cell, respectively). Due to the low quality crystals of complex [**4.8**]$_2$, one *p*-benzyl group was highly disordered and could not be located in the density map. All other carbon atoms in the remaining *para*-benzyl groups were treated with isotropic displacements. The structure of complex [**4.7**]$_2$ could not be well refined. The H atoms in all structures were taken in calculated positions. The programs ORTEP32[104] and POV-Ray[105] were used to generate the X-ray structural diagrams pictured in this Chapter.

4.4 Conclusions

A series of bismuth and antimony complexes of the larger calix[n]arenes (n = 6, 7, 8) has been synthesized and fully characterized by NMR, UV/vis and X-ray crystallography. The large cavity size of the calix[n]arenes (n = 6-8) allowed the preparation of a variety of complexes featuring mono- to tetranuclear structures. Monometallic complexes were only obtained when **RC6(H)$_6$** ligands were used. The larger calix[n]arenes (n = 7, 8) produced multinuclear complexes even working with 1:1 calixarene/metal ratios. In our previous work it was observed that even-membered **RC4(H)$_4$** ligands tend to produce fully saturated Bi or Sb complexes, while the odd-membered **RC5(H)$_5$** produced partially metallated complexes with free OH groups.[159] The large calixarenes behave similarly. Calix[n]arenes (n = 6, 8) produced fully saturated complexes when using excess M(O^{t}Bu)$_3$ (M = Bi, Sb), while the odd-membered **^{t}BuC7(H)$_7$**

produced the partially metallated complex **4.6**. All crystal structures of bismuth complexes are dimeric with the calixarenes in cone-like conformations while the antimony complexes are monomeric in partial cone or 1,2,3-alternate conformations. Binuclear complex **4.6** and tetranuclear complexes [**4.7**]$_2$ and [**4.8**]$_2$ contain Bi_4O_6 motifs similar to our previously reported bismuth calixarene clusters.[57,159]

CHAPTER 5

SILYLATED BISMUTH(III) AND ANTIMONY(III) CALIX[5]ARENE COMPLEXES

5.1 Introduction

The lower and/or upper rim modification of calix[n]arene ligands[47] have been extensively utilized as methodologies for the complexation of specific metal centers, guest molecules or ions.[50,51,178] Usually, the addition of pendant arms (aldehydes, ketones, amines, esters, etc)[47,82,178,179] enhances the calixarene affinity toward certain substrates by changing the ring conformation or by decreasing the number of available hydroxide groups. Functionalized calixarenes have a wide range of applications including sensors, catalysts, drug design, biological and separation processes, enzymatic models and others.[106,180-184]

In coordination chemistry, functionalized calix[n]arenes have been successfully employed in the synthesis of transition, main group and f-block metal complexes.[51,61,73] For instance, the use of 1,2- or 1,3-lower rim substituted calix[4]arenes allowed the preparation of monometallic main group complexes (M = Ge, Sn, Al, Mg, Bi) that were inaccessible by other methods.[58,95,113,116] Ladipo et al. have synthesized a series of titanium(IV) complexes supported by silicon-containing calix[4]arenes and discovered that they were able to catalyze alkyne cyclotrimerization or induce Ti-C bond formation.[185-188] Lattman et al. have reported that the use of phosphorus mono-substituted calix[5]arene ligands allowed the easy insertion of tungsten, titanium or zirconium centers in the lower rim, and that the resulting complexes featured interesting metal-phosphorus interactions.[130,131] For the calix[n]arene ligands (n = 6, 8) where the large cavity usually favors the production of multinuclear complexes, the use of upper and/or lower rim substituted precursors has permitted the preparation of monometallic complexes impossible to prepare by other procedures.[61]

One of our research interests lies in the synthesis of bismuth(III) or antimony(III) calixarenes as precursors for heterobimetallic models of the Bi/Mo SOHIO catalyst. We have recently reported that the reaction of calix[5]arene [**RC5(H)$_5$**] trianions M'$_3$·**RC5(H)**$_2$ (M' = Li, Na, K)[120] with MCl_3 (M = Bi, Sb) or the reaction of parent **RC5(H)$_5$** (R = H, ^{t}Bu, Bn) with M(O^tBu)$_3$[159] produced mono or bimetallic complexes containing unreacted OH groups. However, the solubility of some of these complexes is limited, decreasing their potential as building blocks.

Lattman has reported that the addition of silicon moieties (-SiR_2) to the lower rim of the calix[n]arenes (n = 4, 5) is relatively easy and that the silylated ligands feature high solubility and free OH groups that facilitate the preparation of monometallic complexes.[123,125,126] We decided to take advantage of these features by blocking the 1,2 positions of **^{t}BuC5(H)$_5$** ligands with -SiR_2 moieties, targeting the design of trivalent templates for the complexation of bismuth(III) and antimony(III) centers.

In this chapter we will describe the synthesis of monosilylated calix[5]arene ligands obtained by the reaction of the Na_2·**^{t}BuC5(H)$_3$**[120] salt with one equivalent of R_2SiCl_2 or by treatment of the monobenzyl substituted **^{t}BuC5(H)$_5$** ligand [**^{t}BuC5(Bn)(H)$_4$**] with $Me_2Si(NMe_2)_2$. The reactivity of the **^{t}BuC5(SiRR')(H)$_3$** (**5.1-5.5**) and **^{t}BuC5(Bn)(SiMe$_2$)(H)$_2$** (**5.6**) ligands with M(O^tBu)$_3$ (M = Bi, Sb) or $Sb(NMe_2)_3$ was tested and successfully employed for the synthesis of a series of highly soluble monometallic bismuth(III) and antimony(III) complexes. We will discuss the solution and solid state features encountered upon change of substitution level in the calixarene ligands and the strength of the base used in the complex synthesis.

5.2 Results and discussion

5.2.1 Synthesis of silylated calix[5]arenes **^{t}BuC5(SiRR'$_2$)(H)$_3$**

In order to access monosilylated ligands of the type **^{t}BuC5(SiRR'$_2$)(H)$_3$**, a salt metathesis approach was employed. From the dianionic **^{t}BuC5(H)$_5$** salt precursors M_2·**^{t}BuC5(H)$_3$** (M = Na, K, Rb and Cs) that we have previously prepared,[120] only Na_2·**^{t}BuC5(H)$_3$** was used, as it produces the best yields and clean reactions. The reaction of Na_2·**^{t}BuC5(H)$_3$**[120] with one equivalent of RR'$SiCl_2$ (R, R' = Me, ^{i}Pr, Ph, CH=CH_2) in THF, produces the monosilylated **^{t}BuC5(SiRR'$_2$)(H)$_3$** ligands **5.1**-**5.5** as depicted in equation 5.1. In general, the reaction gives a mixture of the **^{t}BuC5(SiRR'$_2$)(H)$_3$** product and parent calixarene. Purification of the products is performed by slow evaporation of a concentrated pentane (or hexane) solution of the crude mixture for ligands **5.2-5.4** or by successive pentane/hexane washing cycles to remove parent calixarene in the case of **^{t}BuC5(SiMe$_2$)(H)$_3$** (**5.1**) and **^{t}BuC5(SiMeVinyl)(H)$_3$** (**5.5**).

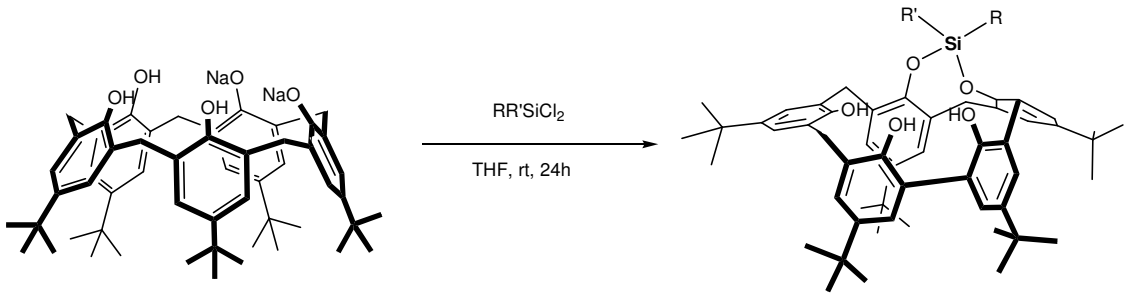

(5.1)

Na_2·**^{t}BuC5(H)$_3$**

R, R' = Me	**5.1**
R = Me, R' = Ph	**5.2**
R, R' = Ph	**5.3**
R, R' = ^{i}Pr	**5.4**
R = Me, R' = C_2H_3	**5.5**

Lattman and coworkers have previously reported the synthesis of ligands **5.1** and **5.2** by the reaction of **^{t}BuC5(H)$_5$** and $Me_2Si(NMe_2)_2$.[126] When a 1:1 ratio was used, a mixture of mono- and di-substituted products was observed. The di-substituted products could only be avoided when the reaction ratio was changed to 1:0.35 [**^{t}BuC5(H)$_5$**:$R_2Si(NMe_2)_2$]. However, under these reaction conditions, a large amount of unreacted **^{t}BuC5(H)$_5$** had to be removed and the yields

(based on calixarene) were too low. In addition, the insertion of bulkier silane groups such as -$SiPh_2$ was unsuccessful when applying this methodology.

On the other hand, by utilizing our **^{t}BuC5**·Na_2 precursor, we were able to isolate the ligands **5.1**, **5.2** and **5.3** in good yields (74-85%, based on calixarene) after an easy purification. The success of this reaction could be due to the use of a true dianionic precursor that favors the insertion of a single -SiR_2 moiety in the lower rim of the calixarene.

With these successful results, we decided to utilize the calixanion methodology for the preparation of silylated versions of the **^{t}BuC5(Bn)(H)$_4$** ligand. When the *in situ* prepared dianionic Na_2·**^{t}BuC5Bn(H)$_2$** salt (using 2 equivalents of NaO^tBu) was reacted with one equivalent of $RR'SiCl_2$, the reaction mixture showed only traces of the desired product in addition to parent calixarene. The large amount of unreacted parent calixarene suggested that the deprotonation of the parent ligand with NaO^tBu was not as efficient as in the case of **^{t}BuC5(H)$_5$**.[120]

An alternate procedure for the preparation of silylated calix[4]arenes consists of the deprotonation of the calixarene ligand with triethylamine (Et_3N) followed by addition of $SiCl_4$ or $RSiCl_3$.[125,189,190] We employed this pathway by treating the **^{t}BuC5(Bn)(H)$_4$** ligand with 2 equivalents of Et_3N followed by the addition of the appropriate silane dichloride. The ^{1}H NMR spectra in this case showed a smaller amount of unreacted **^{t}BuC5Bn(H)$_4$**, but a complex mixture of products was observed. It was necessary to treat **^{t}BuC5(Bn)(H)$_4$** with one equivalent of $Me_2Si(NMe_2)_2$ in toluene in order to afford the desired **^{t}BuC5(Bn)(SiMe$_2$)(H)$_2$** ligand (**5.6**). The reaction mixture showed quantitative conversion to the silylated ligand **5.6**, and after recrystallization from hexane an isolated yield of 78% was attained (Equation 5.2).

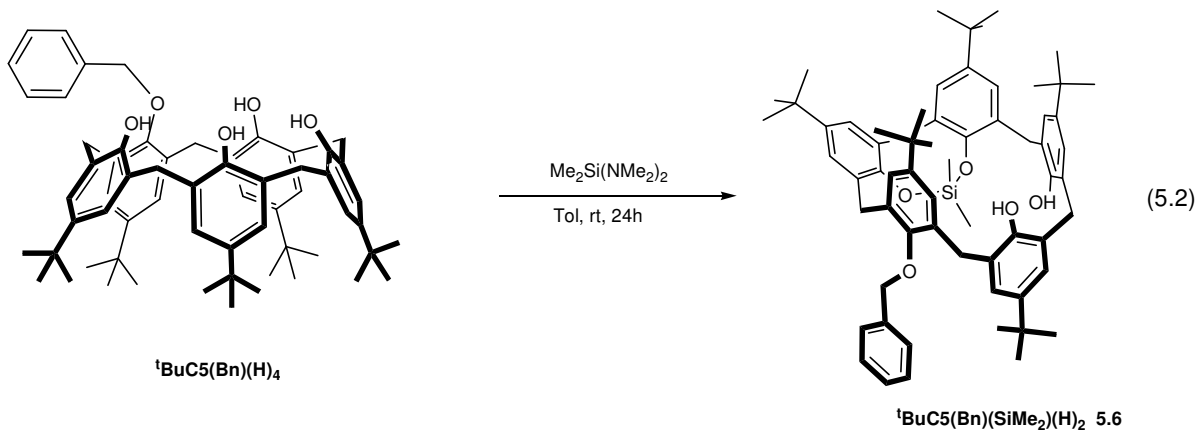

(5.2)

We attempted the preparation of analogous silylated complexes of **^{t}BuC5Bn(H)$_4$** containing bulkier -$SiPh_2$ or -$Si^{i}Pr_2$ groups by the addition of $R_2Si(NMe)_2$ to the parent calixarene, but in all cases we observed a mixture of mono and di-substituted ligands that were hard to separate.

Silylated ligands **5.1-5.5** are all white solids, soluble in most organic solvents, and stable up to three weeks in air.

5.2.2 Synthesis of bismuth(III) and antimony(III) complexes supported by **^{t}BuC5(SiRR')(H)$_3$** ligands (**5.1-5.5**)

The addition of a silicon group in the 1,2 positions of the calix[5]arene ligands left three neighboring hydroxyl groups available for reactivity. We expected that the disposition of the remaining OH groups could facilitate the lower rim coordination of the bismuth(III) and antimony(III) centers. However, we observed that the choice of the right metal reagent is critical for obtaining the desired products.

Relatively few examples of the insertion of main group or transition metals to silylated calixarenes can be found in literature. Ladipo and coworkers reported that complexation of Ti(IV) centers to several **RC4(SiR$_2$)(H)$_2$** ligands was achieved after the stoichiometric addition of $TiCl_4$ at low temperature.[185] Following this methodology, we treated the **^{t}BuC5(SiRR')(H)$_3$**

ligands with one equivalent of MCl_3 (M = Bi, Sb) in THF at -78 ^oC. The ^1H NMR spectra in all cases showed only a trace of new products in mixture with parent calixarene. Our attempts to improve the yield of the products by increasing the temperature or the number of MCl_3 equivalents failed in all cases. We believe that the poor performance observed in these reactions could be related to the release of HCl (protonating agent) that may be responsible for the regeneration of parent calixarene.

The most common pathway for the preparation of main group calix[n]arenes (n = 4, 6, 8) involves the reaction of the parent calix[n]arene ligands with metal amides, organometals or metal alkoxides in exchange reactions.[112-115,117-119] Lattman et al. have shown that mono-phosphorus substituted ligands of the type **^{t}BuC5(PNMe$_2$)(H)$_3$** readily react with transition metal amides (M = Ti, Zr, W) to produce metallated complexes of the type [M{**^{t}BuC5(PNMe$_2$)**}].[130,131] We have reported that $M(O^tBu)_3$ (M = Bi, Sb) or $Sb(NMe_2)_3$ are excellent reagents for the preparation of metallocalix[n]arenes (n = 4-8).[58,121,159]

We decided to employ the latter routes by treating the **^{t}BuC5(SiRR')(H)$_3$** ligands with one equivalent of $M(O^tBu)_3$ (M = Bi, Sb) or $Sb(NMe_2)_2$ in THF or toluene, as depicted in equation 3. Under these reaction conditions, the formation of the metallated calixarenes **5.7-5.16** was readily achieved (equation 5.3). The products were obtained in moderate to good yields (52-91%) as yellow (Bi) and white (Sb) solids after purification by recrystallization from THF or DME. As desired, the complexes **5.7-5.16** displayed excellent solubility in most organic solvents including alkanes (pentane and hexane), and no decomposition was observed after 12 h in air. Most of the complexes are stable in solution, but complexes **5.13**, **5.14**, and **5.16** start to decompose to parent silylated ligand after 2 h in benzene.

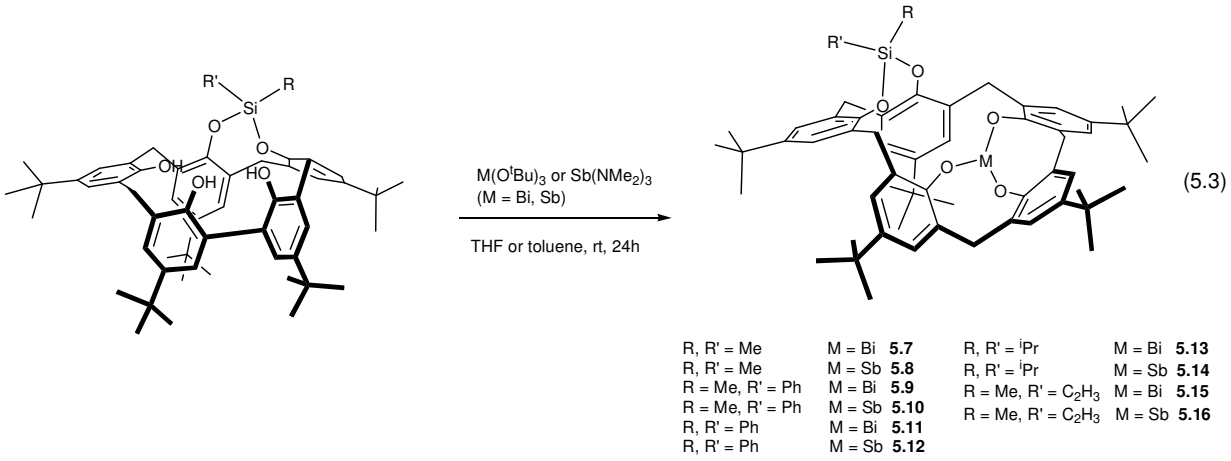

5.2.3 Synthesis of bismuth(III) and antimony (III) complexes supported by the **^{t}BuC5(Bn)(SiMe$_2$)(H)$_2$** ligand (**5.6**).

The silylated calix[5]arene **^{t}BuC5(Bn)(SiMe$_2$)(H)$_2$** (**5.6**) resembles the **RC4(SiR$_2$)(H)$_2$** ligands by containing two unreacted OH groups, but the larger cavity size in **5.6** allows the calixarene ring to adopt a partial cone conformation rather than 1,2-alternate. In the partial cone conformation, the two unreacted OH groups in **5.6** point in different directions so the insertion of a metal could be difficult.

Experimentally, we observed that the treatment of **^{t}BuC5(Bn)(SiMe$_2$)(H)$_2$** with one equivalent of M(O^{t}Bu)$_3$ (M = Bi, Sb) or Sb(NMe$_2$)$_3$ in toluene readily yielded the expected complexes **5.17-5.19**, as shown in equation 5.4.

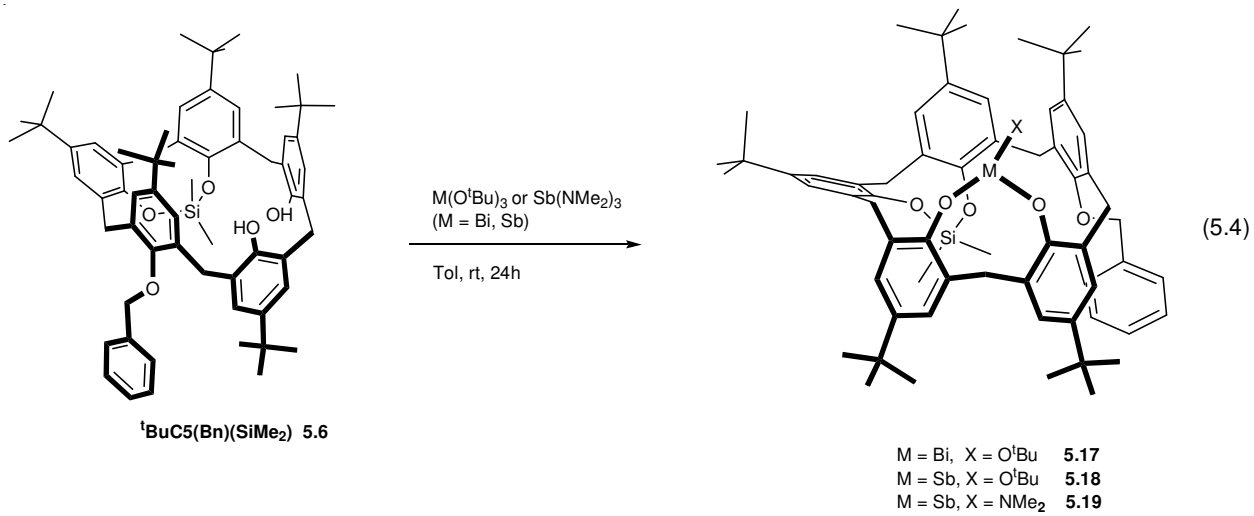

^{t}BuC5(Bn)(SiMe$_2$) 5.6

(5.4)

The crude reaction mixture showed quantitative conversion to the products at room temperature. Recrystallization at -35 ^oC from concentrated pentane/THF (or DME) gave the complexes in 83-87% yields. Compounds **5.17-5.19** are soluble in most organic solvents and moderately air and moisture sensitive (decomposition to silylated ligands is observed after 2 days in air).

5.3 NMR spectroscopy

The excellent solubility of complexes **5.1-5.19** allowed their solution analysis by ^1H NMR spectroscopy. The monosilylated ligands **5.1-5.5** all give very similar patterns (Figure 5.1). Three pairs of doublets for the methylene protons (geminal coupling due to nonequivalent methylene hydrogens), in a 1:2:2 ratio, range from 3.13 to 4.73 ppm.[79] Ligands **5.1-5.5** display three *tert*-butyl resonances (with 2:2:1 intensities) located between 1.13 to 1.31 ppm. Overall the ^1H NMR spectra for ligands **5.1-5.5** are similar to those observed in phosphorus and silicon calix[5]arene complexes reported in literature, and consistent with a C_s symmetry.[126,136]

The groups attached to the silicon atoms are chemically nonequivalent (*endo* and *exo* orientation), giving two different signals in the ^1H NMR spectra. The methyl groups in ligands

5.1, **5.2** and **5.5** are located in high fields ranging from -2.03 to -0.105 ppm. The OH groups can only be observed for ligands **5.1** and **5.5** as the OH signals for ligands **5.2**-**5.4** are too broad to be observed at room temperature.

An interesting conformational behavior was observed for ligand **^{t}BuC5(Si^{i}Pr$_2$)(H)$_3$** (**5.4**). When the ^{1}H NMR spectrum of **5.4** is taken in C_6D_6, the pattern indicates the presence of two different conformations in an approximate 1:3 ratio. Each conformer displays a set of three ^{t}Bu peaks and three pairs of doublets for the $ArCH_2Ar$ groups. On the other hand, if the ^{1}H NMR of ligand **5.4** is taken in DMSO-d_6, the spectrum shows only a single conformer (Figure 5.1) probably due to the insertion of the DMSO inside the cavity of the calixarene. This ^{1}H NMR behavior could also be related to the influence of the solvent polarity on the rate of conformational inversion in calixarene complexes.[74,120]

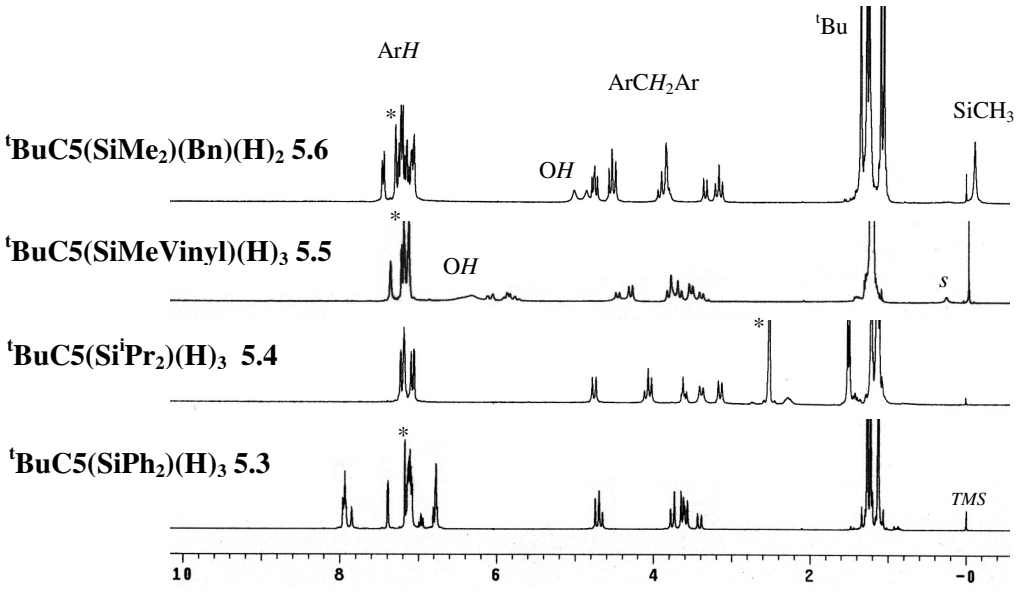

Figure 5.1. ^{1}H NMR spectra for ligands **5.3**, **5.5**, and **5.6** in *C_6D_6 and **5.4** in *DMSO-d_6. Second $SiCH_3$ group in **5.6** is not shown. s = residual solvent.

The presence of the benzyl group in the lower rim of ligand **5.6** changes the patterns of its ^{1}H NMR spectrum with respect to ligands **5.1-5.5**. Five single peaks for the ^{t}Bu groups, eight

doublets in the methylene area and two broad signals for the unreacted OH groups are observed (Figure 5.1). The complicated ^{1}H NMR spectrum in ligand **5.6** resembles the patterns observed in some bimetallic calix[5]arene antimony complexes reported recently by our group.[159] The methylene protons of the benzyl group appear as a singlet at 3.87 ppm and the methyl groups attached to the silicon atoms are nonequivalent, appearing at -2.45 and -0.11 ppm.

The metallated complexes **5.7-5.16** all display similar ^{1}H NMR patterns to those of their parent ligands (Figure 5.2). The presence of the metals resolves the *tert*-butyl peaks as three sharp singlets ranging from 0.97 to 1.38 ppm, and the six methylene doublets range from 3.32 to 5.30 ppm. The $SiMe_3$ groups in complexes **5.7** and **5.8** are nonequivalent, resonating upfield in a range from 0.13 to 0.92 ppm.

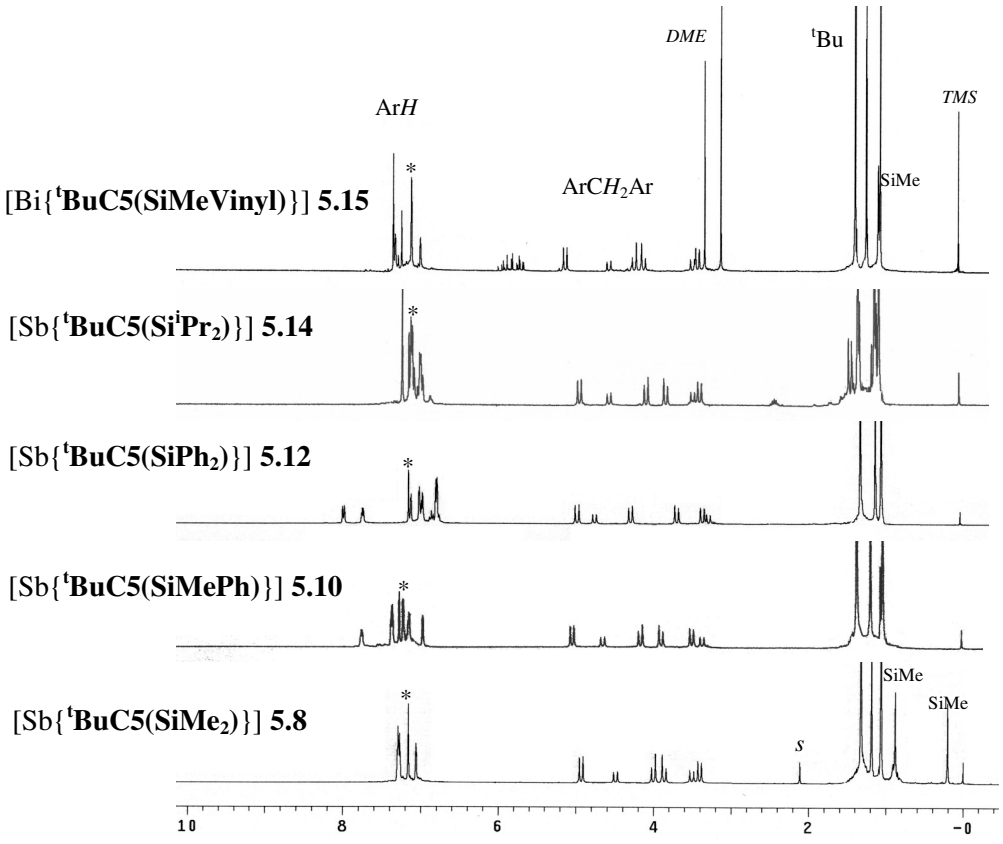

Figure 5.2. Representative ^{1}H NMR spectra of the M^{III} (M^{III} = Bi, Sb) complexes supported by **^{t}BuC5(SiRR')(H)$_3$** ligands in $*C_6D_6$. *s* = residual solvent, DME = dimethoxyethane.

Complexes **5.17**-**5.19** show similar ^{1}H NMR patterns (Figure 5.3) to those for the **^{t}BuC5(Bn)(SiMe$_2$)(H)$_2$** ligand **5.6** (Figure 5.1). However, the metallation in complexes **5.17** and **5.19** resolves the calixarene methylene groups into five pairs of doublets. Likewise, the methylene hydrogens from the benzyl group are no longer equivalent, appearing as a pair of doublets. The *endo* -SiCH$_3$ groups in **5.17**-**5.19** remain nonequivalent as in their parent ligand **5.6**, and they are strongly shielded (δ = -1.19, -1.20 and -1.16 ppm, respectively). A *tert*-butyl group belonging to the remaining M-O^{t}Bu bond is observed for complexes **5.17** and **5.18** at 1.90 and 1.82 ppm, respectively, and in the case of complex **5.19** a singlet at 2.96 ppm belongs to the Sb-NMe$_2$ group. The presence of reactive -O^{t}Bu and -NMe$_2$ groups in complexes **5.17**-**5.19** may be useful for the preparation of more complex structures.

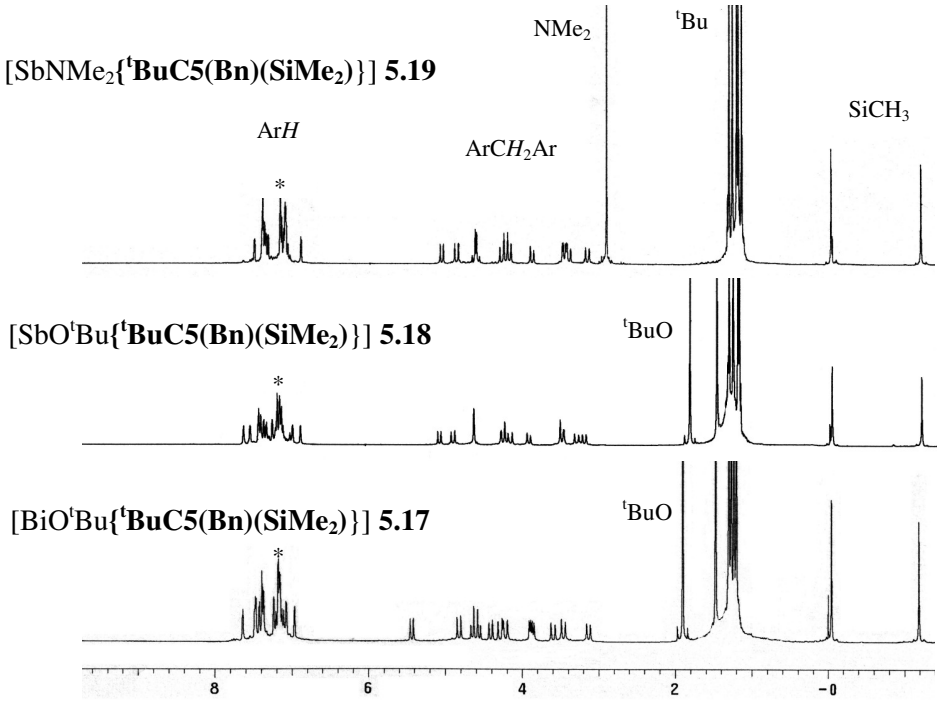

Figure 5.3. ^{1}H NMR spectra of complexes **5.17**-**5.19** in *C_6D_6**.**

5.4 Crystal and molecular structures

5.4.1 Monosilylated ligands.

Crystal structures of the ligands **^{t}BuC5(SiPh$_2$)(H)$_3$** (**5.3**) and **^{t}BuC5(Bn)(SiMe$_2$)(H)$_2$** (**5.6**) are illustrated in Figures 5.4 and 5.5, respectively, and selected bond distances and angles are shown in Table 5.1. Ligands **5.3** and **5.6** are monomeric units with a silicon center located in the lower rim of the cavity. The silicon center displays a tetrahedral geometry with O-Si-O, C-Si-O and C-Si-C angles ranging from 104.8 to 117.8^{o}, close to the expected 109^{o}.

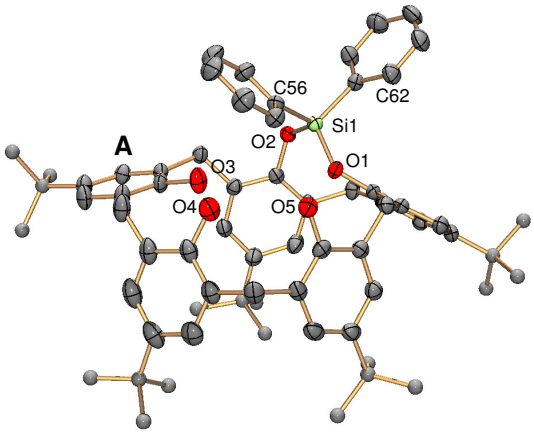

Figure 5.4. Crystal structure of ligand **5.3** with thermal ellipsoids at the 50% probability level. H atoms and non-coordinated solvent are omitted for clarity.

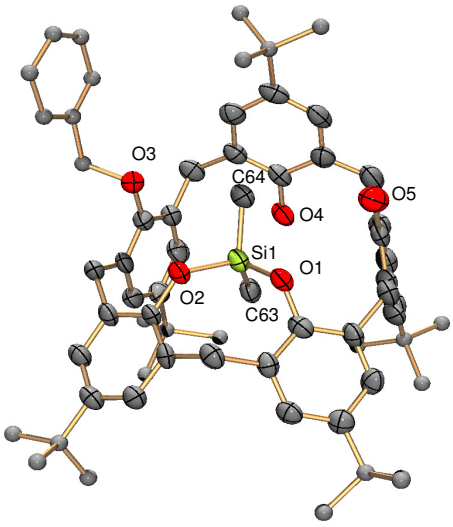

Figure 5.5. Crystal structure of ligand **5.6** with thermal ellipsoids at the 50% probability level. H atoms and non-coordinated solvent are omitted for clarity.

Table 5.1. Selected bond lengths (Å) and angles (°) of ligands **5.3** and **5.6**.

5.3		**5.6**	
Si(1)-O(1)	1.6454(18)	Si(1)-O(1)	1.661(6)
Si(1)-O(2)	1.6590(19)	Si(1)-O(2)	1.652(5)
Si(1)-C(56)	1.858(3)	Si(1)-C(63)	1.825(8)
Si(1)-C(62)	1.856(3)	Si(1)-C(64)	1.819(7)
O(1)-Si(1)-O(2)	109.64(9)	O(1)-Si(1)-O(2)	107.6(3)
O(1)-Si(1)-C(56)	106.04(10)	O(1)-Si(1)-C(63)	108.6(3)
O(1)-Si(1)-C(62)	114.31(11)	O(1)-Si(1)-C(64)	106.3(3)
O(2)-Si(1)-C(56)	107.19(11)	O(2)-Si(1)-C(63)	111.2(3)
O(2)-Si(1)-C(62)	107.17(11)	O(2)-Si(1)-C(64)	104.8(3)
C(56)-Si(1)-C(62)	112.29(12)	C(63)-Si(1)-C(64)	117.8(4)

The silicon centers each form an eight membered ring by bonding to two aryloxide groups from the calixarene ligand. The conformation of the eight membered rings could be described as twisted boat (TB) in the case of ligand **5.3**, while for ligand **5.6** the conformation is close to boat chair (BC).[140] These conformations are similar to those observed in silicon, phosphorus and antimony **^{t}BuC5(H)$_5$** complexes[126,136,159] and in some silicon bisphenolates.[191] The Si-OAr bond lengths are in the range of 1.6454(18) to 1.661(6) Å while the Si-C bond distances range from 1.819(7) to 1.858(3) Å. All these distances fall in the normal ranges for silicon calixarene complexes.[125,126,185-188,192-194] The methyl groups attached to the silicon center are *endo* and *exo* oriented, consistent with their ^{1}H NMR analyses.

The calixarene ring in **5.3** displays a distorted cone conformation with the ring **A** close to the plane of the lower rim (Figure 5.4). In ligand **5.6** the presence of the monobenzyl ether moiety causes the ligand to adopt a partial cone conformation (Figure 5.5) similar to that observed in the mono-*n*-propyl calix[5]arene ether.[79]

5.4.2 Bi(III) and Sb(III) complexes with **^{t}BuC5(SiRR')(H)$_3$** ligands.

The crystal structures of complexes **5.8**, **5.9**, **5.12**, **5.15**, and **5.16** are illustrated in Figures 5.6-5.8 and selected bond distances and angles are presented in Table 5.2. Complexes **5.9**, **5.12**, **5.15** and **5.16** all crystallize in the triclinic *P*-1 space group while complex **5.8** crystallizes in the orthorhombic space group *P*na2$_1$. All monometallic complexes **5.8**, **5.9**, **5.12**, **5.15** and **5.16** are monomeric units with the calixarene ligand in an approximate 1,2-alternate conformation. This conformation is similar to that observed in [W(N^{t}Bu)(HN^{t}Bu){ **^{t}BuC5(PNMe$_2$)**}] and [Ti(NMe$_2$){**^{t}BuC5(PNMe$_2$)**}].[130,131]

The silicon centers remain tetrahedral as in the parent ligands with their R and R' groups coordinated *endo* and *exo* with respect to the calixarene lower rim, consistent with their ^{1}H NMR spectra. All the Si-O and Si-C bond distances and O-Si-O and C-Si-O angles fall in the normal ranges for silylated calixarene[123,125] and aryloxide[191,195-198] complexes (Table 5.2). The conformation of the eight-membered rings formed around the silicon center in **5.8**, **5.9**, **5.12**, **5.15** and **5.16** is twisted boat (TB) in all cases regardless of the R,R' groups attached to the silicon atom, or the metal center coordinated in the lower rim.

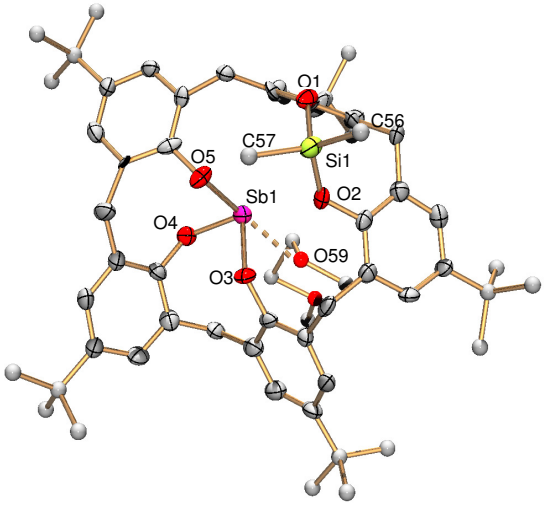

Figure 5.6. Crystal structure of complex **5.8** with thermal ellipsoids at the 50% probability level. H atoms and non-coordinated solvent are omitted for clarity.

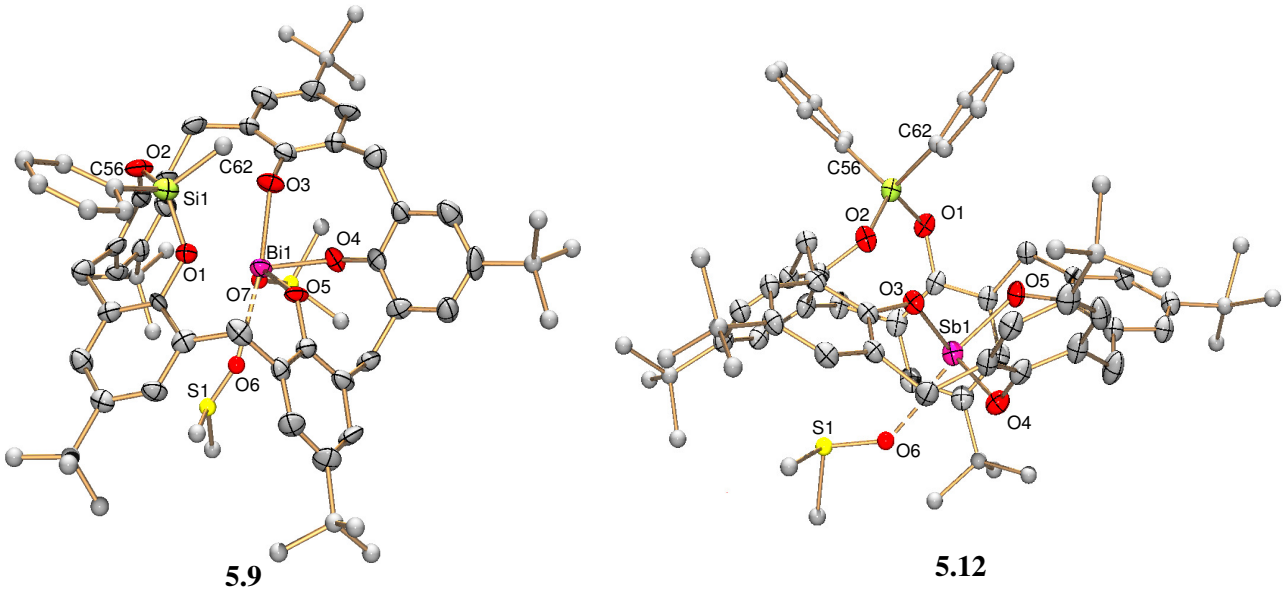

Figure 5.7. Crystal structures of complexes **5.9** and **5.12** with thermal ellipsoids at the 50% probability level. H atoms and non-coordinated solvent are omitted for clarity.

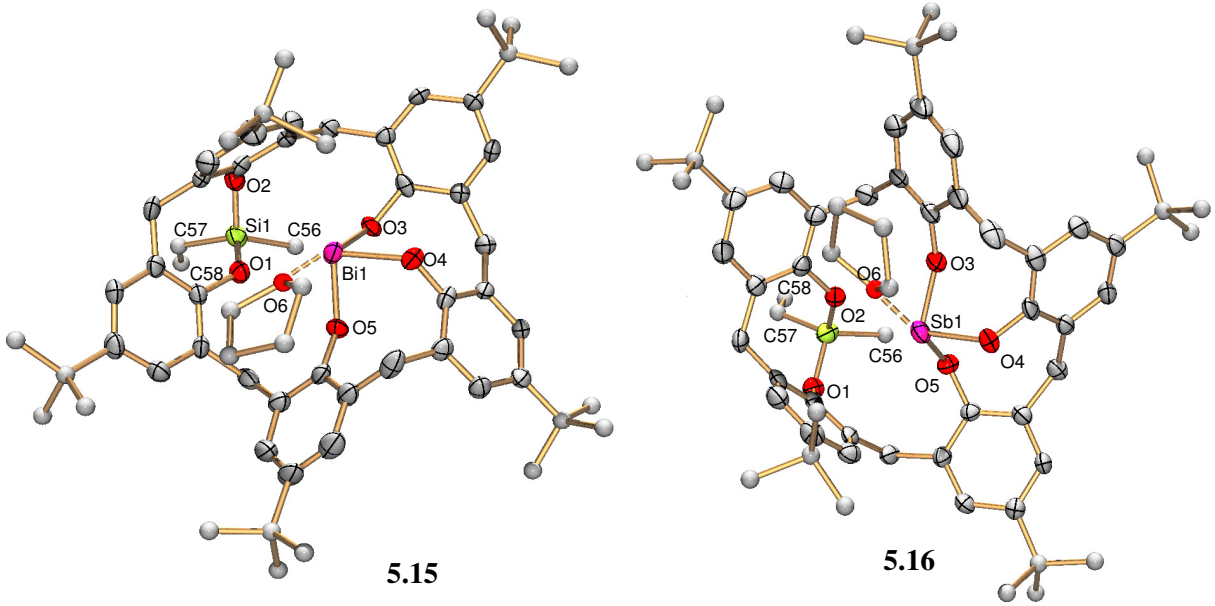

Figure 5.8. Crystal structures of complexes **5.15** and **5.16** with thermal ellipsoids at the 50% probability level. H atoms and non-coordinated solvent are omitted for clarity.

Table 5.2. Selected bond lengths (Å) and angles (°) of complexes **5.8**, **5.9**, **5.12**, **5.15** and **5.16**.

	5.8	**5.9**	**5.12**	**5.15**	**5.16**
Si(1)-OAr	1.644(7), 1.645(7)	1.646(9), 1.666(9)	1.630(3), 1.651(3)	1.640(6), 1.650(5)	1.643(4), 1.648(4)
Si(1)-C	1.826(10), 1.840(11)	1.821(18), 1.831(14)	1.848(5), 1.850(4)	1.833(10), 1.844(8)	1.830(8), 1.852(7)
O(1)-Si-O(2)	106.2(3)	104.4(4)	105.94(14)	105.3(3)	105.3(2)
C-Si-OAr	107.3(5)-114.8(5)	108.5(6)-112.1(6)	105.51(18)-116.78(18)	107.5(3)-113.0(4)	107.3(3)-112.6(3)
C-Si-C	111.1(6)	110.6(7)	110.1(2)	112.8(4)	112.7(4)
M-O(3)	1.959(6)	2.207(8)	1.988(2)	2.131(5)	1.959(4)
M-O(4)	1.969(6)	2.125(8)	1.985(3)	2.094(5)	1.971(4)
M-O(5)	2.013(6)	2.119(7)	2.011(3)	2.069(5)	2.010(4)
ArO-M-OAr	89.9(3)-94.8(2)	83.5(3)-90.5(3)	89.41(11)-95.22(11)	86.99(19)-92.68(18)	89.82(16)-93.49(16)
M-$O_{solvent}$	3.028(12)	2.53(2)- 2.73(2)	2.565(3)	2.981(9)	3.128(14)

The metal centers in complexes **5.8**, **5.12**, **5.15**, and **5.16** are tetracoordinated having primary bonds with three aryloxides, and have a secondary interaction with one solvent molecule (DME for **5.8**, DMSO for **5.12** and THF for **5.15** and **5.16**), to give an overall see-saw geometry. The antimony center in complex **5.8** is weakly coordinated to one DME molecule with a bond distance of 3.028(4) Å, while complex **5.12** contains a Sb-O(DMSO) bond distance of 2.565(3) Å similar to those observed in [Sb_2Cl_2{**RC4**}] and [Sb_2O**RC5(H)**}] complexes [2.503(7)-2.569(2) Å].[58,159] The *trans* effect of solvent coordination is noticed in the slight elongation of bonds [Sb-O(5) 2.013(6) and Sb-O(5) 2.011(3) Å] in **5.8** and **5.12**, respectively. The metal centers in complexes **5.15** and **5.16** are weakly coordinated to one THF molecule each with bond distances of 2.981(9) and 3.128(14) Å, respectively. These Sb-O(THF) bond distances are much longer than that observed in the calixarene complex [Sb_2Cl_2{^{t}**BuC4**}]·4THF [2.631(2) Å], indicating relatively weak coordination.[57] A similar solvent coordination *trans* effect in

complexes **5.15** and **5.16** is evidenced by the elongation of the Bi-O(3) and Sb-O(5) bonds with distances of 2.131(5) and 2.010(4) Å, respectively.

In complex **5.9** two DMSO molecules coordinate to the bismuth center, providing a distorted square-based pyramidal geometry. This geometry is similar to the one observed in the central rings of bismuth calixarene clusters of the type $[Bi_2O\{\mathbf{RC5(H)}\}]_2$ and $[Bi_4O_2\{\mathbf{RC8}\}]_2$.[57,121,159] The Bi-O(7) bond distance is 2.589(10) Å while Bi-(O6) and Bi-O(6A) bond distances from the disordered DMSO molecule are 2.53(2) and 2.73(2) Å, respectively (2.63 Å average).

The conformation of the calixarene ligands in complexes **5.8**, **5.9**, **5.12**, **5.15** and **5.16** allows metal π-arene interactions with a single aromatic ring in the calixarene ligand. The M-C(aryl) distances and M···centroid(aryl) distances are shown in Table 5.3, and they are comparable with those reported in literature.[57,58,141-143,199-202] Due to the 1,2-alternate conformation in the calixarene ring, the silicon atoms and the metal centers are oriented on opposite sides of the ring, avoiding any Si···metal interactions.

Table 5.3 Comparison of M-C(aryl) and M···centroid(aryl) interactions

	M-C(aryl)/ Å	M···centroid(aryl)/ Å
5.8	3.502-4.260	3.661
5.9	3.524-4.042	3.543
5.12	3.492-4.116	3.562
5.15	3.411-3.875	3.391
5.16	3.477-4.073	3.538
5.17	3.343-4.218	3.537
5.18	3.358-4.377	3.655
5.19	3.431-4.390	3.689

5.4.3 Bi(III) and Sb(III) complexes with **^{t}BuC5(Bn)(SiMe$_2$)(H)$_2$** (**5.6**) ligand

The crystal structures of complexes **5.17**, **5.18** and **5.19** are depicted in Figures 5.9 and 5.10 and selected bond distances and angles are shown in Table 5.4. Complexes **5.17-5.19** are all monomeric with an approximate 1,2-alternate conformation. The calixarene ligands in complexes **5.17-5.19** display a C_1 symmetry and the two methyl groups in the tetrahedral silicon centers are coordinated *endo* and *exo,* consistent with their ^{1}H NMR spectra. The bismuth center in complex **5.17** is primarily coordinated to two aryloxides and to one unreacted O^{t}Bu group that faces away from the calixarene cavity. In addition, a secondary interaction with a THF molecule with bond distance of 2.806(16) Å is observed, providing a see-saw geometry. The Bi-O^{t}Bu bond distance is 2.008(8) Å, similar to that in the [Bi(O^{t}Bu){**^{t}BuC4(Bn)$_2$**}] complex [2.061(3) Å] prepared in our lab.[58]

The antimony centers in complexes **5.18** and **5.19** are bonded to two neighboring aryloxides and one O^{t}Bu and NMe$_2$, respectively, displaying a trigonal pyramidal geometry. This geometry is usually observed in antimony(III) calixarene and aryloxide complexes.[57,58,139,159] The Sb-O^{t}Bu and Sb-NMe$_2$ bond distances are 1.906(3) and 1.976(4) Å, respectively, and as in complex **5.17**, they point away from the calixarene cavity.

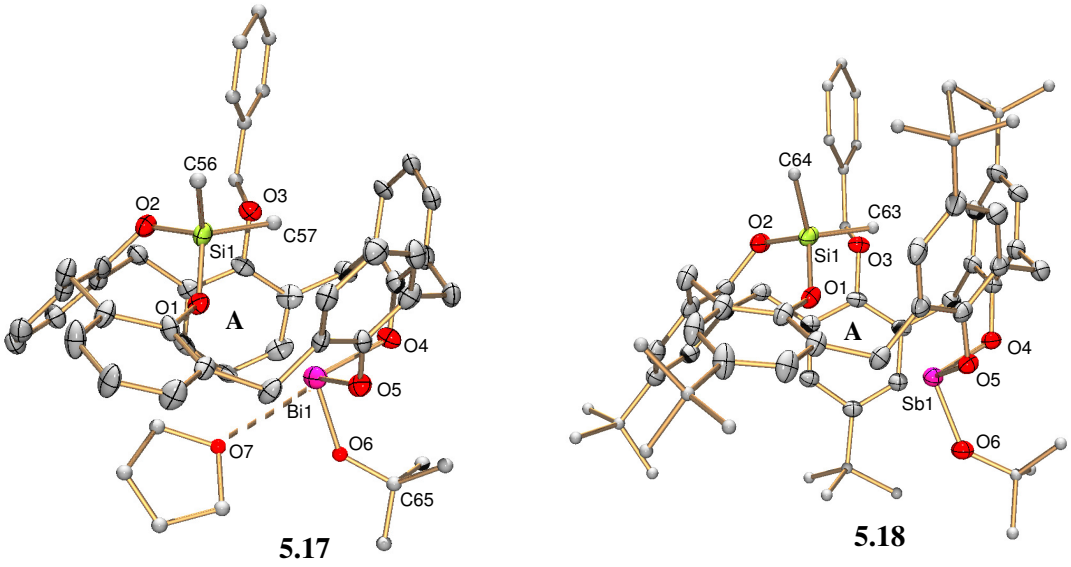

Figure 5.9. Crystal structures of complex **5.17** and **5.18** with thermal ellipsoids at the 50% probability level. *tert*-Butyl groups in **5.17**, H atoms and non-coordinated solvent are omitted for clarity.

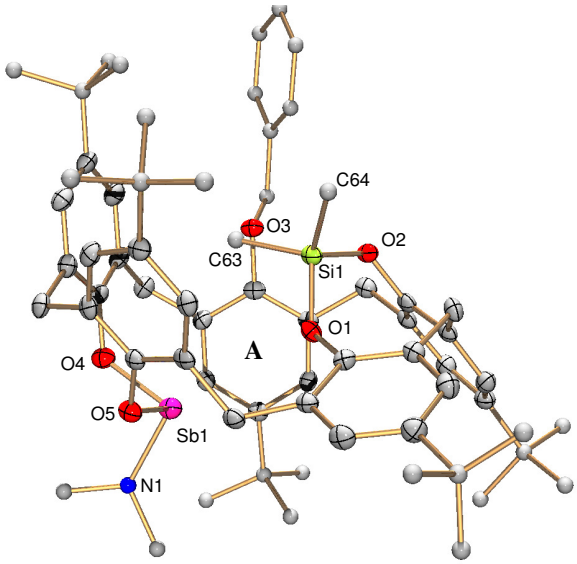

Figure 5.10. Crystal structure of complex **5.19** with thermal ellipsoids at the 50% probability level. H atoms and non-coordinated solvent are omitted for clarity.

Table 5.4 Selected bond lengths (Å) and angles (°) of complexes **5.17**-**5.19**.

	5.17	**5.18**	**5.19**
Si(1)-OAr	1.642(6), 1.664(6)	1.640(3), 1.661(3)	1.650(3), 1.663(2)
Si(1)-C	1.814(11), 1.820(10)	1.823(5), 1.830(5)	1.818(4), 1.847(4)
O(1)-Si-O(2)	105.5(3)	106.66(14)	106.65(12)
C-Si-OAr	108.1(4)-112.6(4)	107.19(18)-111.21(18)	108.05(16)-111.89(17)
C-Si-C	109.0(5)	111.6(2)	110.5(2)
M-O(4)	2.124(6)	1.982(3)	1.992(3)
M-O(5)	2.128(6)	1.995(3)	2.014(2)
M-X	2.008(8)	1.906(3)	1.976(4)
O-M-X	93.4(3), 94.0(3)	94.35(12), 94.74(11)	89.06(14), 94.38(13)
O(4)-M-O(5)	92.4(2)	94.52(11)	95.32(10)
M-$O_{solvent}$	2.806(16)	----------	----------

X = O^{t}Bu, NMe_2

The M-OAr bond distances and O-M-O angles in structures **5.17-5.19** fall in the normal ranges for bismuth(III) and antimony(III) calixarene complexes.[57,58,121,159] In complex **5.17-5.19**, the *endo* coordination (with respect to the lower rim) of the bismuth and antimony centers allows several metal-arene π interactions with ring **A** (Table 5.3). The Bi-C interactions in **5.17** are comparable with those observed in complexes **5.9** and **5.15** (Table 5.3), while the Sb-C interactions in complexes **5.18** and **5.19** are similar to those observed in [Sb_2Cl_2{**RC4**}],[58] [SbX_3·(arene)],[203-206] and organoantimony(III) complexes.[207,208]

5.5 Experimental Section

5.5.1 General information

Unless otherwise noted, all manipulations were carried out in a nitrogen filled glovebox. Starting materials were obtained from commercial suppliers and used without further purification. *p-tert*-Butylcalix[5]arene,[97] monobenzyl-*p-tert*-butylcalix[5]arene,[79] [Na_2·**^{t}BuC5(H)$_3$**],[120] Bi(O^{t}Bu)$_3$,[145] and Sb(O^{t}Bu)$_3$[156] were prepared by the literature procedures. $Sb(NMe_2)_3$ was purchased from Strem Chemicals and used as received. *p-tert*-Butylcalix[5]arene

was dried at 110 ^{o}C at least 24 hrs under vacuum before use. Tetrahydrofuran and toluene were freshly distilled from Na/benzophenone. Other anhydrous solvents were purchased from Aldrich and stored over molecular sieves under nitrogen before using. Deuterated benzene and dimethyl sulfoxide were dried over CaH_2. The melting points of all compounds were taken in sealed and evacuated capillary tubes on a Mel-temp apparatus (Laboratory Devices, Cambridge, MA) using a 500 ^{o}C thermometer. A melting temperature preceded by a " >" sign indicates that the compound starts to decompose at that temperature but appears to actually melt at some higher temperature. ^{1}H NMR and ^{13}C spectra were recorded at room temperature on a Varian XL-300 spectrometer at 300 and 75 MHz, respectively. Analytical samples were dried under vacuum for at least 24 hrs. Microanalyses were performed by Atlantic Microlab, Inc, Norcross, GA. IR and UV/Vis spectra were obtained with an Infinity Gold^{TM} FTIR spectrometer and Agilent 8453 spectrophotometer, respectively. Filtrations used a medium sintered glass filter. All X-ray diffraction experiments were performed in a Bruker SMART 1000 CCD detector at variable low temperature using Mo Kα radiation. In most cases the crystals for X-ray diffraction included solvents of crystallization, as shown in Table 5.5. For analytical samples the crystals were dried under vacuum at room temperature for 24 hrs.

5.5.2 General procedure for preparation of **^{t}BuC5(SiRR')(H)$_3$** ligands (**5.1-5.5**)

A solution of NaO^{t}Bu (0.102 g, 1.06 mmol) in 4 mL of THF was added dropwise to a solution of **^{t}BuC5(H)$_5$** (0.412 g, 0.508 mmol) in 8 mL of THF and the reaction mixture was allowed to stir for 24 hrs. To the resulting yellowish solution of the $Na_2\cdot$**^{t}BuC5(H)$_3$**^{120} salt, a colorless solution of the appropriate silane precursor (RR'$SiCl_2$, 0.508 mmol) in 3 ml of THF was added, and the reaction was allowed to stir for 24 h.

The resulting cloudy solution was centrifuged (or filtered) to yield a colorless solution that was vacuum dried to yield a white solid.

^{t}BuC5(SiMe$_2$)(H)$_3$ (**5.1**): The white solid was stirred in 15 mL of pentane for 24 h and centrifuged. This washing procedure was repeated to yield 0.374 g of pure **^{t}BuC5(SiMe$_2$)(H)$_3$** as a white powder (0.432 mmol, 85% yield). ^{1}H NMR (C_6D_6): δ -2.03 (bs, 3H, SiC*H*$_3$), -0.10 (bs, 3H, SiC*H*$_3$), 1.15 (s, 18H, C(C*H*$_3$)$_3$), 1.28 (s, 18H, C(C*H*$_3$)$_3$), 1.31 (s, 9H, C(C*H*$_3$)$_3$), 3.34 (d, *J* = 14.1 Hz, 2H, ArC*H*$_2$Ar), 3.37 (d, *J* = 13.2 Hz, 1H, ArC*H*$_2$Ar), 3.78 (d, *J* = 14.1 Hz, 2H, ArC*H*$_2$Ar), 3.89 (d, *J* = 14.1 Hz, 2H, ArC*H*$_2$Ar), 4.34 (d, *J* = 14.1 Hz, 2H, ArC*H*$_2$Ar), 4.47 (d, *J* = 13.2 Hz, 1H, ArC*H*$_2$Ar), 5.53 (b, 3H, O*H*), 7.09 (d, *J* = 2.4 Hz, 2H, Ar*H*), 7.21 (d, *J* = 2.4 Hz, 2H, Ar*H*), 7.30 (s, 6H, Ar*H*). ^{13}C{^{1}H} NMR (C_6D_6): δ 151.9, 150.4, 149.2, 144.7, 143.8, 142.9, 131.7, 131.4, 127.1, 127.0, 126.7, 126.2, 126.1, 125.9 (aromatic carbons) [two signals missing, probably overlapping with C_6H_6 peaks], 35.6, 34.9 (*C*(CH$_3$)$_3$), 34.0, 33.9 (Ar*C*H$_2$Ar), 31.8 (*C*(CH$_3$)$_3$), 31.6, 31.5, 31.4 (C(*C*H$_3$)$_3$), 30.7 (Ar*C*H$_2$Ar), -2.9, -8.4 (Si*C*H$_3$). IR (KBr, cm^{-1}): 3548bs (OH), 2962vs, 2906vs, 2868vs, 1603m, 1479vs, 1439m, 1402w, 1393w, 1362s, 1310m, 1291s, 1264s, 1202vs, 1125m, 1105w, 1056w, 944m, 927m, 899s, 878s, 824s, 789m. UV/Vis λ_{max}/nm (C_6H_6) (ε/dm^{3}mol^{-1}cm^{-1}): 281 (1.61 x 10^4).

^{t}BuC5(SiMePh)(H)$_3$ (**5.2**): The white solid was dissolved in 8 mL of pentane and the solution was allowed to evaporate slowly to yield 0.382 g of colorless single block crystals of pure **^{t}BuC5(SiMePh)(H)$_3$** (0.411 mmol, 81% yield). ^{1}H NMR (C_6D_6): δ -0.29 (b, SiC*H*$_3$), 1.15 (s, 9H, C(C*H*$_3$)$_3$), 1.20 (s, 18H, C(C*H*$_3$)$_3$), 1.30 (s, 18H, C(C*H*$_3$)$_3$), 3.33 (d, *J* = 14.1 Hz, 1H, ArC*H*$_2$Ar), 3.53 (d, *J* = 14.1 Hz, 2H, Ar*CH*$_2$Ar), 3.75 (d, *J* = 14.7 Hz, 2H, ArC*H*$_2$Ar), 3.83 (d, *J* = 14.1 Hz, 2H, ArC*H*$_2$Ar), 4.39 (d, *J* = 14.7 Hz, 2H, ArC*H*$_2$Ar), 4.50 (d, *J* = 14.1 Hz, 1H, ArC*H*$_2$Ar), 7.01 (b, 2H, Ar*H*), 7.10 (d, *J* = 2.4 Hz, 2H, Ar*H*), 7.13 (d, *J* = 2.4 Hz, 1H, ArH), 7.19

(d, *J* = 2.4 Hz, 2H, Ar*H*), 7.23 (d, *J* = 2.4 Hz, 2H, Ar*H*), 7.25 (d, *J* = 2.4 Hz, 2H, Ar*H*), 7.48 (d, *J* = 2.4 Hz, 2H, Ar*H*), 7.73-7.76 (m, 2H, Ar*H*). No OH peak was observed at room temperature. $^{13}C\{^{1}H\}$ NMR (C_6D_6): δ 150.9, 148.7, 148.5, 145.5, 144.2, 143.7, 143.1, 134.4, 133.9, 130.9, 130.6, 130.3, 127.4, 127.5, 127.0, 126.9, 126.7, 126.5, 126.4, 125.9 (aromatic carbons), 35.7, 34.5 ($C(CH_3)_3$), 34.2, 34.0, 33.9 ($ArCH_2Ar$), 32.7 ($C(CH_3)_3$), 31.8, 31.6, 31.5 ($C(CH_3)_3$), -2.7 ($SiCH_3$). IR (KBr, cm^{-1}): 3576m, 3516vs, 3073w, 3049m, 2963vs, 2910vs, 2868vs, 1771w, 1593w, 1512w, 1503m, 1479vs, 1431s, 1392m, 1362s, 1323s, 1291vs, 1258vs, 1202vs, 1124vs, 996w, 931vs, 900vs, 872vs, 813m, 793s, 757m. UV/Vis λ_{max}/nm (C_6H_6) (ε/$dm^3mol^{-1}cm^{-1}$): 282 (1.63×10^4).

^{t}BuC5(SiPh$_2$)(H)$_3$ (**5.3**): The white solid was dissolved in 8 mL of hexane and allowed to evaporate slowly to yield 0.373 g of **^{t}BuC5(SiPh$_2$)(H)$_3$** as colorless crystals suitable for X-ray diffraction (0.376 mmol, 74% yield). Mp: 273-275 ^{o}C. ^{1}H NMR (C_6D_6): δ 1.13 (s, 18H, $C(CH_3)_3$), 1.23 (s, 9H, $C(CH_3)_3$), 1.27 (s, 18H, $C(CH_3)_3$), 3.41 (d, *J* = 15 Hz, 1H, $ArCH_2Ar$), 3.59 (d, *J* = 15 Hz, 2H, $ArCH_2Ar$), 3.62 (d, *J* = 14.1 Hz, 2H, $ArCH_2Ar$), 3.76 (d, *J* = 14.1 Hz, 2H, $ArCH_2Ar$), 4.67 (d, *J* = 15 Hz, 1H, $ArCH_2Ar$), 4.72 (d, *J* = 15 Hz, 2H, $ArCH_2Ar$), 6.76-6.81(m, 4H, Ar*H*), 6.96 (t, *J* = 7.5 Hz, 1H, Ar*H*), 7.08-7.14 (m, 8H, Ar*H*), 7.39 (d, *J* = 2.4 Hz, 2H, Ar*H*), 7.85 (s, 1H, Ar*H*), 7.92-7.96 (m, 4H, Ar*H*). The OH peak was too broad to be observed at room temperature. $^{13}C\{^{1}H\}$ NMR (C_6D_6): δ 149.9, 148.8, 148.4, 145.2, 143.6, 142.6, 134.8, 134.2, 133.4, 132.8, 131.0, 130.7, 129.9, 129.4, 128.6, 128.2, 127.2, 127.1, 126.8, 126.6, 126.4, 126.1, 126.0, 125.7 (aromatic carbons), 36.7 ($C(CH_3)_3$), 34.0, 33.9, 33.8 ($ArCH_2Ar$), 32.4, 32.1 ($C(CH_3)_3$), 31.6, 31.5, 31.3 ($C(CH_3)_3$). IR (KBr, cm^{-1}): 3558s (OH), 3401vs (OH), 3047m, 3007m, 2962vs, 2905vs, 2868vs, 2743w, 2709w, 2591w, 2557w, 1758w, 1592m, 1481vs, 1430s, 1393s, 1363vs, 1297vs, 1247vs, 1201vs, 1123vs, 1027w, 997w, 953s, 928s, 909vs, 889vs.

UV/Vis λ_{max}/nm (C_6H_6) (ε/$dm^3mol^{-1}cm^{-1}$): 283 (1.41 x 10^4). Anal. Calcd for $C_{67}H_{78}O_5Si$: C 81.17, H 7.93. Found: C 80.90, H 8.06.

^{t}BuC5(Si^{i}Pr$_2$)(H)$_3$ (**5.4**): The white solid was redissolved in 3 mL of pentane and was placed in the freezer at -35 ^{o}C overnight to yield 0.127 g of block colorless crystals of pure **^{t}BuC5(Si^{i}Pr$_2$)(H)$_3$** (0.137 mmol, 27% yield). Single crystals were obtained by slow evaporation of a concentrated pentane/DME solution (5:1) of product. Mp: 139-140 ^{o}C. ^{1}H NMR (DMSO-d_6): δ 1.11 (d, *J* = 7.5 Hz, 6H, CH(C*H*$_3$)$_2$), 1.13 (s, 9H, C(C*H*$_3$)$_3$), 1.14 (s, 18H, C(C*H*$_3$)$_3$), 1.21 (s, 18H, C(C*H*$_3$)$_3$), 1.41 (broad septet, 1H, C*H*(CH$_3$)$_2$), 1.49 (d, *J* = 7.5 Hz, 6H, CH(C*H*$_3$)$_2$), 2.26 (broad septet, 1H, C*H*(CH$_3$)$_2$), 3.13 (d, *J* = 13.5 Hz, 2H, ArC*H*$_2$Ar), 3.36 (d, *J* = 13.8 Hz, 2H, Ar*CH*$_2$Ar), 3.57 (d, *J* = 14.1 Hz, 1H, Ar*CH*$_2$Ar), 4.03 (d, *J* = 13.5 Hz, 2H, Ar*CH*$_2$Ar), 4.07 (d, *J* = 14.1 Hz, 1H, Ar*CH*$_2$Ar), 4.73 (d, *J* = 13.8 Hz, 2H, ArC*H*$_2$Ar), 7.03 (b, 2H, Ar*H*), 7.06 (bs, 2H, Ar*H*), 7.16 (b, 4H, Ar*H*), 7.20 (s, 2H, Ar*H*). OH peak not observed at room temperature. ^{13}C{^{1}H} NMR (DMSO-d_6): δ 148.9, 143.4, 130.5, 128.9, 128.3, 128.1, 127.3, 126.6, 126.3, 125.9, 125.7 (aromatic carbons, one carbon peak not observed), 36.2 (*C*(CH$_3$)$_3$), 34.4, 34.2 (Ar*C*H$_2$Ar), 34.1 (*C*(CH$_3$)$_3$), 32.1, 31.9 (two peaks overlapping, C(*C*H$_3$)$_3$), 27.9 (Ar*C*H$_2$Ar), 25.8 (*C*(CH$_3$)$_3$), 18.6, 18.4 (*C*H(CH$_3$)$_2$), 14.8 (CH(*C*H$_3$)$_2$) [one (CH(*C*H$_3$)$_2$) peak not observed]. IR (KBr, cm^{-1}): 3368m, 3055w, 2962s, 2910m, 2868s, 2717w, 1602w, 1503w, 1481s, 1422m, 1363s, 1296m, 1246m, 1202s, 1126m, 1117m, 1069w, 1046m, 1019w, 995w, 927m, 884s, 820m, 8052w, 795w. UV/Vis λ_{max}/nm (C_6H_6) (ε/$dm^3mol^{-1}cm^{-1}$): 213 (1.05 x 10^4), 284 (6.036 x 10^3). Anal. Calcd for $C_{61}H_{82}O_5Si \cdot C_4H_{10}O_2$: C 77.03, H 9.15. Found: C 77.11, H 9.36.

^{t}BuC5(SiMeVinyl)(H)$_3$ (**5.5**): The white solid was stirred for 24 hrs in 10 mL of pentane and centrifuged to yield a white solid. This washing procedure was repeated to yield 0.277 g of pure **^{t}BuC5(SiMeVinyl)(H)$_3$** as a white powder (0.315 mmol, 62% yield). Mp: 268-270 ^{o}C. ^{1}H

NMR (C_6D_6): δ -1.05 (b, 3H, SiCH_3), 1.22 (bs, 9H, C(CH_3)$_3$), 1.24 (bs, 18H, C(CH_3)$_3$), 1.25 (b, 18H, C(CH_3)$_3$), 3.42 (d, *J* = 14.1 Hz, 1H, ArCH_2Ar), 3.55 (d, *J* = 14.4 Hz, 2H, ArCH_2Ar), 3.69 (d, *J* = 14.1 Hz, 2H, ArCH_2Ar), 3.83 (d, *J* = 14.1 Hz, 2H, ArCH_2Ar), 4.32 (d, *J* = 14.4 Hz, 2H, ArCH_2Ar), 4.48 (d, *J* =14.1 Hz, 1H, ArCH_2Ar), 5.74-5.93 (m, 2H, CH=CH_2), 6.11 (dd, *J* = 4.5 Hz, *J* = 14.7 Hz, 1H, C*H*=CH_2), 6.36 (b, 3H, O*H*), 7.22 (b, 6H, Ar*H*), 7.25 (d, *J* = 2.1 Hz, 2H, Ar*H*), 7.39 (b, 2H, Ar*H*). $^{13}C\{^1H\}$ NMR (C_6D_6): δ 150.5, 150.1, 148.8, 145.2, 143.8, 143.2, 136.5, 133.2, 130.9, 130.7, 127.5, 127.4, 127.3, 126.7, 126.4 (aromatic carbons), 126.3 (*C*H=CH_2), 126.2 (aromatic carbons), 35.6 (*C*(CH_3)$_3$), 34.4 (Ar*C*H_2Ar), 34.2, 34.1, (*C*(CH_3)$_3$), 34.0 (Ar*C*H_2Ar) , 32.5 (CH=*C*H_2), 31.7, 31.6, 31.5 (C(*C*H_3)$_3$), 22.7 (Ar*C*H_2Ar), -5.8 (Si*C*H_3). IR (KBr, cm^{-1}): 3537m (OH), 3047m, 2961vs, 2906vs, 2867s, 2743w, 2702w, 1762w, 1596w, 1479vs, 1393m, 1362s, 1310m, 1291m, 1261m, 1202vs, 1125s, 1104m, 1004m, 961m, 946s, 926m, 899s, 878s, 859m. UV/Vis λ_{max}/nm (C_6H_6) (ε/$dm^3mol^{-1}cm^{-1}$): 283 (5.68 x 10^3). Anal. Calcd for $C_{58}H_{74}O_5Si$: C 79.23, H 8.48. Found: C 79.47, H 8.76.

^{t}BuC5(Bn)(SiMe$_2$)(H)$_2$ (**5.6**): A colorless solution of $Me_2Si(NMe_2)_2$ in 4 mL of toluene (0.0743 g, 0.508 mmol) was added dropwise to a solution of **^{t}BuC5(Bn)(H)$_4$** (0.458 g, 0.508 mmol) in 8 mL of toluene and the reaction mixture was allowed to stir for 24 hrs. The final yellowish solution was vacuum dried to yield a yellowish solid. This solid was dissolved in 10 mL of hexane and the solution was allowed to slowly evaporate to give 0.379 g of pure **^{t}BuC5(Bn)(SiMe$_2$)(H)$_2$** as X-ray quality colorless block crystals (0.396 mmol, yield 78%). Mp: 279-281 ^oC. ^1H NMR (C_6D_6): δ -2.45 (s, 3H, SiCH_3), -0.11 (s, 3H, SiCH_3), 1.06 (s, 9H, C(CH_3)$_3$), 1.10 (s, 9H, C(CH_3)$_3$), 1.25 (s, 9H, C(CH_3)$_3$), 1.28 (s, 9H, C(CH_3)$_3$), 1.36 (s, 9H, C(CH_3)$_3$), 3.17 (d, *J* = 14.1 Hz, 1H, ArCH_2Ar), 3.21 (d, *J* = 14.1 Hz, 1H, ArCH_2Ar), 3.36 (d, *J* = 13.2 Hz, 1H, ArCH_2Ar), 3.85 (partially overlapping, d, *J* = 13.2 Hz, 1H, ArCH_2Ar), 3.87 (s, 2H, OCH_2Ar),

3.95 (d, *J* = 13.2 Hz, 1H, ArC*H*$_2$Ar), 4.54 (d, *J* = 14.1 Hz, 2H, ArC*H*$_2$Ar), 4.58 (d, *J* = 11.4 Hz, 1H, ArC*H*$_2$Ar), 4.77 (d, *J* = 14.1 Hz, 1H, Ar*CH*$_2$Ar), 4.80 (d, *J* = 11.4 Hz, 1H, ArC*H*$_2$Ar), 4.88 (b, 1H, O*H*), 5.05 (b, 1H, O*H*), 7.12 (b, 2H, Ar*H*), 7.15 (d, *J* = 2.4 Hz, 1H, ArH), 7.18 (b, 1H, Ar*H*), 7.21 (d, *J* = 2.4 Hz, 1H, Ar*H*), 7.24 (b, 1H, Ar*H*), 7.26 (b, 2H, Ar*H*), 7.28 (b, 2H, Ar*H*), 7.31 (d, *J* = 2.4 Hz, 1H, Ar*H*), 7.36 (b, 2H, Ar*H*), 7.51 (d, *J* = 6.9 Hz, 2H, Ar*H*). $^{13}C\{^1H\}$ NMR (C_6D_6): δ 153.5, 152.3, 150.1, 149.5, 149.4, 146.4, 144.2, 144.1, 143.4, 143.0, 137.9, 133.6, 132.3, 132.1 (two signals overlapping), 131.9, 131.8, 129.1, 128.8 (three signals overlapping), 128.0 (two signals overlapping) 127.6, 127.3, 127.2, 127.1, 126.3, 126.2, 126.0, 125.8, 125.7, 125.5, 125.3 (aromatic carbons), 75.5 (O*C*H$_2$Ar), 36.5, 36.1 (*C*(CH$_3$)$_3$), 34.8 (Ar*C*H$_2$Ar), 34.1, 34.0, 33.96 (*C*(CH$_3$)$_3$), 33.9, 33.8 (Ar*C*H$_2$Ar), 31.63, 31.61, 31.5, 31.4, 31.3 (C(*C*H$_3$)$_3$), 29.7, 28.8 (Ar*C*H$_2$Ar), -3.55, -9.79 (Si*C*H$_3$). IR (KBr, cm^{-1}): 3535bs (OH), 3032m, 2960vs, 2867vs, 2750w, 2716w, 1763w, 1601m, 1513m, 1478vs, 1392m, 1372m, 1363s, 1310s, 1290vs, 1257vs, 1201vs, 1122s, 1107m, 987m, 943m, 902vs, 879s, 822s, 787m. UV/Vis λ_{max}/nm (C_6H_6) (ε/dm^{3}mol^{-1}cm^{-1}): 284 (2.36 x 10^4). Anal. Calcd for $C_{64}H_{80}O_5Si$: C 80.29, H 8.42. Found: C 79.90, H 8.77.

5.5.3 General synthesis of silylated bismuth and antimony complexes of the type **[M{^{t}BuC5(SiRR')}]** (**5.7-5.19**).

A solution of M(O^{t}Bu)$_3$ (M = Bi, Sb) or Sb(NMe$_2$)$_3$ (0.126 mmol) in 4 mL of toluene was added dropwise to a colorless solution of the **^{t}BuC5(SiRR')(H)$_3$** ligand (0.125 mmol) in 10 mL of toluene. The resulting yellow (Bi) or colorless (Sb) solution was allowed to stir for 24 h at room temperature. The solvent was vacuum removed to yield the crude products as white (antimony) or yellow (bismuth) solids. The crude product was dissolved in 2 mL of pentane and centrifuged to remove the small amount of insoluble material. To the resulting solution 0.5 mL

of THF (or dimethoxyethane) were added and then placed in the freezer at -35 ^{o}C for four days to yield pure products as crystalline powders.

[Bi{^{t}**BuC5(SiMe$_2$)**}] (**5.7**): Single crystals of **5.7** (poor quality) were obtained from a mixture of pentane/DMSO (2:0.3 mL) at room temperature. Yield 83% (0.104 mmol, 0.111 g). Mp: 258-260 ^{o}C. ^{1}H NMR (C_6D_6): δ 0.13 (s, 3H, SiC*H*$_3$), 0.92 (s, 3H, SiC*H*$_3$), 1.03 (s, 18H, C(C*H*$_3$)$_3$), 1.20 (s, 9H, C(C*H*$_3$)$_3$), 1.35 (s, 18H, C(C*H*$_3$)$_3$), 3.42 (d, *J* = 13.8 Hz, 2H, ArC*H*$_2$Ar), 3.47 (d, *J* = 15.0 Hz, 1H, ArC*H*$_2$Ar), 4.11 (d, *J* = 15.3 Hz, 2H, ArC*H*$_2$Ar), 4.24 (d, *J* = 15.3 Hz, 2H, ArC*H*$_2$Ar), 4.40 (d, *J* = 15.0 Hz, 1H, Ar*CH*$_2$Ar), 5.12 (d, *J* =13.8 Hz, 2H, ArC*H*$_2$Ar), 7.04 (d, *J* = 2.1 Hz, 2H, Ar*H*), 7.28 (s, 2H, Ar*H*), 7.37 (d, J = 2.1 Hz, 2H, Ar*H*), 7.39 (s, 4H, Ar*H*). ^{13}C{^{1}H} NMR (C_6D_6): δ 152.7, 152.3, 148.6, 146.7, 144.6, 135.9, 135.4, 135.2, 134.3, 131.3, 129.2, 126.6, 125.7, 125.6, 125.2, 123.4 (aromatic carbons), 36.4, 35.9 (*C*(CH$_3$)$_3$), 34.1 (Ar*C*H$_2$Ar), 33.7 (*C*(CH$_3$)$_3$), 33.5 (Ar*C*H$_2$Ar), 32.0 (two peaks overlapping), 31.3 (C(*C*H$_3$)$_3$), 30.1 (Ar*C*H$_2$Ar), 1.0, -1.5 (Si*C*H$_3$). IR (KBr, cm^{-1}): 3042m, 2970vs, 2922vs, 2870vs, 1606m, 1481vs, 1397s, 1296vs, 1256vs, 1196vs, 1123s, 1053w, 1029w, 989w, 946s, 930m, 894m, 873s, 825m, 753w. UV/Vis λ_{max}/nm (C_6H_6) (ε/dm^{3}mol^{-1}cm^{-1}): 283 (1.72 x 10^4). Anal. Calcd for $C_{57}H_{71}O_5BiSi\cdot 1.5C_2H_6SO$: C 60.54, H 6.77. Found: C 60.84, H 6.65.

[Sb{^{t}**BuC5(SiMe$_2$)**}] (**5.8**): Single crystals of **5.8** were obtained from a mixture of pentane/DME (2:0.3 mL) at -35 ^{o}C. Yield 87% (0.109 mmol, 0.107 g). Mp: 344-346 ^{o}C. ^{1}H NMR (C_6D_6): δ 0.20 (s, 3H, SiC*H*$_3$), 0.88 (s, 3H, SiC*H*$_3$), 1.06 (s, 18H, C(C*H*$_3$)$_3$), 1.18 (s, 9H, C(C*H*$_3$)$_3$), 1.32 (s, 18H, C(C*H*$_3$)$_3$), 3.40 (d, *J* = 13.8 Hz, 2H, ArC*H*$_2$Ar), 3.51 (d, *J* = 15.0 Hz, 1H, ArC*H*$_2$Ar), 3.86 (d, *J* = 15.0 Hz, 2H, ArC*H*$_2$Ar), 4.00 (d, *J* = 15.0 Hz, 2H, ArC*H*$_2$Ar), 4.49 (d, *J* = 15.0 Hz, 1H, Ar*CH*$_2$Ar), 4.93 (d, *J* =13.8 Hz, 2H, ArC*H*$_2$Ar), 7.06 (d, *J* = 2.4 Hz, 2H, Ar*H*), 7.26 (d, *J* = 2.4 Hz, 2H, Ar*H*), 7.28-7.30 (m, 6H, Ar*H*). ^{13}C{^{1}H} NMR (C_6D_6): δ 152.2, 151.1,

148.7, 146.2, 144.6, 144.3, 134.4, 134.2, 133.6, 131.3, 131.2, 126.6, 126.4, 126.1, 125.7, 124.4 (aromatic carbons), 36.8, 36.6 ($C(CH_3)_3$), 34.1 ($ArCH_2Ar$), 33.9 ($C(CH_3)_3$), 33.9, 31.8 ($ArCH_2Ar$), 31.6, 31.5, 31.4 ($C(CH_3)_3$), 0.9, -1.3 ($SiCH_3$). IR (KBr, cm^{-1}): 3054w, 2960vs, 2866vs, 1598w, 1477vs, 1422w, 1392m, 1362s, 1291s, 1239s, 1187vs, 1122s, 1052w, 904m, 873m, 801w, 736m. UV/Vis λ_{max}/nm (C_6H_6) (ε/$dm^3mol^{-1}cm^{-1}$): 283 (5.57 x 10^3). Anal. Calcd for $C_{57}H_{71}O_5SbSi \cdot 0.5C_4H_{10}O_2$: C 68.73, H 7.43. Found: C 68.87, H 7.74.

[Bi{**^{t}BuC5(SiMePh)**}] (**5.9**): Single crystals of **5.9** were obtained from a mixture of pentane/DMSO (2:0.3 mL) at room temperature. Yield 81% (0.101 mmol, 0.115 g). Mp: 215-217 ^oC. ^1H NMR (C_6D_6): δ 0.97 (s, 18H, $C(CH_3)_3$), 1.13 (s, 3H, $SiCH_3$), 1.21 (s, 9H, $C(CH_3)_3$), 1.38 (s, 18H, $C(CH_3)_3$), 3.32 (d, *J* = 15.0 Hz, 1H, $ArCH_2Ar$), 3.47 (d, *J* = 13.8 Hz, 2H, $ArCH_2Ar$), 4.13 (d, *J* = 15.3 Hz, 2H, $ArCH_2Ar$), 4.27 (d, *J* = 15.3 Hz, 2H, $ArCH_2Ar$), 4.50 (d, *J* = 15.0 Hz, 1H, $ArCH_2Ar$), 5.25 (d, *J* = 13.8 Hz, 2H, $ArCH_2Ar$), 6.87 (d, *J* = 2.4 Hz, 2H, Ar*H*), 7.02-7.04 (m, 3H, Ar*H*), 7.31 (s, 2H, Ar*H*), 7.32 (d, *J* = 2.4 Hz, 2H, Ar*H*), 7.40 (d, *J* = 2.4 Hz, 2H, Ar*H*), 7.42 (d, *J* = 2.4 Hz, 2H, Ar*H*), 7.57 (d, *J* = 2.4 Hz, 1H, Ar*H*), 7.60 (d, *J* = 2.4 Hz, 1H, Ar*H*). $^{13}C\{^1H\}$ NMR (C_6D_6): δ 152.6, 152.4, 148.6, 146.7, 144.7, 144.6, 136.0, 135.4, 134.9, 134.2, 133.5, 133.4, 131.4, 129.2, 128.4, 126.3, 125.6, 125.5, 125.3, 123.4 (aromatic carbons), 36.4, 36.0 ($C(CH_3)_3$), 34.1, 33.8 ($ArCH_2Ar$), 33.5 ($C(CH_3)_3$), 32.0, 31.9 ($C(CH_3)_3$), 31.6 ($ArCH_2Ar$), 31.2 ($C(CH_3)_3$), 1.6 ($SiCH_3$). IR (KBr, cm^{-1}): 3049w, 3109w, 2961vs, 2867vs, 2717w, 1759w, 1591m, 1504m, 1474vs, 1429s, 1412s, 1393s, 1362vs, 1299s, 1250s, 1196vs, 1121vs, 1028w, 990w, 949s, 924vs, 894vs, 877vs, 817vs, 808s. UV/Vis λ_{max}/nm (C_6H_6) (ε/$dm^3mol^{-1}cm^{-1}$): 279 (3.71 x 10^4), 347 (1.46 x 10^3). Anal. Calcd for $C_{62}H_{73}O_5BiSi \cdot C_4H_{10}O_2$: C 64.69, H 6.83. Found: C 64.97, H 7.10.

[Sb{^{t}**BuC5(SiMePh)**}] (**5.10**): Yield 77% (0.0964 mmol, 0.101 g). Mp: 367-369 ^{o}C. ^{1}H NMR (C_6D_6): δ 1.01 (s, 18H, C(C*H*$_3$)$_3$), 1.04 (s, 3H, SiC*H*$_3$), 1.17 (s, 9H, C(C*H*$_3$)$_3$), 1.35 (s, 18H, C(C*H*$_3$)$_3$), 3.32 (d, *J* = 14.7 Hz, 1H, ArC*H*$_2$Ar), 3.46 (d, *J* = 14.4 Hz, 2H, ArC*H*$_2$Ar), 3.85 (d, *J* = 15.0 Hz, 2H, ArC*H*$_2$Ar), 4.11 (d, *J* = 15.0 Hz, 2H, ArC*H*$_2$Ar), 4.59 (d, *J* = 14.7 Hz, 1H, Ar*CH*$_2$Ar), 4.99 (d, *J* = 14.4 Hz, 2H, ArC*H*$_2$Ar), 6.90 (d, *J* = 2.4 Hz, 2H, Ar*H*), 7.06-7.08 (m, 3H, Ar*H*), 7.15 (s, 2H, Ar*H*), 7.20 (s, 2H, Ar*H*), 7.29 (d, *J* = 2.4 Hz, 2H, Ar*H*), 7.31 (d, *J* = 2.4 Hz, 2H, Ar*H*), 7.67 (d, *J* = 2.1 Hz, 1H, Ar*H*), 7.69 (d, *J* = 2.1 Hz, 1H, Ar*H*). ^{13}C{^{1}H} NMR (C_6D_6): δ 151.5, 151.4, 148.5, 146.1, 144.6, 144.5, 134.3, 134.1, 134.0, 133.5, 133.2, 131.5, 131.3, 130.7, 129.2, 128.4, 126.7, 125.5, 125.4, 124.5 (aromatic carbons), 36.9, 36.4 (*C*(CH$_3$)$_3$), 34.1 (Ar*C*H$_2$Ar), 34.0 (*C*(CH$_3$)$_3$), 33.9, 31.9 (Ar*C*H$_2$Ar), 31.7, 31.5, 31.3 (C(*C*H$_3$)$_3$), 1.2 (Si*C*H$_3$). IR (KBr, cm^{-1}): 3051w, 2961vs, 2868vs, 1775w, 1604w, 1474vs, 1392m, 1362s, 1293s, 1243s, 1198vs, 1115m, 1050w, 910m, 874m, 820s, 796m. UV/Vis λ_{max}/nm (C_6H_6) (ε/dm^{3}mol^{-1}cm^{-1}): 289 (2.84 x 10^4). Anal. Calcd for $C_{62}H_{73}O_5SbSi\cdot 2C_4H_8O$: C 70.52, H 7.52. Found: C 70.23, H 7.25.

[Bi{^{t}**BuC5(SiPh$_2$)**}] (**5.11**): Yield 92% (0.115 mmol, 0.138 g). Mp: 245-246 ^{o}C. ^{1}H NMR (C_6D_6): δ 1.02 (s, 18H, C(C*H*$_3$)$_3$), 1.19 (s, 9H, C(C*H*$_3$)$_3$), 1.36 (s, 18H, C(C*H*$_3$)$_3$), 3.38 (d, *J* = 14.7 Hz, 2H, ArC*H*$_2$Ar), 3.40 (d, *J* = 15.0 Hz, 1H, ArC*H*$_2$Ar), 4.10 (d, *J* = 15.3 Hz, 2H, ArC*H*$_2$Ar), 4.44 (d, *J* = 15.3 Hz, 2H, ArC*H*$_2$Ar), 4.74 (d, *J* = 15.0 Hz, 1H, Ar*CH*$_2$Ar), 5.30 (d, *J* = 14.7 Hz, 2H, ArC*H*$_2$Ar), 6.96 (d, *J* = 2.4 Hz, 2H, Ar*H*), 6.99-7.01 (m, 3H, Ar*H*), 7.05-7.06 (m, 3H, Ar*H*), 7.15 (s, 2H, Ar*H*), 7.27 (d, *J* = 2.4 Hz, 2H, Ar*H*), 7.36 (d, *J* = 2.4 Hz, 2H, Ar*H*), 7.44 (s, 2H, Ar*H*), 7.80 (dd, *J* = 2.4 Hz, *J* = 6.9 Hz, 2H, Ar*H*), 8.23 (dd, *J* = 2.4 Hz, *J* = 6.9 Hz, 2H, Ar*H*). ^{13}C{^{1}H} NMR (C_6D_6): δ 154.1, 150.6, 149.1, 146.2, 145.2, 144.5, 136.0, 135.7, 135.4, 134.9, 134.4, 133.2, 132.3, 132.0, 131.3, 131.2, 129.7, 128.42, 128.40, 125.8, 125.7, 125.6, 125.3, 123.4

(aromatic carbons), 36.5, 36.1 ($C(CH_3)_3$), 34.1, 33.7 (ArCH_2Ar), 33.6 ($C(CH_3)_3$), 32.0, 31.9 ($C(CH_3)_3$), 31.8 (ArCH_2Ar), 31.3 ($C(CH_3)_3$). IR (KBr, cm^{-1}): 3049m, 2959vs, 2906s, 2867s, 1592m, 1505w, 1474vs, 1429m, 1413m, 1392m, 1362m, 1300m, 1250m, 1198vs, 1076w, 1045w, 1030w, 996w, 952m, 952m, 925s, 896m, 876m, 853m, 823s, 807w, 787m, 764w. UV/Vis λ_{max}/nm (C_6H_6) ($\varepsilon/dm^3mol^{-1}cm^{-1}$): 279 (1.42 x 10^4), 356 (7.70 x 10^3). Anal. Calcd for $C_{67}H_{75}O_5BiSi \cdot C_4H_{10}O_2$: C 66.23, H 6.65. Found: C 65.96, H 6.73.

[Sb{**^{t}BuC5(SiPh$_2$)**}] (**5.12**): Single crystals of **5.12** can be obtained from a mixture of pentane/DMSO (2:0.3 mL) at room temperature. Yield 80% (0.100 mmol, 0.111 g). Mp: 105-106 ^oC. ^1H NMR (C_6D_6): δ 1.05 (s, 18H, C(C*H*$_3$)$_3$), 1.13 (s, 9H, C(C*H*$_3$)$_3$), 1.32 (s, 18H, C(C*H*$_3$)$_3$), 3.33 (d, *J* = 14.4 Hz, 1H, ArC*H*$_2$Ar), 3.41 (d, *J* = 15.3 Hz, 2H, ArC*H*$_2$Ar), 3.75 (d, *J* = 15.0 Hz, 2H, ArC*H*$_2$Ar), 4.37 (d, *J* = 15.0 Hz, 2H, ArC*H*$_2$Ar), 4.84 (d, *J* = 14.4 Hz, 1H, Ar*CH*$_2$Ar), 5.07 (d, *J* = 15.3 Hz, 2H, ArC*H*$_2$Ar), 6.92 (d, *J* = 2.4 Hz, 4H, Ar*H*), 6.94 (b, 2H, Ar*H*) 7.11-7.13 (m, 4H, Ar*H*), 7.17 (s, 2H, Ar*H*), 7.27 (d, *J* = 2.4 Hz, 2H, Ar*H*), 7.30 (s, 2H, Ar*H*), 7.91 (dd, *J* = 2.4 Hz, *J* = 6.9 Hz, 2H, Ar*H*), 8.16 (dd, *J* = 2.4 Hz, *J* = 6.9 Hz, 2H, Ar*H*). $^{13}C\{^1H\}$ NMR (C_6D_6): δ 152.2, 149.9, 148.9, 145.8, 144.9, 144.5, 135.3, 134.3, 133.61, 133.59, 133.4, 133.2, 133.2, 131.4, 131.0, 130.9, 129.2, 128.5, 128.4, 127.2, 126.7, 125.2, 124.8, 124.5 (aromatic carbons), 36.9, 36.5 ($C(CH_3)_3$), 34.1, 33.9 (ArCH_2Ar), 33.9 ($C(CH_3)_3$), 32.5 (ArCH_2Ar), 31.6, 31.5, 31.4 ($C(CH_3)_3$). IR (KBr, cm^{-1}): 3049w, 2962vs, 2869vs, 1759w, 1592m, 1478vs, 1431s, 1393m, 1363vs, 1295vs, 1252vs, 1199vs, 1121vs, 1054w, 994w, 955m, 929s, 876m, 822m, 807w, 777m. UV/Vis λ_{max}/nm (C_6H_6) ($\varepsilon/dm^3mol^{-1}cm^{-1}$): 281 (2.17 x 10^4). Anal. Calcd for $C_{67}H_{75}O_5SbSi \cdot 0.25C_2H_6SO$: C 71.77, H 6.83. Found: C 71.73, H 7.05.

[Bi{**^{t}BuC5(Si^{i}Pr$_2$)**}] (**5.13**): Single crystals of **5.13** (poor quality) can be obtained from a mixture of pentane/DMSO (2:0.3 mL) at room temperature. Yield 81% (0.101 mmol, 0.114 g).

Mp: 260-262 °C. ^{1}H NMR (C_6D_6): δ 1.16 (s, 18H, C(CH_3)$_3$), 1.26 (s, 9H, C(CH_3)$_3$), 1.33 (d, *J* = 7.2 Hz, 6H, CH(CH_3)$_2$), 1.37 (s, 18H, C(CH_3)$_3$), 1.63 (d, *J* = 7.2 Hz, 6H, CH(CH_3)$_2$), 2.51 (broad septet, 1H), 2.72 (broad septet, 1H), 3.38 (d, *J* = 14.4 Hz, 2H, ArCH_2Ar), 3.51 (d, *J* = 14.7 Hz, 1H, ArCH_2Ar), 4.08 (d, *J* = 15.3 Hz, 2H, ArCH_2Ar), 4.23 (d, *J* = 15.3 Hz, 2H, ArCH_2Ar), 4.65 (d, *J* = 14.7 Hz, 1H, ArCH_2Ar), 5.00 (d, *J* = 14.4 Hz, 2H, ArCH_2Ar), 7.03 (d, *J* = 2.4 Hz, 2H, Ar*H*), 7.27 (s, 2H, Ar*H*), 7.29 (s, 2H, Ar*H*), 7.37 (s, 4H, Ar*H*). ^{13}C NMR not available due to fast decomposition in solution. IR (KBr, cm^{-1}): 3045w, 2961vs, 2910vs, 2868vs, 1759w, 1602w, 1504w, 1467vs, 1413m, 1392m, 1362s, 1299s, 1251s, 1199vs, 1123m, 1117m, 1071w, 1020m, 994w, 924s, 883s, 822m, 805w, 784w. UV/Vis λ_{max}/nm (C_6H_6) (ε/dm^{3}mol^{-1}cm^{-1}): 281 (1.66 x 10^4), 340 (4.40 x 10^3). Anal. Calcd for $C_{61}H_{79}O_5BiSi \cdot 1.5C_2H_6SO$: C 61.67, H 7.12. Found: C 61.65, H 7.18.

[Sb{^{t}**BuC5(Si^{i}Pr$_2$)**}] (**5.14**): Yield 52% (0.0651 mmol, 0.0678 g). Mp: 188-189 °C. ^{1}H NMR (C_6D_6): δ 1.07 (s, 18H, C(CH_3)$_3$), 1.13 (s, 9H, C(CH_3)$_3$), 1.135 (broad septet, 1H, C*H*(CH$_3$)$_2$), 1.14 (d, *J* = 11.7 Hz, 6H, CH(CH_3)$_2$), 1.34 (s, 18H, C(CH_3)$_3$), 1.44 (d, *J* = 11.7 Hz, 6H, CH(CH_3)$_2$), 2.42 (broad septet, 1H, C*H*(CH$_3$)$_2$), 3.39 (d, *J* = 14.4 Hz, 2H, ArCH_2Ar), 3.48 (d, *J* = 14.7 Hz, 1H, ArCH_2Ar), 3.84 (d, *J* = 15.3 Hz, 2H, ArCH_2Ar), 4.09 (d, *J* = 15.3 Hz, 2H, ArCH_2Ar), 4.58 (d, *J* = 14.7 Hz, 1H, ArCH_2Ar), 4.96 (d, *J* = 14.4 Hz, 2H, ArCH_2Ar), 7.04 (d, *J* = 2.4 Hz, 2H, Ar*H*), 7.13 (s, 2H, Ar*H*), 7.18 (s, 2H, Ar*H*), 7.27 (s, 4H, Ar*H*). ^{13}C NMR not available due to fast decomposition in solution. IR (KBr, cm^{-1}): 3048m, 2964vs, 2906vs, 2869vs, 1602w, 1585w, 1503m, 1475vs, 1413m, 1392s, 1363s, 1302s, 1248s, 1195vs, 1153s, 1056w, 1020m, 996w, 952m, 925s, 882s, 827s. UV/Vis λ_{max}/nm (C_6H_6) (ε/dm^{3}mol^{-1}cm^{-1}): 282 (1.44 x 10^4). Anal. Calcd for $C_{61}H_{79}O_5SiSb$: C 70.30, H 7.64. Found: C 70.56, H 7.44.

[Bi{^{t}**BuC5(SiMeVinyl)**}] (**5.15**): Single crystals of **5.15** were obtained from a mixture of pentane/THF (2:0.3 mL) at -35 ^{o}C. Yield 67% (0.0838 mmol, 0.0909 g). Mp: 236-237 ^{o}C. ^{1}H NMR (C_6D_6): δ 1.03 (s, 18H, C(C*H*$_3$)$_3$), 1.05 (s, 3H, SiC*H*$_3$), 1.21 (s, 9H, C(C*H*$_3$)$_3$), 1.35 (s, 18H, C(C*H*$_3$)$_3$), 3.42 (d, *J* = 13.5 Hz, 2H, ArC*H*$_2$Ar), 3.48 (d, *J* = 15.3 Hz, 1H, ArC*H*$_2$Ar), 4.12 (d, *J* = 15.3 Hz, 2H, ArC*H*$_2$Ar), 4.24 (d, *J* = 15.3 Hz, 2H, ArC*H*$_2$Ar), 4.57 (d, *J* = 15.3 Hz, 1H, Ar*CH*$_2$Ar), 5.14 (d, *J* = 13.5 Hz, 2H, ArC*H*$_2$Ar), 5.68-5.84 (m, 2H, CH=C*H*$_2$), 5.90-6.02 (m, 1H, C*H*=CH$_2$), 7.04 (d, *J* = 2.1 Hz, 2H, Ar*H*), 7.29 (s, 2H, Ar*H*), 7.37 (d, *J* = 2.1 Hz, 2H, Ar*H*), 7.40 (s, 4H, Ar*H*). ^{13}C{^{1}H} NMR (C_6D_6): δ 152.5, 148.7, 146.9, 144.7, 138.1, 137.9, 136.1, 135.5, 135.2, 134.5, 134.1, 132.3, 131.3, 126.8, 125.8 (aromatic carbons), 125.4 (*C*H$_2$=CH), 123.5 (aromatic carbons), 36.5, 36.2 (*C*(CH$_3$)$_3$), 36.1, 34.4, 34.3 (Ar*C*H$_2$Ar), 33.9 (CH=*C*H$_2$), 33.7 (*C*(CH$_3$)$_3$), 32.1 (two carbons overlapping), 31.4 (C(*C*H$_3$)$_3$), -1.0 (Si*C*H$_3$). IR (KBr, cm^{-1}): 3050w, 2961vs, 2906vs, 2868vs, 1596w, 1504w, 1475vs, 1413m, 1393m, 1362s, 1295s, 1251s, 1201vs, 1123m, 1006w, 928m, 903m, 879m, 819m, 809m, 744w. UV/Vis λ_{max}/nm (C_6H_6) (ε/dm^{3}mol^{-1}cm^{-1}): 280 (2.03 x 10^4), 332 (7.05 x 10^3). Anal. Calcd for $C_{58}H_{71}O_5BiSi \cdot C_4H_8O$: C 64.34, H 6.88. Found: C 64.19, H 7.17.

[Sb{^{t}**BuC5(SiMeVinyl)**}] (**5.16**): Single crystals of **5.16** were obtained from a mixture of pentane/THF (2:0.3 mL) at -35 ^{o}C. Yield 79% (0.0988 mmol, 0.0986 g). Mp: 180-181 ^{o}C. ^{1}H NMR (C_6D_6): δ 1.06 (s, 18H, C(C*H*$_3$)$_3$), 1.18 (s, 9H, C(C*H*$_3$)$_3$), 1.24 (s, 3H, SiC*H*$_3$), 1.32 (s, 18H, C(C*H*$_3$)$_3$), 3.40 (d, *J* = 14.1 Hz, 2H, ArC*H*$_2$Ar), 3.51 (d, *J* = 15.3 Hz, 1H, ArC*H*$_2$Ar), 3.86 (d, *J* = 15.3 Hz, 2H, ArC*H*$_2$Ar), 4.01 (d, *J* = 15.3 Hz, 2H, ArC*H*$_2$Ar), 4.66 (d, *J* = 15.3 Hz, 1H, Ar*CH*$_2$Ar), 4.95 (d, *J* = 14.1 Hz, 2H, ArC*H*$_2$Ar), 5.72-5.91 (m, 2H, CH=C*H*$_2$), 6.05 (dd, *J* = 4.5 Hz, *J* = 14.5 Hz, 1H, C*H*=CH$_2$), 7.05 (d, *J* = 2.1 Hz, 2H, Ar*H*), 7.19 (s, 2H, Ar*H*), 7.22 (d, *J* = 2.1 Hz, 2H, Ar*H*), 7.27 (b, 4H, Ar*H*). No ^{13}C NMR available due to fast decomposition of product in

solution. IR (KBr, cm^{-1}): 3050m, 2963vs, 2905vs, 2869s, 1759w, 1560w, 1478vs, 1414m, 1393m, 1363s, 1293s, 1257s, 1202vs, 1122s, 1056m, 1008m, 930s, 904s, 879s, 809s, 788m, 749m, 680m. UV/Vis λ_{max}/nm (C_6H_6) (ε/$dm^3mol^{-1}cm^{-1}$): 282 (1.56 x 10^4). Anal. Calcd for $C_{58}H_{71}O_5SiSb \cdot C_4H_{10}O_2$: C 68.43, H 7.50. Found: C 68.70, H 7.41.

[Bi(O^{t}Bu){^{t}**BuC5(Bn)(SiMe$_2$)**}] (**5.17**): Single crystals of **5.17** were obtained from a mixture of pentane/THF (2:0.3 mL) at -35 ^{o}C. Yield 85% (0.106 mmol, 0.131 g). Mp: 244-245 ^{o}C. ^{1}H NMR (C_6D_6): δ -1.19 (s, 3H, SiCH_3), -0.04 (s, 3H, SiCH_3), 1.20 (s, 9H, C(CH_3)$_3$), 1.24 (s, 9H, C(CH_3)$_3$), 1.27 (s, 9H, C(CH_3)$_3$), 1.30 (s, 9H, C(CH_3)$_3$), 1.48 (s, 9H, C(CH_3)$_3$), 1.90 (s, 9H, OC(CH_3)$_3$), 3.13 (d, *J* = 14.4 Hz, 1H, ArCH_2Ar), 3.46 (d, *J* = 15.3 Hz, 1H, ArCH_2Ar), 3.60 (d, *J* = 16.2 Hz, 1H, ArCH_2Ar), 3.87 (d, *J* = 13.2 Hz, 1H, ArCH_2Ar), 3.89 (d, *J* = 12.3 Hz, 1H, ArCH_2Ar), 4.22 (d, *J* = 15.3 Hz, 1H, ArCH_2Ar), 4.29 (d, *J* = 16.2 Hz, 1H, ArCH_2Ar), 4.41 (d, *J* = 13.2 Hz, 1H, ArCH_2Ar), 4.56 (d, *J* = 11.4 Hz, 1H, OCH_2Ar), 4.65 (d, *J* = 11.4 Hz, 1H, OCH_2Ar), 4.82 (d, *J* = 14.4 Hz, 1H, ArCH_2Ar), 5.44 (d, *J* = 12.3 Hz, 1H, ArCH_2Ar), 6.97 (d, *J* = 2.4 Hz, 1H, Ar*H*), 7.07 (d, *J* = 2.1 Hz, 1H, Ar*H*), 7.16-7.18 (m, 4H, Ar*H*), 7.24 (d, *J* = 2.4 Hz, 1H, Ar*H*), 7.37-7.39 (m, 3H, Ar*H*), 7.43 (d, *J* = 2.4 Hz, 1H, Ar*H*), 7.47-7.49 (m, 3H, Ar*H*), 7.64 (d, *J* = 2.1 Hz, 1H, Ar*H*). ^{13}C{^{1}H} NMR (C_6D_6): δ 155.1, 153.2, 151.9, 150.0, 149.5, 147.7, 144.8, 143.9, 143.5, 143.4, 137.8, 137.4, 136.6, 136.1, 134.8, 133.0, 131.8, 131.2, 129.7 (two signals overlapping), 128.7 (two signals overlapping), 128.6, 128.5, 128.4, 128.1, 127.4, 126.8, 126.5, 126.4, 126.1, 125.6, 124.6, 121.7 (aromatic carbons), 80.3 (O*C*(CH$_3$)$_3$), 74.2 (O*C*H$_2$Ar), 38.4, 36.8 (*C*(CH$_3$)$_3$), 35.5 (OC(*C*H$_3$)$_3$), 34.9 (*C*(CH$_3$)$_3$), 34.0, 33.9, 33.7 (Ar*C*H$_2$Ar), 31.84, 31.81, 31.7, 31.6, 31.5 (C(*C*H$_3$)$_3$), 30.6, 29.4 (*C*(CH$_3$)$_3$), 29.3, 28.2 (Ar*C*H$_2$Ar), -0.56, -0.98 (Si*C*H$_3$). IR (KBr, cm^{-1}): 3031m, 2963vs, 2868vs, 2737w, 2712w, 1757w, 1601w, 1513w, 1493s, 1476vs, 1417s, 1392s, 1362vs, 1293vs, 1258vs, 1201vs, 1122vs, 1106m, 1085m, 1018m, 1000w, 942s,

931s, 899vs, 879vs, 821vs, 790w, 742m, 728m, 694m, 675w. UV/Vis λ_{max}/nm (C_6H_6) (ε/$dm^3mol^{-1}cm^{-1}$): 284 (1.35 x 10^4). Anal. Calcd for $C_{68}H_{87}O_6BiSi$: C 66.00, H 7.09. Found: C 65.73, H 7.34.

[Sb(O^{t}Bu){**^{t}BuC5(Bn)(SiMe$_2$)**}] (**5.18**): Single crystals of **5.18** were obtained from a mixture of pentane/DME (2:0.3 mL) at -35 ^{o}C.Yield 87% (0.109 mmol, 0.125 g). Mp: 186-188 ^{o}C. ^{1}H NMR (C_6D_6): δ -1.20 (s, 3H, SiC*H*$_3$), -0.03 (s, 3H, SiC*H*$_3$), 1.18 (s, 9H, C(C*H*$_3$)$_3$), 1.20 (s, 9H, C(C*H*$_3$)$_3$), 1.26 (s, 9H, C(C*H*$_3$)$_3$), 1.31 (s, 9H, C(C*H*$_3$)$_3$), 1.47 (s, 9H, C(C*H*$_3$)$_3$), 1.82 (s, 9H, OC(C*H*$_3$)$_3$), 3.19 (d, *J* = 14.1 Hz, 1H, ArC*H*$_2$Ar), 3.29 (d, *J* = 16.2 Hz, 1H, ArC*H*$_2$Ar), 3.49 (d, *J* = 13.2 Hz, 2H, ArC*H*$_2$Ar), 3.91 (d, *J* = 13.5 Hz, 1H, ArC*H*$_2$Ar), 4.16 (d, *J* = 16.2 Hz, 1H, Ar*CH*$_2$Ar), 4.25 (d, *J* = 13.2 Hz, 2H, ArC*H*$_2$Ar), 4.63 (s, 2H, OC*H*$_2$Ar), 4.90 (d, *J* = 14.1 Hz, 1H, ArC*H*$_2$Ar), 5.08 (d, *J* = 13.5 Hz, 1H, ArC*H*$_2$Ar), 6.88 (d, *J* = 2.1 Hz, 1H, Ar*H*), 6.99 (d, *J* = 2.4 Hz, 1H, Ar*H*), 7.13 (d, *J* = 2.4 Hz, 2H, Ar*H*), 7.19 (b, 3H, Ar*H*), 7.25 (d, *J* = 2.4 Hz, 1H, Ar*H*), 7.33 (d, *J* = 2.4 Hz, 1H, Ar*H*), 7.36 (d, *J* = 2.1 Hz, 1H, Ar*H*), 7.40 (b, 1H, Ar*H*), 7.42-7.44 (two doublets overlapping, 2H, Ar*H*), 7.54 (d, *J* = 2.4 Hz, 1H, Ar*H*), 7.62 (d, *J* = 2.1 Hz, 1H, Ar*H*). ^{13}C{^{1}H} NMR (C_6D_6): δ 155.1, 151.5, 150.0, 149.9, 149.7, 147.4, 144.4, 143.8, 143.7, 143.6, 138.0, 136.0, 135.7, 134.9, 133.6, 132.2, 131.1, 130.8, 129.9, 129.7, 129.2, 128.7, 128.6, 128.4, 128.0, 127.9, 127.8, 127.4, 127.0, 126.4, 126.0, 125.9, 124.8, 122.1 (aromatic carbons), 80.9 (O*C*(CH$_3$)$_3$), 74.4 (O*C*H$_2$Ar), 38.7, 36.8, 34.7 (*C*(CH$_3$)$_3$), 34.1, 34.0, 33.9, 33.8 (Ar*C*H$_2$Ar), 33.7 (OC(*C*H$_3$)$_3$), 33.4, 31.9 (*C*(CH$_3$)$_3$), 31.8, 31.63, 31.62, 31.5, 31.4 (C(*C*H$_3$)$_3$), 28.0 (Ar*C*H$_2$Ar), -0.57, -0.81 (Si*C*H$_3$). IR (KBr, cm^{-1}): 3030m, 2963vs, 2910vs, 2867vs, 1755w, 1602w, 1478vs, 1416m, 1392m, 1363vs, 1292s, 1260vs, 1200vs, 1121s, 1108m, 1055w, 1021w, 994s, 934s, 905s, 879s, 822s, 810m, 790m, 747m, 729m. UV/Vis λ_{max}/nm (C_6H_6) (ε/$dm^3mol^{-1}cm^{-1}$): 272 (1.56 x 10^4), 283 (2.25 x10^4). Anal. Calcd for $C_{68}H_{87}O_6SiSb\cdot 1.5C_4H_{10}O_2$: C 69.14, H 8.00. Found: C 69.49, H 7.80.

[Sb(NMe$_2$){^{t}**BuC5(Bn)(SiMe$_2$)**}] (**5.19**): Single crystals of **5.19** were obtained from a mixture of pentane/THF (2:0.3 mL) at -35 ^{o}C. Yield 83% (0.104 mmol, 0.117 g). Mp: 175-176 ^{o}C. ^{1}H NMR (C_6D_6): δ -1.16 (s, 3H, SiC*H*$_3$), 0.02 (s, 3H, SiC*H*$_3$), 1.19 (s, 9H, C(C*H*$_3$)$_3$), 1.24 (s, 9H, C(C*H*$_3$)$_3$), 1.26 (s, 9H, C(C*H*$_3$)$_3$), 1.31 (s, 9H, C(C*H*$_3$)$_3$), 1.36 (s, 9H, C(C*H*$_3$)$_3$), 2.96 (s, 6H, N(C*H*$_3$)$_2$), 3.21 (d, *J* = 14.4 Hz, 1H, ArC*H*$_2$Ar), 3.45 (d, *J* = 13.8 Hz, 1H, ArC*H*$_2$Ar), 3.50 (d, *J* = 12.6 Hz, 1H, OC*H*$_2$Ar), 3.51 (d, *J* = 12.6 Hz, 1H, OC*H*$_2$Ar), 3.93 (d, *J* = 13.8 Hz, 1H, Ar*CH*$_2$Ar), 4.20-4.35 (three doublets overlapping, 3H, ArC*H*$_2$Ar), 4.64 (d, *J* = 16.8 Hz, 1H, ArC*H*$_2$Ar), 4.68 (d, *J* = 16.8 Hz, 1H, ArC*H*$_2$Ar), 4.92 (d, *J* = 14.4 Hz, 1H, C*H*$_2$Ar), 5.11 (d, *J* = 12.3 Hz, 1H, OC*H*$_2$Ar), 6.94 (d, *J* = 2.4 Hz, 1H, Ar*H*), 7.11-7.17 (m, 3H, Ar*H*), 7.20 (s, 1H, Ar*H*), 7.22 (b, 3H, Ar*H*), 7.37 (d, *J* = 2.4 Hz, 1H, Ar*H*), 7.40 (d, *J* = 2.4 Hz, 1H, Ar*H*), 7.42 (s, 1H, Ar*H*), 7.45 (b, 2H, Ar*H*), 7.46 (s, 1H, Ar*H*), 7.55 (d, *J* = 2.4 Hz, 1H, Ar*H*). ^{13}C{^{1}H} NMR (C_6D_6): δ 155.0, 152.6, 151.0, 150.2, 149.8, 146.6, 144.4, 143.7, 143.5, 143.1, 138.1, 135.8, 135.2, 134.6, 133.4, 131.5, 131.4, 130.6, 130.3, 129.9, 129.5, 129.2, 128.7, 128.5, 128.4, 128.3, 128.0, 127.0, 126.6, 126.5, 126.1, 126.0, 124.6, 122.1 (aromatic carbons), 74.4 (O*C*H$_2$Ph), 38.9 (*C*(CH$_3$)$_3$), 38.4 (N(*C*H$_3$)$_2$), 37.4, 37.0, 34.5 (*C*(CH$_3$)$_3$), 34.1, 34.0, 33.9 (Ar*C*H$_2$Ar), 33.9 (*C*(CH$_3$)$_3$), 32.9 (Ar*C*H$_2$Ar), 31.62 (two peaks overlapping), 31.59 (two peaks overlapping), 31.4 (C(*C*H$_3$)$_3$), 28.1 (Ar*C*H$_2$Ar), -0.41, -1.02 (Si*C*H$_3$). IR (KBr, cm^{-1}): 3031m, 2961vs, 2905vs, 2868s, 1767w, 1600w, 1479vs, 1416m, 1393m, 1362s, 1293s, 1259s, 1202vs, 1122s, 1019w, 945m, 904s, 879s, 823s, 729m. UV/Vis λ_{max}/nm (C_6H_6) (ε/dm^{3}mol^{-1}cm^{-1}): 283 (1.80 x 10^4). Anal. Calcd for $C_{66}H_{84}NO_5SbSi \cdot C_4H_8O$: C 70.45, H 7.77. Found: C 70.18, H 7.49.

5.5.4 General X-ray structure information

X-ray data for **5.3**, **5.4**, **5.5**, **5.9**, **5.12**, **5.15**, **5.16** and **5.17**-**5.19** were collected on a SMART Bruker 1000 CCD detector diffractometer at low temperature using Mo Kα radiation. The crystallographic data and some details of the data collection and refinement of the structures are given in Table 7.5. Absorption corrections in all cases were applied by SADABS.[101] All structures were solved by direct methods and subsequent difference Fourier syntheses and refined by full matrix least-squares methods against F^2 (SHELX 97).[102] Disorder for some *tert*-butyl groups was due to a 2-fold axis, and was modeled using partial occupancies (PART instruction).[102] The O(6) and S(1) atoms in a DMSO molecule of complex **5.9** presented disorder and were modeled using a 50/50 percent atom occupancy. Some other disordered molecules and solvents were refined using a combination of restraints on the distances while keeping the disordered parts similar (use of the SADI and SAME instructions).[102] All non-hydrogen atoms were refined with anisotropic displacement coefficients, except atoms of disordered fragments, which were refined with isotropic thermal parameters. The H atoms in structures were taken in calculated positions. In the crystal structures of complexes **5.18** and **5.19**, highly disordered molecules (6 DME molecules in **5.18** and 1 THF molecule in **5.19**) were treated with the program SQUEEZE.[103] Corrections of the X-ray data for **5.18** and **5.19** by SQUEEZE (309 and 42 electron cell, respectively), were close to the required values (300 and 40 electron cell, respectively). The programs ORTEP32[104] and POV-ray[105] were used to generate the X-ray structural diagrams pictured in this chapter.

Table 5.5. Crystallographic Data and Summary of Data Collection and Structure Refinement

	5.3	**5.6**·0.5C_6H_{14}	**5.8**·DME	**5.9**·3DMSO	**5.12**·DMSO·C_5H_{12}
Formula	$C_{67}H_{78}O_5Si$	$C_{67}H_{87}O_5Si$	$C_{61}H_{81}O_7SiSb$	$C_{68}H_{91}O_8S_3SiBi$	$C_{74}H_{93}O_6SSiSb$
Fw	991.38	1000.46	1076.14	1369.66	1260.38
cryst syst	Triclinic	Monoclinic	Orthorhombic	Triclinic	Triclinic
space group	*P*-1	$P2_1/c$	$Pna2_1$	*P*-1	*P*-1
T, K	213(2)	228(2)	218(2)	218(2)	228(2)
a, Å	10.980(3)	15.970(4)	27.843(5)	11.377(3)	13.675(3)
b, Å	17.101(5)	15.753(4)	15.306(3)	17.416(4)	13.858(2)
c, Å	18.085(5)	27.162(5)	13.221(2)	20.856(4)	18.553(3)
α, deg	100.073(6)	90	90	112.877(4)	88.196(3)
β, deg	107.479(5)	120.270(10)	90	92.901(4)	77.019(3)
γ, deg	101.844(5)	90	90	102.414(4)	86.717(4)
V, A^3	3066.5(15)	5902(2)	5634.3(18)	3676.8(15)	3419.8(11)
Z	2	4	4	2	2
$d_{calcd.}$ g·cm^{-3}	1.074	1.126	1.264	1.237	1.224
μ, mm^{-1}	0.084	0.088	0.561	2.546	0.501
Refl collected	13355	23868	22348	14957	14053
T_{min}/T_{max}	0.996	0.995	0.968	0.860	0.972
N_{measd}	8660	8460	7520	10473	9727
[R_{int}]	[0.0367]	[0.0848]	[0.1022]	[0.0823]	[0.0975]
R [I>2sigma(I)]	0.0528	0.1157	0.0574	0.0700	0.0506
R_w[I>2sigma(I)]	0.1371	0.2860	0.1198	0.1687	0.1300
GOF	0.979	1.074	0.910	0.958	1.020

	5.15·2THF	**5.16**·2THF	**5.17**·THF	**5.18**·DME	**5.19**·2.5THF
Formula	$C_{66}H_{87}O_7SiBi$	$C_{66}H_{87}O_7SiSb$	$C_{72}H_{95}O_7SiBi$	$C_{72}H_{97}O_8SiSb$	$C_{76}H_{104}NO_{7.5}SiSb$
Fw	1229.43	1142.20	1309.55	1240.38	1301.48
cryst syst	Triclinic	Triclinic	Monoclinic	Hexagonal	Triclinic
space group	*P*-1	*P*-1	C2/c	*P*-3	*P*-1
T, K	223(2)	223(2)	228(2)	223(2)	223(2)
a, Å	13.033(4)	13.0513(16)	30.143(9)	31.122(3)	16.080(3)
b, Å	15.050(5)	15.1142(19)	31.624(9)	31.222(3)	16.736(3)
c, Å	18.679(6)	18.546(2)	17.105(7)	14.5433(18)	17.447(3)
α, deg	66.401(5)	66.643(2)	90	90	99.445(3)
β, deg	75.309(6)	76.027(2)	93.469(7)	90	116.548(3)
γ, deg	67.587(5)	67.568(2)	90	120	108.152(3)
V, A^3	3081.7(17)	3086.9(6)	16275(9)	12199(2)	3728.4(12)
Z	2	2	8	6	2
$d_{calcd.}$ g·cm^{-3}	1.325	1.229	1.069	1.013	1.159
μ, mm^{-1}	2.930	0.516	2.223	0.392	0.434
Refl collected	15150	14195	32203	60352	17582
T_{min}/T_{max}	0.863	0.956	0.875	0.981	0.983
N_{measd}	8831	8860	11671	11707	10608
[R_{int}]	[0.0843]	[0.0625]	[0.1144]	[0.0672]	[0.0506]
R [I>2sigma(I)]	0.0474	0.0579	0.0657	0.0488	0.0426
R_w[I>2sigma(I]	0.1079	0.1383	0.1617	0.1311	0.1002
GOF	0.979	0.959	0.0902	0.969	0.903

5.6 Conclusions

We have synthesized and fully characterized a series of calix[5]arene bismuth(III) and antimony(III) complexes supported by silylated ligands. The use of calixanions as precursors for the preparation of monosilylated ligands was only successful when using the **^{t}BuC5(H)$_5$** ligand. For the **^{t}BuC5(Bn)(H)$_4$** ligand, the use of $Me_2Si(NMe_2)_2$ yielded the desired product. The free OH groups in ligands **5.1-5.6** are reactive, and the addition of $M(O^tBu)_3$ (M = Bi, Sb) or $Sb(NMe_2)_3$ readily yields the respective metallated complexes. All of the complexes are monomeric in the solid state with the calixarene ring in cone conformation for ligand **^{t}BuC5(SiPh$_2$)(H)$_3$** (**5.3**) and partial cone for ligand **^{t}BuC5(Bn)(SiMe$_2$)(H)$_2$** (**5.6**). All bismuth and antimony complexes display distorted 1,2-alternate conformations in the solid state despite the fact that complexes **5.17-5.19** contain a monobenzyl group in the lower rim. The *endo* coordination of the metal centers and the 1,2-alternate conformation of the calixarene rings allow metal-arene π interactions in most of the complexes. The monometallic complexes **5.7**-**5.19** have high solubility in most organic solvents making them interesting precursors for more extended structures.

CHAPTER 6

HETEROMETALLIC BISMUTH(III)/MOLYBDENUM(VI) AND ANTIMONY(III)/MOLYBDENUM(VI) CALIX[5]ARENE COMPLEXES

6.1 Introduction

The SOHIO process is the predominant methodology for the selective oxidation and ammoxidation of propene to produce acrolein and acrylonitrile, used on large scales on industry.[6,13] Commercial interest in replacing the substrate with propane has increased the need for the improvement of the bismuth molybdate catalyst.[8-12] Although the SOHIO process has been used for more than 4 decades, the mechanistic details of the ammoxidation and oxidation by the multicomponent $n MoO_3/Bi_2O_3$ catalyst remain controversial.[6,13] The proposal that Bi(μ-O)Mo linkages are the active oxo transfer sites in propene oxidation[209] has provided incentive for the preparation of soluble Bi/Mo model compounds, ideally with pure oxo environments around the metals. However, to date only a few Bi/Mo heterobimetallic complexes are available and none of them has fulfilled the requirements above. In this chapter we will describe the synthesis and characterization of the first examples of soluble M^{III}/Mo^{VI} (M = Bi, Sb) complexes with both surrounded by oxygen environments, utilizing the *p-tert*-butylcalix[5]arene [^{t}**BuC5(H)$_5$**] ligand as an oxygen-rich platform. This work also provides the first rational synthesis of metallocalixarene complexes containing both transition metals and main group metals.

Limberg et al. synthesized and structurally characterized a series of $Mo^{II/IV}/Bi^{III}$ heterobimetallic complexes bridged by alkoxide groups,[37,38,210] and complexes with covalent Mo^{VI}-O-$Bi^{III/V}$ linkages.[35,40] Most of their compounds have good solubility but the metal centers are stabilized by organic ligands such as cyclopentadienyl or allylic anions (Figure 6.1).

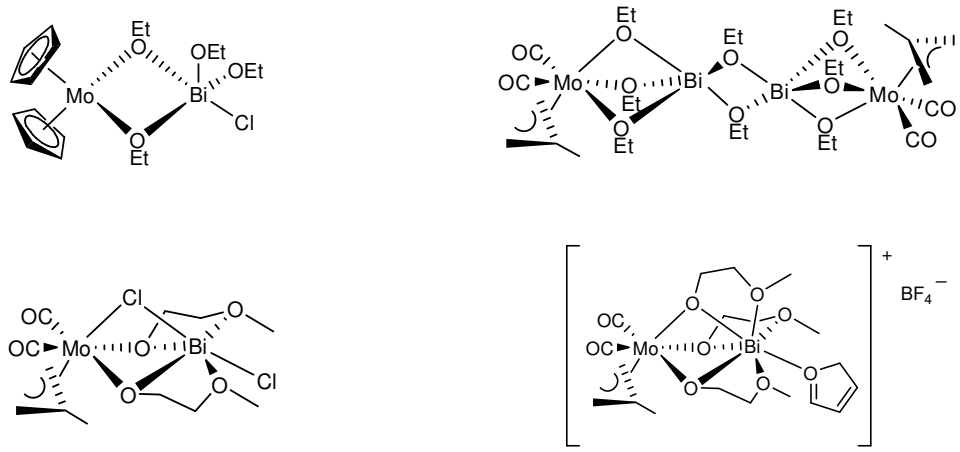

Figure 6.1. Alkoxide bridged [Mo](μ-OR)[Bi] complexes.

The heteropolyanions $[Bi^{III}\{Mo_5O_{13}(OMe)_4(NO)\}_2]^{3-}$,[36] $[Bi^{III}Mo_6O_{21}(O_2C(CH_2)_2NH_3\}_3]^{3-}$, $[Bi^{III}Mo_6O_{21}\{O_2C(CH_2)_3NH_3\}_3]^{3-}$and $[Bi^{III}Mo_6O_{21}\{_L\text{-}O_2CCH[(CH_2)_4NH_2]NH_3\}_3]^{3-}$[211] contain multiple Bi(μ-O)Mo linkages. These anions feature metallic cores in pure oxo environments (Figure 6.2), but their limited solubility in organic solvents and the unavailability of the bismuth atom (buried inside the oxo cage) make them unsuitable as SOHIO model compounds.

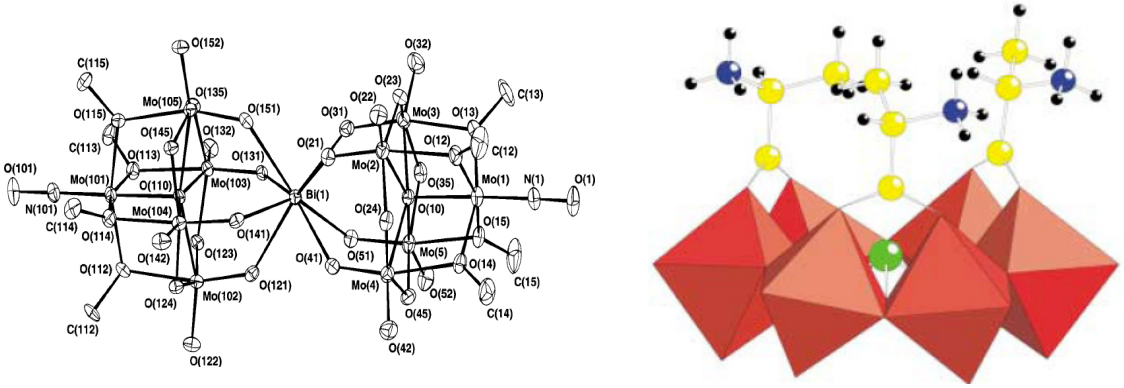

Figure 6.2. Oxygen rich Bismuth/Molybdenum heteropolyanions.

For several years now, we have sought to prepare soluble complexes featuring Bi^{III}(μ-O)Mo^{VI} interactions in pure oxo environments, in order to resemble the proposed SOHIO

catalyst active site. We have been interested in the use of calixarene ligands due to their potential to mimic features of heterogeneous catalyst surfaces and their ability to hold several metals simultaneously. In particular, calix[5]arene has proved to be excellent for the insertion of more than one metal in the lower rim.[159] In the present chapter we report the synthesis, structure and full characterization of the first examples of soluble M^{III}/Mo^{VI} (M = Bi, Sb) complexes with both metals surrounded by oxygen environments, utilizing the *p-tert*-butylcalix[5]arene [^{t}**BuC5(H)$_5$**] ligand as an oxygen-rich platform. This work also provides the first rational synthesis of metallocalixarene complexes containing Group15 and transition metals in the lower rim, aiming to model of the SOHIO catalyst.

6.2 Results and discussion

We have described in Chapter 3 the synthesis of monometallic [M{^{t}**BuC5(H)$_2$**}] (M = Bi, Sb) complexes,[159] prepared by the metathesis reaction of the M'$_3$·^{t}**BuC5(H)$_3$** precursors (M' = Li, Na, K) with MCl_3. The [M{^{t}**BuC5(H)$_2$**}] complexes contain two unreacted OH groups that permit the formation of bimetallic complexes of the type [M_2O\{^{t}**BuC5(H)**\}],[159] upon treatment with $M(O^tBu)_3$. These bimetallic complexes display M(μ-O)M interactions and pure oxo environments that are key features for our heterometallic model. With this successful background, we decided to treat the [Bi{^{t}**BuC5(H)$_2$**}] and [Sb{^{t}**BuC5(H)$_2$**}] complexes with molybdenum precursors in the hope of obtaining analogous complexes of the type [BiOMo{^{t}**BuC5(H)**}].

The synthesis of complexes [$Bi_2Mo_4O_{11}$\{^{t}**BuC5(H)**\}$_2$] **6.1** and [$Sb_2Mo_4O_{11}$\{^{t}**BuC5(H)**\}$_2$] **6.2** is depicted in equation 6.1. Our first attempt to introduce a molybdenum center in the calix[5]arene lower rim involved the treatment of the monometallic [M{^{t}**BuC5(H)$_2$**}] (M = Bi, Sb) precursors with one equivalent of $MoO_2(O^tBu)_2$ in THF or DME at high temperatures.

Unfortunately, under these reaction conditions, the resulting dark brown solutions showed complex mixtures of products by ^{1}H NMR spectroscopy. All our attempts to isolate a single compound failed due to fast decomposition of products to parent calixarene. However, when the ratio of $MoO_2(O^tBu)_2$ was increased to 1.5 equivalents, complexes $[Bi_2Mo_4O_{11}\{^t\mathbf{BuC5(H)}\}_2]$ **6.1** and $[Sb_2Mo_4O_{11}\{^t\mathbf{BuC5(H)}\}_2]$ **6.2** were readily obtained as red solids in 55 and 45% yields, respectively (equation 6.1).

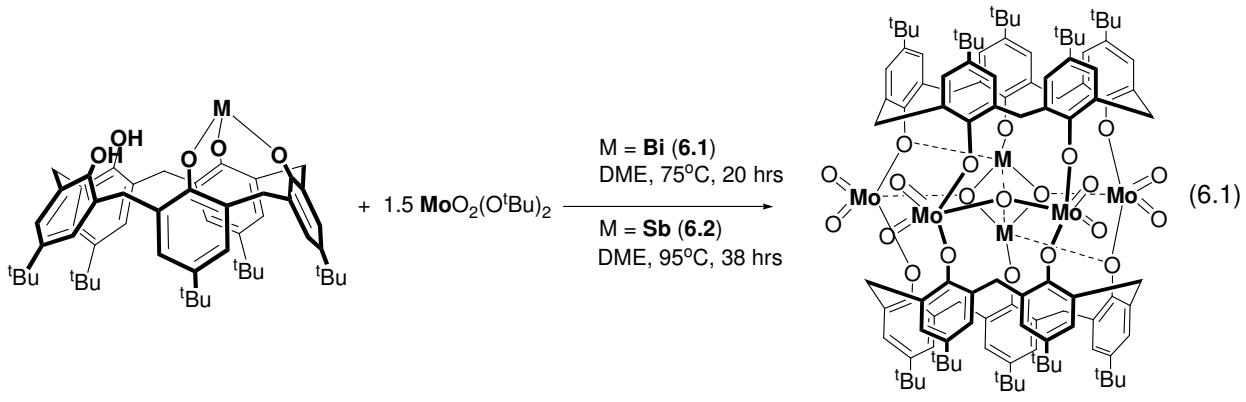

(6.1)

*Each calixarene ring contains an OH group (not located).

The high solubility of complexes **6.1** and **6.2** in $CHCl_3$, THF and DMSO and stability in the solid state (up to two months under inert conditions) facilitated their solution and solid state characterization. In solution the ^{1}H NMR patterns for **6.1** and **6.2** are characteristic of a C_s symmetry (Figure 6.3). There are three pairs of doublets for the methylene protons (germinal coupling due to nonequivalent methylene hydrogens), three singlets in a 1:2:2 ratio for the tert-butyl groups, and no OH groups were observed at room temperature.

The IR spectra of complexes **6.1** and **6.2** showed the intense two-band pattern characteristic of the stretching vibrations of the MoO_2^{2+} group between 822-870 cm^{-1}. There are several strong signals in the region of 3000-2800 cm^{-1} due to the *v*(C-H) of the *tert*-butyl of methylene groups. A broad band around 3400 cm^{-1} suggested the presence of calixarene OH

groups, consistent with our analogously prepared [$M_2O\{^t$**BuC5(H)**$\}$] complexes that also contained an unreacted OH group.[159]

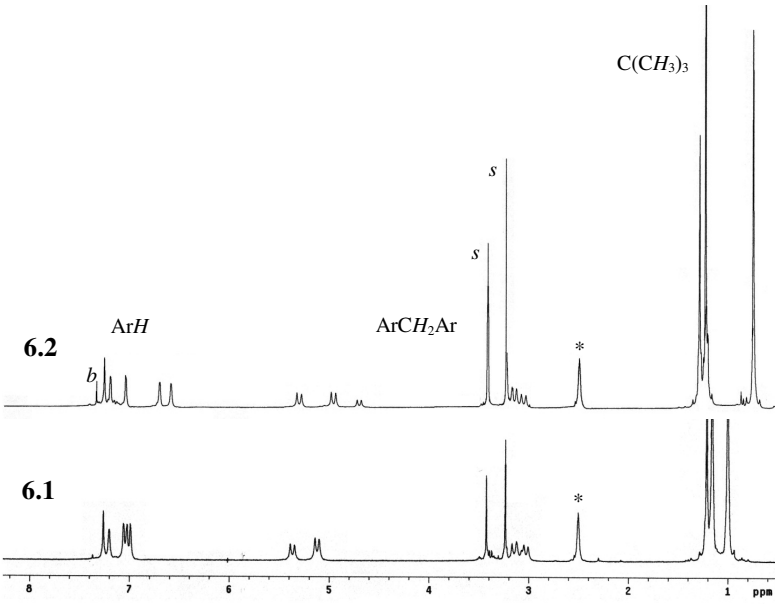

Figure 6.3 ^{1}H NMR spectrum of complexes **6.1** and **6.2** in *DMSO-d_6. Crystals obtained from DME (*s*). *b* = residual benzene.

We obtained single crystals of complex **6.1** from a concentrated Et_2O solution at room temperature and single crystals of **6.2** from an Et_2O solution at -35 ^oC (poor quality). The crystal structure of complex **6.1** is displayed in Figure 6.4 and selected bond distances and angles are presented in Table 6.1. Complex **6.1** crystallizes in the *P*-1 space group and consists of a dimeric heterometallic Bi/Mo (1:2 ratio) unit with the calixarene ligands adopting a distorted flattened-cone conformation(Figure 6.5b). Complex **6.1** represents the first example of a calix[5]arene containing one heavy Group 15 element and two transition metals in the lower rim and one of the very rare examples of rationally designed bimetallocalixarenes.[212] The calixarene ligands adopt a distorted flattened-cone conformation where one of the rings tilts and its *tert*-butyl group blocks the cavity (Figure 6.4a).

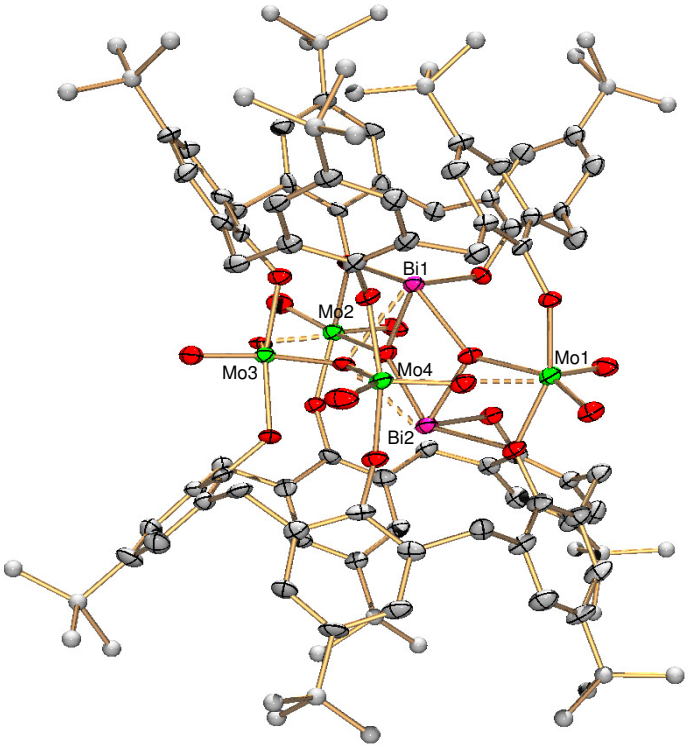

a)

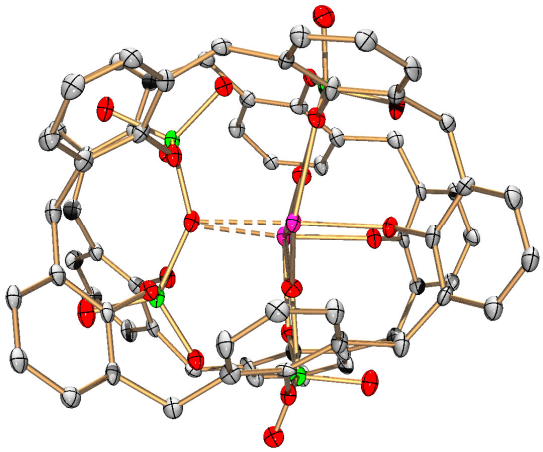

b)

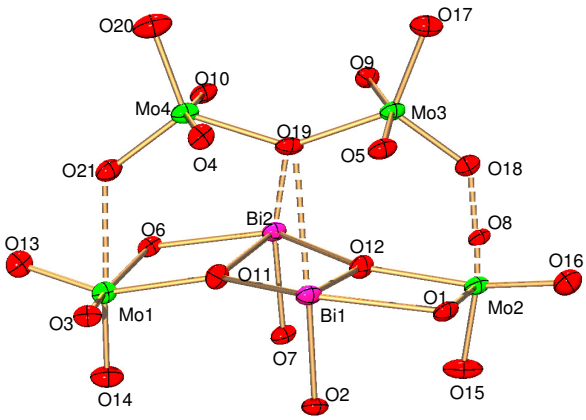

c)

Figure 6.4. X-ray structure of complex **6.1**: a) front view, b) top view, c) $Bi_2Mo_4O_{21}$ core. Ellipsoids shown at 40% probability. H atoms and ^{t}Bu groups in b) are not shown for clarity.

Table 6.1 Bond distances (Å) and angles (°) for complex **6.1**

Bi(1)-O(2)	2.158(5)	O(2)-Bi(1)-Bi(2)	90.69(13)	O(16)-Mo(2)-O(12)	153.4(2)
Bi(1)-O(12)	2.166(5)	O(11)-Bi(1)-O(1)	139.00(17)	O(8)-Mo(2)-O(12)	88.8(2)
Bi(1)-O(11)	2.189(5)	O(12)-Bi(1)-Bi(2)	39.19(12)	O(1)-Mo(2)-O(12)	72.30(18)
Bi(1)-O(1)	2.407(5)	O(11)-Bi(1)-Bi(2)	37.33(14)	O(15)-Mo(2)-O(18)	175.5(2)
Bi(1)-Bi(2)	3.4386(5)	O(1)-Bi(1)-Bi(2)	103.77(11)	O(16)-Mo(2)-O(18)	81.2(2)
Mo(1)-O(14)	1.691(5)	O(14)-Mo(1)-O(13)	105.4(3)	O(8)-Mo(2)-O(18)	80.19(18)
Mo(1)-O(13)	1.697(5)	O(14)-Mo(1)-O(3)	98.6(2)	O(1)-Mo(2)-O(18)	83.88(18)
Mo(1)-O(3)	1.925(5)	O(13)-Mo(1)-O(3)	99.8(2)	O(12)-Mo(2)-O(18)	76.21(18)
Mo(1)-O(6)	2.063(5)	O(14)-Mo(1)-O(6)	94.8(2)	O(17)-Mo(3)-O(18)	108.3(3)
Mo(1)-O(11)	2.140(5)	O(13)-Mo(1)-O(6)	91.6(2)	O(17)-Mo(3)-O(19)	127.8(3)
Mo(1)-O(21)	2.352(5)	O(3)-Mo(1)-O(6)	159.46(18)	O(18)-Mo(3)-O(19)	123.9(2)
O(1)-Mo(2)	2.045(5)	O(14)-Mo(1)-O(11)	91.7(2)	O(17)-Mo(3)-O(9)	93.8(2)
Bi(2)-O(7)	2.151(5)	O(13)-Mo(1)-O(11)	157.9(2)	O(18)-Mo(3)-O(9)	98.6(2)
Bi(2)-O(11)	2.155(5)	O(3)-Mo(1)-O(11)	91.26(19)	O(19)-Mo(3)-O(9)	81.8(2)
Bi(2)-O(12)	2.230(5)	O(6)-Mo(1)-O(11)	72.78(18)	O(17)-Mo(3)-O(5)	93.2(2)
Bi(2)-O(6)	2.417(5)	O(14)-Mo(1)-O(21)	167.5(2)	O(18)-Mo(3)-O(5)	95.2(2)
Mo(2)-O(15)	1.677(5)	O(13)-Mo(1)-O(21)	86.6(2)	O(19)-Mo(3)-O(5)	80.57(19)
Mo(2)-O(16)	1.719(5)	O(3)-Mo(1)-O(21)	82.48(17)	O(9)-Mo(3)-O(5)	161.7(2)
Mo(2)-O(8)	1.904(5)	O(6)-Mo(1)-O(21)	81.13(17)	O(20)-Mo(4)-O(21)	107.8(2)
Mo(2)-O(12)	2.109(5)	O(11)-Mo(1)-O(21)	75.85(18)	O(20)-Mo(4)-O(19)	128.7(2)
Mo(2)-O(18)	2.404(5)	Mo(2)-O(1)-Bi(1)	107.98(19)	O(21)-Mo(4)-O(19)	123.4(2)
Mo(3)-O(17)	1.677(5)	O(7)-Bi(2)-O(11)	84.15(18)	O(20)-Mo(4)-O(4)	93.3(2)
Mo(3)-O(18)	1.734(5)	O(7)-Bi(2)-O(12)	87.08(18)	O(21)-Mo(4)-O(4)	98.5(2)
Mo(3)-O(19)	1.960(5)	O(11)-Bi(2)-O(12)	74.98(18)	O(19)-Mo(4)-O(4)	81.92(19)
Mo(3)-O(9)	1.963(5)	O(7)-Bi(2)-O(6)	80.99(17)	O(20)-Mo(4)-O(10)	93.0(2)
Mo(3)-O(5)	1.972(5)	O(11)-Bi(2)-O(6)	65.83(16)	O(21)-Mo(4)-O(10)	96.4(2)
Mo(4)-O(20)	1.693(5)	O(12)-Bi(2)-O(6)	139.90(18)	O(19)-Mo(4)-O(10)	80.3(2)
Mo(4)-O(21)	1.730(5)	O(7)-Bi(2)-Bi(1)	90.76(13)	O(4)-Mo(4)-O(10)	161.2(2)
Mo(4)-O(19)	1.947(5)	O(11)-Bi(2)-Bi(1)	38.01(12)	Mo(1)-O(6)-Bi(2)	106.98(18)
Mo(4)-O(4)	1.958(5)	O(12)-Bi(2)-Bi(1)	37.87(13)	Mo(1)-O(11)-Bi(2)	114.2(2)
Mo(4)-O(10)	1.972(5)	O(6)-Bi(2)-Bi(1)	103.82(11)	Mo(1)-O(11)-Bi(1)	141.1(3)
Bi(1)-O(19)	2.852(6)	O(15)-Mo(2)-O(16)	103.2(3)	Bi(2)-O(11)-Bi(1)	104.7(2)
Bi(2)-O(19)	2.812(8)	O(15)-Mo(2)-O(8)	97.8(2)	Mo(2)-O(12)-Bi(1)	115.1(2)
O(2)-Bi(1)-O(12)	88.06(19)	O(16)-Mo(2)-O(8)	101.0(2)	Mo(2)-O(12)-Bi(2)	141.9(2)

The unexpected 1:2 Bi/Mo ratio observed in the core structure of **6.1** could explain why the reaction of [M{^{t}**BuC5(H)$_2$**}] and one equivalent of $MoO_2(O^tBu)_2$ was unsuccessful. Attempts to increase the yield of the products by using two or more equivalents of $MoO_2(O^tBu)_2$ failed, producing intractable mixtures in all cases.

The overall $Mo_4Bi_2O_{21}$ core in complex **6.1** (Figure 6.4c) contains two pentacoordinated bismuth(III) centers with primary bonds to one aryloxide [Bi(1)-O(2), 2.158(5) Å] and two bridging oxygens [Bi(1)-O(11) 2.189(5) and Bi(1)-O(12) 2.166(5) Å] and secondary bonds to one aryloxide and one μ_4-oxygen [Bi(1)-O(1) 2.407(5) and Bi(1)-O(19) 2.852(6) Å].[213] The Bi(1) and Bi(2) centers are covalently linked through O(11) and O(12) to form a central $Bi_2(\mu\text{-}O)_2$ four-membered ring similar to those found in bismuth calixarene complexes. All the Bi-OAr and Bi-Bi bond distances, and O-Bi-O and Bi-O-Bi angles, fall in the normal ranges for bismuth(III) calixarene complexes.[57,58,121,159]

There are two types of Mo^{VI} centers within the core structure of **6.1**. The Mo(1) and Mo(2) centers are hexacoordinated with distorted octahedral geometries. Each molybdenum is bonded to two aryloxides, two dioxo groups, one bridging oxygen, and one dioxo group of a vicinal Mo center. The apical positions are defined by the aryloxide groups with the Mo(1)-O(6) [2.063(5) Å] and Mo(2)-O(1) [2.045(5) Å] bond distances longer than the Mo(1)-O(3) [1.925(5) Å] and Mo(2)-O(8) [1.904(5) Å] distances due to their bridging interactions with the Bi(2) and Bi(1) atoms, respectively. The Mo(3) and Mo(4) centers, on the other hand, are coordinated to two aryloxides, two dioxo groups, and one bridging oxygen O(19) in a distorted trigonal bipyramidal geometry. The apical positions in Mo(3) and Mo(4) are occupied again by aryloxide groups with ArO-Mo-OAr angles around 160^o, close to the expected 180^o. The Mo(3) and Mo(4) atoms are covalently linked through O(19)[132] with bond distances of 1.960(5) and 1.947(5) Å, respectively.

Each calixarene ring in complex **6.1** contains an OH proton that could not be located on the crystal structure density map. Using bond valence sum calculations,[214,215] we found that the Mo-O and Mo=O bonds should have distances of approximately 1.907 and 1.605 Å, respectively. In complex **6.1,** we observed that the Mo(1)-O(3) [1.925(5) Å] and Mo(2)-O(8) [1.904(5) Å] distances are close to the calculated Mo-O values. However, the Mo(3)-O(5) [1.972(5) Å], Mo(3)-O(9) [1.963(5) Å], Mo(4)-O(10) [1.972(5) Å], and Mo(4)-O(4) [1.958(5) Å] distances are larger than the calculated Mo-O values. These bond distance elongations suggest that the two remaining hydrogen atoms are delocalized between the O(5)-Mo(3)-O(9) and the O(4)-Mo(4)-O(10) bonds.

The dioxo groups in all the Mo^{VI} centers are cis to each other, as usually observed in MoO_2^{2+} centers, and have bond distances comparable to those observed in Mo^{VI} calixarene complexes.[65] The Mo(3)=O(18) [1.734(5) Å] and Mo(4)=O(21) [1.730(5) Å] bond distances display slight elongations due to their bridging interactions with Mo(2) and Mo(1), respectively.

A key feature of complex **6.1** is the formation of several Bi(μ-O)Mo interactions as a result of the Lewis acidity of the bismuth atoms and the proximity of the metal centers provided by the calixarene template. Bi(1) is singly bridged to Mo(1) by O(11), doubly bridged to Mo(2) by O(1) and O(12) and bridged to Mo(3) and Mo(4) by O(19). Likewise, Bi(2) is oxo bridged to Mo(2) by O(12), doubly bridged to Mo(1) by O(6) and O(11) and bridged to Mo(3) and Mo(4) by O(19). In the Bi(1)Bi(2)Mo(1)Mo(2) ladder the Bi-OMo bond distances range from 2.155(5) to 2.417(5) Å, while Mo-OBi distances range from 2.045(5)-2.140(5) Å. All of these oxo bridging distances lie in the normal ranges found in alkoxide bridged Bi/Mo complexes.[37,38,210] and they are similar to Bi-OMo distances observed in the crystal structure of the heterogeneous $Bi_2Mo_2O_9$ catalyst.[216]

The four-coordinate O(19)[132] weakly bridges Bi(1) and Bi(2) with Mo(2) and Mo(4). The Bi-O bond distances of 2.812(8) and 2.852(6) Å are longer than the Bi···O=Mo interactions observed in the $[Bi\{Mo_5O_{13}(OMe)(NO)_2\}]^{3-}$anion [Figure 6.2, 2.42(1)-2.519(9) Å],[36] but noticeably shorter than the sum of the Van der Waals radii (3.67 Å).

We have pointed out that a trademark "ladder" motif appears in many bismuth oxo complexes.[6,57,121,159] In the core structure of **6.1**, the Bi(μ-O)Mo interactions between Bi(1), Bi(2), Mo(1) and Mo(2) build up a ladder system that contains a central $Bi_2(\mu\text{-}O)_2$ and two terminal $Bi(\mu\text{-}O)_2Mo$ rings. The three four-membered rings display individual planarity (torsion angles range from 1.71-10.47°) and they are coplanar with each other, similar to Uchiyama's bismuth-oxo ladder complex.[150] The ladder system resembles a fragment of the Graselli's proposed SOHIO active catalyst site, with alternate $Bi^{III}(\mu\text{-}O)Mo^{VI}$ arrangements, and the Mo^{VI} centers containing two terminal dioxo groups (Figure 6.5a).[5] Likewise, the ladder system contains $Bi(\mu\text{-}O)_2Bi$, and several $Mo(\mu\text{-}O)Bi(\mu\text{-}O)Mo$ moieties similar to those found in the crystal structure of $Bi_2Mo_2O_9$ (the best oxidation catalyst among bismuth molybdates) (Figure 6.5b).[216]

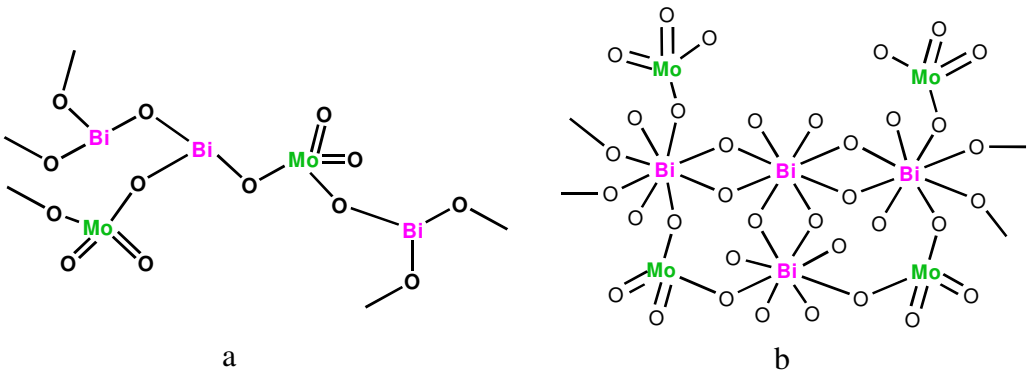

a b

Figure 6.5. Graselli SOHIO proposed active site (a) and fragment of the crystal structure of the $Bi_2Mo_2O_9$ catalyst (b).[5]

The Bi···Mo distances in the Bi(μ-O)$_2$Mo rings are close to 3.61 Å, and the Bi-O-Mo angles range from 106.98(18) to 115.1(2)^o. These angles are comparable to those observed in Limberg's Bi(μ-OR)$_2$Mo and Bi(μ-OR)$_3$Mo alkoxide bridged complexes [93.88(11)-115.2(3)^o].[37,38,210] No metal-arene π-interactions were observed.

6.3 Experimental section

6.3.1 General Information

All manipulations were carried out in a nitrogen filled glovebox. Complexes [Bi{^{t}**BuC5(H)$_2$**}],[159] [Sb{^{t}**BuC5(H)$_2$**}],[159] and MoO$_2$(O^{t}Bu)$_2$[217] were obtained by the literature procedures. Tetrahydrofuran was freshly distilled from Na/benzophenone; other anhydrous solvents were purchased from Aldrich and stored over molecular sieves under nitrogen before using. Dimethyl sulfoxide was dried over CaH_2. The melting points were taken in capillary tubes on a Mel-temp apparatus (Laboratory devices, Cambridge, MA) using a 500 ^{o}C thermometer. ^{1}H NMR and ^{13}C spectra were recorded on a Varian XL-300 spectrometer at 300 and 75 MHz, respectively. Analytical samples were dried under vacuum for at least 72 hrs. Microanalyses were performed by Atlantic Microlab, Inc, Norcross, GA. IR and UV/Vis spectra were obtained with an Infinity Gold^{TM} FTIR spectrometer and Agilent 8453 spectrophotometer, respectively. Filtrations used a medium sintered glass filter. X-ray diffraction of complex **6.1** was performed in a Bruker SMART 1000 CCD detector at 213(2) K using Mo Kα radiation.

6.3.2 Synthesis of compounds **6.1** and **6.2**

*Synthesis of complex [Bi$_2$Mo$_4$O$_{11}${^{t}**BuC5(H)**}$_2$]* (**6.1**)**:** A solution of MoO$_2$(O^{t}Bu)$_2$ (0.0103 g, 0.0376 mmol) in dimethoxyethane (DME) (3 mL) and a yellow suspension of [Bi{^{t}**BuC5(H)$_2$**}] (0.0254 g, 0.0250 mmol) in DME (5 mL) were placed together in a solvent bomb. The resulting dark brown suspension was placed in an isotemp bath at 75 ^{o}C and allowed

to heat for 20 hrs. Some red crystals were obtained on the bottom and side walls of the flask. The crystals were removed from the mixture by centrifugation (or filtration), washed with DME (2 mL) and dried under vacuum to yield 0.0030 g of $[Bi_2Mo_4O_{11}\{^t\mathbf{BuC5(H)}\}_2]$ (**6.1**). The remaining dark solution was centrifuged (or filtered) to remove the small amount of solid remaining, and then dried under vacuum. The dark brown solid was dissolved in diethyl ether (Et_2O) (3 mL) and centrifuged to remove any insoluble material. The final dark solution was allowed to stand for 14 hrs at rt yielding red single crystals. The supernatant was removed by pipette and the crystals were washed three times with 2 mL portions of Et_2O to yield 0.0103 g of pure $[Bi_2Mo_4O_{11}\{^t\mathbf{BuC5(H)}\}_2]$ (**6.1**). Total yield 55% (0.0133 g, 0.00513 mmol). m.p. 338-340 ^oC; ^1H NMR (300 MHz, DMSO-d_6, 25^{o}C, TMS): δ 1.00 (s, 18H, C(CH_3)$_3$), 1.16 (s, 18H, C(CH_3)$_3$), 1.21 (s, 9H, C(CH_3)$_3$), 3.03 (d, *J* = 12.9 Hz, 2H, ArCH_2Ar), 3.05 (d, *J* = 12.3 Hz, 1H, ArCH_2Ar), 3.15 (d, *J* = 12.9 Hz, 2H, ArCH_2Ar), 5.12 (two doublets overlapping, 3H, ArCH_2Ar), 5.37 (d, *J* = 12.9 Hz, 2H, ArCH_2Ar), 6.99 (s, 2H, Ar*H*), 7.03 (s, 2*H*, Ar*H*), 7.07 (s, 2H, Ar*H*), 7.20 (s, 2H, Ar*H*), 7.26 (s, 2H, Ar*H*), no OH peaks were observed at rt; ^{13}C NMR (75 MHz, DMSO-d_6, 25^{o}C, TMS): δ = 25.8, 29.9 (Ar*C*H$_2$Ar), 31.3, 32.2, 32.6 (C(*C*H$_3$)$_3$), 33.8 (ArCH$_2$Ar), 34.0, 34.1, 36.3 (*C*(CH$_3$)$_3$), 124.4, 124.5, 131.5, 132.9, 133.5, 134.2, 134.8, 135.0, 138.1, 140.3, 141.1, 142.5, 152.3, 154.7, 158.0, 162.6 ppm (aromatic carbons). IR (KBr): *v* = 3438w (OH), 2959vs, 2910m, 2870m, 1598w, 1574w, 1459vs, 1393w, 1362m, 1290m, 1250s, 1198vs, 1125s, 1079w, 938m, 906m, 870s, 824s, 802m, 771m, 664m; UV/Vis (DMSO) λ_{max} (ε) = 217 (5620), 279 (1200), 489 nm (813). Elemental analysis calcd (%) for $C_{110}H_{132}Bi_2Mo_4O_{21}$: C 50.97, H 5.13; Found C 51.18, H 5.36.

Synthesis of complex $[Sb_2Mo_4O_{11}\{^t\mathbf{BuC5(H)}\}_2]$ (**6.2**) : A solution of $MoO_2(O^tBu)_2$ (0.0103 g, 0.0376 mmol) in DME (2 mL) and a white suspension of $[Sb\{^t\mathbf{BuC5(H)_2}\}]$ (0.0232g,

0.0250 mmol) in DME (3 mL) were placed together in a solvent bomb. The resulting yellowish suspension was placed in an isotemp bath at 95 ^{o}C and allowed to heat for 36 h yielding a light yellow solution and a red solid. The solution was removed by pipette, the red solid was dissolved with THF (7 mL), and the THF solution was centrifuged to remove any insoluble material. The red THF solution was dried under vacuum to give the crude product as a red solid. This solid was dissolved with Et_2O (or DME) (3 mL), centrifuged to remove any insoluble material and then placed in the freezer at -35 ^{o}C to yield pure $[Sb_2Mo_4O_{11}\{^{t}\mathbf{BuC5(H)}\}_2]$ (**6.2**) in 45% yield (0.0102 g, 0.00422 mmol) as red needle crystals. m.p. 242-244 ^{o}C; ^{1}H NMR (300 MHz, [D_6]DMSO, 25^{o}, TMS): δ 0.74 (s, 18H, C(CH_3)$_3$), 1.22 (s, 18H, C(CH_3)$_3$), 1.28 (s, 9H, C(CH_3)$_3$), 3.06 (d, *J* = 13.8 Hz, 2H, ArCH_2Ar), 3.15 (two doublets overlapping, 3H, ArCH_2Ar), 4.72 (d, *J* = 12.3 Hz, 1H, ArCH_2Ar), 4.98 (d, *J* = 13.5 Hz, 2H, ArCH_2Ar), 5.32 (d, *J* = 13.8 Hz, 2H, ArCH_2Ar), 6.62 (s, 2H, Ar*H*), 6.73 (s, 2*H*, Ar*H*), 7.08 (s, 2H, Ar*H*), 7.22 (s, 2H, Ar*H*), 7.29 (s, 2H, Ar*H*), no OH peaks were observed at rt; No ^{13}C NMR was obtained due to limited solubility in DMSO. IR (KBr): *v* = 3306w (OH), 2960vs, 2906m, 2869m, 1602w, 1478vs, 1459vs, 1393w, 1362m, 1293m, 1251m, 1198vs, 1124s, 1045w, 947m, 910m, 890m, 874m, 822m, 800m, 771m, 751m, 675m. UV/Vis (DMSO): λ_{max} (ε) = 218 (6310, 278 (1150), 486 nm (734). Elemental analysis calcd (%) for $C_{110}H_{132}Sb_2Mo_4O_{21}$: C 54.65, H 5.50; Found C 54.93, H 5.76.

6.3.3 General X-ray structure information

The crystallographic data and some details of the data collection and refinement of complex **6.1** are given in Table 6.2. Absorption corrections were applied by SADABS.[101] The X-ray structure of **6.1** was solved by direct methods and subsequent difference Fourier syntheses and refined by full matrix least-squares methods against F^2 (SHELX 97).[102] Disorder for some *tert*-butyl groups was due to a two-fold axis, and was modeled using partial occupancies (PART

instruction)[102] and isotropic displacement parameters. The H atoms in structures were taken in calculated positions. In the crystal structure of complex **6.1** highly disordered Et_2O molecules were treated with the program SQUEEZE.[103] PLATON/SQUEEZE estimated the solvent-accessible region void to occupy 1912.8 $Å^3$ and contain 231 electrons. The electron density was modeled as 6 diethyl ether (Et_2O) molecules (3 Et_2O per asymmetric unit) which accounts for 252 electrons. The 3 Et_2O molecules were added to the formula weight of the asymmetric unit. The two hydrogen atoms remaining in the calixarene ligands could not be located on the density map but they were added in the formula weight of the asymmetric unit. The programs ORTEP32[104] and POVRay[105] were used to generate the X-ray structural diagrams pictured in this Chapter.

Table 6.2. Crystallographic data for complex **6.1**

	6.1·$3C_4H_{10}O$
Formula	$C_{122}H_{162}Bi_2Mo_4O_{24}$
Fw	2814.30
cryst syst	Triclinic
space group	*P*-1
T, K	213(2)
a, Å	15.9705(13)
b, Å	18.4194(15)
c, Å	23.3498(18)
α, deg	97.864(2)
β, deg	101.8890(10)
γ, deg	96.2080(10)
V, A^3	6592.0(9)
Z	2
d_{calcd} g·cm^{-3}	1.418
μ, mm^{-1}	3.083
Refl collected	33803
T_{min}/ T_{max}	0.889
N_{measd}	18756
[R_{int}]	[0.0615]
R [I>2sigma(I)]	0.0435
R (all data)	0.0686
R_w [I>2sigma(I)]	0.0993
R_w (all data)	0.1052
GOF	0.916

6.4 Conclusions

We have synthesized and characterized the first calixarene M(III)/Mo(VI) (M = Bi, Sb) heterometallic complexes $[Bi_2Mo_4O_{11}\{^{t}\mathbf{BuC5(H)}\}_2]$ **6.1** and $[Sb_2Mo_4O_{11}\{^{t}\mathbf{BuC5(H)}\}_2]$ **6.2** by the reaction of monometallic $[M\{^{t}\mathbf{BuC5(H)_2}\}]$ (M = Bi, Sb) precursors with $MoO_2(O^{t}Bu)_2$. Complexes **6.1** and **6.2** have good solubility in organic solvents such as THF, Et_2O and DMSO, and display all-oxygen environments around the metal centers. The remarkable oxo-rich core structure of **6.1** contains Bi(μ-O)Mo, Mo(μ-O)Mo, Mo=O···Mo, and Bi-O-Bi interactions that are promising features for catalytic and mechanistic studies related to the SOHIO process.

CHAPTER 7

SYNTHESIS AND INTRAMOLECULAR ANTIMONY-CARBON BOND FORMATION IN ANTIMONY(III) BISPHENOLATES

7.1 Introduction

In Chapter 1, we described the importance of bismuth in the SOHIO process. It is generally accepted that the activation of the propene takes place in the bismuth site and that this is the rate determining step of the SOHIO process at 400 ^{o}C (structure C, Scheme 1.1).[218] Several studies have focused on the elucidation of the C-H bond breaking and the nature of the resulting organic species.[6]

We have shown that bismuth aryloxides of the type [Bi(OAr)$_3$] (Ar = 2,6-RC$_6$H$_3$, R = ^{i}Pr, ^{t}Bu) readily decomposed to produce C-C coupled products (equation 1.3, Chapter 1),[33] supporting the proposal that propene activation occurs by a radical species formed by Bi^{III}-O bond homolysis. Also we have observed that the complex Bi(OAr)$_3$ (Ar = 2,6-^{i}Pr-4-BrC$_6$H$_3$) underwent an intramolecular C-H activation to form an organometallic ladder Bi complex **2** (equation 1.4, Chapter 1).[43]

Our interest in the use of oxygen donor ligands for complexation of bismuth and antimony centers motivated us to explore the coordination capabilities of a series of bisphenol ligands that can be viewed as "half calixarenes."[219] There are several interesting features associated with ligands containing two oxygen donor atoms. First, these ligands with good π-donor atoms are expected to stabilize high oxidation states with covalent M-O (phenolate) bonds. Bisphenol ligands also may produce, in the presence of air, phenoxy radicals to be used as bioinspired radical catalysts for the conversion of different organic substrates.[220-223]

We have recently reported the synthesis of bismuth(III) bisphenolates of the type [Bi(O^{t}Bu){2,2'-CH(4-RC$_6$H$_4$)(O-4,6-^{t}Bu$_2$C$_6$H$_2$)$_2$-κ^2*O,O'*}] (R = OMe, NO$_2$).[224] Upon heating

these complexes at 80-100 °C for a period of 12 to 24 h, they form intramolecular Bi-C bonds (equation 7.1).[224] These results indicate that the bismuth(III) center is capable of produce C-H bond activation, a feature that is generally observed only in transition metal complexes.[225-227]

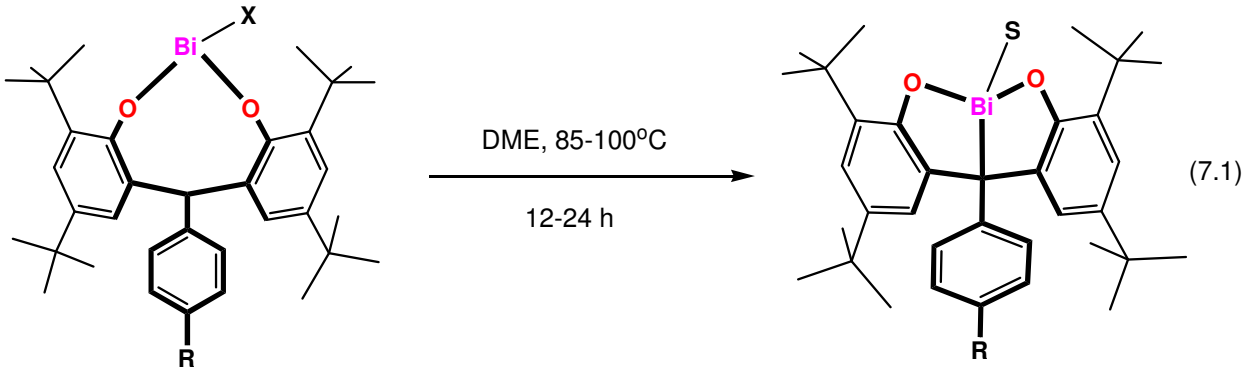

(7.1)

R = OMe, NO_2, CF_3, F
X = O^{t}Bu, $N(SiMe_3)_2$

S = coordination solvent

As the activation of C-H bonds has a broad range of applications, the development of a useful synthetic methodology for selectively functionalizing C-H bonds with a main group metal catalyst could be of great interest. In order to expand our knowledge related to the heavy Group 15 elements, we decided to synthesize a series of antimony(III) bisphenolates by the reaction of parent bisphenolates in reaction with SbX_3 (X = O^{t}Bu, NMe_2) precursors. We have discovered that they are also able to undergo intramolecular Sb-C bond formation upon heating of the parent complexes.

In this chapter we will describe the synthesis of a series of antimony(III) bisphenolates, the Sb-C bond formation, and the role of the electron-donating or electron-withdrawing groups attached to the bisphenol ligands. The solution and solid state characterization of the products will also be discussed.

7.2 Results and discussion.

7.2.1 Synthesis of the bisphenol ligands

The general method for the synthesis of bisphenol ligands **7.1**-**7.7** involves the reaction of two equivalents of 2,4-di-*tert*-butylphenol with one equivalent of the respective aldehyde in acidic media (equation 7.2).[228]

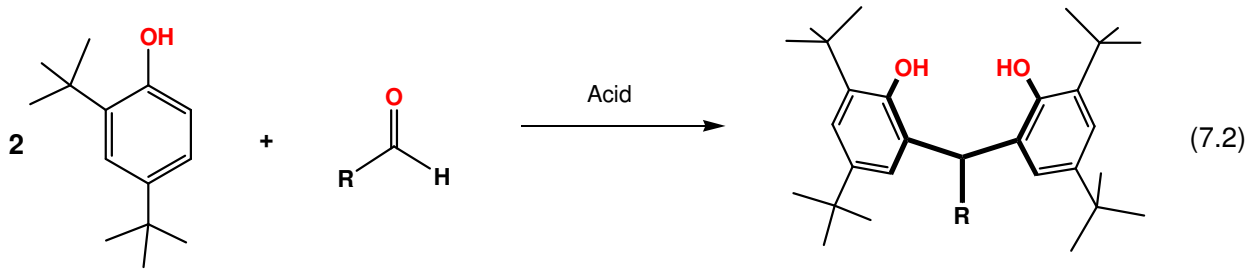

(7.2)

R = CH_2Ph **7.1** R = 4-MeC_6H_4 **7.5**
4-$NO_2C_6H_4$ **7.2** 4-$CF_3C_6H_4$ **7.6**
4-$OMeC_6H_4$ **7.3** 4-FC_6H_4 **7.7**
3-OMe-5-BrC_6H_3 **7.4**

In general the reaction mixture shows the expected bisphenol product along with unreacted starting materials. Purification of the bisphenols requires crystallization by solvent diffusion or low temperature, or chromatographic column separation. The bisphenol 2'2-CHMe(4,6-$^tBu_2C_6H_2OH)_2$, 2,2'-methylidenebis(4,6-di-*tert*-butylphenol), (**7.8**) was purchased from Aldrich and 2,2'-methylenebis(6-*tert*-butylphenol-4-methylphenol) **7.9**[229] and (2,2'-CH^iPr(4,6-$^tBu_2C_6H_2OH)_2$) **7.10**[230] were synthesized by literature methods.

All of the bisphenols display very good solubility in most organic solvents including pentane and hexane. In solution the parent bisphenols **7.1**-**7.8** and **7.10** all display very similar ^1H NMR patterns. Due to the symmetry plane that crosses the methylene carbon only two different singlets for the *tert*-butyl groups can be observed in the range from 1.11 to 1.55 ppm. For the bisphenol **7.9**, the ^1H NMR spectrum displays a broad singlet for the two methylene protons and

a single peak for the methyl and *tert*-butyl groups. The OH groups in ligands **7.1-7.10** are observed as single peaks (ranging from 4.81 to 7.52 ppm) indicating that ligands freely rotate around the methylene bridge.

Single crystals of ligand **7.10** were obtained by slow evaporation of a pentane solution and its crystal structure is depicted in Figure 7.1.

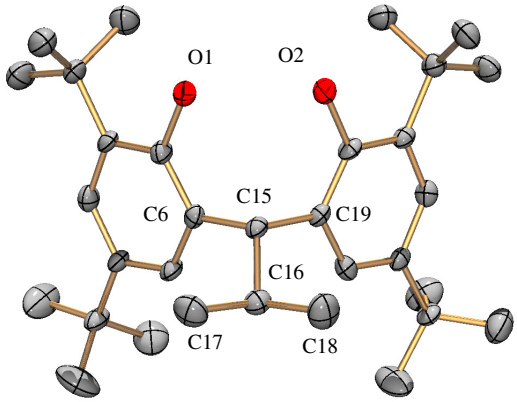

Figure 7.1. Crystal structure of ligand **7.10**.

Ligand **7.10** crystallizes in the monoclinic space group $P2_1/n$, with an approximate σ_v plane crossing the methylene carbon. This symmetry is consistent with the ^{1}H NMR patterns observed in all the bisphenol ligands. The isopropyl group in **7.10** points away from the OH groups and the C(6)-C(15)-C(19) angle is 110.3(2)^o.

7.2.2 Synthesis of antimony(III) bisphenolates

The treatment of the parent bisphenols **7.1-7.10** with one equivalent of SbX_3 (X = O^{t}Bu, NMe_2) at room temperature in pentane or THF produces the antimony complexes **7.11-7.30** in good to excellent isolated yields (64 to 95%), as depicted in Scheme 7.1. In general, the reaction produces a mixture of the antimony(III) complexes with parent bisphenols. The product is isolated by recrystallizing the crude materials by slow evaporation of a hexane solution, cooling

a pentane solution down to -35 °C, or by pentane diffusion into a concentrated THF (or DME) solution.

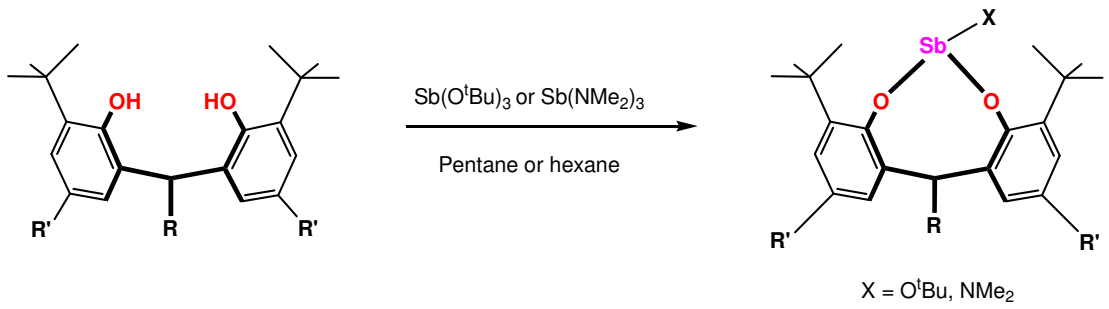

Compound	R	R'	X	Yield (%)
7.11	H	Me	O^{t}Bu	87
7.12	H	Me	NMe_2	91
7.13	4-$NO_2C_6H_4$	^{t}Bu	O^{t}Bu	89
7.14	4-$NO_2C_6H_4$	^{t}Bu	NMe_2	94
7.15	4-$OMeC_6H_4$	^{t}Bu	O^{t}Bu	84
7.16	4-$OMeC_6H_4$	^{t}Bu	NMe_2	87
7.17	^{i}Pr	^{t}Bu	O^{t}Bu	85
7.18	^{i}Pr	^{t}Bu	NMe_2	88
7.19	4-MeC_6H_4	^{t}Bu	O^{t}Bu	80
7.20	4-MeC_6H_4	^{t}Bu	NMe_2	78
7.21	Me	^{t}Bu	O^{t}Bu	83
7.22	Me	^{t}Bu	NMe_2	92
7.23	4-FC_6H_4	^{t}Bu	O^{t}Bu	90
7.24	4-FC_6H_4	^{t}Bu	NMe_2	81
7.25	4-$CF_3C_6H_4$	^{t}Bu	O^{t}Bu	73
7.26	4-$CF_3C_6H_4$	^{t}Bu	NMe_2	84
7.27	CH_2Ph	^{t}Bu	O^{t}Bu	92
7.28	CH_2Ph	^{t}Bu	NMe_2	88
7.29	2-OMe-5-BrC_6H_3	^{t}Bu	O^{t}Bu	68
7.30	2-OMe-5-BrC_6H_3	^{t}Bu	NMe_2	64

Scheme 7.1 Synthesis of antimony complexes **7.11-7.30**.

In an attempt to synthesize complexes containing terminal Sb-Cl bonds, we synthesized the lithium salts of ligands **7.2** and **7.3** by reaction of the bisphenol with two equivalents of ^{n}BuLi. The resulting white powders were slightly soluble in pentane and moderately soluble in THF and DMSO. The addition of one equivalent of $SbCl_3$ to the bisphenol lithium salts in THF

resulted in a mixture of traces of new complexes along with parent bisphenol, indicating that the products were very unstable in solution.

As the bismuth(III) bisphenolates containing terminal Bi-$N(SiMe_3)_2$ groups synthesized previously by our group[224] favored the intramolecular formation of Bi-C bonds, we decided to prepare analogous antimony complexes containing terminal $N(SiMe_3)_2$ groups. We synthesized the precursor $Sb[N(SiMe_3)_2]_3$ by the reaction of $SbCl_3$ with three equivalents of $LiN(SiMe_3)_2$ in THF as reported in literature.[155] The reaction of the parent bisphenol ligands with one equivalent of $Sb[N(SiMe_3)_2]_3$ at room temperature using pentane or THF showed only unreacted ligand after periods of 1-4 days. In order to favor the preparation of the desired antimony complexes, we increased the number of equivalents of $Sb[N(SiMe_3)_2]_3$ to 2-4 or the temperature of reaction in the range of 70-100 ^oC, but in all cases we still observed unreacted parent bisphenols. It is probable that the smaller size of antimony in comparison to that of bismuth and the bulkiness of the $N(SiMe_3)_2$ group hinder the close approach of the antimony amide to the OH groups of the parent bisphenol ligands.

All antimony complexes **7.11-7.30** have excellent solubility in most organic solvents and are stable both in solution and in the solid state under nitrogen. However, benzene solutions of complexes **7.11-7.30** start to decompose to parent bisphenols after six hours in air.

The ^1H NMR spectra of the complexes **7.11-7.30** in C_6D_6, as expected, lack the OH peak belonging to the parent ligands and reveal the existence of a mirror plane that crosses each molecule through the methylene bridge. The number of hydrogen signals observed for all the antimony complexes is therefore halved due to magnetic equivalence of the nuclei in opposite sides of the mirror plane with a bridging methylene as center of symmetry. Some representative ^1H NMR spectra are shown in Figure 7.2.

For the complexes **7.13-7.30** containing *tert*-butyl groups in the 4 and 6 positions two different singlets are observed in the range of 1.28 to 1.58 ppm, and the proton in the methylene bridge shifts upfield in a range from 5.06 to 7.16 ppm. This large chemical shift indicates that the methylene protons are close to the antimony centers.

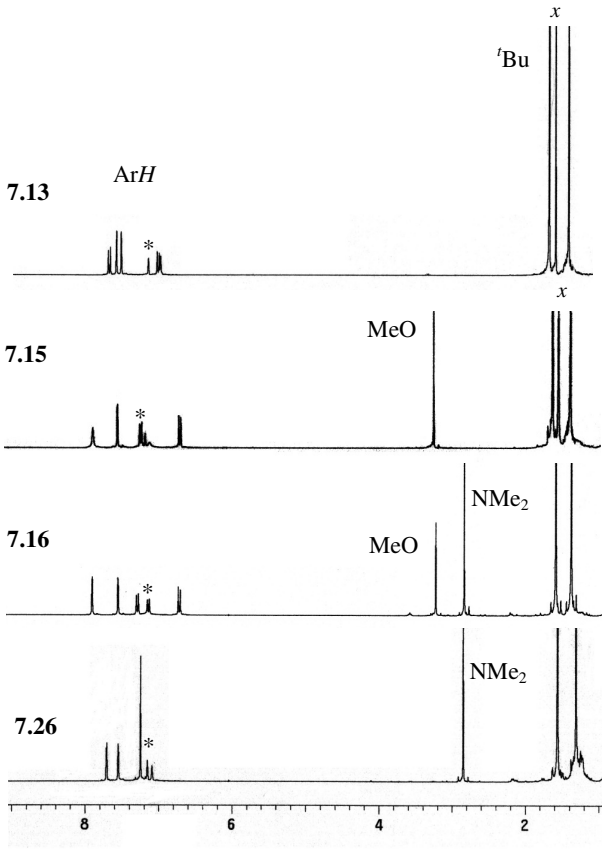

Figure 7.2. Representative ^{1}H NMR spectra in $*C_6D_6$ of the antimony(III) bisphenolates. *x* = O^{t}Bu peaks.

In the case of complexes **7.11** and **7.12**, a single peak is observed for each pair of *tert*-butyl and methyl groups that are located in the 4 and 6 positions of the aromatic rings, respectively. The methylene protons in the chelate backbone are diastereotopic, indicating that they are exposed to different magnetic environments. One of the methylene protons is pointing to the metal center (*endo*) and the other pointing down from the coordination sphere (*exo*),

producing two doublets in the ^{1}H NMR spectrum (in the parent phenol the methylene protons appear as a singlet).

The presence of the Sb-O^{t}Bu and Sb-NMe_2 is easily observed by the presence of sharp singlets around 1.5 and 2.9 ppm, respectively. These terminal Sb-X groups make complexes **7.11-7.30** interesting building blocks for more extended structures.

Selected IR data for complexes **7.11-7.30** are given in the experimental section. The broad *v*(OH) band for the free ligands in the region 3400-3200 cm^{-1} is lost once the antimony centers are coordinated. There are several strong signals in the region of 3000-2800 cm^{-1} due to the *v*(C-H) of the *tert*-butyl and the methylene groups.

7.2.3 Intramolecular antimony-carbon bond formation

We recently reported a series of mono and bimetallic antimony(III) calixarene complexes where we observed by ^{1}H NMR that the ligand methylene protons usually range from 2.76 to 6.02 ppm.[58,121,159] In the antimony bisphenolates **7.13-7.16**, **7.19**, **7.20**, **7.23-7.26**, **7.29** and **7.30**, the higher ^{1}H NMR shifts for all the methylene hydrogens (6.98 to 7.16 ppm) suggested that this hydrogen atom was relatively close to the metal center. In our previously reported bismuth(III) bisphenolates[224] (equation 7.1) we observed that the proximity between the methylene hydrogen and the bismuth center was an important feature for the Bi-C intramolecular bond formation. Having observed this similarity, we expected that under analogous reaction conditions, the antimony bisphenolates could also allow intramolecular Sb-C bond formation.

We performed a large series of experiments utilizing several temperatures and reaction solvents (including all of the bisphenolate complexes **7.11-7.30**) targeting the intramolecular Sb-C bond formation. However, we only observed significant Sb-C bond formation in the complexes supported by ligands **7.2**, **7.3**, and **7.5-7.7** (equation 7.3). The latter results are similar

to those observed for the intramolecular Bi-C bond formation in the bismuth(III) bisphenolates (see equiation 7.2), however, in the antimony complexes we were able to additionally induce Sb-C bond formation utilizing ligand **7.5**.

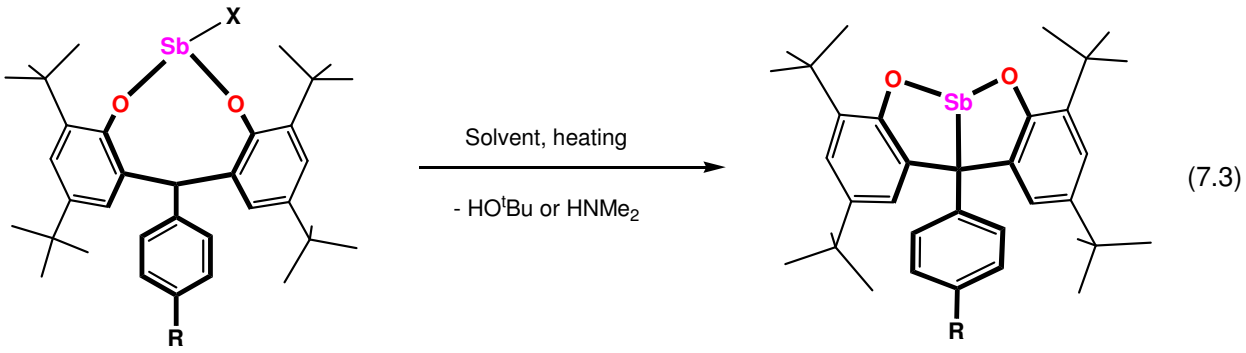

(7.3)

X = O^{t}Bu, NMe$_2$

R = -OMe **7.31** R = -F **7.34**
-CF$_3$ **7.32** -Me **7.35**
-NO$_2$ **7.33**

The activation of the C-H bond and the intramolecular Sb-C bond formation is possible, but the selection of the right solvent, temperature, and time of reaction is very important (see Table 7.1). For example, the preparation of complex **7.31** requires the heating of the precursor **7.16** for 48 h in a mixture of C_6H_6/THF (1:5) at 95 ^oC. The use of any other solvents or temperatures results in a mixture of complex **7.31** and parent bisphenol, or in some cases no reaction at all.

Intramolecular Sb-C formation is faster when using complexes containing terminal Sb-NMe$_2$ bonds. For instance, complex **7.35** is obtained after heating complex **7.20** (see Scheme 7.3) in a mixture of C_6H_6/THF (1:5) for 3 days at 95 ^oC, while the treatment of complex **7.19** (containing terminal Sb-O^{t}Bu) under the same conditions yields complex **7.35** only after 6 days of reaction. Also, complex **7.32** can only be obtained by heating the precursor **7.26** (containing terminal Sb-NMe$_2$) at 95 ^oC**.** All the attempts to obtain **7.32** by employing the precursor **7.25** (see Scheme 7.3) were unsuccessful.

Table 7.1. Different reaction conditions for Sb-C bond formation in complexes **7.31-7.35**

Parent compd	Solvent	Temp	Time	Sb-C (Product)	Yield(%)
7.15	C_6H_6/THF (1:1)	95 ^oC	58 h	**7.31**	82
7.16	C_6H_6	95 ^oC	7 d	----------	--------
7.16	C_6H_6/THF (1:5)	95 ^oC	48 h	**7.31**	78
7.16	THF	95 ^oC	6 d	**7.31**	64
7.26	C_6H_6	95 ^oC	48 h	**7.32**	76
7.26	THF	95 ^oC	48 h	NR	--------
7.26	C_6H_6/THF (1:5)	95 ^oC	3 d	**7.32 + 7.6**	--------
7.14	C_6H_6/THF (1:5)	75 ^oC	48 h	**7.33**	89
7.14	C_6H_6	95 ^oC	2 weeks	**7.33**	62
7.23	C_6H_6/THF (1:5)	95 ^oC	4 d	**7.34**	80
7.24	C_6H_6/THF (1:5)	95 ^oC	3 d	**7.34**	84
7.19	C_6H_6/THF (1:5)	95 ^oC	6 d	**7.35**	78
7.20	C_6H_6/THF (1:5)	95 ^oC	3 d	**7.35**	71

The activation of C-H bonds is well established to occur by five basic pathways: oxidative addition, σ-bond metathesis, 1,2-addition, electrophilic displacement of H^+, and four center cleavage by two metalloradicals.[227,231-233] In our antimony(III) bisphenolates the C-H/Sb-X system (X = O^tBu, NMe_2) appears to undergo an acid/base reaction with the release of *tert*-butanol or dimethyl amine. We also think that the enhanced basicity of the -NMe_2, in comparison with that of the O^tBu terminal groups, is responsible for the faster Sb-C bond formation in complexes **7.31-7.35**.

In solution, the ^1H NMR spectra of complexes **7.31-7.35** all display very similar patterns as their parent complexes (Figure 7.3). The four *tert*-butyl groups on each complex display only two singlets, ranging from 1.26 to 1.58 ppm, indicating C_s symmetry. As expected for complexes **7.31-7.35**, the methylene hydrogen signal is lost.

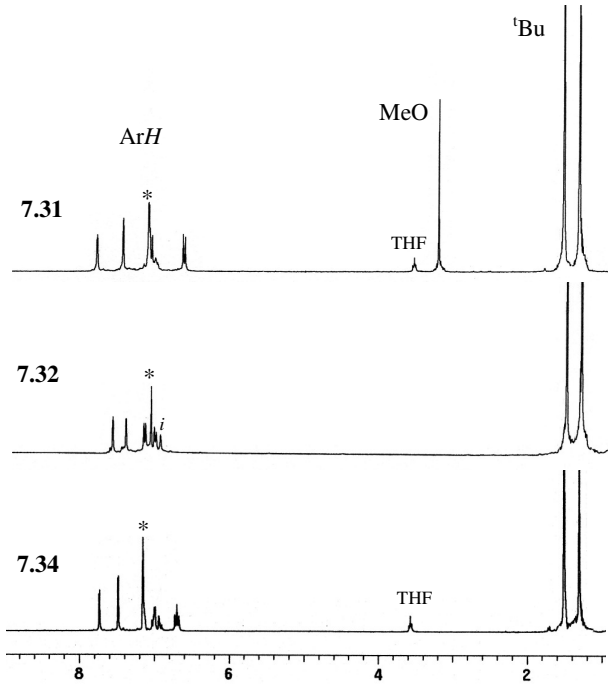

Figure 7.3. Representative ^{1}H NMR spectra in $*C_6D_6$ of complexes containing Sb-C bonds. *i* = impurity.

Single crystals of complex **7.33** were obtained as light-yellow blocks by the slow evaporation of a benzene/DMSO mixture (6/1) for two weeks at room temperature. The crystal structure of complex **7.33** and selected bond distances and angles are depicted in Figure 7.4. Complex **7.33** crystallizes in the monoclinic space group $P2_1/c$ as a monomeric unit with an antimony center bound to two aryloxides and one carbon atom. The Sb(1)-C(15) covalent bonding in **7.33** changes the overall hapticity of the bisphenol ligand from two to three, now resembling transition metal complexes supported by calixarenes and bisphenols that display similar covalent M-C bonds (M = Mo, W, Ti, Zr, Ta)[219,234-238] and metal complexes supported by O,X,O-donor ligands (X = S, N, Se, P, PO).[239-245]

The Sb-OAr distances are 2.017(3) and 2.030(3) Å, in the normal range of Sb-OAr bond distances for aryloxide and alkoxide complexes.[121,138,139,159] The Sb-C bond distance is 2.217(4) Å and is also similar to those Sb-C distances observed in several organoantimony complexes.[137]

The antimony center has secondary interactions with two DMSO molecules to form a distorted square pyramidal coordination sphere around the metal center. The Sb-O(DMSO) bond distances are 2.578(9) and 2.688(12) Å, similar to those observed in other antimony aryloxide and calixarene complexes.[58,138,159]

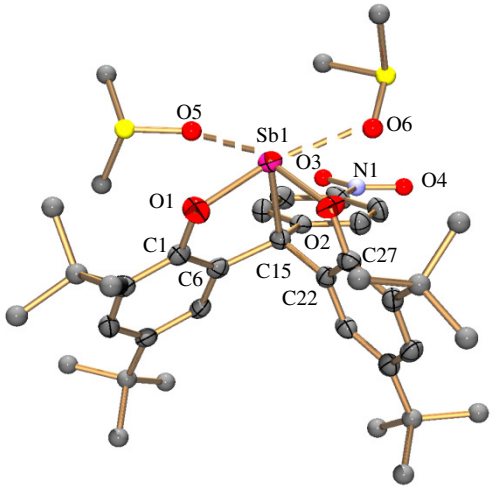

Figure 7.4 Crystal structure and selected bond distances (Å) and angles (°) of complex **7.33**. Ellipsoids are shown at 50% probability. Hydrogen atoms and uncoordinated solvents omitted for clarity. Sb(1)-O(1) 2.030(3), Sb(1)-O(2) 2.017(3), Sb(1)-C(15) 2.217(4), Sb(1)-O(5) 2.688(12), Sb(1)-O(6) 2.578(9), O(1)-Sb(1)-(O)2 90.04(12), O(1)-Sb(1)-C(15) 81.88(14), O(2)-Sb(1)-C(15) 83.92(13), C(6)-C(15)-C(22) 107.5(3).

The basal plane of the square pyramidal geometry at the antimony center is defined by the O(1), O(2), O(5), and O(6) atoms and the apical position is occupied by the C(15) atom. Two fused five membered rings are formed by Sb(1), O(1), C(1), C(6) and C(15), and Sb(1), O(2), C(27), C(22) and C(15). The $ArNO_2$ group does not have much effect on the geometry of the metal center as it points away from the core structure.

7.3 Experimental section

7.3.1 General information:

Unless otherwise noted, all manipulations were carried out in a nitrogen filled glove-box or using standard Schlenk techniques. 2'2-CHMe(4,6-$^{t}Bu_2C_6H_2OH)_2$, 2,2'-methylidenebis(4,6-di-tert-butylphenol) (**7.8**), was purchased from Aldrich, 2,2'-methylenebis(6-*tert*-butylphenol-4-methylphenol) (**7.9**) was synthesized from 2-*tert*-butylphenol and *para*-formaldehyde in anhydrous xylenes following a literature procedure.[229] 2,2'-isobutylidenebis(4,6-di-tert-butylphenol), (2,2'-$CH^{i}Pr(4,6\text{-}^{t}Bu_2C_6H_2OH)_2$) (**7.10**), was prepared from 2,4-di-tert-butylphenol, isobutyraldehyde, boron trifluoride diethyl etherate and acetic acid as described elsewere.[230] Other starting materials were obtained from commercial suppliers and used without further purification. All the other bisphenol ligands were synthesized in our lab and dried at 110 ^{o}C for at least 24 hrs under vacuum before use. $Sb(O^{t}Bu)_3$ was synthesized by the literature method.[156] Hexanes, diethyl ether (Et_2O) and tetrahydrofuran (THF) were freshly distilled from Na/benzophenone. Benzene was dried by refluxing over Na/benzophenone and stored over 4Å molecular sieves. Other anhydrous solvents were purchased from Aldrich and stored over molecular sieves under nitrogen before using. Deuterated benzene was dried over CaH_2. The melting points of all the compounds were taken in capillary tubes on a Mel-temp apparatus (Laboratory devices, Cambridge, MA) using a 500 ^{o}C thermometer. ^{1}H NMR and ^{13}C spectra were recorded at room temperature on a Varian XL-300 spectrometer at 300 and 75 MHz, respectively. Analytical samples were dried under vacuum for at least 24 hrs. Microanalyses were performed by Atlantic Microlab, Inc, Norcross, GA. IR and UV/Vis spectra were obtained with an Infinity Gold^{TM} FTIR spectrometer and an Agilent 8453 spectrophotometer, respectively.

Filtrations used a medium sintered glass filter. X-ray data for **7.10** and **7.33** were collected on a Bruker SMART APEX CCD diffractometer at variable low temperature using Mo Kα radiation.

7.3.2 Preparation of compounds

7.3.2.1 Synthesis of bisphenols

Bisphenols **7.1-7.8** were prepared according to a literature procedure.[246]

2,2'-CHBn(4,6-^{t}Bu$_2$C$_6$H$_2$OH)$_2$, 2,2'-phenylethylenebis(4,6-di-*tert*-butylphenol) (7.1): 2,4-di-*tert*-butylphenol (2.063 g, 10.00 mmol), phenylacetaldehyde (0.661 g, 5.50 mmol), heptane (30 mL) and conc. H_2SO_4 (1 mL) were combined with strong stirring in a 100 mL round bottomed flask adapted with a condenser. The reaction mixture was allowed to reflux for 8 hrs and allowed to cool down to room temperature. The reaction mixture was washed twice with a saturated solution of $NaHCO_3$ and the organic phase separated and dried with $MgSO_4$. The solvent was removed to yield an orange residue. A water/methanol mixture (1:6, 50 mL) was added to the orange residue followed by 25 minutes of boiling, then the yellow mixture was allowed to reach room temperature. The yellow precipitate was then recrystallized from a 20 mL mixture of chloroform and hexanes (1:10). Yield 78% (2.01 g, 3.91 mmol). ^{1}H NMR (C_6D_6): δ 1.27 (s, 18H, C(C*H*$_3$)$_3$), 1.39 (s, 18H, C(C*H*$_3$)$_3$), 3.40 (d, *J* = 7.8 Hz, 2H, CH(C*H*$_2$Ph)), 4.64 (t, *J* = 7.8 Hz, 1H, C*H*(CH$_2$Ph)), 5.35 (s, 2H, O*H*), 6.97 (m, 3H, Ar*H*), 6.86 (m, 2H, Ar*H*), 7.36 (d, *J* = 2.4 Hz, 2H, Ar*H*), 7.38 (d, *J* = 2.4 Hz, 2H, Ar*H*).

2,2'-CH[4-NO$_2$C$_6$H$_4$](4,6-^{t}Bu$_2$C$_6$H$_2$OH)$_2$, 2,2'-(4-nitrobenzylene)bis(4,6-di-*tert*-butylphenol) (7.2): 2,6-di-*tert*-butylphenol (2.063 g, 10.00 mmol) and 4-nitrobenzaldehyde (0.831 g, 5.50 mmol) were dissolved in anhydrous methanol (40 mL) in a 100 mL three neck flask. The first neck was attached to a mild argon flow, the second neck was equipped with a glass sintered bubbler that provided a mild anhydrous hydrogen chloride gas flow during the

course of the reaction, and the third neck was connected to a trap used to quench the excess of HCl gas with a saturated solution of K_2CO_3. The reaction mixture was stirred at room temperature. After 2 days, stirring was stopped, the precipitate was collected by filtration, and it was recrystallized from hexanes (20 mL) at -15 ^oC yielding a yellowish crystalline solid. Yield 72% (1.97 g, 3.61 mmol). ^1H NMR ($CDCl_3$): δ 1.16 (s, 18H, C(C*H*$_3$)$_3$), 1.39 (s, 18H, C(C*H*$_3$)$_3$), 4.89 (s, 2H, O*H*), 5.85 (s, 1H, bridge C*H*), 6.65 (d, *J* = 2.4 Hz, 2H, Ar*H*), 7.27 (d, *J* = 2.4 Hz, 2H, Ar*H*), 7.33 (d, *J* = 8.7 Hz, 2H, Ar*H*), 8.19 (d, *J* = 8.7 Hz, 2H, Ar*H*). ^1H NMR (C_6D_6): δ (ppm) 1.18 (s, 18H, C(C*H*$_3$)$_3$), 1.44 (s, 18H, C(C*H*$_3$)$_3$), 5.00 (s, 2H, O*H*), 5.77 (s, 1H, bridge C*H*)), 6.90 (d, *J* = 2.4 Hz, 2H, Ar*H*), 6.95 (d, *J* = 8.7 Hz, 2H, Ar*H*), 7.45 (d, *J* = 2.4 Hz, 2H, Ar*H*), 7.76 (d, *J* = 8.7 Hz, 2H, Ar*H*).

2'2-CH[4-OMeC$_6$H$_4$](4,6-^{t}Bu$_2$C$_6$H$_2$OH)$_2$, 2,2'-(4-methoxybenzylene)bis(4,6-di-*tert*-butylphenol) (7.3): 2,6-di-*tert*-butylphenol (2.063 g, 10.00 mmol) and 4-methoxybenzaldehyde (0.749 g, 5.50 mmol) were dissolved in anhydrous methanol (40 mL) in a 100 mL three neck flask. The reaction mixture was stirred at room temperature using the same reaction set up as for ligand **7.2**. After 2 days, stirring was stopped, the precipitate was collected by filtration, and it was recrystallized from hexanes (20 mL) at -15 ^oC yielding a white powder. Yield 76% (2.01 g, 3.78 mmol). ^1H NMR (C_6D_6): δ 1.21 (s, 18H, C(C*H*$_3$)$_3$), 1.55 (s, 18H, C(C*H*$_3$)$_3$), 3.17 (s, 3H, OC*H*$_3$), 4.95 (s, 2H, O*H*), 5.60 (s, 1H, bridge C*H*)), 6.65 (d, *J* = 8.7 Hz, 2H, Ar*H*), 7.03 (two doublets overlapping, 4H, Ar*H*), 7.52 (d, *J* = 2.4 Hz, 2H, Ar*H*).

2,2'-CH(2-OMe-5-BrC$_6$H$_3$)(4,6-^{t}Bu$_2$C$_6$H$_2$OH)$_2$, 2,2'-(5-bromo-2-methoxybenzylene)bis(4,6-di-*tert*-butylphenol) (7.4): 2,4-di-*tert*-butylphenol (5.202 g, 25.21 mmol) and 5-bromo-2-methoxybenzaldehyde (2.712 g, 12.61 mmol) were dissolved in anhydrous methanol (65 mL) in a 250 mL three neck flask. The reaction mixture was allowed to

stir for 48 hrs at room temperature (using the same reaction set up as for ligand **7.2**) yielding a white suspension. The precipitate was separated by filtration and then recrystallized from 15 mL of methanol-chloroform (1:1) to give colorless crystals of the product. Yield 86% (6.603 g, 10.83 mmol). ^{1}H NMR ($CDCl_3$): δ 1.18 (s, 18H, C(C*H*$_3$)$_3$), 1.38 (s, 18H, C(C*H*$_3$)$_3$), 3.76 (s, 3H, OC*H*$_3$), 4.90 (s, 2H, O*H*), 5.88 (s, 1H, bridge C*H*), 6.70 (d, *J* = 2.4 Hz, 2H, Ar*H*), 6.82 (d, *J* = 9.0 Hz, 1H, Ar*H*), 7.09 (d, *J* = 2.7 Hz, 1H, Ar*H*), 7.25 (d, *J* = 2.4 Hz, 2H, Ar*H*), 7.39 (dd, *J* = 2.7 Hz, *J* = 9.0 Hz, 1H, Ar*H*).

2,2'-CH(4-MeC$_6$H$_4$)(4,6-^{t}Bu$_2$C$_6$H$_2$OH)$_2$, 2,2'-(4-methylbenzylene)bis(4,6-di-*tert*-butylphenol) (7.5): 2,4-di-*tert*-butylphenol (5.202 g, 25.21 mmol) and tolualdehyde (1.604 g, 13.35 mmol) were dissolved in absolute methanol (65 mL) in a 250 mL round three neck flask. The reaction mixture was allowed to stir for 48 hrs at room temperature (using the same reaction set up as for ligand **7.2**) yielding a white suspension. The precipitate was separated by filtration, dried under vacuum and recrystallized from hexane (15 mL) at -15 ^{o}C to give the product as a white powder. Yield 83% (5.398 g, 10.49 mmol). ^{1}H NMR (C_6D_6): δ 1.21 (s, 18H, C(C*H*$_3$)$_3$), 1.53 (s, 18H, C(C*H*$_3$)$_3$), 1.98 (s, 3H, C*H*$_3$), 4.93 (s, 2H, O*H*), 5.63 (s, 1H, bridge C*H*), 6.88 (d, *J* = 8.7 Hz, 2H, Ar*H*), 7.03 (d, *J* = 2.4 Hz, 2H, Ar*H*), 7.07 (d, *J* = 8.7 Hz, 2H, Ar*H*), 7.51 (d, *J* = 2.4 Hz, 2H, Ar*H*).

2,2'-CH(4-CF$_3$C$_6$H$_4$)(4,6-^{t}Bu$_2$C$_6$H$_2$OH)$_2$, 2,2'-(4-trifluoromethylbenzylene)bis(4,6-di-*tert*-butylphenol) (7.6): 2,4-di-*tert*-butylphenol (5.202 g, 25.21 mmol) and 4-trifluoromethylbenzaldehyde (2.201 g, 12.64 mmol) were dissolved in absolute methanol (65 mL) in a 250 mL three neck flask. The reaction mixture was allowed to stir for 48 hrs at room temperature (using the same reaction set up as for ligand **7.2**) yielding a white suspension. The methanol was removed under vacuum yielding a yellow residue, which was dissolved in 200 mL

of hexane and washed with a saturated $NaHCO_3$ solution (15 mL) and H_2O (10 mL). The organic phase was separated and dried to give a yellow residue. The product was isolated by flash chromatography [ethyl acetate:hexane (1:5)] as a yellow waxy solid. Yield 64% (4.60 g, 8.08 mmol). ^{1}H NMR (C_6D_6): δ 1.17 (s, 18H, C(C*H*$_3$)$_3$), 1.45 (s, 18H, C(C*H*$_3$)$_3$), 4.93 (s, 2H, O*H*), 5.72 (s, 1H, bridge C*H*), 6.94 (d, *J* = 2.4 Hz, 2H, Ar*H*), 7.05 (d, *J* = 8.7 Hz, 2H, Ar*H*), 7.27 (d, *J* = 8.7 Hz, 2H, Ar*H*), 7.47 (d, *J* = 2.4 Hz, 2H, Ar*H*).

2,2'-CH(4-FC$_6$H$_4$)(4,6-^{t}Bu$_2$C$_6$H$_2$OH)$_2$, 2,2'-(4-fluorobenzylene)bis(4,6-di-*tert*-butylphenol) (7.7): 2,4-di-*tert*-butylphenol (5.202 g, 25.21 mmol) and 4-fluoroaldehyde (1.604 g, 12.92 mmol) were dissolved in absolute methanol (65 mL) in a 250 mL three neck round bottom flask. The reaction mixture was allowed to stir for 48 hrs at room temperature (using the same reaction set up as for ligand **7.2**) yielding a white suspension. The precipitate was separated by filtration, dried under vacuum and recrystallized from hexane (20 mL) at -15 ^{o}C to give the product as colorless crystals. Yield 94% (6.11 g, 11.8 mmol). ^{1}H NMR (C_6D_6): δ 1.15 (s, 18H, C(C*H*$_3$)$_3$), 1.46 (s, 18H, C(C*H*$_3$)$_3$), 4.81 (s, 2H, O*H*), 5.54 (s, 1H, bridge C*H*), 6.65 (dd, *J* = 8.4 Hz, *J* = 13.2 Hz, 2H, Ar*H*), 6.87 (dd, *J* = 8.4 Hz, *J* = 13.2 Hz, 2H, Ar*H*), 6.89 (d, *J* = 2.4 Hz, 2H, Ar*H*), 7.44 (d, *J* = 2.4 Hz, 2H, Ar*H*).

2,2'-CHMe(4,6-^{t}Bu$_2$C$_6$H$_2$OH)$_2$, 2,2'-methylidenebis(4,6-di-*tert*-butylphenol) (7.8): Purchased from Aldrich. ^{1}H NMR (C_6D_6): δ 1.29 (s, 18H, C(C*H*$_3$)$_3$), 1.41 (s, 18H, C(C*H*$_3$)$_3$), 1.61 (d, *J* = 7.2 Hz, 3H, CH(C*H*$_3$)), 4.42 (q, *J* = 7.2 Hz, 1H, bridge C*H*), 5.60 (s, 2H, O*H*), 7.38 (d, *J* = 2.1 Hz, 2H, Ar*H*), 7.42 (d, *J* = 2.4 Hz, 2H, Ar*H*).

2,2'-CH$_2$(6-^{t}Bu-4-MeC$_6$H$_2$OH)$_2$, 2,2'-methylenebis(6-*tert*-butylphenol-4-methylphenol) (7.9): Bisphenol prepared according to literature procedure.[229] ^{1}H NMR (C_6D_6):

δ 1.35 (s, 18H, C(CH_3)$_3$), 2.06 (s, 6H, CH_3), 3.65 (s, 2H, ArCH_2Ar), 5.53 (s, 2H, O*H*), 6.81 (d, *J* = 1.8 Hz, 2H, Ar*H*), 6.97 (d, *J* = 1.8 Hz, 2H, Ar*H*).

2,2'-CH^{i}Pr(4,6-^{t}Bu$_2$C$_6$H$_2$OH)$_2$, 2,2'-isobutylidenebis(4,6-di-*tert*-butylphenol) (**7.10**): Bisphenol prepared according to literature procedure.[230] ^{1}H NMR (C_6D_6): δ 1.02 (d, *J* = 6.6 Hz, 6H, CH(CH_3)$_2$), 1.32 (s, 18H, C(CH_3)$_3$), 1.35 (s, 18H, C(CH_3)$_3$), 2.73 (broad septet, 1H, C*H*(CH$_3$)$_2$), 4.36 (d, *J* = 10.8 Hz, 1H, bridge C*H*), 6.08 (s, 2H, O*H*), 7.27 (d, *J* = 2.4 Hz, 2H, Ar*H*), 7.52 (d, *J* = 2.4 Hz, 2H, Ar*H*).

7.3.2.2 General procedure for preparation of antimony bisphenolates

The detailed preparation for compounds **7.11** and **7.12** is described below. The rest of the antimony bisphenolates were synthesized following similar procedures and using the same number of moles of the respective starting materials.

[Sb(O^{t}Bu){2,2'-CH$_2$(O-6-^{t}Bu-4-MeC$_6$H$_2$)$_2$-κ^2*O,O'*}] (7.11): A colorless solution of Sb(O^{t}Bu)$_3$ (0.103 g, 0.302 mmol) in 5 mL of pentane was added dropwise to a solution of 2,2'-CH$_2$(6-^{t}Bu-4-MeC$_6$H$_2$OH)$_2$ (**7.9**) (0.102 g, 0.300 mmol) in 12 mL of pentane and the resulting clear solution was allowed to stir for 48 hrs at room temperature. The final colorless solution was dried under vacuum to give the crude product as a white solid. Pure product was obtained either by redissolving the crude product in 10 mL of pentane and cooling it down to -35 ^{o}C inside the freezer for 3 days or by recystallization by pentane diffusion into a concentrated THF (or DME) solution. Yield 87% (0.139 g, 0.261 mmol). ^{1}H NMR (C_6D_6): δ 1.51 (s, 18H, C(CH_3)$_3$), 1.51 (s, 9H, OC(CH_3)$_3$), 2.19 (s, 6H, CH_3), 3.32 (d, *J* = 13.5 Hz, 1H, ArCH_2Ar), 4.66 (b, 1H, ArCH_2Ar), 7.10 (b, 2H, Ar*H*), 7.13 (b, 2H, Ar*H*). ^{13}C{^{1}H} NMR (C_6D_6): δ 151.5, 140.6, 134.6, 130.5, 129.5,

126.1 (aromatic carbons), 35.1 (Ar*C*H_2Ar), 33.7 (*C*(CH_3)$_3$ and O*C*(CH_3)$_3$), 31.0 (C(*C*H_3)$_3$ and OC(*C*H_3)$_3$), 20.9 (*C*H_3).

[Sb(NMe$_2$){2,2'-CH$_2$(O-6-^{t}Bu-4-MeC$_6$H$_2$)$_2$-κ^2*O,O'*}] (7.12): A colorless solution of Sb(NMe$_2$)$_3$ (0.0764 g ,0.301 mmol) in 5 mL of pentane was added dropwise to a solution of 2,2'-CH$_2$(6-^{t}Bu-4-MeC$_6$H$_2$OH)$_2$ (**7.9**) (0.102 g, 0.300 mmol) in 12 mL of pentane and the resulting clear solution was allowed to stir for 24 hrs at room temperature. The final colorless solution was dried under vacuum to give the crude product as a white solid. Pure product was obtained either by redissolving the crude product in 10 mL of pentane and cooling it down to -35 ^{o}C inside the freezer for 3 days or by slow evaporation of a hexane solution (12 mL). Yield 91% (0.137 g, 0.272 mmol). ^{1}H NMR (C$_6$D$_6$): δ 1.50 (s, 18H, C(C*H*$_3$)$_3$), 2.22 (s, 6H, C*H*$_3$), 2.91 (s, 6H, N(C*H*$_3$)$_2$), 3.57 (d, *J* = 13.2 Hz, 1H, ArC*H*$_2$Ar), 4.74 (d, *J* = 12.3 Hz, 1H, ArC*H*$_2$Ar), 7.14 (b, 2H, Ar*H*), 7.21 (b, 2H, Ar*H*). ^{13}C{^{1}H} NMR (C$_6$D$_6$): δ 152.7, 140.5, 135.1, 130.3, 129.6, 125.9 (aromatic carbons), 39.2 (N(*C*H$_3$)$_2$), 35.1 (Ar*C*H$_2$Ar), 31.8 (*C*(CH$_3$)$_3$), 31.1 (C(*C*H$_3$)$_3$), 21.0 (*C*H$_3$).

[Sb(O^{t}Bu){2,2'-CH(4-NO$_2$C$_6$H$_4$)(O-4,6-^{t}Bu$_2$C$_6$H$_2$)$_2$-κ^2*O,O'*}] (7.13): Yield 89% (0.197 g, 0.267 mmol). ^{1}H NMR (C$_6$D$_6$): δ 1.30 (s, 18H, C(C*H*$_3$)$_3$), 1.48 (s, 9H, OC(C*H*$_3$)$_3$), 1.57 (s, 18H, C(C*H*$_3$)$_3$), 6.98 (s, 1H, bridge C*H*), 7.02 (d, *J* = 9.3 Hz, 2H, Ar*H*), 7.53 (d, *J* = 2.4 Hz, 2H, Ar*H*), 7.60 (d, *J* = 2.4 Hz, 2H, Ar*H*), 7.70 (d, *J* = 9.3 Hz, 2H, Ar*H*). ^{13}C{^{1}H} NMR (C$_6$D$_6$): δ 153.3, 151.7, 146.2, 144.7, 140.5, 137.9, 129.8, 125.2, 122.7, 122.4 (aromatic carbons), 42.0 (bridge *C*H), 35.5, 34.6, 33.7 (*C*(CH$_3$)$_3$), 31.5 (two ^{t}Bu peaks overlapping), 31.2 (C(*C*H$_3$)$_3$).

[Sb(NMe$_2$){2,2'-CH(4-NO$_2$C$_6$H$_4$)(O-4,6-^{t}Bu$_2$C$_6$H$_2$)$_2$-κ^2*O,O'*}] (7.14): Yield 94% (0.200 g, 0.280 mmol). ^{1}H NMR (C$_6$D$_6$): δ 1.32 (s, 18H, C(C*H*$_3$)$_3$), 1.56 (s, 18H, C(C*H*$_3$)$_3$), 2.84 (s, 6H,

N(CH_3)$_2$), 7.03 (s, 1H, bridge C*H*), 7.10 (d, *J* = 9.3 Hz, 2H, Ar*H*), 7.55 (d, *J* = 2.4 Hz, 2H, Ar*H*), 7.63 (d, *J* = 2.4 Hz, 2H, Ar*H*), 7.74 (d, *J* = 9.3 Hz, 2H, Ar*H*). ^{13}C{^{1}H} NMR (C_6D_6): δ 153.7, 153.3, 146.2, 144.4, 140.2, 137.6, 129.9, 125.2, 122.7, 122.3 (aromatic carbons), 41.9 (bridge *C*H), 38.8 (N(*C*H_3)$_2$), 35.5, 34.6 (*C*(CH_3)$_3$), 31.6, 31.4 (C(*C*H_3)$_3$).

[Sb(O^{t}Bu){2,2'-CH(4-OMeC$_6$H$_4$)(O-4,6-^{t}Bu$_2$C$_6$H$_2$)$_2$-*κ*^{2}*O,O'*}] (7.15): Yield 84% (0.182 g, 0.252 mmol). ^{1}H NMR (C_6D_6): δ 1.34 (s, 18H, C(C*H*$_3$)$_3$), 1.50 (s, 9H, OC(C*H*$_3$)$_3$), 1.58 (s, 18H, C(C*H*$_3$)$_3$), 3.21 (s, 3H, OC*H*$_3$), 6.68 (d, *J* = 9.0 Hz, 2H, Ar*H*), 7.09 (s, 1H, bridge C*H*), 7.21 (d, *J* = 9.0 Hz, 2H, Ar*H*), 7.53 (d, *J* = 2.4 Hz, 2H, Ar*H*), 7.87 (b, 2H, Ar*H*). ^{13}C{^{1}H} NMR (C_6D_6): δ 157.9, 151.8, 144.1, 140.1, 139.4, 138.1, 130.4, 126.0, 121.8, 113.4 (aromatic carbons), 54.5 (O(*C*H_3), 40.9 (bridge *C*H), 35.5, 34.6, 33.7 (*C*(CH_3)$_3$), 31.6 (two ^{t}Bu peaks overlapping), 31.3 (C(*C*H_3)$_3$).

[Sb(NMe$_2$){2,2'-CH(4-OMeC$_6$H$_4$)(O-4,6-^{t}Bu$_2$C$_6$H$_2$)$_2$-*κ*^{2}*O,O'*}] (7.16): Yield 87% (0.181 g, 0.261 mmol). ^{1}H NMR (C_6D_6): δ 1.37 (s, 18H, C(C*H*$_3$)$_3$), 1.58 (s, 18H, C(C*H*$_3$)$_3$), 2.83 (s, 6H, N(C*H*$_3$)$_2$), 3.22 (s, 3H, OC*H*$_3$), 6.72 (d, *J* = 9.0 Hz, 2H, Ar*H*), 7.12 (s, 1H, bridge C*H*), 7.29 (d, *J* = 9.0 Hz, 2H, Ar*H*), 7.55 (d, *J* = 2.4 Hz, 2H, Ar*H*), 7.90 (d, *J* = 2.4 Hz, 2H, Ar*H*). ^{13}C{^{1}H} NMR (C_6D_6): δ 157.9, 153.4, 143.8, 139.8, 139.1, 138.4, 130.5, 125.9, 121.6, 113.3 (aromatic carbons), 54.5 (O(*C*H_3)), 40.7 (bridge *C*H), 38.9 (N(*C*H_3)$_2$), 35.5, 34.6 (*C*(CH_3)$_3$), 31.7, 31.5 (C(*C*H_3)$_3$).

[Sb(O^{t}Bu){2,2'-CH^{i}Pr(O-4,6-^{t}Bu$_2$C$_6$H$_2$)$_2$-*κ*^{2}*O,O'*}] (7.17): Yield 85% (0.168 g, 0.255 mmol). ^{1}H NMR (C_6D_6): δ 0.91 (d, *J* = 6.3 Hz, 6H, CH(C*H*$_3$)$_2$), 1.40 (s, 18H, C(C*H*$_3$)$_3$), 1.55 (s, 18H, C(C*H*$_3$)$_3$), 1.56 (s, 9H, OC(C*H*$_3$)$_3$), 2.61 (dsept, *J* = 6.3 Hz, *J* = 11.4 Hz, 1H, C*H*(CH_3)$_2$), 5.06 (d, *J* = 11.4 Hz, 1H, bridge C*H*), 7.45 (d, *J* = 2.4 Hz, 2H, Ar*H*), 7.78 (d, *J* = 2.4 Hz, 2H,

Ar*H*). $^{13}C\{^{1}H\}$ NMR (C_6D_6): δ 151.5, 144.2, 140.1, 139.1, 122.5, 121.1 (aromatic carbons), 44.5 (bridge *C*H), 35.4 (*C*H(CH_3)$_2$), 34.6, 34.2, 33.7 (*C*(CH_3)$_3$), 31.7 (two ^{t}Bu peaks overlapping), 31.2 (C(*C*H_3)$_3$), 21.6 (CH(*C*H_3)$_2$).

[Sb(NMe$_2$){2,2'-CH^{i}Pr(O-4,6-^{t}Bu$_2$C$_6$H$_2$)$_2$-*κ*^{2}*O,O'*}] (7.18): Yield 88% (0.166 g, 0.263 mmol). ^{1}H NMR (C_6D_6): δ 0.97 (d, *J* = 6.3 Hz, 6H, CH(C*H*$_3$)$_2$), 1.42 (s, 18H, C(C*H*$_3$)$_3$), 1.53 (s, 18H, C(C*H*$_3$)$_3$), 2.66 (dsept, *J* = 6.3 Hz, *J* = 11.4 Hz, 1H, C*H*(CH_3)$_2$), 2.93 (s, 6H, N(C*H*$_3$)$_2$), 5.07 (d, *J* = 11.4 Hz, 1H, bridge C*H*), 7.45 (d, *J* = 2.4 Hz, 2H, Ar*H*), 7.80 (d, *J* = 2.4 Hz, 2H, Ar*H*). $^{13}C\{^{1}H\}$ NMR (C_6D_6): δ 153.1, 143.8, 139.8, 138.9, 122.5, 120.9 (aromatic carbons), 44.4 (bridge *C*H), 38.9 (N(*C*H_3)$_2$), 35.4 (*C*H(CH_3)$_2$), 34.6, 34.1, (*C*(CH_3)$_3$), 31.8, 31.3 (C(*C*H_3)$_3$), 21.8 (CH(*C*H_3)$_2$).

[Sb(O^{t}Bu){2,2'-CH(4-MeC$_6$H$_4$)(O-4,6-^{t}Bu$_2$C$_6$H$_2$)$_2$-*κ*^{2}*O,O'*}] (7.19): Yield 80% (0.170 g, 0.240 mmol). ^{1}H NMR (C_6D_6): δ 1.34 (s, 18H, C(C*H*$_3$)$_3$), 1.50 (s, 9H, OC(C*H*$_3$)$_3$), 1.58 (s, 18H, C(C*H*$_3$)$_3$), 2.02 (s, 3H, ArC*H*$_3$), 6.91 (d, *J* = 8.1 Hz, 2H, Ar*H*), 7.16 (s, 1H, bridge C*H*), 7.25 (d, *J* = 8.1 Hz, 2H, Ar*H*), 7.54 (d, *J* = 2.4 Hz, 2H, Ar*H*), 7.87 (b, 2H, Ar*H*). $^{13}C\{^{1}H\}$ NMR (C_6D_6): δ 151.8, 144.1, 143.2, 140.1, 139.2, 134.7, 129.4, 128.6, 126.0, 121.8 (aromatic carbons), 41.4 (bridge *C*H), 35.5, 34.6, 33.7 (*C*(CH_3)$_3$), 31.6 (two ^{t}Bu signals overlapping), 31.3 (C(*C*H_3)$_3$), 30.0 (ArC*H*$_3$).

[Sb(NMe$_2$){2,2'-CH(4-MeC$_6$H$_4$)(O-4,6-^{t}Bu$_2$C$_6$H$_2$)$_2$-*κ*^{2}*O,O'*}] (7.20): Yield 78% (0.159 g, 0.234 mmol). ^{1}H NMR (C_6D_6): δ 1.36 (s, 18H, C(C*H*$_3$)$_3$), 1.57 (s, 18H, C(C*H*$_3$)$_3$), 2.03 (s, 3H, ArC*H*$_3$), 2.82 (s, 6H, N(C*H*$_3$)$_2$), 6.94 (d, *J* = 8.1 Hz, 2H, Ar*H*), 7.16 (s, 1H, bridge C*H*), 7.32 (d, *J* = 8.1 Hz, 2H, Ar*H*), 7.55 (d, *J* = 2.1 Hz, 2H, Ar*H*), 7.90 (d, *J* = 2.4 Hz, 2H, Ar*H*). $^{13}C\{^{1}H\}$ NMR (C_6D_6): δ 153.4, 143.8, 143.6, 139.8, 139.0, 134.7, 129.5, 128.6, 126.0, 121.6 (aromatic

carbons), 41.3 (bridge *C*H), 38.9 (N(*C*H_3)$_2$), 35.5, 34.6 (*C*(CH_3)$_3$), 31.7, 31.5 (C(*C*H_3)$_3$), 20.7 (ArC*H*$_3$).

[Sb(O^{t}Bu){2,2'-CHMe(O-4,6-^{t}Bu$_2$C$_6$H$_2$)$_2$-κ^2*O,O'*}] (7.21): Yield 83% (0.157 g, 0.249 mmol). ^{1}H NMR (C_6D_6): δ 1.38 (d, *J* = 7.5 Hz, 3H, CH-C*H*$_3$), 1.39 (s, 18H, C(C*H*$_3$)$_3$), 1.55 (s, 18H, C(C*H*$_3$)$_3$), 1.57 (s, 9H, OC(C*H*$_3$)$_3$), 5.68 (q, *J* = 7.5 Hz, 1H, bridge C*H*), 7.45 (d, *J* = 2.4 Hz, 2H, Ar*H*), 7.85 (d, *J* = 2.4 Hz, 2H, Ar*H*). ^{13}C{^{1}H} NMR (C_6D_6): δ 150.6, 144.3, 140.7, 140.2, 122.4, 121.4 (aromatic carbons), 35.4 (*C*(CH_3)$_3$), 34.7 (bridge *C*H), 33.8 (*C*(CH_3)$_3$), 31.7 (two ^{t}Bu peaks overlapping), 31.4 (C(*C*H_3)$_3$), 30.3 (*C*(CH_3)$_3$), 23.0 (CH-*C*H_3).

[Sb(NMe$_2$){2,2'-CHMe(O-4,6-^{t}Bu$_2$C$_6$H$_2$)$_2$-κ^2*O,O'*}] (7.22): Yield 92% (0.166 g, 0.276 mmol). ^{1}H NMR (C_6D_6): δ 1.41 (s, 18H, C(C*H*$_3$)$_3$), 1.54 (s, 18H, C(C*H*$_3$)$_3$), 1.66 (d, *J* = 7.8 Hz, 3H, CH-C*H*$_3$), 2.93 (s, 6H, N(C*H*$_3$)$_2$), 5.74 (q, *J* = 7.8 Hz, 1H, bridge C*H*), 7.47 (d, *J* = 2.4 Hz, 2H, Ar*H*), 7.88 (d, *J* = 2.4 Hz, 2H, Ar*H*). ^{13}C{^{1}H} NMR (C_6D_6): δ 152.2, 143.9, 140.4, 139.9, 122.3, 121.3 (aromatic carbons), 39.0 (N(*C*H_3)$_2$), 35.4, 34.7 (*C*(CH_3)$_3$), 31.83 (bridge *C*H), 31.81, 31.4 (C(*C*H_3)$_3$), 22.9 (CH-*C*H_3).

[Sb(O^{t}Bu){2,2'-CH(4-FC$_6$H$_4$)(O-4,6-^{t}Bu$_2$C$_6$H$_2$)$_2$-κ^2*O,O'*}] (7.23): Yield 90% (0.192 g, 0.270 mmol). ^{1}H NMR (C_6D_6): δ 1.32 (s, 18H, C(C*H*$_3$)$_3$), 1.49 (s, 9H, OC(C*H*$_3$)$_3$), 1.57 (s, 18H, C(C*H*$_3$)$_3$), 6.69 (dd, *J* = 8.7 Hz, 12.7 Hz, 2H, Ar*H*), 7.02 (s, 1H, bridge C*H*), 7.10 (dd, *J* = 8.7 Hz, 12.7 Hz, 2H, Ar*H*), 7.52 (d, *J* = 2.4 Hz, 2H, Ar*H*), 7.75 (d, *J* = 2.4 Hz, 2H, Ar*H*). ^{13}C{^{1}H} NMR (C_6D_6): δ 151.7, 144.3, 140.2, 138.9, 131.0, 139.9, 125.7, 122.0, 114.6, 144.3 (aromatic carbons), 41.2 (bridge *C*H), 35.5, 34.6, 33.7 (*C*(CH_3)$_3$), 31.6 (two ^{t}Bu peaks overlapping), 31.3 (C(*C*H_3)$_3$).

[Sb(NMe$_2$){2,2'-CH(4-FC$_6$H$_4$)(O-4,6-^{t}Bu$_2$C$_6$H$_2$)$_2$-κ^2*O,O'*}] (7.24): Yield 83% (0.169 g, 0.248 mmol). ^{1}H NMR (C_6D_6): δ 1.34 (s, 18H, C(C*H*$_3$)$_3$), 1.56 (s, 18H, C(C*H*$_3$)$_3$), 2.83 (s, 6H, N(C*H*$_3$)$_2$), 6.73 (dd, *J* = 8.7 Hz, *J* = 13.4 Hz, 2H, Ar*H*), 7.07 (s, 1H, bridge C*H*), 7.17 (dd, *J* = 8.7 Hz, *J* = 13.4 Hz, 2H, Ar*H*), 7.54 (d, *J* = 2.4 Hz, 2H, Ar*H*), 7.78 (d, *J* = 2.4 Hz, 2H, Ar*H*).

[Sb(O^{t}Bu){2,2'-CH(4-CF$_3$C$_6$H$_4$)(O-4,6-^{t}Bu$_2$C$_6$H$_2$)$_2$-κ^2*O,O'*}] (7.25): Yield 73% (0.167 g, 0.219 mmol). ^{1}H NMR (C_6D_6): δ 1.29 (s, 18H, C(C*H*$_3$)$_3$), 1.49 (s, 9H, OC(C*H*$_3$)$_3$), 1.57 (s, 18H, C(C*H*$_3$)$_3$), 7.05 (s, 1H, bridge C*H*), 7.16 (dd, *J* = 8.7 Hz, *J* = 13.4 Hz, 2H, Ar*H*), 7.22 (dd, *J* = 8.7 Hz, *J* = 13.4, 2H, Ar*H*), 7.53 (d, *J* = 2.4 Hz, 2H, Ar*H*), 7.68 (d, *J* = 2.4 Hz, 2H, Ar*H*).

[Sb(NMe$_2$){2,2'-CH(4-CF$_3$C$_6$H$_4$)(O-4,6-^{t}Bu$_2$C$_6$H$_2$)$_2$-κ^2*O,O'*}] (7.26): Yield 84% (0.185 g, 0.253 mmol). ^{1}H NMR (C_6D_6): δ 1.31 (s, 18H, C(C*H*$_3$)$_3$), 1.56 (s, 18H, C(C*H*$_3$)$_3$), 2.85 (s, 6H, N(C*H*$_3$)$_2$), 7.09 (s, 1H, bridge C*H*), 7.25 (s, 4H, Ar*H*), 7.55 (d, *J* = 2.1 Hz, 2H, Ar*H*), 7.71 (d, *J* = 2.4 Hz, 2H, Ar*H*).

[Sb(O^{t}Bu){2,2'-CHBn(O-4,6-^{t}Bu$_2$C$_6$H$_2$)$_2$-κ^2*O,O'*}] (7.27): Note: The solvent in this reaction was THF (same amounts as in general procedure).Yield 92% (0.195 g, 0.276 mmol). ^{1}H NMR (C_6D_6): δ 1.38 (s, 18H, C(C*H*$_3$)$_3$), 1.44 (s, 18H, C(C*H*$_3$)$_3$), 1.56 (s, 9H, OC(C*H*$_3$)$_3$), 3.38 (d, *J* = 8.1 Hz, 2H, CH-C*H*$_2$Ph), 5.81 (t, *J* = 8.1 Hz, 1H, bridge C*H*), 6.84 (t, *J* = 7.2 Hz, 1H, Ar*H*), 6.95 (t, *J* = 7.2 Hz, 2H, Ar*H*), 7.04 (m, *J* = 6.9 Hz, 2H, Ar*H*), 7.35 (d, *J* = 2.4 Hz, 2H, Ar*H*), 7.86 (d, *J* = 2.4 Hz, 2H, Ar*H*).

[Sb(NMe$_2$){2,2'-CHBn(O-4,6-^{t}Bu$_2$C$_6$H$_2$)$_2$-κ^2*O,O'*}] (7.28): Note: The solvent in this reaction was THF (same amounts as in general procedure).Yield 88% (0.179 g, 0.264 mmol). ^{1}H NMR (C_6D_6): δ 1.40 (s, 18H, C(C*H*$_3$)$_3$), 1.46 (s, 18H, C(C*H*$_3$)$_3$), 3.02 (s, 6H, N(C*H*$_3$)$_2$), 3.47 (d, *J* = 8.1 Hz, 2H, CH-C*H*$_2$Ph), 5.83 (t, *J* = 8.1 Hz, 1H, bridge C*H*), 6.88 (t, *J* = 7.5 Hz, 1H, Ar*H*),

6.99 (t, *J* = 7.5 Hz, 2H, Ar*H*), 7.14 (d, *J* = 8.1 Hz, 2H, Ar*H*), 7.33 (d, *J* = 2.4 Hz, 2H, Ar*H*), 7.89 (d, *J* = 2.4 Hz, 2H, Ar*H*).

[Sb(O^{t}Bu){2,2'-CH(2-OMe-5-BrC$_6$H$_3$)(O-4,6-^{t}Bu$_2$C$_6$H$_2$)$_2$-κ^2*O,O'*}] (7.29): Note: The solvent in this reaction was THF (same amounts as in general procedure). Yield 68% (0.164 g, 0.204 mmol). ^{1}H NMR (C_6D_6): δ 1.30 (s, 18H, C(C*H*$_3$)$_3$), 1.57 (s, 18H, C(C*H*$_3$)$_3$), 1.63 (s, 9H, OC(C*H*$_3$)$_3$), 3.02 (s, 3H, OC*H*$_3$), 6.25 (d, *J* = 8.7 Hz, 1H, Ar*H*), 7.15 (s, 1H, bridge C*H*), 7.19 (b, 1H, Ar*H*), 7.36 (d, *J* = 2.4 Hz, 2H, Ar*H*), 7.67 (d, *J* = 2.4 Hz, 2H, Ar*H*), 8.03 (b, 1H, Ar*H*).

[Sb(NMe$_2$){2,2'-CH(2-OMe-5-BrC$_6$H$_4$)(O-4,6-^{t}Bu$_2$C$_6$H$_2$)$_2$-κ^2*O,O'*}] (7.30): Note: The solvent in this reaction was THF (same amounts as in general procedure). Yield 64% (0.149 g, 0.193 mmol). ^{1}H NMR (C_6D_6): δ 1.28 (s, 18H, C(C*H*$_3$)$_3$), 1.51 (s, 18H, C(C*H*$_3$)$_3$), 3.07 (s, 3H, OC*H*$_3$), 3.13 (s, 6H, N(CH$_3$)$_2$), 6.51 (d, *J* = 8.7 Hz, 1H, Ar*H*), 7.07 (s, 1H, bridge C*H*), 7.27 (b, 1H, Ar*H*), 7.33 (d, *J* = 2.1 Hz, 2H, Ar*H*), 7.63 (d, *J* = 2.1 Hz, 2H, Ar*H*), 7.97 (b, 1H, Ar*H*).

7.3.2.3 Experiments for intramolecular Sb-C bond formation.

The detailed preparation for compounds **7.31** and **7.32** is described below. For complexes **7.33-7.35** the mole numbers, solvents, and temperatures of reactions are specified and their purifications follow similar procedures as those for **7.31** and **7.32**.

[Sb{2,2'-C(4-OMeC$_6$H$_4$)(O-4,6-^{t}Bu$_2$C$_6$H$_2$)$_2$-κ^3*C,O,O'*}] (7.31) : Method A: A colorless solution of compound **7.16** (0.0251 g, 0.0361 mmol) in 15 mL of a C_6H_6:THF (1:5) mixture was transferred into a solvent bomb that was closed under nitrogen. The colorless solution was allowed to heat in an isotemp bath set at 95 ^{o}C for 48 hrs. The small amount of insoluble material was removed by centrifugation and the light-yellow solution obtained was dried under vacuum to yield a yellowish solid. The solid was redissolved in 7 mL of pentane and the small amount of

insoluble material was removed by centrifugation to give a colorless solution. Once again the solvent was removed under vacuum to yield the product as a white solid in 78% yield (0.0183 g, 0.0282 mmol). The product **7.31** could also be obtained in 64% yield (0.0150 g, 0.0231 mmol) by using 10 mL of a THF:C_6H_6 (1:1) solvent mixture, but it was necessary to heat the reaction mixture for at least 6 days at 95 ^oC. Attempts to obtain the product using THF or C_6H_6 separately were unsuccessful.

Method B: A colorless solution of compound **7.15** (0.0261 g, 0.0361 mmol) in 15 mL of a C_6H_6:THF (1:1) mixture, was transferred into a solvent bomb that was closed under nitrogen. The colorless solution was allowed to heat in an isotemp bath set at 95 ^oC for 58 hrs. The final light-yellow solution was centrifuged to remove the small amount of solid and vacuum dried to yield a light-yellow solid. The solid was redissolved in 7 mL of pentane to give a colorless solution after removal of the insoluble material by centrifugation. The solvent was removed by vacuum to give the product as a white solid in 88% yield (0.0206 g, 0.0317 mmol). ^1H NMR (C_6D_6): δ 1.34 (s, 18H, C(C*H*$_3$)$_3$), 1.55 (s, 18H, C(C*H*$_3$)$_3$), 3.24 (s, 3H, OC*H*$_3$), 6.68 (d, *J* = 9.0 Hz, 2H, Ar*H*), 7.12 (d, *J* = 9.0 Hz, 2H, Ar*H*), 7.50 (d, *J* = 2.1 Hz, 2H, Ar*H*), 7.85 (d, *J* = 2.1 Hz, 2H, Ar*H*).

[Sb{2,2'-C(4-$CF_3C_6H_4$)(O-4,6-^{t}Bu$_2C_6H_2$)$_2$-κ^3*C,O,O'*}] (7.32) : Method A: A colorless solution of compound **7.26** (0.0265 g, 0.0362 mmol) in 15 mL of C_6H_6 was transferred into a solvent bomb that was closed under nitrogen. The colorless solution was allowed to heat in an isotemp bath set at 95 ^oC for 48 hrs. The small amount of insoluble material was removed by centrifugation and the yellowish solution obtained was dried under vacuum to yield a light-yellow solid. The solid was redissolved in 5 mL of pentane and the small amount of insoluble material was removed by centrifugation to give a light-yellow solution. The solvent was removed

under vacuum to yield the product as an off-yellow solid in 75% yield (0.0188 g, 0.0273 mmol). Attempts to obtain the product using THF or a 1:5 THF:C_6H_6 mixture were unsuccessful, yielding only decomposition to the parent bisphenol. ^{1}H NMR (C_6D_6): δ 1.29 (s, 18H, C(CH_3)$_3$), 1.49 (s, 18H, C(CH_3)$_3$), 7.09 (d, *J* = 8.4 Hz, 2H, Ar*H*), 7.24 (d, *J* = 8.4 Hz, 2H, Ar*H*), 7.49 (d, *J* = 2.1 Hz, 2H, Ar*H*), 7.67 (d, *J* = 2.1 Hz, 2H, Ar*H*).

[Sb{2,2'-C(4-$NO_2C_6H_4$)(O-4,6-^{t}Bu$_2$$C_6H_2$)$_2$-$\kappa^3$*C,O,O'*}] (7.33) : Method A: A colorless solution of compound **7.14** (0.0256 g, 0.0358 mmol) in 15 mL of C_6H_6:THF (1:5) was transferred into a solvent bomb that was closed under nitrogen. The colorless solution was allowed to heat in an isotemp bath set at 75 ^{o}C for 48 hrs. After workup and purification (see **7.32** procedure) the product was obtained as an off-yellow solid in 90% yield (0.0213 g, 0.0321 mmol).

Method B: The product **7.33** could also be obtained in 63% yield (0.0149 g, 0.0224 mmol) by heating complex **7.14** at 95 ^{o}C in 10 mL of C_6H_6, but it was necessary to heat the reaction mixture for at least 2 weeks. Attempts to obtain complex **7.33** from the heating of precursor **7.13** in different solvents and temperatures always resulted in mixtures of unknown products that were hard to isolate. ^{1}H NMR (C_6D_6): δ 1.26 (s, 18H, C(CH_3)$_3$), 1.58 (s, 18H, C(CH_3)$_3$), 6.82 (d, *J* = 8.7 Hz, 2H, Ar*H*), 7.25 (d, *J* = 2.1 Hz, 2H, Ar*H*), 7.33 (d, *J* = 2.1 Hz, 2H, Ar*H*), 7.82 (d, *J* = 8.7 Hz, 2H, Ar*H*).

[Sb{2,2'-C(4-FC_6H_4)(O-4,6-^{t}Bu$_2$$C_6H_2$)$_2$-$\kappa^3$*C,O,O'*}] (7.34) : Method A: A colorless solution of compound **7.24** (0.0247 g, 0.0362 mmol) in 15 mL of C_6H_6:THF (1:5), was transferred into a solvent bomb that was closed under nitrogen. The colorless solution was allowed to heat in an isotemp bath set at 95 ^{o}C for 72 hrs. After workup and purification (see **7.32** procedure) the product was obtained as a white solid in 84% yield (0.0193 g, 0.0303 mmol).

Method B: A colorless solution of compound **7.23** (0.0257 g, 0.0361 mmol) in 10 mL of a 1:5 C_6H_6:THF mixture was transferred into a solvent bomb that was closed under nitrogen. The colorless solution was allowed to heat in an isotemp bath set at 95 ^oC for 4 d. After purification (see **7.32** procedure) the product was isolated as a white solid in 80% yield (0.0184 g, 0.0289 mmol). ^1H NMR (C_6D_6): δ 1.31 (s, 18H, C(C*H*$_3$)$_3$), 1.51 (s, 18H, C(C*H*$_3$)$_3$), 6.70 (dd, *J* = 8.7 Hz, *J* = 13.4 Hz, 2H, Ar*H*), 7.01 (m, 2H, Ar*H*), 7.49 (d, *J* = 2.4 Hz, 2H, Ar*H*), 7.74 (d, *J* = 2.1 Hz, 2H, Ar*H*).

[Sb{2,2'-C(4-MeC$_6$H$_4$)(O-4,6-^{t}Bu$_2$C$_6$H$_2$)$_2$-*κ*^{3}*C,O,O'*}] (7.35): Method A: A colorless solution of compound **7.20** (0.0245 g, 0.0361 mmol) in 15 mL of C_6H_6:THF (1:5) was transferred into a solvent bomb that was closed under nitrogen. The colorless solution was allowed to heat in an isotemp bath set at 95 ^oC for 72 h. After workup and purification (see **7.32** procedure) the product was isolated as a white solid in 71% yield (0.0162 g, 0.0256 mmol).

Method B: A colorless solution of compound **7.19** (0.0256 g, 0.0362 mmol) in 10 mL of a C_6H_6:THF (1:5) mixture was transferred into a solvent bomb that was closed under nitrogen. The colorless solution was allowed to heat in an isotemp bath set at 95 ^oC for 6 d. After workup and purification (see **7.32** procedure) the product was isolated as a white solid in 77% yield (0.0176 g, 0.0278 mmol). ^1H NMR (C_6D_6): δ 1.33 (s, 18H, C(C*H*$_3$)$_3$), 1.53 (s, 18H, C(C*H*$_3$)$_3$), 2.05 (s, 3H, ArC*H*$_3$), 6.91 (d, *J* = 8.1 Hz, 2H, Ar*H*), 7.25 (d, *J* = 8.1 Hz, 2H, ArH), 7.50 (d, *J* = 2.4 Hz, 2H, Ar*H*), 7.84 (d, *J* = 2.4 Hz, 2H, Ar*H*).

7.3.3 General X-ray Information.

X-ray data for **7.9** and **7.33** were collected on a SMART Bruker 1000 CCD detector diffractometer at low temperature using Mo Kα radiation. The crystallographic data and some details of the data collection and refinement of the structures are given in Table 7.2. Absorption

corrections in all cases were applied by SADABS.[101] All structures were solved by direct methods and subsequent difference Fourier syntheses and refined by full matrix least-squares methods against F^2 (SHELX 97).[102] All non-hydrogen atoms were refined with anisotropic displacement coefficients, except atoms of disordered fragments which were refined with isotropic thermal parameters. The H atoms in structures were taken in calculated positions. The programs ORTEP32[104] and POV-ray[105] were used to generate the X-ray structural diagrams pictured in this Chapter.

Table 7.2. Crystallographic data for complexes **7.9** and **7.33**

	7.10	**7.33·3DMSO**
Formula	$C_{32}H_{50}O_2$	$C_{41}H_{62}NO_7S_3Sb$
Fw	466.72	898.85
cryst syst	Monoclinic	Monoclinic
space group	$P2_1/n$	$P2_1/c$
T, K	213(2)	218(2)
a, Å	15.152(2)	14.941(3)
b, Å	11.9261(17)	18.681(3)
c, Å	17.225(2)	17.587(3)
α, deg	90	90
β, deg	107.118(4)	112.470(3)
γ, deg	90	90
V, A^3	2974.7(7)	4536.1(14)
Z	4	4
d_{calcd} g·cm^{-3}	1.042	1.316
μ, mm^{-1}	0.062	0.791
Refl collected	4793	18118
T_{min}/ T_{max}	0.992	0.956
N_{measd}	4156	6507
[R_{int}]	[0.0689]	[0.0628]
R [I>2sigma(I)]	0.0506	0.0404
R (all data)	0.1073	0.0630
R_w [I>2sigma(I)]	0.1091	0.0964
R_w (all data)	0.1304	0.1052
GOF	0.849	0.931

7.4 Conclusions

We have reported the preparation of a series of antimony(III) bisphenolates **7.11-7.30** containing terminal Sb-O^{t}Bu and Sb-NMe_2 groups**.** The synthesis of these complexes consists of the simple addition of M(O^{t}Bu)$_3$ (M = Bi, Sb) or Sb(NMe_2)$_3$ to the parent bisphenol in pentane or

hexane. ^{1}H NMR spectra show that the bisphenol ligands on complexes **7.11-7.30** contain C_s symmetry with a bridging methylene as center of symmetry. Complexes **7.11-7.30** all have very good solubility in most organic solvents and terminal Sb-O^{t}Bu or Sb-NMe_2 groups that make them interesting precursors for more extended structures.

We performed a series of experiments to induce intramolecular Sb-C bond formation in all of the bisphenolate complexes **7.11-7.30**, using several temperatures and reaction solvents. However, we only observed significant Sb-C bond formation in the complexes supported by ligands **7.2**, **7.3**, and **7.5-7.7**.

Complexes **7.31-7.35** with Sb-C bonds were prepared by heating the appropriate antimony precursor but we found that the selection of the right solvent, temperature, and time of reaction is very important for yielding clean products. Intramolecular Sb-C bond formation is faster when using complexes containing terminal Sb-NMe_2 bonds. The crystal structure of complex **7.31** is monomeric and confirms the presence of the Sb-C bond and the mirror plane observed in solution.

References:

(1) Gates, B. C.; Katzer, J. R.; Schuit, G. C. A. *Chemistry of Catalytic Processes*; McGraw-Hill: New York, 1979.

(2) Idol, J. D., Process for the Manufacture of Acrylonitrile. US Patent 2,904,580, September 15, 1959.

(3) Callahan, J. L.; Foreman, R. W.; Veatch, F., Attrition Resistant Oxidation Catalyst. U.S. Patent 3,044,966, July 17, 1962.

(4) Limberg, C. *Top. Organomet. Chem.* **2007**, *22*, 79-95.

(5) Graselli, R. K. In *Handbook of Heterogeneous Catalysis*; Ertl, G., Knozinger, H., Weitkamp, J., Eds.; VCH Verlagsgesellschaft mbH: Weinheim, 1997; Vol. 5, pp 2302-2326.

(6) Hanna, T. A. *Coord. Chem. Rev.* **2004**, *248*, 429-440.

(7) Jang, Y. H.; Goddard, W. A., III. *Top. Catal.* **2001**, *15*, 273-289.

(8) Kim, Y. C.; Ueda, W.; Moro-oka, Y. *Appl. Catal.* **1991**, *70*, 189-196.

(9) Kim, Y. C.; Ueda, W.; Moro-oka, Y. *Catal. Today* **1992**, *13*, 673-678.

(10) Kim, J. S.; Woo, S. I. *Appl. Catal., A* **1994**, *110*, 207-216.

(11) Kim, J. S.; Woo, S. I. *Appl. Catal., A* **1994**, *110*, 173-184.

(12) Ushikubo, T.; Oshima, K.; Kayou, A.; Vaarkamp, M.; Hatano, M. *J. Catal.* **1997**, *169*, 394-396.

(13) Limberg, C. *Angew. Chem. Int. Ed.* **2003**, *42*, 5932-5954.

(14) Hall, K. A.; Mayer, J. M. *J. Am. Chem. Soc.* **1992**, *114*, 10402-10411.

(15) Borgmann, C.; Limberg, C.; Cunskis, S.; Kircher, P. *Eur. J. Inorg. Chem.* **2001**, 349-352.

(16) Green, M. L. H.; Konidaris, P. C.; Mountford, P. *J. Chem. Soc., Dalton Trans.* **1994**, 2975-2982.

(17) Radius, U.; Sundermeyer, J.; Peters, K.; Von Schnering, H. G. *Z. Anorg. Allg. Chem.* **2002**, *628*, 1226-1235.

(18) Rodrigues, C. W.; Limberg, C.; Pritzkow, H. *Eur. J. Inorg. Chem.* **2004**, 3644-3650.

(19) Rodrigues, C. W.; Antelmann, B.; Limberg, C.; Kaifer, E.; Pritzkow, H. *Organometallics* **2001**, *20*, 1825-1831.

(20) Chan, D. M. T.; Fultz, W. C.; Nugent, W. A.; Roe, D. C.; Tulip, T. H. *J. Am. Chem. Soc.* **1985**, *107*, 251-253.

(21) Chan, D. M. T.; Nugent, W. A. *Inorg. Chem.* **1985**, *24*, 1422-1424.

(22) Belgacem, J.; Kress, J.; Osborn, J. A. *J. Am. Chem. Soc.* **1992**, *114*, 1501-1502.

(23) Belgacem, J.; Kress, J.; Osborn, J. A. *J. Mol. Cat.* **1994**, *86*, 267-285.

(24) Du, Y.; Rheingold, A. L.; Maatta, E. A. *Inorg. Chem.* **1994**, *33*, 6415-6418.

(25) Maatta, E. A.; Du, Y.; Rheingold, A. L. *J. Chem. Soc., Chem. Commun.* **1990**, 756-757.

(26) Maatta, E. A.; Du, Y. *J. Am. Chem. Soc.* **1988**, *110*, 8249-8250.

(27) Du, Y.; Rheingold, A. L.; Maatta, E. A. *J. Chem. Soc., Chem. Commun.* **1994**, 2163-2164.

(28) Du, Y.; Rheingold, A. L.; Maatta, E. A. *J. Am. Chem. Soc.* **1992**, *114*, 345-346.

(29) Mohs, T. R.; Du, Y.; Plashko, B.; Maatta, E. A. *Chem. Commun.* **1997**, 1707-1708.

(30) Proust, A.; Thouvenot, R.; Chaussade, M.; Robert, F.; Gouzerh, P. *Inorg. Chim. Acta* **1994**, *224*, 81-95.

(31) Kinne, M.; Heidenreich, A.; Rademann, K. *Angew. Chem. Int. Ed.* **1998**, *37*, 2509-2511.

(32) Fielicke, A.; Rademann, K. *J. Phys. Chem. A* **2000**, *104*, 6979-6982.

(33) Hanna, T. A.; Rieger, A. L.; Rieger, P. H.; Wang, X. *Inorg. Chem.* **2002**, *41*, 3590-3592.

(34) Klemperer, W. G.; Liu, R.-S. *Inorg. Chem.* **1980**, *19*, 3863-3864.

(35) Roggan, S.; Limberg, C.; Ziemer, B. *Angew. Chem. Int. Ed.* **2005**, *44*, 5259-5262.

(36) Villanneau, R.; Proust, A.; Robert, F.; Gouzerh, P. *J. Chem. Soc., Dalton Trans.* **1999**, 421-426.

(37) Hunger, M.; Limberg, C.; Kircher, P. *Angew. Chem. Int. Ed.* **1999**, *38*, 1105-1108.

(38) Hunger, M.; Limberg, C.; Kircher, P. *Organometallics* **2000**, *19*, 1044-1050.

(39) Hunger, M.; Limberg, C.; Kaifer, E.; Rutsch, P. *J. Organomet. Chem.* **2002**, *641*, 9-14.

(40) Roggan, S.; Limberg, C.; Brandt, M.; Ziemer, B. *J. Organomet. Chem.* **2005**, *690*, 5282-5289.

(41) Roggan, S.; Schnakenburg, G.; Limberg, C.; Sandhöfner, S.; Pritzkow, H.; Ziemer, B. *Chem. Eur. J.* **2005**, *11*, 225-234.

(42) Roggan, S.; Limberg, C.; Ziemer, B.; Brandt, M. *Angew. Chem. Int. Ed.* **2004**, *43*, 2846-2849.

(43) Kou, X.; Wang, X.; Mendoza-Espinosa, D.; Zakharov, L. N.; Brien, K. A.; Jayarathna, L. K.; Rheingold, A. L.; Watson, W. H.; Hanna, T. A. **2009**, Submitted to *Inorg. Chem.*

(44) Hanna, T. A.; Incarvito, C. D.; Rheingold, A. L. *Inorg. Chem.* **2000**, *39*, 630-631.

(45) Hanna, T. A.; Ghosh, A. K.; Ibarra, C.; Mendez-Rojas, M. A.; Rheingold, A. L.; Watson, W. H. *Inorg. Chem.* **2004**, *43*, 1511-1516.

(46) Hanna, T. A.; Ghosh, A. K.; Ibarra, C.; Zakharov, L. N.; Rheingold, A. L.; Watson, W. H. *Inorg. Chem.* **2004**, *43*, 7567-7569.

(47) Gutsche, C. D. *Calixarenes Revisited: Monographs In Supramolecular Chemistry*; The Royal Society of Chemistry: Cambridge, UK, 1998.

(48) Thondorf, I.; Shivanyuk, A.; Böhmer, V. In *Calixarenes 2001*; Asfari, Z., Böhmer, V., Harrowfield, J., Vicens, J., Eds.; Kluwer Academic Publishers: Boston, 2001, p 26-53.

(49) Gutsche, C. D. *Calixarenes*; Royal Society of Chemistry: Cambridge, 1989.

(50) Böhmer, V. *Angew. Chem. Int. Ed.* **1995**, *34*, 713-745.

(51) Sliwa, W. *J. Inclusion Phenom. Macrocyclic Chem.* **2005**, *52*, 13-37.

(52) Corazza, F.; Floriani, C.; Chiesi-Villa, A.; Guastini, C. *J. Chem. Soc., Chem. Commun.* **1990**, 640-641.

(53) Giannini, L.; Solari, E.; Zanotti-Gerosa, A.; Floriani, C.; Chiesi-Villa, A.; Rizzoli, C. *Angew. Chem. Int. Ed.* **1997**, *36*, 753-754.

(54) Giannini, L.; Solari, E.; Dovesi, S.; Floriani, C.; Re, N.; Chiesi-Villa, A.; Rizzoli, C. *J. Am. Chem. Soc.* **1999**, *121*, 2784-2796.

(55) Giannini, L.; Guillemot, G.; Solari, E.; Floriani, C.; Re, N.; Chiesi-Villa, A.; Rizzoli, C. *J. Am. Chem. Soc.* **1999**, *121*, 2797-2807.

(56) Guillemot, G.; Solari, E.; Floriani, C.; Re, N.; Rizzoli, C. *Organometallics* **2000**, *19*, 5218-5230.

(57) Liu, L.; Zakharov, L. N.; Rheingold, A. L.; Hanna, T. A. *Chem. Commun.* **2004**, 1472-1473.

(58) Liu, L.; Zakharov, L. N.; Golen, J. A.; Rheingold, A. L.; Hanna, T. A. *Inorg. Chem.* **2008**, *47*, 11143-11153.

(59) Young, C. G. *Comprehensive Coordination Chemistry II*; McCleverty, J. A.; Meyer, T. J Eds.; Elsevier: Amsterdam, 2004; Vol. 4.

(60) Redshaw, C.; Elsegood, M. R. J. *Eur. J. Inorg. Chem.* **2003**, 2071-2074.

(61) Redshaw, C. *Coord. Chem. Rev.* **2003**, *244*, 45-70.

(62) Radius, U. *Inorg. Chem.* **2001**, *40*, 6637-6642.

(63) Millar, A. J.; White, J. M.; Doonan, C. J.; Young, C. G. *Inorg. Chem.* **2000**, *39*, 5151 5155.

(64) Mongrain, P.; Douville, J.; Gagnon, J.; Drouin, M.; Decken, A.; Fortin, D.; Harvey, P. D. *Can. J. Chem.* **2004**, *82*, 1452-1461.

(65) Liu, L.; Zakharov, L. N.; Golen, J. A.; Rheingold, A. L.; Watson, W. H.; Hanna, T. A. *Inorg. Chem.* **2006**, *45*, 4247-4260.

(66) Gutsche, C. D. In *Topics in Current Chemistry*; Boschke, F. L., Ed.; Springer-Verlag: 1984; Vol. 123, p 1-47.

(67) Arnecke, R.; Böhmer, V.; Caccipaglia, R.; Cort, A. D.; Mandollini, L. *Tetrahedron* **1997**, *53*, 4901-4908.

(68) Haino, T.; Yanase, M.; Fukazawa, Y. *Angew. Chem. Int. Ed.* **1997**, 259-260.

(69) Schwing, M. J.; McKervey, M. A. In *Calixarenes: A Versatile Class of Macrocyclic Compounds*; Vicens, J., Böhmer, V., Eds.; Kluwer, Dordrecht: 1991, p 149-172.

(70) Floriani, C.; Floriani-Moro, R. *Adv. Organomet. Chem.* **2001**, *147*, 167-233.

(71) Floriani, C. *Chem. Eur. J.* **1999**, *5*, 19-23.

(72) Coleman, A. W.; Bott, S. G.; Morley, S. D.; Means, C. M.; Robinson, K. D.; Zhang, H.; Atwood, J. L. *Angew. Chem. Int. Ed.* **1988**, *27*, 1361-1362.

(73) Weiser, C.; Dieleman, C. B.; Matt, D. *Coord. Chem. Rev.* **1997**, *165*, 93-161.

(74) Hanna, T. A.; Liu, L.; Angeles-Boza, A. M.; Kou, X.; Gutsche, C. D.; Ejsmont, K.; Watson, W. H.; Zakharov, L. N.; Incarvito, C. D.; Rheingold, A. L. *J. Am. Chem. Soc.* **2003**, *125*, 6228-6238.

(75) Hanna, T. A.; Liu, L.; Zakharov, L. N.; Rheingold, A. L.; Watson, W. H.; Gutsche, C. D. *Tetrahedron* **2002**, 9751-9757.

(76) Hamada, F.; Robinson, K. D.; Orr, G. W.; Atwood, J. *Supramol. Chem.* **1993**, 19-24.

(77) Gueneau, D. E.; Fromm, K. M.; Goesmann, H. *Chem. Eur. J.* **2003**, *9*, 509-514.

(78) Charbonniere, L. J.; Balsiger, C.; Schenk, K. J.; Bünzli, J.-L. G. *J. Chem. Soc., Dalton Transactions* **1998**, 505-510.

(79) Stewart, D. R.; Krawiec, M.; Kashyap, R. P.; Watson, W. H.; Gutsche, C. D. *J. Am. Chem. Soc.* **1995**, *117*, 586-601.

(80) Arnaud-Neu, F.; Asfari, Z.; Souley, B.; Vicens, J.; Thuéry, P.; Nierlich, M. *J. Chem. Soc., Perkin Trans. 2* **2000**, 495-499.

(81) Petrella, A.; Roberts, N. K.; Craig, D. C.; Raston, C. L.; Lamb, R. N. *Chem. Commun.* **2003**, 1728-1729.

(82) Bell, S. E. J.; Browne, J. K.; McKee, V.; McKervey, M. A.; Malone, J. F.; O'Leary, M.; Walker, A. *J. Org. Chem.* **1998**, *63*, 489-501.

(83) Martino, M.; Gregoli, L.; Gaeta, C.; Neri, P. *Org. Lett.* **2002**, *4*, 1531-1534.

(84) Martino, M.; Gaeta, C.; Neri, P. *Tetrahedron Lett.* **2004**, *45*, 3387-3391.

(85) Gaeta, C.; Martino, M.; Neri, P. *Org. Lett.* **2006**, *8*, 4409-4412.

(86) Jin, T.; Kinjo, M.; Kobayashi, Y.; Hirata, H. *J. Chem. Soc., Faraday Trans.* **1998**, *94*, 3135-3140.

(87) Stewart, D. R.; Gutsche, C. D. *J. Am. Chem. Soc.* **1999**, *121*, 4136-4146.

(88) Thuéry, P.; Asfari, Z.; Vicens, J.; Lamare, V.; Dozol, J. F. *Polyhedron* **2002**, *21*, 2497-2503.

(89) Harrowfield, J. M.; Ogden, M. I.; Richmond, W. R.; White, A. H. *J. Chem. Soc., Chem. Commun.* **1991**, 1159-1161.

(90) Murayama, K.; Aoki, K. *Inorg. Chim. Acta* **1998**, *281*, 36-42.

(91) Boyle, T. J.; Pedrotty, D. M.; Alam, T. M.; Vick, S. C.; Rodriguez, M. A. *Inorg. Chem.* **2000**, *39*, 5133-5146.

(92) Bradley, D. C.; Mehrotra, R. C.; Rothwell, I. P.; Singh, A. *Alkoxo and Aryloxo Derivatives of Metals*; Academic Press: New York, 2001.

(93) Gordon, B. W.; Scott, M. J. *Inorg. Chim. Acta* **2000**, *297*, 206-216.

(94) Davidson, M. G.; Howard, J. A.; Lamb, S.; Lehmann, C. W. *Chem. Commun.* **1997**, 1607-1608.

(95) Guillemot, G.; Solari, E.; Rizzoli, C.; Floriani, C. *Chem. Eur. J.* **2002**, *8*, 2072-2080.

(96) Steed, J. W.; Johnson, C. P.; Barnes, C. L.; Juneja, R. K.; Atwood, J. L.; Reilly, S.; Hollis, R. L.; Smith, P. H.; Clark, D. L. *J. Am. Chem. Soc.* **1995**, *117*, 11426-11433.

(97) Stewart, D. R.; Gutsche, C. D. *Org. Prep. Proc. Int.* **1993**, *25*, 137-139.

(98) Gutsche, C. D.; Bauer, L. J. *J. Am. Chem. Soc.* **1985**, *107*, 6052-6059.

(99) Kanamathareddy, S.; Gutsche, C. D. *J. Org. Chem.* **1994**, *59*, 3871-3879.

(100) Friebolin, H. *Basic One- and Two-Dimensional NMR Spectroscopy* Wiley-VCH: Weinheim, 1998.

(101) Sheldrick, G. M. *SADABS, Program for Empirical Absorption Correction of Area Detector Data*; University of Göttingen: Göttingen, Germany, 1996.

(102) Sheldrick, G. M. *SHELXS-97, Program for Crystal Structure Solution and Refinement*; Institut Für Anorganische Chemie: Gottingen, Germany, 1998.

(103) van der Sluis, P. V.; Spek, A. L. *Acta Crystallogr.* **1990**, *A46*, 194-201.

(104) Farrugia, L. J. *J. Appl. Crystallogr.* **1997**, *30*, 565-566.

(105) POVRAY v. 3.5 Persistence of Vision Raytracer, Williamston, Victoria, Australia 2002. Retrieved from http://www.povray.org.

(106) Homden, D. M.; Redshaw, C. *Chem. Rev.* **2008**, *108*, 5086-5130.

(107) Quinlan, E.; Matthews, S. E.; Gunnlaugsson, T. *Tetrahedron Lett.* **2006**, *47*, 9333-9338.

(108) Quinlan, E.; Matthews, S. E.; Gunnlaugsson, T. *J. Org. Chem.* **2007**, *72*, 7497-7503.

(109) Matthews, S. E.; Schmitt, P.; Felix, V.; Drew, M. G. B.; Beer, P. D. *J. Am. Chem. Soc.* **2002**, *124*, 1341-1353.

(110) Matthews, S. E.; Parzuchowski, P.; Garcia-Carrera, A.; Gruttner, C.; Dozol, J. F.; Böhmer, V. *Chem. Commun.* **2001**, 417-418.

(111) Mehring, M. *Coord. Chem. Rev.* **2007**, *251*, 974-1006.

(112) McBurnett, B. G.; Cowley, A. H. *Chem. Commun.* **1999**, 17-18.

(113) Hascall, T.; Rheingold, A. L.; Guzei, I.; Parkin, G. *Chem. Commun.* **1998**, 101-102.

(114) Shang, S.; Khasnis, D. V.; Zhang, H.; Small, A. C.; Fan, M.; Lattman, M. *Inorg. Chem.* **1995**, *34*, 3610-3615.

(115) Gardiner, M. G.; Lawrence, S. M.; Raston, C. L.; Skelton, B. W.; White, A. H. *Chem. Commun.* **1996**, 2491-2492.

(116) Atwood, J. L.; Gardiner, M. G.; Jones, C.; Raston, C. L.; Skelton, B. W.; White, A. H. *Chem. Commun.* **1996**, 2487-2488.

(117) Wetherby, A. E.; Goeller, L. R.; DiPascale, A. G.; Rheingold, A. L.; Weinert, C. S. *Inorg. Chem.* **2007**, *46*, 7579-7586.

(118) Arimori, S.; Davidson, M. G.; Fyles, T. M.; Hibbert, T. G.; James, T. D.; Kociok-Köhn, G. I. *Chem. Commun.* **2004**, 1640-1641.

(119) Redshaw, C.; Elsegood, M. R. J. *Chem. Commun.* **2005**, 5056-5058.

(120) Mendoza-Espinosa, D.; Martínez-Ortega, B. A.; Quiroz-Guzmán, M.; Golen, J. A.; Rheingold, A. L.; Hanna, T. A. *J. Organomet. Chem.* **2009**, *694*, 1509-1523.

(121) Mendoza-Espinosa, D.; Rheingold, A. L.; Hanna, T. A. *Dalton Trans.* **2009**, 5226-5238.

(122) Khasnis, D. V.; Lattman, M.; Gutsche, C. D. *J. Am. Chem. Soc.* **1990**, *112*, 9422-9423.

(123) Fan, M.; Shevchenko, I. V.; Voorhies, R. H.; Eckert, S. F.; Zhang, H.; Lattman, M. *Inorg. Chem.* **2000**, *39*, 4704-4712.

(124) Shang, S.; Khasnis, D. V.; Burton, J. M.; Santini, C. J.; Fan, M.; Small, A. C.; Lattman, M. *Organometallics* **1994**, *13*, 5157-5159.

(125) Fan, M.; Zhang, H.; Lattman, M. *Organometallics* **1996**, *15*, 5216-5219.

(126) Sood, P.; Zhang, H.; Lattman, M. *Organometallics* **2002**, *21*, 4442-4447.

(127) Paalasmaa, S.; Mansfeld, D.; Schurmann, M.; Mehring, M. *Z. Anorg. Allg. Chem.* **2005**, *631*, 2433-2438.

(128) Veith, M.; Yu, E. C.; Huch, V. *Chem. Eur. J.* **1995**, *1*, 26-32.

(129) Mehring, M.; Mansfeld, D.; Costisella, B.; Schurmann, M. *Eur. J. Inorg. Chem.* **2006**, 735-739.

(130) Fan, M.; Zhang, H.; Lattman, M. *Chem. Commun.* **1998**, 99-100.

(131) Fan, M.; Zhang, H.; Lattman, M. *Inorg. Chem.* **2006**, *45*, 6490-6496.

(132) Attempts to perform VT-NMR for a more accurate conformational analysis of complexes **5** and **8** were unsuccessful due to their limited solubility.

(133) Gibson, V.; Redshaw, C.; Clegg, W.; Elsegood, M. R. J. *Polyhedron* **1997**, *16*, 4385-4387.

(134) Bukhaltsev, E.; Goldberg, I.; Vigalok, A. *Organometallics* **2004**, *23*, 4540-4543.

(135) Bukhaltsev, E.; Goldberg, I.; Vigalok, A. *Organometallics* **2005**, *24*, 5732-5736.

(136) Sood, P.; Koutha, M.; Fan, M.; Klichko, Y.; Zhang, H.; Lattman, M. *Inorg. Chem.* **2004**, *43*, 2975-2980.

(137) Breunig, H. J.; Kruger, T.; Lork, E. *J. Organomet. Chem.* **2002**, *648*, 209-213.

(138) Tanski, J. M.; Kelly, B. V.; Parkin, G. *Dalton Trans.* **2005**, 2442-2447.

(139) Horley, G. A.; Mahon, F. M.; Molloy, K. C.; Venter, M. M.; Haycock, P. W.; Myers, C. P. *Inorg. Chem.* **2002**, *41*, 1652-1657.

(140) Evans, D. G.; Boeyens, J. C. A. *Acta Cryst.* **1988**, *B44*, 663-671.

(141) Mansfeld, D.; Mehring, M.; Schurmann, M. *Z. Anorg. Allg. Chem.* **2004**, *630*, 1795-1797.

(142) Jones, C. M.; Burkart, M. D.; Whitmire, K. H. *Angew. Chem. Int. Ed.* **1992**, *31*, 451-452.

(143) Turner, L. E.; Davidson, M. G.; Jones, M. D.; Ott, H.; Schulz, V. S.; Wilson, P. J. *Inorg. Chem.* **2006**, *45*, 6123-6125.

(144) Mansfeld, D.; Mehring, M.; Schurmann, M. *Angew. Chem. Int. Ed.* **2005**, *44*, 245-249.

(145) Evans, W. J.; Hain, J. H.; Ziller, J. W. *J. Chem. Soc. Chem. Commun.* **1989**, 1628-1629.

(146) Whitmire, K. H.; Hoppe, S.; Sydora, O.; Jolas, J. L.; Jones, M. C. *Inorg. Chem.* **2000**, *39*, 85-97.

(147) Mehring, M.; Paalasmaa, S.; Schurmann, M. *Eur. J. Inorg. Chem.* **2005**, 4891-4901.

(148) Mehring, M.; Mansfeld, D.; Paalasmaa, S.; Schurmann, M. *Chem. Eur. J.* **2006**, *12*, 1767-1781.

(149) Hinz-Hübner, D. *Z. Anorg. Allg. Chem.* **2002**, *628*, 1811-1814.

(150) Uchiyama, Y.; Kano, N.; Kawashima, T. *Organometallics* **2001**, *20*, 2440-2442.

(151) Massiani, M. C.; Papiernik, R.; Hubert-Pfalzgraf, L. G.; Daran, J. C. *J. Chem. Soc. Chem. Commun.* **1990**, 301-302.

(152) Cass, E. M.; Hii, K. K.; Rzepa, H. S. *J. Chem. Educ.* **2006**, *83*, 336.

(153) Souley, B.; Asfari, Z.; Vicens, J. *Pol. J. Chem.* **1992**, *66*, 959-961.

(154) Böhmer, D.; Rathay, H.; Kammerer, H. *Org. Prep. Proc. Int.* **1978**, *10*, 113-121.

(155) Bochmann, M.; Song, X.; Hursthouse, M. B.; Karaulov, A. *J. Chem. Soc. Dalton Trans.* **1995**, 1649-1652.

(156) Russias, C.; Damm, F.; Deluzarche, A.; Maillard, A. *Bull. Soc. Chim. Fr.* **1966**, *7*, 2275-2277.

(157) Hubert-Pfalzgraf, L. G. *Coord. Chem. Rev.* **1998**, *178-180*, 967-997.

(158) Radius, U. *Z. Anorg. Allg. Chem.* **2004**, *630*, 957-972.

(159) Mendoza-Espinosa, D.; Hanna, T. A. *Dalton Trans.* **2009**, 5211-5225.

(160) Petrella, A. J.; Roberts, N. K.; Craig, D. C.; Raston, C. L.; Lamb, R. N. *Chem. Commun.* **2003**, 1014-1015.

(161) Redshaw, C.; Elsegood, M. R. J. *Polyhedron* **2000**, *19*, 2657-2659.

(162) Rondelez, Y.; Bertho, G.; Reinaud, O. *Angew. Chem. Int. Ed.* **2002**, *41*, 1044-1046.

(163) Izzet, G.; Zeng, X.; Over, D.; Douziech, B.; Zeitouny, J.; Giorgi, M.; Jabin, I.; Le Mest, Y.; Reinaud, O. *Inorg. Chem.* **2007**, *46*, 375-377.

(164) Seneque, O.; Rager, M. N.; Giorgi, M.; Reinaud, O. *J. Am. Chem. Soc.* **2000**, *122*, 6183-6189.

(165) Parlevliet, F. J.; Zuideveld, M. A.; Kiener, C.; Kooijman, H.; Speck, A. L.; Kamer, P. C. J.; van Leeuwen, P. W. N. M. *Organometallics* **1999**, *18*, 3394-3405.

(166) Salmon, L.; Thuéry, P.; Ephritikhine, M. *Chem. Commun.* **2006**, 856-858.

(167) Gibson, V. C.; Redshaw, C.; Elsegood, M. R. J. *J. Chem. Soc. Dalton Trans.* **2001**, 767-769.

(168) Atwood, J. L.; Hardie, M. J.; Raston, C. L.; Sandoval, C. A. *Org. Lett.* **1999**, *1*, 1523-1526.

(169) Thuéry, P.; Nierlich, M.; Souley, B.; Asfari, Z.; Vicens, J. *J. Chem. Soc. Dalton Trans.* **1999**, 2589-2594.

(170) Li, H.; Xiong, D.; Chen, Y.; Xie, P.; Wan, J. *J. Inclusion Phenom. Macrocyclic Chem.* **2008**, *60*, 169-172.

(171) Fleming, S.; Gutsche, C. D.; Harrowfield, J. M.; Ogden, M. I.; Skelton, B. W.; Stewart, D.; White, A. H. *Dalton Trans.* **2003**, 3319-3327.

(172) Rogers, R. D.; Bond, A. H.; Aguinaga, S. *J. Am. Chem. Soc.* **1992**, *114*, 2960-2967.

(173) Stavila, V.; Wignacourt, J. P.; Holt, E. M.; Conflant, P.; Drache, M.; Gulea, A. *Inorg. Chim. Acta* **2003**, *353*, 43-50.

(174) Stavila, V.; Gulea, A.; Shova, S.; Simonov, Y. A.; Petrenko, P.; Lipkowski, J.; Riblet, F.; Helm, L. *Inorg. Chim. Acta* **2004**, *357*, 2060-2068.

(175) Georgopoulou, A. S.; Ulvenlund, S.; Mingos, D. M. P.; Baxter, I.; Williams, D. J. *J. Chem. Soc. Dalton Trans.* **1999**, 547-551.

(176) Gutsche, C. D.; Dhawan, B.; Leonis, M.; Stewart, D. *Org. Synth.* **1990**, *68*, 238-242.

(177) Gutsche, C. D.; Lin, L.-G. *Tetrahedron* **1986**, *42*, 1633-1640.

(178) Harvey, P. D. *Coord. Chem. Rev.* **2002**, *233-234*, 289-309.

(179) *Calixarenes 2001*; Asfari, Z.; Böhmer,V.; Harrowfield, J; Vicens, J. ed.; Kluwer Academic Publishers: Boston, 2001.

(180) Diamond, D.; McKervey, M. A. *Chem. Soc. Rev.* **1996**, 15-24.

(181) Jose, P.; Menon, S. *Bioinorg. Chem. Appl.* **2007**, *2007*, 1-16.

(182) Diamond, D.; Nolan, K. *Anal. Chem.* **2001**, *73*, 22A-29A.

(183) Ludwig, R. *Microchim. Acta* **2005**, *152*, 1-19.

(184) Creaven, B. S.; Donlon, D. F.; McGinley, J. *Coord. Chem. Rev.* **2009**, *253*, 893-962.

(185) Ozerov, O. V.; Ladipo, F. T.; Patrick, B. O. *J. Am. Chem. Soc.* **1999**, *121*, 7941-7942.

(186) Ozerov, O. V.; Parkin, S.; Brock, C. P.; Ladipo, F. T. *Organometallics* **2000**, *19*, 4187-4190.

(187) Ozerov, O. V.; Brock, C. P.; Carr, S. D.; Ladipo, F. T. *Organometallics* **2000**, *19*, 5016-5025.

(188) Ozerov, O. V.; Patrick, B. O.; Ladipo, F. T. *J. Am. Chem. Soc.* **2000**, *122*, 6423-6431.

(189) Notestein, J. M.; Iglesia, E.; Katz, A. *J. Am. Chem. Soc.* **2004**, *126*, 16478-16486.

(190) Katz, A.; Da Costa, P.; Lam, A. C. P.; Notestein, J. M. *Chem. Mater.* **2002**, *14*, 3364-3368.

(191) Burke, L. P.; DeBellis, A. D.; Fuhrer, H.; Meier, H.; Pastor, S. D.; Rihs, G.; Rist, G.; Rodebaugh, R. K.; Shum, S. P. *J. Am. Chem. Soc.* **1997**, *119*, 8313-8323.

(192) Kingston, J. V.; Ozerov, O. V.; Parkin, S.; Brock, C. P.; Ladipo, F. T. *J. Am. Chem. Soc.* **2002**, *124*, 12217-12224.

(193) Ladipo, F. T.; Sarveswaran, V.; Kingston, J. V.; Huyck, R. A.; Bylikin, S. Y.; Carr, S. D.; Watts, R.; Parkin, S. *J. Organomet. Chem.* **2004**, *689*, 502-514.

(194) Kingston, J. V.; Sarveswaran, V.; Parkin, S.; Ladipo, F. T. *Organometallics* **2003**, *22*, 136-144.

(195) Wagler, J.; Doert, T.; Roewer, G. *Angew. Chem. Int. Ed.* **2004**, *43*, 2441-2444.

(196) Kobayashi, J.; Kawaguchi, K.; Kawashima, T. *J. Am. Chem. Soc.* **2004**, *126*, 16318-16319.

(197) Timosheva, N. V.; Chandrasekaran, A.; Day, R. O.; Holmes, R. R. *Organometallics* **2000**, *19*, 5614-5622.

(198) Timosheva, N. V.; Chandrasekaran, A.; Day, R. O.; Holmes, R. R. *Organometallics* **2001**, *20*, 2331-2337.

(199) Jones, C. M.; Burkart, M. D.; Bachman, R. E.; Serra, D. L.; Hwu, S. J.; Whitmire, K. H. *Inorg. Chem.* **1993**, *32*, 5136-5144.

(200) Hanna, T. A.; Keitany, G.; Ibarra, C.; Sommer, R. D.; Rheingold, A. L. *Polyhedron* **2001**, *20*, 2451-2455.

(201) Mehring, M.; Schürmann, M. *Chem. Commun.* **2001**, 2354-2355.

(202) Breeze, S. R.; Wang, S. *Angew. Chem. Int. Ed.* **1993**, *32*, 589-591.

(203) Hulme, R.; Szymanski, J. T. *Acta Cryst.* **1969**, *B25*, 753-761.

(204) Hulme, R.; Mullen, J. E. D. *J. Chem. Soc. Dalton, Trans.* **1976**, 802-804.

(205) Lipka, V. A.; Mootz, D. *Z. Anorg. Allg. Chem.* **1978**, *440*, 217-223.

(206) Mootz, D.; Handler, V. *Z. Anorg. Allg. Chem.* **1986**, *533*, 23-29.

(207) Avarvari, N.; Fourmigué, M.; Canadell, E. *Eur. J. Inorg. Chem.* **2004**, 3409-3414.

(208) Pohl, S.; Saak, W.; Haase, D. *Angew. Chem. Int. Ed.* **1987**, *26*, 467-468.

(209) Ono, T.; Numata, H.; Ogata, N. *J. Mol. Catal. A: Chem.* **1996**, *105*, 31-37.

(210) Limberg, C.; Hunger, M.; Habicht, W.; Kaifer, E. *Inorg. Chem.* **2002**, *41*, 3359-3365.

(211) Kortz, U.; Savelieff, M. G.; Abou Ghali, F. Y.; Khalil, L. M.; Maalouf, S. A.; Sinno, D. I. *Angew. Chem. Int. Ed.* **2002**, *41*, 4070-4073.

(212) Petrella, A. J.; Craig, D. C.; Lamb, R. N.; Raston, C. L.; Roberts, N. K. *Dalton Trans.* **2004**, 327-333.

(213) Several mechanisms have been proposed for bismuth oxo formation in cluster systems, but in this case residual water is the most plausible source of the oxo groups, as previously observed in our [$M_2O\{^tBuC5(H)\}$] complexes (M = Bi, Sb).

(214) Hormillosa, C.; Healy, S. Valence for DOS, Bond Valence Calculator 1993. Retrieved from http://www.physics.mcmaster.ca/people/faculty/Brown ID.html.

(215) Orlov, I. P.; Popov, K. Bond Valence Wizard, Lausanne, Switzerland, 2004. Retrieved from http:/orlov.ch/bondval/.

(216) Chen, H.-Y.; Sleight, A. W. *J. Solid State Chem.* **1986**, *63*, 70-75.

(217) Jolly, M.; Mitchell, J. P.; Gibson, V. C. *J. Chem. Soc., Dalton Trans.* **1992**, 1331-1332.

(218) Adams, C. R.; Jennings, T. J. *J. Catal.* **1963**, *2*, 63-68.

(219) Buccella, D.; Tanski, J. M.; Parkin, G. *Organometallics* **2007**, *26*, 3275-3278.

(220) Chaudhuri, P.; Hess, M.; Weyhermüller, T.; Wieghardt, K. *Angew. Chem. Int. Ed.* **1999**, *38*, 1095-1098.

(221) Chaudhuri, P.; Hess, M.; Müller, J.; Hildenbrand, K.; Bill, E.; Weyhermüller, T.; Wieghardt, K. *J. Am. Chem. Soc.* **1999**, *121*, 9599-9610.

(222) Wang, Y.; Stack, T. D. P. *J. Am. Chem. Soc.* **1996**, *118*, 13097-13098.

(223) Thomas, F.; Gellon, G.; Gautier-Luneau, I.; Saint-Aman, E.; Pierre, J.-L. *Angew. Chem. Int. Ed.* **2002**, *41*, 3047-3050.

(224) Liu, L.; Quiroz-Guzmán, M.; Mendoza-Espinosa, D.; Hanna, T. A. **2009**, Manuscript in preparation.

(225) Shilov, A. E.; Shul'pin, G. B. *Russ. Chem. Rev.* **1990**, *59*, 853-866.

(226) Davies, M. L. H.; Beckwith, R. E. J. *Chem. Rev.* **2003**, *103*, 2861-2904.

(227) Labinger, J. A.; Bercaw, J. E. *Nature* **2002**, *417*, 507-514.

(228) Liu, L.; Hanna, T. A., Manuscript in preparation.

(229) Casiraghi, G.; Casnati, G.; Pochini, A.; Puglia, G.; Ungaro, R.; Sartori, G. *Synthesis* **1981**, 143-146.

(230) Kolly, S.; Meier, H.; Rihs, G.; Winkler, T. *Helv. Chim. Acta* **1988**, *71*, 1101-1107.

(231) Dick, A. R.; Sanford, M. S. *Tetrahedron* **2006**, *62*, 2439-2463.

(232) Janowicz, A. H.; Bergman, R. G. *J. Am. Chem. Soc.* **1982**, *104*, 352-354.

(233) Vastine, B. A.; Hall, M. B. *J. Am. Chem. Soc.* **2007**, *129*, 12068-12069.

(234) Buccella, D.; Parkin, G. *J. Am. Chem. Soc.* **2006**, *128*, 16358-16364.

(235) Akagi, F.; Matsuo, T.; Kawaguchi, K. *J. Am. Chem. Soc.* **2005**, *127*, 11936-11937.

(236) Kawaguchi, K.; Matsuo, T. *J. Am. Chem. Soc.* **2003**, *125*, 14254-14255.

(237) Watanabe, T.; Matsuo, T.; Kawaguchi, K. *Inorg. Chem.* **2006**, *45*, 6580-6582.

(238) Kawaguchi, K.; Matsuo, T. *J. Organomet. Chem.* **2005**, *690*, 5333-5345.

(239) Paine, T. K.; Weyhermüller, T.; Slep, L. D.; Neese, F.; Bill, E.; Bothe, E.; Weighardt, K.; Chaudhuri, P. *Inorg. Chem.* **2004**, *43*, 7324-7338.

(240) Chaudhuri, P.; Hess, M.; Flörke, U.; Wieghardt, K. *Angew. Chem. Int. Ed.* **1998**, *37*, 2217-220.

(241) Siefert, R.; Weyhermüller, T.; Chaudhuri, P. *J. Chem. Soc. Dalton Trans.* **2000**, 4656-4663.

(242) Weyhermüller, T.; Paine, T. K.; Bothe, E.; Bill, E.; Chaudhuri, P. *Inorg. Chim. Acta* **2002**, *337*, 344-356.

(243) Paine, T. K.; Weyhermüller, T.; Wieghardt, K.; Chaudhuri, P. *Inorg. Chem.* **2002**, *41*, 6538-6540.

(244) Paine, T. K.; Weyhermüller, T.; Bothe, E.; Weighardt, K.; Chaudhuri, P. *Dalton Trans.* **2003**, 3136-3144.

(245) Sernetz, F. G.; Mülhaupt, R.; Fokken, S.; Okuda, J. *Macromolecules* **1997**, *30*, 1562-1569.

(246) Liu, L.; Hanna, T. A., Unpublished results.

VITA

Daniel Mendoza-Espinosa was born on March 12, 1982 in Mexico City, Mexico. He is the son of Margarito Mendoza-Cureno and Emma Espinosa-García. He received his Bachelor in Sciences degree with a major in Inorganic Chemistry from Universidad Autónoma del Estado de Hidalgo, Pachuca de Soto Hidalgo, Mexico, *magna cum laude*, in 2004.

In 2004 he enrolled in graduate study at Texas Christian University, Fort Worth, TX, to pursue a Ph. D. in Inorganic Chemistry. While working on his doctorate in Chemistry, he worked as a Graduate Teaching Assistant for four semesters and was awarded the Graduate Student Teaching Award from the College of Sciences and Engineering in the spring of 2007. He is member of the American Chemical Society.

ABSTRACT

SYNTHESIS AND CHARACTERIZATION OF METALLOCALIXARENES AS PRECURSORS FOR THE SOHIO MODEL CATALYST

by Daniel Mendoza-Espinosa
Department of Chemistry
Texas Christian University

Dissertation Advisor: Tracy A. Hanna, Associate Professor

The Standard Oil of Ohio Company (SOHIO) process refers to the selective oxidation and ammoxidation of propene to produce acrolein and acrylonitrile, used on large scales in industry. The outstanding performance of the SOHIO process has stimulated much fundamental research on its mechanistic details, but four decades after its discovery, the mode of action of the "simple" $Bi_2O_3 \cdot MoO_3$ catalyst remains controversial (Chapter 1).

For several years now, we have sought to prepare soluble complexes featuring $Bi^{III}(\mu\text{-}O)Mo^{VI}$ interactions in pure oxo environments, in order to resemble the proposed SOHIO catalyst active site. During our quest, we have employed calixarene ligands as oxygen rich platforms that can hold the Bi and Mo centers simultaneously. We took advantage of the oxygen-donor lower rim of the calixarenes to prepare a series of Bi^{III} and Sb^{III} metallated complexes that display a broad structural diversity. We synthesized a series of deprotonated calixarenes "calix[n]anions" (including mono- to pentaanionic species) by the reaction of parent calix[n]arenes (n = 5, 7) with alkali metal bases (Chapter 2). The calix[5]arene anions were employed to successfully synthesize for the first time, mono- and bimetallic Bi^{III} and Sb^{III} calix[5]arene complexes containing unreacted OH groups (Chapter 3).

In order to expand the number of bismuth and antimony precursors, we decided to explore the reactivity of the calix[n]arenes (n = 6-8) taking advantage of the larger cavity size and conformational exchange. The treatment of parent calix[n]arenes (n = 6-8) with several

bismuth and antimony precursors allowed the preparation of a series of metal complexes featuring mono- to tretranuclear structures (Chapter 4).

As the chemistry of bismuth and antimony complexes usually has an issue of low solubility, we synthesized mono-silylated calix[5]arenes that upon treatment with bismuth and antimony alkoxides permitted the preparation of highly soluble Bi^{III} and Sb^{III} compounds (Chapter 5). The reactivity of the monometallic Bi^{III} and Sb^{III} calixarene complexes was tested and successfully utilized on the synthesis of the first M/Mo (M = Sb, Bi) heterometallic models supported by calixarene ligands (Chapter 6).

Finally, as part of our studies on C-H activation (rate determining step in the SOHIO process) observed in Bi^{III} bisphenolates, we have synthesized the analogous Sb^{III} complexes and discovered that they are able to undergo such bond activations under similar reaction conditions (Chapter 7).